

1964

Strength of soil aggregates

Andrew Stanislaw Rogowski
Iowa State University

Follow this and additional works at: <https://lib.dr.iastate.edu/rtd>



Part of the [Agriculture Commons](#)

Recommended Citation

Rogowski, Andrew Stanislaw, "Strength of soil aggregates " (1964). *Retrospective Theses and Dissertations*. 2716.
<https://lib.dr.iastate.edu/rtd/2716>

This Dissertation is brought to you for free and open access by the Iowa State University Capstones, Theses and Dissertations at Iowa State University Digital Repository. It has been accepted for inclusion in Retrospective Theses and Dissertations by an authorized administrator of Iowa State University Digital Repository. For more information, please contact digirep@iastate.edu.

This dissertation has been 65-3773
microfilmed exactly as received

ROGOWSKI, Andrew Stanislaw, 1931-
STRENGTH OF SOIL AGGREGATES.

Iowa State University of Science and Technology
Ph.D., 1964
Agriculture, general

University Microfilms, Inc., Ann Arbor, Michigan

STRENGTH OF SOIL AGGREGATES

by

Andrew Stanislaw Rogowski

A Dissertation Submitted to the
Graduate Faculty in Partial Fulfillment of
The Requirements for the Degree of
DOCTOR OF PHILOSOPHY

Major Subject: Soil Physics

Approved:
Signatures have been redacted for privacy.

Iowa State University
Of Science and Technology
Ames, Iowa

1964

TABLE OF CONTENTS

	Page
ORGANIZATION OF THIS THESIS	vii
INTRODUCTION	1
METHODS	7
Soils	7
Gravity Fractionation	9
Introduction: an example	9
Apparatus	17
Procedure	18
Carbon	21
Procedure	21
Calculation	22
Clay	23
Water Stability	23
Strength Measurements	24
Equilibration	25
Apparatus	25
Procedure	30
Calculations	31
Strain	31
Stress	33
Conclusions	34
Experimental Design and Methods of Averaging	35
Gravity fractionation	35
Carbon, clay, and water stability analyses	35
Strength measurements	38
Rupture stress, Z_{zr} , and rupture strain, e_{zr}	40
Average stress, Z_z , and average strain, e_z	41
Aggregate size (polar diameter)	41
Numerical size of groups	41

	Page
Conclusions	43
THEORY I	45
Shape of Soil Aggregates	45
Theoretical volume V_c	45
Experimental volume V_e	45
Correction factor	50
THEORY II	54
Gravity Fractionation of Soil Aggregates	54
Introduction	54
Use of pore liquids for fractionation	57
Criteria of pore liquid selection	58
Liquid to be readily driven off	58
Liquid to be non-polar	59
Liquid to be immiscible	61
Computation of aggregate bulk density	66
Straight line equation	66
Algebraic solution	69
Experimental verification of the theory	70
Porous ceramics	70
Soil aggregates	74
Chepil's (1950) results	77
Sources of error	82
Conclusions	94
THEORY III	
Theoretical Treatment of Soil Aggregate Rupture	96
General concepts	96
Statement of a problem and assumptions	97
Elementary concepts of elastic theory	98
Stress	98
Strain	111
Hooke's law	113

	Page
Griffith theory of rupture	119
Influence of moisture on soil aggregate strength	121
Statistical theory of the strength of materials	123
RESULTS	128
Influence of Aggregate Size on Aggregate Strength	129
Influence of Aggregate density on aggregate Strength	144
Influence of the Type of Soil on the Aggregate Strength	156
Statistical	161
Analysis of variance	161
Size groups	163
Density groups	163
Soil as a whole	166
DISCUSSION OF RESULTS	168
Influence of Aggregate Size on Aggregate Strength	168
General information	168
Aggregate size	168
Weight percent	170
Constancy of stress/strain ratio	171
Crushing strength	172
Relationship of strength measurements to other variables tested	179
Aggregates in air-dry condition	179
Aggregates at 15 atm. moisture tension	180
Griffith crack theory	185
Tensile strength in air-dry condition	185
Tensile strength at 15 atm. moisture tension	187
Rupture strain	188
Change in energy of rupture	189
Water stability	192
Induced strain	192
Aggregate stability	192
Weibull theory	193

	Page
Parameters	193
Shift of Weibull lines	195
Tensile and crushing strength values in psi	197
Influence of Aggregate Density on Aggregate Strength	197
General information	197
Aggregate density	197
Weight percent	200
Constancy of the stress/strain ratio	200
Crushing strength	201
Relationship of strength measurements to other variables tested	207
Aggregates in air-dry condition: tensile strength	207
Aggregates in air-dry condition: tensile rupture strain	215
Aggregates at 15 atm. moisture tension	217
Change in energy of rupture	217
Water stability	219
Weibull parameters	219
Three anomalous Density groups; the influence of carbon	220
Tensile and crushing strength in psi	224
Influence of the Type of Soil on the Aggregate Strength	226
General information	226
Constancy of the stress/strain ratio	226
Crushing strength	226
Relationship of strength measurements to other variables tested	227
Aggregates in air-dry condition	227
Aggregates at 15 atm. moisture tension	232
Griffith crack theory	233
Tensile strength in air-dry condition	233
Tensile strength at 15 atm. moisture tension	234
Change in energy of rupture	236
Tensile and crushing strength values in psi	242

	Page
SUMMARY AND CONCLUSIONS	243
LITERATURE CITED	252
ACKNOWLEDGEMENTS	261
APPENDIX I	263
Detailed Results and Calculations Pertaining to Strength Measurements for Respective Size Groups of Clarion s.l., Webster c.l., and Luton si.c. Aggregates.	263
APPENDIX II	278
Detailed Results and Calculations Pertaining to Strength Measurements for Respective Density Groups of Clarion s.l., Webster c.l., and Luton si.c. Aggregates.	278
APPENDIX III	291
Detailed Results and Calculations Pertaining to Strength Measurements for Soil as a Whole for Clarion s.l., Webster C.l., and Luton si.c. Aggregates.	291
APPENDIX IV	300
Statistical Analysis	300
APPENDIX V	305
List of Symbols and Definitions	305
Page Numbers of Tables, Figures and Equations	311
Tables	311
Figures	314
Equations	315

ORGANIZATION OF THIS THESIS

This dissertation is organized along the following lines:

- (a) Initially in the Introduction (pp. 1-6) the definition of a soil aggregate is given and the scope of this work is outlined.
- (b) On the next 38 pages (pp. 7-44) methods used are given. The methods describe the soils and procedures employed for determination of soil aggregate strength parameters and soil aggregate strength.
- (c) On the next 83 pages (pp. 45-127) the theoretical basis of experimental measurements is given. This includes Theory I: Shape of soil aggregates, Theory II: Gravity fractionation of aggregates, and Theory III: Theoretical treatment of soil aggregate rupture.
- (d) The detailed computations of soil aggregate strength, related parameters and statistical analyses are given in Tables of Appendix I, Appendix II, Appendix III and Appendix IV. The principal results abstracted from the appendices are presented in the tables and figures of Results section (pp. 128-167).
- (e) In the Discussion of Results section (pp. 168-242) our results are contrasted and compared with the results of other research workers.
- (f) The findings are summarized and conclusions are given in the Summary and Conclusions section (pp. 243-251).
- (g) The Literature cited, arranged alphabetically and chronologically, and the Acknowledgements (pp. 252-262) complete this presentation.
- (h) Finally in Appendix V, at the end, the crossreference material is presented. This includes List of Symbols and Definitions and Page Numbers of Tables, Figures and Equations.

INTRODUCTION

Soil supports and sustains us. In a sense we are all affected directly or indirectly by its properties. In soil physics we are concerned with physical properties of the soil as a scientific basis for our own investigations and as a framework for the work of others. It is our purpose in this study to examine some of these properties and to record them in terms of numbers and equations subject to the laws of science.

The basic experimental unit used throughout this investigation is a soil aggregate. A soil aggregate may be thought of as a number of primary particles of sand silt and clay connected together in a spatial distribution in the state of equilibrium at a given temperature and moisture content. When aggregation occurs the specific surface area and with it the total surface free energy of the solid particles within the soil diminishes. The reduction of surface energy may be thought of as the mechanism for the driving force for aggregation. As the surfaces of two solids approach one another, their fields of force begin to overlap, resulting in adhesion whenever they come close enough together. Adhesion manifests itself by internal friction, siezure of two solids, or aggregation of primary particles (Gregg 1961, p. 137).

The surface energy of the solids is generally reduced by adsorption of films and impurities on their surfaces. Although the adhesive power is a universal property of surfaces, the effect is shown best if one of the solids is thin as well as clean. Generally clay micelles can be thought of as thin plates. We would suspect therefore that within a soil mass it is the nature, distribution, and orientation of the clay fraction which determines the properties of a given aggregate. Since the distribution of clay within the soil

is perfectly random, subject only to the redistributing action of soil water, we would expect great variability of strength properties between different aggregates. However, as pointed out before, each aggregate would represent a state of equilibrium of the particles that compose it. Under these circumstances the amount of energy required to rupture an aggregate should be a definite measurable quantity for a given soil.

Grossman (1959) has shown by thin section examinations that the aggregate surface was composed in part of blanched silt-rich areas and in part of clay-rich areas. The latter were shown to contain large quantities of silicate clays in preferential orientation (oriented clay coatings). Immediately to the inside of an aggregate or void surface there occurred a relatively clay-poor zone in which clay also showed preferential orientation. The proportion of degradational surface was greater on the aggregate surface than on the walls of larger non-capillary pores in the aggregate interior. Grossman suggests that the morphology of the aggregate surface reflects the large amount of water movement per unit area across the surface of aggregates. The preferential orientation of clay fields within the till soil matrix was also observed, suggesting a certain amount of orderly deposition independent of the voids.

This preferential orientation of clay on the aggregate surface, along the walls of voids and finally in a form of fields within the matrix, would certainly have a bearing on the mechanical properties of individual aggregates. With this in mind we decided to approach the problem of aggregate strength from the standpoint of elastic theory and soil mechanics. We have also incorporated in our work the ideas put forward by Griffith (1921 and 1924) and Weibull (1939a and 1939b), as well as the statistical treatment

of data to compensate for variability among the aggregates. In this way we were able to compute the energy of rupture and describe the strength of soil aggregates for soils of differing clay content in terms of crushing and tensile strength.

We would expect the soil strength to vary as the number of contact points within a given aggregate since the number of contact points would vary as does the density, any increase in density, provided other factors are held constant, should be reflected by a corresponding increase of strength. To evaluate the effect of density, a method for a densimetric, non-destructive separation of aggregates had to be developed first, since a review of literature did not show any method available.

In reviewing the literature we noticed that the effect of aggregate size on soil strength was either overlooked entirely (Richards, 1953), or seemed to give erroneous results (Martinson and Olmstead, 1949).^a Furthermore, no concrete evidence with relation to soils could be found regarding the mean distribution of sizes within any given sieving class.

The theoretical development of the Griffith crack theory (Griffith, 1924) and subsequent studies by Orowan (1949) and Millard et al. (1955) have enabled us to obtain the representative values of rupture energy and soil aggregate strength for the size classes studies. Experimental data furnished partial answers with regard to the mean distribution of sizes within a given sieving class.

We have pointed out earlier that the reduction of surface area may be

^aMartinson and Olmstead (1949) claim that the aggregate strength increased as did the size. Since their values are in terms of load only, and the cross-sectional aggregate area was not taken into account, the results are not surprising.

associated with the driving force of aggregation. Since organic matter and clay possess a very large surface area, we have investigated, compared, and contrasted the effects of both on aggregate strength. Excellent studies dealing with the influence of clay on soil strength have been conducted previously (Stauffer, 1927; Hooghoudt, 1950; Grossman, 1957; Knox, 1957; Koenigs, 1961). However, no attempt was made to ascertain the influence of clay on the strength of individual aggregates. Stauffer (1927) and Hooghoudt (1950) worked with synthetic soils. Grossman (1957) and Knox (1957) studied large clods from fragipan horizons. Koenigs' (1961) approach was more from the standpoint of chemical nature of clay, swelling, and cohesion.

Organic matter has consistently appeared in the soils literature (Baver, 1956; De Leenheer, 1961b) as a factor favorably influencing "soil structure". We have attempted to establish the nature of the influence of organic matter on aggregate strength.

A commonly accepted index of soil structure is usually some modification of Yoder's (1936) wet sieving technique (De Leenheer and De Boodt, 1959; van Bavel, 1953). We have felt for a very long time that the results obtained by this technique are inconsistent and perhaps unrelated to the true aggregate strength. Furthermore, a wide variation in the way workers have presented the results renders data from the method practically useless for comparison purposes. With that in mind we have investigated the nature of the wet sieving method as it might relate to true soil aggregate strength.

Finally, the search of literature revealed that the so-called modulus of rupture of the soil and soil strength have been subject to a conflicting

number of methods and presentation of results. There appear to be five types of methods available. The first type measures the inter-aggregate strength of soil (Richards, 1953; Vomocil, 1961). The second type measures the true strength of soil using synthetic or compacted material (Stauffer, 1927; Gill, 1959; Hooghoudt, 1950). In the third type of methods, use is made of a soil engineering approach (McMurdie, 1963; McMurdie and Day, 1958; Barley, 1963). The fourth type of methods employs the relationship between soil resistance and strength (Taylor and Gardner, 1963; Phillips, 1959; Phillips and Kirkham, 1962). Finally, in the fifth type of methods, a soil strength of undisturbed soil samples is determined (Kirkham et al., 1958; Grossman and Cline, 1957).

We have attempted to obtain the crushing and tensile strength values on the individual soil aggregates in air-dry condition and at 15 atm. moisture tension. Furthermore, we have computed the energy of rupture for different size and density groups of soils studied.

We will show from the theoretical considerations that we may assume the aggregates of the soils studied to approximate spheres. Using aggregates of known size and density we will establish the theoretical and experimental basis of our approach to the soil strength on the "per aggregate" basis. We must emphasize that all the values of strength measurements obtained are based on a large number of individual determinations.

We shall compare our results with results obtained by other research workers, bearing in mind that in all instances (unless otherwise specified) their results are for the assemblies of aggregates in contrast to the individual aggregate determinations carried out by us.

We will attempt to show the relationship between soil strength and

soil resistance. We will also point out the correspondence between our values and those values obtained by a method used by Moldenhauer and Long (1964) in the study of erosion.

The literature on soil structure is very large and comprehensive. In this study we have made use of several excellent reviews (Russell, 1938; van Schuylenborgh, 1947; Kirkham, 1960; De Leenheer 1961a and 1961b).

In concluding this introduction we would like to say that our investigation has been suggested by the great confusion that exists in soil literature with regard to soil strength, its measurement, and its relationship in a useful index, to other variables within the soil mass.

Table 1. Selected properties of soils used in subsequent analyses

Soil	Textural Class	Sand %	Silt %	Clay %	Carbon %	Bulk Density ^a g cm ⁻³	Porosity ^b %	Remarks
Clarion	sandy loam	57.8	27.1	15.1	0.99	1.74-2.07	24.5-35.5	Ca CO ₃ present
Webster	clay loam	30.2	38.4	31.4	3.26	1.62-2.07	22.2-39.7	
Luton	silty clay	1.9	46.1	52.0	2.96	2.00-2.06	24.1-28.2	

^aAverage bulk density of oven dried soil aggregates as determined by gravity fractionation method described in the next section

^bPorosity % = [1-(bulk density/particle density)] x 100

originating from Missouri River alluvium through sorting and deposition of fine fragments (McClelland et al., 1950). In this dissertation we consider Luton si.c. to be less mature than Webster c.l. . In contrast to the other two, Webster c.l. can be viewed as a relatively developed soil. Though originating from glacial till through sorting and deposition, Webster has undergone changes resulting from leaching, weathering, and extensive cultivation. For Webster c.l., the soil forming process can be thought of as being directed in a downward direction, i.e. from the soil surface down to a depth of about 2 feet.

In all instances the aggregates used in this study come from the plow layer of each soil. For practical reasons we have chosen to work with 0.200 cm. to 0.800 cm. in diameter aggregates. Aggregates smaller than 0.200 cm. in diameter are hard to handle individually especially if visual criteria of rupture, i.e. appearance of cracks, are to be observed. Aggregates larger than 0.800 cm. in diameter were observed to depart more and more from the spherical shape as the size was increased for the three soils used. It will be seen subsequently that the results obtained for the 0.200-0.800 cm. fraction can be extended with suitable corrections to larger or smaller sizes of aggregates.

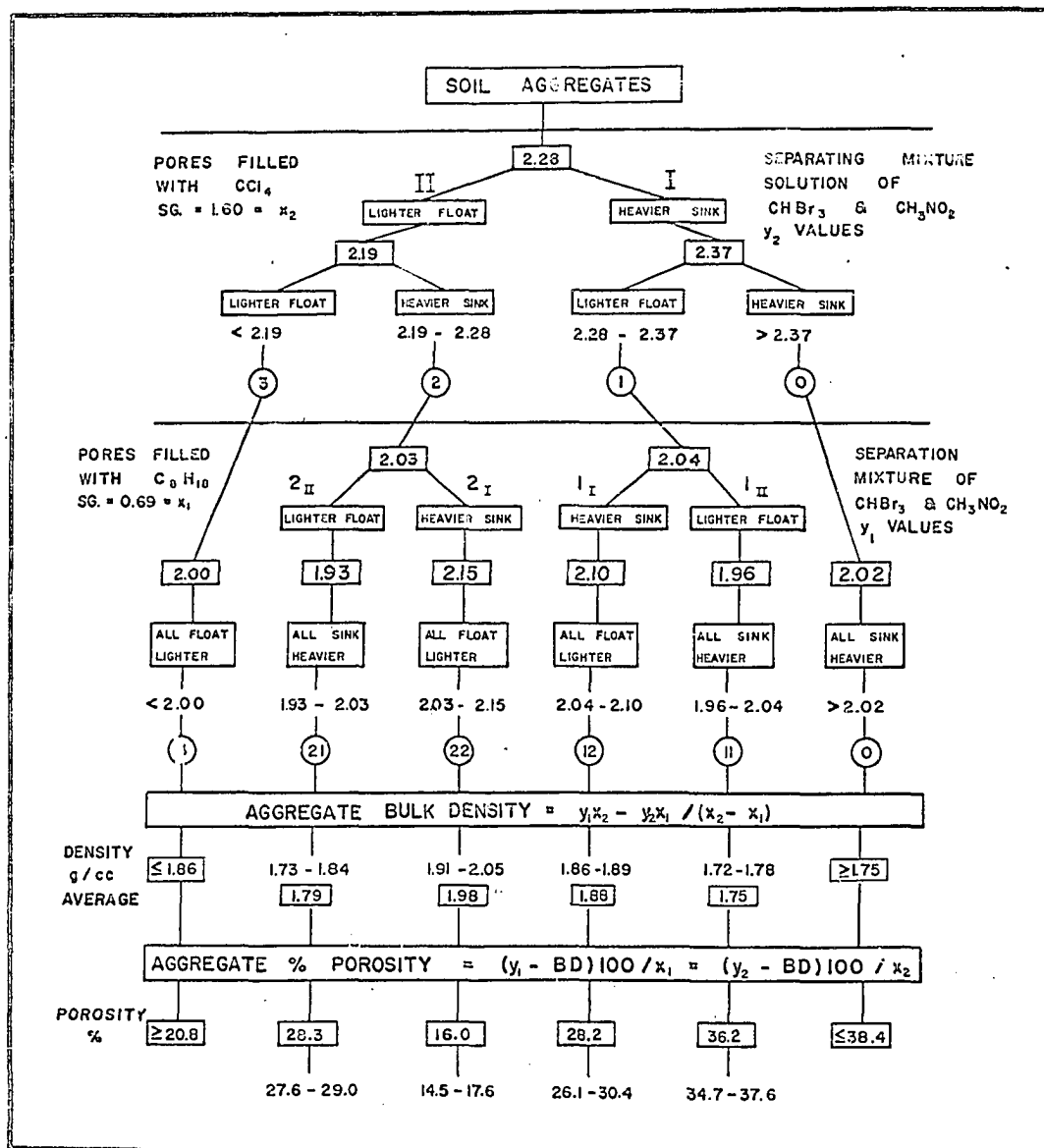
Gravity Fractionation

Introduction: an example

The purpose of gravity fractionation is to separate aggregates of different densities into groups of certain density ranges. The step by step procedure is illustrated by an example in Fig. 1. Four fluids are used: bromoform (CHBr_3) S.G. 2.85 and nitromethane (CH_3NO_2) S.G. 1.12 to prepare

Fig. 1. Schematic illustration of gravity fractionation. The four main groups of aggregates are denoted by encircled numbers 11, 12, 21, and 22 and correspond to Density groups A, C, B and D respectively.

Two other groups are also shown: group denoted by encircled 0 is composed mostly of stones; group denoted by encircled 3 contains very few aggregates whose density limits do not coincide with limits chosen for the other groups. Aggregate porosity is also shown for each group.



a "separating solution" mixture, carbon tetrachloride (CCl_4) S.G. 1.16 and isooctane (C_8H_{18}) S.G. 0.69 to fill the pores.

To accomplish the separation we first fill the pores of the aggregates with carbon tetrachloride (S.G. 1.60) and then pour these aggregates into a fractionating mixture (heavy fluid). Suppose that we have prepared a solution of bromoform and nitromethane such that it has a S.G. 2.28 (see Fig. 1). Then all carbon tetrachloride filled aggregates whose composite density (soil + CCl_4) is more than 2.28 g. cm^{-3} will sink and those whose composite density is less than 2.28 g. cm^{-3} will float. Let us keep these two groups separate, they are denoted by I and II respectively in Fig. 1.

Let us consider the aggregates that sink in the separating solution of S.G. 2.28 (denoted by I in Fig. 1). Were these carbon tetrachloride filled aggregates now poured into a separating solution of S.G. 2.37, then they would separate again into two groups denoted by encircled 1 and encircled 0 in Fig. 1. The group denoted by encircled 1 would consist now of aggregates whose composite density values would be greater than 2.28 g. cm^{-3} but less than 2.37 g. cm^{-3} . The group denoted by encircled 0 would consist of aggregates (mostly stones) whose composite density was greater than 2.37 g. cm^{-3} .

In a similar manner if the carbon tetrachloride filled aggregates that float in separating mixture of S.G. 2.28 are poured into a separating mixture of S.G. 2.19 a further separation into two groups denoted by encircled 2 and encircled 3 in Fig. 1 will result. The group denoted by encircled 2 would consist of aggregates whose composite density would be greater than 2.19 g. cm^{-3} , but less than 2.28 g. cm^{-3} . The group denoted by encircled 3 would consist of aggregates whose composite density was less than 2.19 g. cm^{-3} . For each of the groups encircled 0, 1, 2 and 3, we will call the

values > 2.37 , $2.28-2.37$, $2.19-2.28$ and < 2.19 respectively, the y_2 values in Fig. 1.

Now let us take one of these carbon tetrachloride filled aggregate groups (for example encircled 1 group) remove the carbon tetrachloride (as by oven drying) and then refill the pores with isooctane S.G. 0.69. If we should now pour this group (encircled 1 with pores now filled with isooctane) into a solution of S.G. 2.28 all would float since the isooctane filled aggregates are lighter than before. Therefore we do not pour these aggregates into a separating solution of S.G. 2.28. Let us suppose that we pour these aggregates into a separating solution of S.G. 2.04, then in a manner similar to previous separations the isooctane filled aggregates whose composite density (soil + C_8H_{18}) is greater than 2.04 g. cm^{-3} will sink and those whose composite density is less than 2.04 g. cm^{-3} will float. Let us keep these two subgroups of encircled 1 group separate, they are denoted by 1_I and 1_{II} in Fig. 1 respectively.

If we were now to pour the aggregates of subgroup 1_I (isooctane filled aggregates that sink in a separating solution of 2.04 S.G.) into, for example, a separating solution of S.G. 2.10 we would find that all would float. Similarly if we were to pour the aggregates of subgroup 1_{II} (isooctane filled aggregates that float in a separating solution of 2.04 S.G.) into, for example, a separating solution of S.G. 1.96 we would find that all would sink. In this manner we would obtain two subgroups of encircled group 1. These are shown as encircled group 12 and encircled group 11 in Fig. 1. Encircled group 11 will consist of aggregates filled with isooctane whose composite density will be greater than 1.96 g. cm^{-3} but less than 2.04 g. cm^{-3} . Encircled group 12 will consist of aggregates filled with isooctane whose

Calculated in a similar manner the range of density for subgroup encircled 11 would be 1.72-1.78 g. cm.⁻³, that for subgroup encircled 22, 1.91-2.05 g. cm.⁻³ and that for subgroup encircled 21, 1.73-1.84 g. cm.⁻³. For the group encircled 3' only the upper limit of density can be computed (≤ 1.86 g. cm.⁻³), for the group encircled 0' only the lower limit (≥ 1.75 g. cm.⁻³) can be computed. This situation arises as a result of obtaining only upper (for group 3) or lower (for group 0) limits respectively for composite densities when aggregates of these groups were filled with carbon tetrachloride or isooctane.

Aggregates of group 0 are composed mostly of stones while aggregates of group 3 (very few in number) are those aggregates whose limits do not coincide with the limits of one of the subgroups 11, 12, 21 or 22.

We now arrange subgroups 11, 12, 21 and 22 in order of increasing density i.e. 11, 21, 12 and 22, and denote them by A, B, C and D (not marked on the figure) respectively. From now on these subgroups will be referred to as Density groups A, B, C and D.

Using the values of y_1 or y_2 and values of aggregate bulk density BD from Equation 1, we can compute aggregate porosity from Equation 2 below (Equation 2 is obtained from Equations 43 and 44 in Theory II).

$$\text{Aggregate \% porosity} = (y_1 - \text{BD})100/x_1 = (y_2 - \text{BD})/x_2 \quad (2)$$

For the subgroup encircled 12 of Fig. 1, the calculation would be as follows

$$(2.04 - 1.86)100/0.69 = 26.1\%$$

$$(2.10 - 1.89)100/0.69 = 30.4\%$$

$$(2.28 - 1.86)100/1.60 = 26.3\%$$

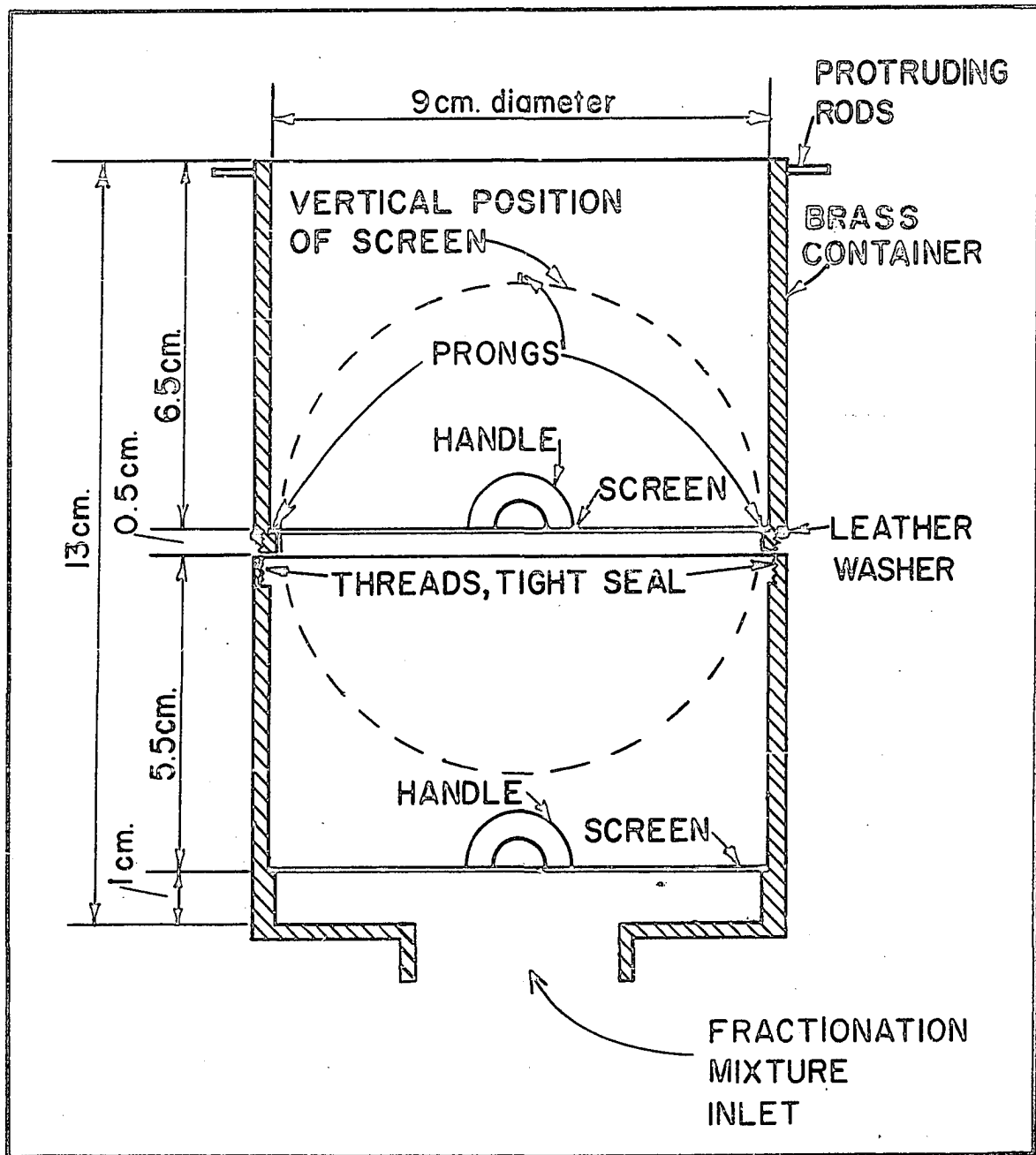


Fig. 2. Apparatus for gravity fractionation of aggregates

$$(2.37 - 1.89)100/1.60 = 30.0\%$$

Average value = 28.2%

In a similar manner the range of porosity for subgroup encircled 11 would be 34.7-37.6%, that for subgroup encircled 21, 27.6-29.0%, and that for subgroup encircled 22, 14.5-17.6%. The lower limit of porosity for group encircled 3' is 20.8% and the upper limit of porosity for group encircled 0 is 38.4%. The reasons why only the lower (group 3) or upper (group 0) limits of porosities can be obtained have been discussed above in connection with the density values.

Apparatus

In Fig. 2 a diagram of the apparatus used initially for gravity fractionation is given. Soil aggregates were placed on a lower screen (bottom screen); when a fractionation mixture was introduced, the lighter aggregates floated to the surface. The screen in the center of the apparatus (top screen), in the vertical position at the start of the separation, was then snapped into a horizontal position. When the fractionation liquid was drained, lighter aggregates were left on the top screen and the heavier ones remained on the bottom one. Following the separation, the top part of the apparatus was unscrewed and both screens and their respective aggregate fractions were removed.

This apparatus suffered from three major drawbacks. First, it was made of brass and we could not see what was happening inside. Second, where the top part joined the bottom part, great difficulty was encountered in keeping the joint leak proof. Third, only small amounts (<50 g.) of soil could be fractionated at any one time. The first of these drawbacks could be corrected by constructing the apparatus from glass. The second is not too

objectionable if the leakage is slow. Finally, insofar as the third drawback is concerned, the dimensions of the apparatus can be made as large as necessary.

For subsequent fractionations we have adopted a simplified procedure. A large glass funnel 300 cm.³ in capacity, called a separating funnel, was fitted with a hose and a clamp. We found that one of the screens from the apparatus described above could be placed about halfway down this funnel. When this screen was introduced at the appropriate time, it provided for an effective separation of aggregates after the fractionation liquid was drained out. By use of the screen we were able, in one procedure, to separate large quantities of aggregates (200 g.).

A large vacuum type desiccator fitted with a separating funnel and a complement of petri and porcelain dishes; also, a hotplate, exhaust hood, oven (110°C.), and a balance completed the list of equipment used.

Procedure

To carry out the gravity fractionation in a manner indicated by the example of Fig. 1, soil aggregates 0.200 to 0.800 cm. in diameter were first dried overnight at 110°C. Approximately 200 g. of soil was weighed out to the nearest gram, put in the porcelain dish, placed in the desiccator and the desiccator was evacuated. Carbon tetrachloride from the separating funnel was now introduced very slowly into the dish containing aggregates under vacuum. When the aggregates were saturated with carbon tetrachloride, enough excess was added to cover them up completely. The aggregates were allowed to soak for 1 minute in the carbon tetrachloride and then air was allowed to enter the desiccator at a fast rate. This procedure further insured complete filling with carbon tetrachloride of all the aggregate

pores. The aggregates were now placed on a coarse sieve and excess carbon tetrachloride was drained off. To insure that as little as possible of carbon tetrachloride remained on the outside of the aggregates, the sieve was placed for 30 seconds on the hotplate and the aggregates were turned frequently.

To prepare the fractionation mixture, bromoform was diluted to a required density with nitromethane using Equation 3 below (De Leenheer, 1961a, p. 79).

$$V_N = V_B \left(\frac{d_B - D_M}{D_M - d_N} \right) \quad (3)$$

V_B = volume of bromoform

V_N = volume of nitromethane to be added

d_B = density of bromoform

d_N = density of nitromethane

D_M = required density of the mixture.

To check the density of a fractionating mixture gravimetrically prior to and after each separation, a 50 ml. high precision graduated flask was filled with the fractionation mixture and weighed to three places of decimals, then

$$\text{Density of fractionation mixture} = \frac{\text{weight of flask \& liquid} - \text{weight of flask}}{\text{volume of flask}}$$

(4)

The hose at the bottom of the funnel which acted as our separation apparatus was now clamped shut. A small piece of wire mesh was placed at the top of funnel stem to prevent the soil aggregates from clogging the stem, and the funnel was filled with the fractionation mixture.

Soil aggregates treated as outlined above with the pores saturated with carbon tetrachloride were now transferred quickly into the fractionation mixture. Some aggregates floated, others began to sink. After 30 seconds a screen was inserted horizontally midway down the funnel. The clamp at the bottom was now opened and the fractionation mixture drained off, leaving behind on the screen the aggregates that floated and in the lower part of the funnel the aggregates that sank. These two sets of aggregates were now dried off, first on a hotplate and later in the oven (110°C.). On drying these two sets of aggregates were saturated with isooctane and the fractionation of each set effected in the same manner as before, with one exception. This exception was that for aggregates saturated with isooctane we inserted the separating screen into the funnel 15 seconds after the aggregates were transferred into the fractionation mixture, and not after 30 seconds as was the procedure with carbon tetrachloride saturated aggregates.

After the gravity fractionation of the soil aggregates was carried out, aggregates 0.200-0.800 cm. in diameter were separated by sieving into three size groups: (1) 0.200-0.283 cm., (2) 0.283-0.476 cm. and (3) 0.476-0.800 cm. All together we obtained four main Density groups A, B, C and D (from gravity fractionation), each composed of three Size groups (1), (2) and (3), (from sieving), yielding a total of twelve Size-density subgroups for a Soil^a.

^aThere were 12 Size-density subgroups for Clarion s.l. and Webster c.l.; however, Luton si.c. separated only into two density groups, hence we only had six Size-density subgroups when working with Luton si.c.

flasks to facilitate cooling. Condensers are left attached while cooling.

When the flasks have cooled for about 15 minutes, the condensers are rinsed and 15 ml. of indicator^a are added. The samples and the blanks (boiled blanks) are titrated with Mohr's salt solution^b at room temperature. The color change, which is quite sudden, is from violet to bright green.

Calculation

The difference ($B_b - T$) between the amount of Mohr's salt added to the boiled blank (B_b) and the amount of Mohr's salt added to the sample (T) is proportional to the amount of soil carbon (C). This value, ($B_b - T$), must be corrected for the amount of the dichromate consumed during boiling. This is done by titrating several (two or more) unboiled blanks (B_u) and determining the normality of Mohr's salt^c from these titrations. Then the correction A (in the range of 0.04) is given by

$$A = (B_b - T)(B_u - B_b)/B_u \quad (5)^a$$

and the corrected value ($B_b - T$)_c is

$$(B_b - T)_c = (B_b - T) + A \quad (6)$$

^aIndicator: N-phenylanthranilic acid, 0.100 g. acid, and 0.107 g. Na_2CO_3 in 100 ml. of H_2O .

^b0.2N Mohr's salt, 78.390 g. of $(\text{NH}_4)_2\text{SO}_4 \cdot \text{FeSO}_4 \cdot 6\text{H}_2\text{O}$ in 50 ml. conc. H_2SO_4 diluted to 1 liter with H_2O . This solution oxidizes slowly and must be standardized daily.

^c N Mohr's salt x ml. Mohr's salt = N dichromate x ml. dichromate, for our purposes N Mohr's salt = $\frac{0.5 \times \text{ml. dichromate}}{\text{ml. Mohr's salt}}$.

^aEquations 5 and 6 are a concise presentation of the material described in words in the original method.

then

$$\text{Percent carbon} = \frac{(B_b - T)_c \times (\text{N Mohr's salt}) \times 0.3}{\text{weight of soil}} \quad (7)$$

Clay

The percent of clay was determined by a standard pipette method (Baver 1956, p. 71-75) as used by the Soil Survey Section at Iowa State University. Carbonates were removed from the oven-dried soils with dilute acetic acid and carbon was removed by digestion in pyrex baby formula bottles with hydrogen peroxide on a hotplate.

After dispersion with Calgon on a shaker overnight, the samples were transferred to 1,000 ml. cylinders, filled up to the mark, shaken, and the required fractions were pipetted out at appropriate times, using a 25 ml. pipette on a rack and pinion arrangement. Applying corrections for Calgon, the amount of clay was calculated for each sample as the fraction < 2 microns in equivalent diameter.

$$\text{Percent clay} = \frac{\text{weight of clay} - \text{correction}}{\text{weight of soil}} \times 4000 \quad (8)$$

Water Stability

To determine water stability of soil aggregates we have used the method of De Leenheer and De Boodt (1959). This method has been used and described by us in detail elsewhere (Rogowski, 1960, and Rogowski and Kirkham, 1962). The method gives the CMWD (change of mean-weight diameter) as an index of water stability of soils. This index is computed from the area enclosed by cumulative percentage curves obtained from the dry and wet sieving procedure.

In this method, dry sieving separates aggregates into size classes

which are subsequently subjected to impact of water drops, simulating slaking and dispersion under natural conditions. Following slaking and dispersion the aggregates are incubated for 24 hours in an atmosphere of 98% relative humidity, wet-sieved for 5 minutes, dried, weighed and the CMWD computed graphically.

This procedure was used to compare mean-weight diameters of two sets of aggregates of each soil which had been subjected to gravity fractionation (treated) with two sets that had not been subjected to gravity fractionation (untreated). Change of mean-weight diameter is, in a sense, a confusing index. In its interpretation we have to remind ourselves constantly that the smaller the CMWD, the more water-stable is the soil. For that reason, and also because we have been working with aggregate size-density groups of a narrow size range (and not with the broad range of aggregates 0.200 to 0.800 cm. in diameter used by De Leenheer and de Boodt), we have found it to be simpler and more convenient to present our water stability results in terms of the percent of water-stable aggregates.

We emphasize: in sections that follow, the term "water stable" (WS) should be taken to mean the percentage of aggregates of a given size-density group that did not break down into smaller aggregates under the influence of slaking, dispersion, and wet-sieving treatments as outlined in the De Leenheer and de Boodt method.

Strength Measurements

Rupture stress and rupture strain were determined on each aggregate individually with about 40 aggregates, on the average, being tested for each size-density subgroup.

Equilibration

The size-density subgroups that had been fractionated by the gravity fractionation procedure and that were to be tested for rupture stress and rupture strain were placed prior to tests for a period of 2 weeks or more in a constant temperature (74°F.) and constant humidity (40% relative humidity) room. Figures given above are not absolute since departures as large as 5°F. and 5% relative humidity could at times be observed. The constant temperature and constant humidity room constituted at the time the best available facility and, since temperature and relative humidity stayed reasonably constant, we arranged to carry out our strength measurements there.

The aggregates that were tested following the equilibration are referred to as "aggregates in air-dry condition". One portion of these aggregates was subjected to saturation and equilibrated at 15 atm. moisture tension on the pressure-membrane apparatus (Richards, 1947). This portion will subsequently be referred to as "aggregates at 15 atm. moisture tension". Moisture contents by weight and by volume, both in the air-dry condition and at 15 atm. moisture tension, were determined for all size-density subgroups tested.

Apparatus

The apparatus for measuring stress and strain relationship for soil aggregates is given in Fig. 3. It consists of a custom-made proving ring mounted on a microscope stand. The stress-recording dial (referred to subsequently as ring dial) mounted in the center of the ring has a sensitivity of .0001 inches, i.e. if a load is applied so as to decrease the polar diameter of the ring by .0001 inches the dial registers 1 division.

Fig. 3. Apparatus for measuring aggregate strength,
bottle of alcohol serves as a weight for
removing backlash in the apparatus

Onto the left-hand side of Fig. 3 we have a second dial (referred to subsequently as strain gauge) with a sensitivity of .01 mm. It is mounted on the ring with its point resting on the base plane. To measure crushing strength, a soil aggregate (assumed to be spherical) is placed on the base plane, its uppermost pole against the ring plate. In the upper portion of the apparatus in Fig. 3 a turning handle can be seen. Turned at the constant rate of 6 revolutions per minute, it provided for a uniform rate of loading of about 50 g. per second. Although an attempt was made to keep this rate constant, we realize that since the apparatus was operated manually the human error in the rate of loading could have been present. It is felt, however, that since large numbers of aggregates were analyzed, this source of error is slight compared to the differences of strength within individual aggregates.

Two custom-made proving rings, supplied and calibrated in grams by Soil Test, Inc., of Chicago, Illinois, were used in this study. The first ring of 12 kg. load capacity was used for strength measurements on Luton si.c. aggregates in air-dry condition, the second one, of 5 kg. capacity, was used for Webster c.l. and Clarion s.l. aggregates in air-dry condition as well as on all three soils for aggregates at 15 atm. moisture tension. We found that even the 5 kg. ring was not sensitive enough to measure adequately the load applied to aggregates at 15 atm. moisture tension on all soils. Ideally we would have preferred to have a 500 g. proving ring for measurements where the load values were low. However, proving rings of that capacity are not commercially available. Each proving ring comes with a calibration chart supplied by the manufacturer. A straight-line relationship between ring dial reading and load in grams is plotted on the

chart which can be seen in the background of Fig. 3. Thus, ring dial readings can be converted to load in grams using the calibration chart.

On the top of the apparatus we placed weight to prevent slippage of pinion gears as the load is applied. A stopwatch and a light source completes the apparatus assembly. A stopwatch was marked in 10-second intervals, corresponding to the intervals at which stress and strain readings were taken. A light source was so directed as to illuminate the aggregate being tested and to facilitate visual observation of the crack appearance.

Proving rings, usually of a much higher load capacity, are used extensively in soil mechanics for unconfined compression testing (Jumikis, 1962, p. 507). Our apparatus was essentially an unconfined compression test assembly, the main difference being in the size and shape of the test sample. Where soil engineers use large, solid cylinders of soil, we have employed a small, spherical aggregate.

Hardesty and Ross (1938), working with fertilizer granules, used an apparatus consisting of a rack and pinion similar to that used in adjusting the elevation of the barrel of a microscope, mounted directly over an anvil resting over a platform of a spring scale. Single fertilizer granules were placed on the anvil under the rack and pressure was applied. The tell-tale hand on the spring scale recorded breaking pressure.

Fitts et al. (1943) and Martinson and Olmstead (1949) adapted an apparatus of Hardesty and Ross to studies of the crushing strength of soil clods. Hooghoudt (1950, p. 41) devised an apparatus where a vertical mechanical movement of a pinion and the crushing resistance it encountered were translated into the reading on a large dial-type scale.

Grossman and Cline (1957), obtained satisfactory results for crushing

strength of clods derived from fragipan horizons of New York soils using a machine designed for triaxial compression tests. Stress was applied to the surface of a cylindrical clod through a proving ring and recorded on a strain gauge with a sensitivity of $1/10000$ of an inch. They used a proving ring of 1000 lbs. capacity, as compared to 10 and 25 lbs. capacity proving rings used by us.

None of these approaches looked satisfactory to us. Hooghout's apparatus, ideal for larger samples prepared in a special way, was too coarse for our purposes. Testing the effectiveness of spring scales used by Fitts et al. and Martinson and Olmstead, we found that they lacked accuracy, sensitivity, and steadiness where small aggregates were concerned. None of the methods mentioned provided for determination of strain along with the stress, and none attempted to relate the values obtained to a stress/strain relationship which was necessary in our work.

Procedure

At the start of each run, a base reading for the strain-recording gauge was taken with the proving ring plate just touching the base plate. The ring assembly was raised and a soil aggregate inserted between the base plate and the proving ring plate. The ring assembly was lowered until the ring plate just touched the aggregate, and the ring dial was adjusted to zero reading. The reading on the strain gauge, when subtracted from the base reading (ring plate just touching the base) gave the aggregate diameter to .01 mm.

The load was now applied at the constant rate by turning the handle in the upper right of Fig. 3. At 10-second intervals the readings on the ring dial and strain gauge were recorded until the aggregate ruptured.

The rupture was usually indicated by a falling back of the ring dial pointer and the appearance of a crack oriented in the polar plane of the aggregate. Maximum value attained on the ring dial constituted the so-called "mth value" or the rupture stress value for a given aggregate. The apparatus was now cleaned, the broken aggregate being removed for determination of moisture content of a given subgroup.

Altogether thirty subgroups containing about 40 aggregates each^a were tested. With five sets of values, on the average, being recorded for each aggregate before it ruptured, an estimated 6,000 observations were made on air-dry aggregates alone, and about 1,000 observations were made on the aggregates at 15 atm. moisture tension. The procedure as outlined required two operators, one to apply the load and read the ring dial, the other to read the strain gauge and to record the results.

Calculations

Strain We have mentioned above that the initial reading on the strain gauge when subtracted from the base reading gave the aggregate diameter d . Subsequent readings on the strain gauge had to be corrected for the deflection of the proving ring, this deflection was given in inches by the ring dial. Strain for each set of readings was computed using Equation 10d derived from Equation 9 below (see Theory III, Equation 90)

$$\text{Strain} = \frac{\Delta d}{d} \quad (9)$$

^aMartinson and Olmstead (1949), in their study of crushing strength of selected Kansas soil, have found that taking 40 aggregates per plot gave statistically significant results.

Here d is the initial aggregate diameter and Δd is the change of the aggregate diameter due to the externally applied stress. If R_o is the initial reading on the strain gauge in cm. and R_b is the base reading on the strain gauge in cm. then we have

$$d = R_b - R_o \quad (10a)$$

Suppose that R_n is nth reading (not to be confused with the mth value) in cm. On a strain gauge at some time $[(0 + 10t)\text{seconds}]$ after the load is applied. Then the apparent change in aggregate diameter $\Delta d'$ is

$$\Delta d' = R_n - R_o \quad (10b)$$

Now $\Delta d'$ has to be corrected for ring deflection. Were it not for this deflection, $\Delta d'$ would be smaller by the amount $(R_{dn})C$, where R_{dn} is the ring dial reading, at some time $[(0 + 10t)\text{seconds}]$, in inches, and $C = 2.54$ is a conversion factor from inches to centimeters. Then for Δd , the actual change in aggregate diameter, we have

$$\Delta d = \Delta d' - (R_{dn})C \quad (10c)$$

Using Equations 10a, 10b and 10c we rewrite Equation 9 as

$$\text{Strain} = \frac{(R_n - R_o) - (R_{dn})C}{(R_b - R_o)} \quad (10d)$$

Equation 10d can now be programmed for a computer.

Numerically our strain values ranged from 0.01 to 0.20 cm. cm.⁻¹. The strain was computed in the manner outlined in Equation 10d above for each observation on every aggregate. This necessitated a very large number of computations which were done on the IBM 7070 computer of the Iowa State University Computation Center.

Stress The stress at the center of each aggregate, normal to the equatorial plane was calculated using Equation 13c derived from Equation 11 given by Sternberg and Rosenthal, (1952) (see Theory III, Equation 84).

$$\text{Stress} = 3F(14 + 5u)/2\pi r^2(7 + 5u) \quad (11)$$

For our purposes Equation 11 can be written

$$\text{Stress} = \frac{F}{Ad^2} \times \frac{6(14 + 5u)}{\pi(7 + 5u)} \quad (12)$$

where F is the force in dynes, A is the correction factor for the area of the equatorial plane (see Theory I, Table 8), u is the Poisson ratio^a, assumed to be 0.5 (see Theory III, Equation 84) and d is the aggregate polar diameter. Suppose we now take

$$C = \frac{6(14 + 5u)}{\pi(7 + 5u)} \quad (13a)$$

Furthermore we wish to write force F in terms of experimental quantities.

We recall that R_{dn} is the ring dial reading at some time $(0 + 10t)$ seconds .

To convert R_{dn} into dynes we use a factor R (where R is the reciprocal of the slope (1./slope) of the ring calibration curve) and a factor 980 (where 1 gram weight = 980 dynes). The load can then be written as a force F in dynes

$$F = R_{dn} \times R \times 980 \quad (13b)$$

Using Equations 12, 13a and 13b we can now write Equation 11 as

$$\text{Stress} = (R_{dn} \times R \times 980 \times C)/Ad^2 \quad (13c)$$

^aPoisson ratio is the ratio of transverseto longitudinal strain, estimated per unit length, produced by a longitudinal stress.

Equation 13c can now be programmed for a computer.

Numerically our stress values ranged from 0.1×10^6 to 100×10^6 dynes cm^{-2} . The stress was computed in the manner outlined in Equation 13c above for each observation on every aggregate.

This again necessitated a very large number of computations which were done on the IBM 7070 computer at the Iowa State University Computation Center.

Conclusions

We also used the IBM 7070 computer to obtain the required average values for stress and strain for pertinent size-density subgroups, as well as the analysis of variance over size and density groups for strength measurements for the air-dry condition. The data for aggregates at 15 atm. tension was so scanty (see discussion of Table 4) that no further purpose could be served by analyzing it statistically.

The apparatus and procedure outlined above, although tedious and slow, gave satisfactory results for aggregates in air-dry condition but as we have mentioned before, the apparatus employed was not sensitive enough to give satisfactory values for aggregates at 15 atm. moisture tension. The results for aggregates at 15 atm. moisture tension should therefore be interpreted in the light of these comments and viewed as trends rather than as adequate factual data.

One way to overcome the inherent drawbacks of the method employed by us here would be to make use of some type of electronic equipment which would be self-recording and easier to operate.

Experimental Design and Methods of Averaging

Gravity fractionation

Gravity fractionation is our basic separation method. The method yields four density groups (A, B, C, D) for Clarion s.l. and Webster c.l. and two density groups (A and B) for Luton si.c. Each density group is then subdivided by sieving into the three size classes (0.200-0.283 cm., 0.283-0.476 cm., and 0.476-0.800 cm.). An assembly of aggregates of any one density and size constitutes a size-density subgroup (SD), the basic unit of analyses.

A schematic illustration of the experimental design is presented in Table 2a. The size-density subgroups S_1D_1 , S_1D_2 , etc. in Table 2a represent measured values of carbon, clay or water stability obtained from two replications. Averaging down the columns of values of Table 2a yields an average value of a property tested for each density group. Averaging the rows of values of Table 2a yields an average value of a property tested for each size group. Averaging values for all size-density subgroups yields average values for a soil as a whole (Total).

Carbon, clay, and water stability analyses

Each Size density subgroup value represents an averaged measured value either of carbon, clay or of water stability for a large number of aggregates of a known density and size range. The original soil taken for analysis was initially subdivided into two lots. Each lot was subjected to a separate gravity fractionation. In this way we obtained two replications. The averages spoken of in this section, are the averages S_{ij} (Equation 14) of all determinations within both replications. In Appendix IV we present a statistical analysis of the measured values of carbon,

clay, water stability based on the following items: two replications, three size, and four density "treatments".

Table 2a. Experimental design for analysis of either the measured values of carbon content or of clay content and water stability of aggregates for various Size-density subgroups

	Density group			
	A	B	C	D
Size group	Size-density subgroup			
1	S_1D_1	S_1D_2	S_1D_3	S_1D_4
2	S_2D_1	S_2D_2	S_2D_3	S_2D_4
3	S_3D_1	S_3D_2	S_3D_3	S_3D_4
				TOTAL

Equation 14 below gives the average values of carbon, clay, or water stability for a Size-density subgroup.

$$S_iD_j = \left(\sum_{l=1}^n \text{Determinations} \right) / n \quad \begin{matrix} i = 1 \dots 3 \\ j = 1 \dots 4 \end{matrix} \quad (14)$$

For carbon, clay and water stability we have taken n to be all the values from two replications.

Equation 15 below gives the average value of a property for a Density group averaged over three Size groups.

$$\text{Density group} = \left(\sum_{i=1}^3 S_iD_j \right) / 3 \quad (15)$$

Equation 16 below gives the average value of a property for a Size group (averaged over four Density groups).

$$\text{Size group} = \left(\sum_{j=1}^4 S_i D_j \right) / 4 \quad (16)$$

Equation 17 below gives the average value of a property for the Soil as a whole (averaged over Size and Density groups).

$$\text{Total} = \left(\sum_{i=1}^3 \left(\sum_{j=1}^4 S_i D_j \right) \right) / 12 \quad (17)$$

In Table 2b a number of determinations comprising each group is listed for carbon, clay, and water stability analyses, of Clarion s.l., Webster c.l., and Luton si.c. aggregates. Poor duplication of carbon values for Webster c.l. is reflected by a large number of determinations that had to be performed before a satisfactory value could be obtained. In general the amount of soil available for carbon, clay, and water stability determinations in Size-density subgroups was small, limiting the number of determinations that could be made. Turning our attention now to the Luton si.c., we have noted before that it separated into two Density groups only. This is reflected by a lower number of determinations composing different groups.

Table 2b. Number of determinations (n) comprising each Size group, Density group, and Soil as a whole for carbon (C), clay, and water stability (WS) of Clarion s.l., Webster c.l., and Luton si.c.

Group	Clarion s.l.			Webster c.l.			Luton si.c.		
	C	clay	WS	C	clay	WS	C	clay	WS
Size									
1	8	7	7	19	7	7	4	4	4
2	8	8	8	16	7	7	4	4	4
3	8	6	6	16	7	7	4	4	4
Density									
A	6	5	5	14	6	6	6	6	6
B	6	5	5	15	6	6	6	6	6
C	6	6	6	12	4	4	-	-	-

Table 2b. Continued

Group	Clarion s.l.			Webster c.l.			Luton si.c.		
	C	clay	WS	C	clay	WS	C	clay	WS
Density									
D	6	5	5	10	5	5	-	-	-
Soil	24	21	21	51	21	21	12	12	12

Strength measurements

The average values of aggregate size and the average values of strength measurements are based on the values obtained for each aggregate individually. Since the aggregates were selected at random from large populations, it is felt that values for each individual aggregate constitute a replication for statistical purposes. The experimental design of size and strength measurement analyses is presented in Table 3, which is identical with Table 2a in so far as the presentation of the Size-density subgroups is concerned. The Table 3 differs from Table 2a in the nature and number of replications composing each Size-density subgroup SD. The values of carbon, clay, and water stability for each Size-density subgroup SD of Table 2a represent an average value of the parameter measured on a given subgroup as a whole. The values of aggregate size and the values of strength measurements for each Size-density subgroup SD in Table 3 represent an average value of the size or strength parameter measured for each aggregate individually. Where there were only two replications composing each Size-density subgroup SD of Table 2a, there are as many replications, composing each Size-density subgroup SD of Table 3, as there are aggregates tested.

For measurement of aggregate size only the first values for each

aggregate are averaged. For certain measurements (rupture stress Z_{zr} and rupture strain e_{zr})^a only the last, or mth, values are averaged. For still other measurements (average stress Z_z and average strain e_z)^b the average values for each individual aggregate are used.

Table 3. Schematic experimental design for size (polar diameter) rupture stress, Z_{zr} , rupture strain, e_{zr} , average stress, Z_z , and average strain, e_z , in equatorial plane

Size group	Density group			
	A	B	C	D
	Size-density subgroup			
1	$S_1 D_1$	$S_1 D_2$	$S_1 D_3$	$S_1 D_4$
	Aggregate number	Value		
	1	1st 2nd : mth or last	$\vdots \vdots$	$\vdots \vdots$
	2	1st 2nd : mth or last	$\vdots \vdots$	$\vdots \vdots$
	\vdots	\vdots	$\vdots \vdots$	$\vdots \vdots$
	n	1st 2nd : mth or last	$\vdots \vdots$	$\vdots \vdots$
2	$S_2 D_1$	$S_2 D_2$	$S_2 D_3$	$S_2 D_4$
	\vdots	\vdots	$\vdots \vdots$	$\vdots \vdots$
	\vdots	\vdots	$\vdots \vdots$	$\vdots \vdots$

^aThe values of Z_{zr} and e_{zr} are at the center of an aggregate on the equatorial plane.

^bSame as (a) above except for Z_z and e_z .

Table 3. Continued

Size group	Density group			
	A	B	C	D
	Size-density subgroup			
3	$S_3 D_1$	$S_3 D_2$	$S_3 D_3$	$S_3 D_4$
	\vdots	\vdots	\vdots	\vdots
	\vdots	\vdots	\vdots	\vdots
				TOTAL

Rupture stress, Z_{zr} , and rupture strain, e_{zr} Maximum values of stress and strain for any one aggregate are called "mth values". They are also the last values recorded since they are followed immediately by aggregate rupture.

Equation 18 gives average values of Z_{zr} and e_{zr} for Size-density subgroup $(S_i D_j)_m$

$$(S_i D_j)_m = \left(\sum_{l=1}^n \text{mth values} \right) / n \quad (18)$$

Here n is the total number of aggregates analyzed individually in each subgroup. For the purposes of statistical analysis each aggregate chosen at random from a large population represents a replication. General equations for the average Density group, average Size group and average for Soil as a whole (Total), have the same form as Equations 15, 16 and 17 before

$$\text{Density group} = \left(\sum_{i=1}^3 (S_i D_j)_m \right) / 3 \quad (19)$$

$$\text{Size group} = \left(\sum_{j=1}^4 (S_i D_j)_m \right) / 4 \quad (20)$$

$$\text{Total} = \left(\sum_{i=1}^3 \sum_{j=1}^4 (S_i D_j)_m \right) / 12 \quad (21)$$

Average stress, Z_z , and average strain, e_z Average stress and strain values represent averages based on averaging m values with each aggregate.

Equation 22 gives average values of Z_z and e_z for each Size-density subgroup $(S_i D_j)_{\text{avg}}$

$$(S_i D_j)_{\text{avg}} = \left(\sum_{l=1}^n \sum_{l=1}^m \text{values} \right) / (m \cdot n) \quad (22)$$

Here m is the number of values of stress or strain readings for each individual aggregate and n is the number of aggregates in each subgroup.

Equations for the average Density group, average Size group and average for Soil as a whole (Total) again have the same form as Equations 15, 16 and 17 before

$$\text{Density group} = \left(\sum_{i=1}^3 (S_i D_j)_{\text{avg}} \right) / 3 \quad (23)$$

$$\text{Size group} = \left(\sum_{j=1}^4 (S_i D_j)_{\text{avg}} \right) / 4 \quad (24)$$

$$\text{Total} = \left(\sum_{i=1}^3 \sum_{j=1}^4 (S_i D_j)_{\text{avg}} \right) / 12 \quad (25)$$

Aggregate size (polar diameter) Averaging techniques for aggregate size follow the same procedure as outlined in Equations 18, 19, 20 and 21 for Z_{zr} and e_{zr} , with the exception that it is the first value for size (and not the last) that is used in calculations.

Numerical size of groups In Table 4 the number of aggregates analyzed in each group is listed for all soils in air-dry condition, (1),

and at 15 atm. moisture tension, (2). The lower number of determinations on Luton si.c. again reflects the two Density groups only, as compared to four for Clarion s.l. and Webster c.l. Now turning our attention to aggregates at 15 atm. moisture tension, we see that we have two sets of figures. Figures in brackets represent a total number of aggregates tested in each subgroup. The other figures (not in brackets) represent the number of aggregates exhibiting a non-zero stress value.

Strength measurements at 15 atm. moisture tension are based on aggregates exhibiting non-zero stress value. Originally we had planned to use the same number of aggregates for strength measurements at 15 atm. moisture tension and in air-dry condition. The values of strength exhibited by aggregates at 15 atm. moisture tension were in general very low. It was felt, at the time of the measurements, that the apparatus used was not sensitive enough to measure the stress in these aggregates with any degree of accuracy and that no additional benefit could be obtained from testing a large number of these aggregates. Therefore the results obtained for strength measurements at 15 atm. moisture tension should be considered as trends and will be treated as such in the sections that follow.

For Size group 1 values of strength measurements gave inconsistent and zero readings. No purpose could be seen in including them in the overall presentation. Therefore values listed for strength of aggregates at 15 atm. moisture tension do not include any values of Size group 1.

Table 4. Number of aggregates (n) analyzed in each Size group, Density group, and Soil as a whole for strength and size parameters of Clarion s.l., Webster c.l., and Luton si.c. in air-dry condition (1) and at 15 atm. moisture tension (2), figures in brackets for (2) indicate total number of aggregates tested

Group	Strength and size parameters					
	Clarion s.l.		Webster c.l.		Luton si.c.	
	(1)	(2)	(1)	(2)	(1)	(2)
Size						
1	165	----	156	----	81	----
2	164	39[72]	163	21[76]	84	21[29]
3	164	65[84]	160	32[63]	93	23[38]
Density						
A	130	41[49]	119	4[35]	125	19[30]
B	126	22[36]	121	17[37]	135	25[37]
C	122	21[38]	120	6[28]	--	----
D	115	20[33]	119	26[39]	--	----
Soil	493	104[156]	479	53[139]	258	44[67]

Conclusions

In concluding we can see from Table 2b and Table 4 that actual results, presented by us elsewhere, (see results section Appendix I, Appendix II and Appendix III) are an average of a large number of individual determinations. When taken individually, the value of a property may vary from determination to determination, but in a statistical sense large number of determinations for Size and Density groups and even more so for a Soil as a whole should closely approximate a true value. This observation is particularly applicable to the strength measurements where large differences between the aggregates within the same group are often observed. It is felt that the results obtained in this study for Clarion s.l., Webster c.l. and Luton si.c. soils are reliable (in the statistical sense) and describe

satisfactorily the differences or similarities that exist between respective Size groups, between respective Density groups, and between Soils as a whole.

THEORY I

Shape of Soil Aggregates

Theoretical volume V_c

Spheroidal aggregates are characteristic of many surface soils, particularly those high in carbon. The term usually applies to the granular soil aggregates not greater than 1.27 cm. in diameter, (Lyon et al., 1952, p. 66). Suppose we assume that the aggregates tested are perfect spheres. Then we define a theoretical (computed) aggregate volume V_c by

$$V_c = \frac{\pi}{6} d_e^3 \quad (26)$$

where d_e is the aggregate equatorial diameter taken as a midpoint of our respective size groups. Thus d_e defines V_c . For 0.200-0.283 cm. aggregates d_e would be 0.242; for 0.283-0.476 cm. aggregates d_e would be 0.380 cm.; and for 0.476-0.800 cm. aggregates d_e would be 0.638 cm.

Experimental volume V_e

The experimental volume (V_e) is computed as follows: 400 aggregates of each size for every soil are counted, weighed, and the average weight per aggregate W_A is computed. From gravity fractionation data we compute an adjusted specific aggregate volume $(V_s)_i$ for each size group of every soil defined by

$$(V_s)_i = \left(\sum_{j=1}^n (\% \text{ Aggs.} \times 1/D)_{ij} \right) / 100 \quad (27)$$

Here $(\% \text{ Aggs.})_{ij}$ refers to the percentage of aggregates of a given Size group that compose a given Size-density subgroup; D_{ij} refers to the respective subgroup density; and the summation is accomplished over n densities

for a given Size group. In Table 5 we illustrate this calculation by an example for Clarion s.l. aggregates (0.200-0.283 cm. in diameter).

Table 5. Adjusted specific volume (Equation 27) of Clarion s.l. aggregates 0.200-0.283 cm. in diameter

1 Size group	2 Density group	3 j	4 % Aggregates	5 1/D cm ³ .g. ⁻¹	6 (4) x (5)
i=1	A	1	15.1	0.568	8.58
i=1	B	2	14.2	0.508	9.96
i=1	C	3	26.7	0.556	7.90
i=1	D	4	19.6	0.521	13.91
i=1	Other	5	0.9	0.500	0.45
i=1	Stones	6	23.7	0.465	11.02
SUM			100.2		51.82

$V_s \text{ adjusted} = 51.82/100 = 0.5182 \text{ cm}^3/\text{g}.$

If we let V_e denote an average experimentally determined volume of an aggregate of the average weight W_A , then we have

$$V_e = V_s \times W_A \quad (28)$$

where V_e will be in cm^3 in our units. The values of d_e , V_c , and V_e are given in Table 6 for each size group of every soil, and the plot of d_e against V_c and V_e for Clarion s.l., Webster c.l., and Luton si.c. are presented in Fig. 4, Fig. 5 and Fig. 6, respectively.

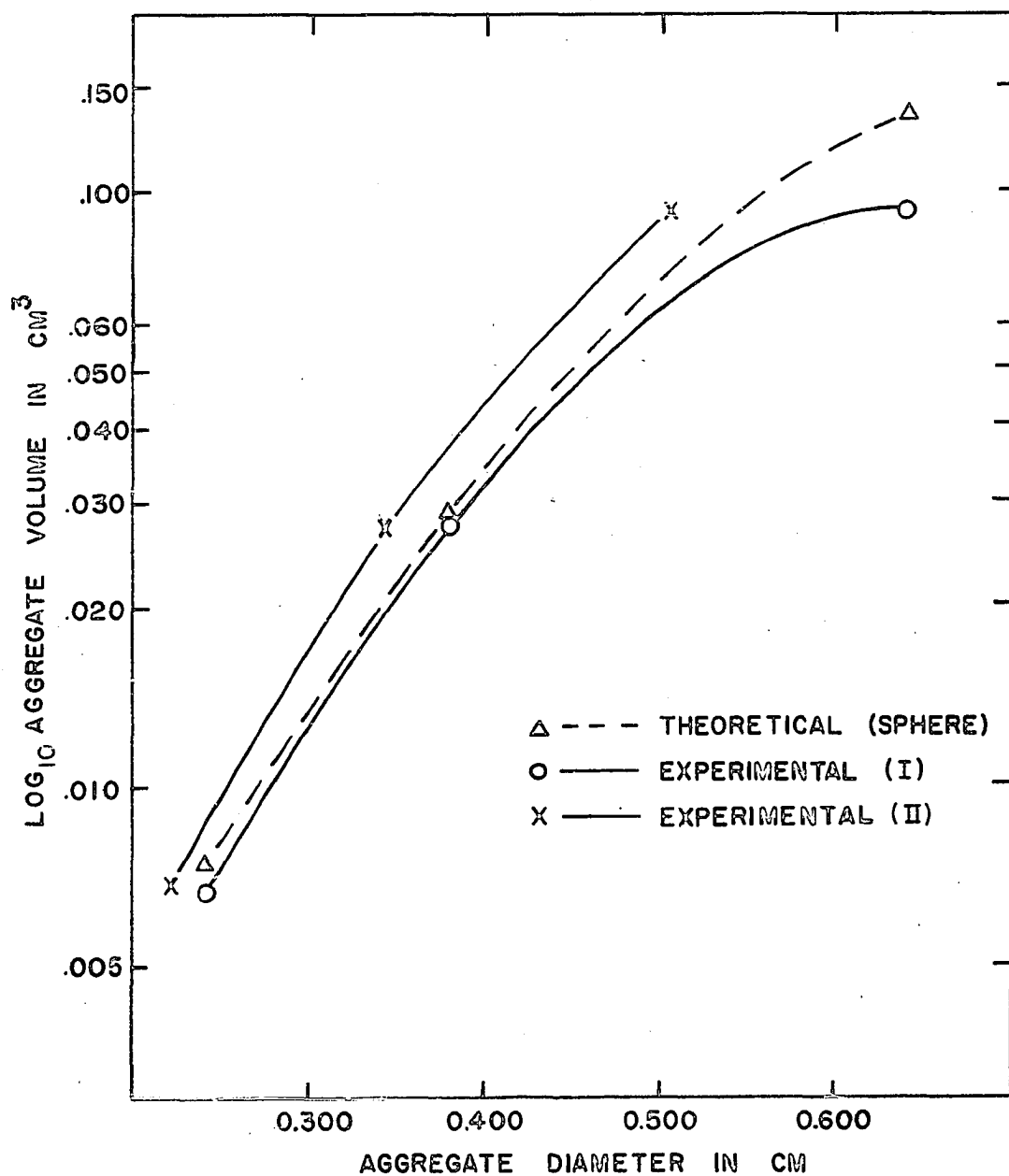


Fig. 4. Theoretical aggregate volume V_c as a function of sphere diameter [Theoretical (sphere)] compared with experimental aggregate volume V_e as a function of equatorial [Experimental (I)] diameter d_e and polar [Experimental (II)] diameter for Clarion s.l. aggregates in air-dry condition

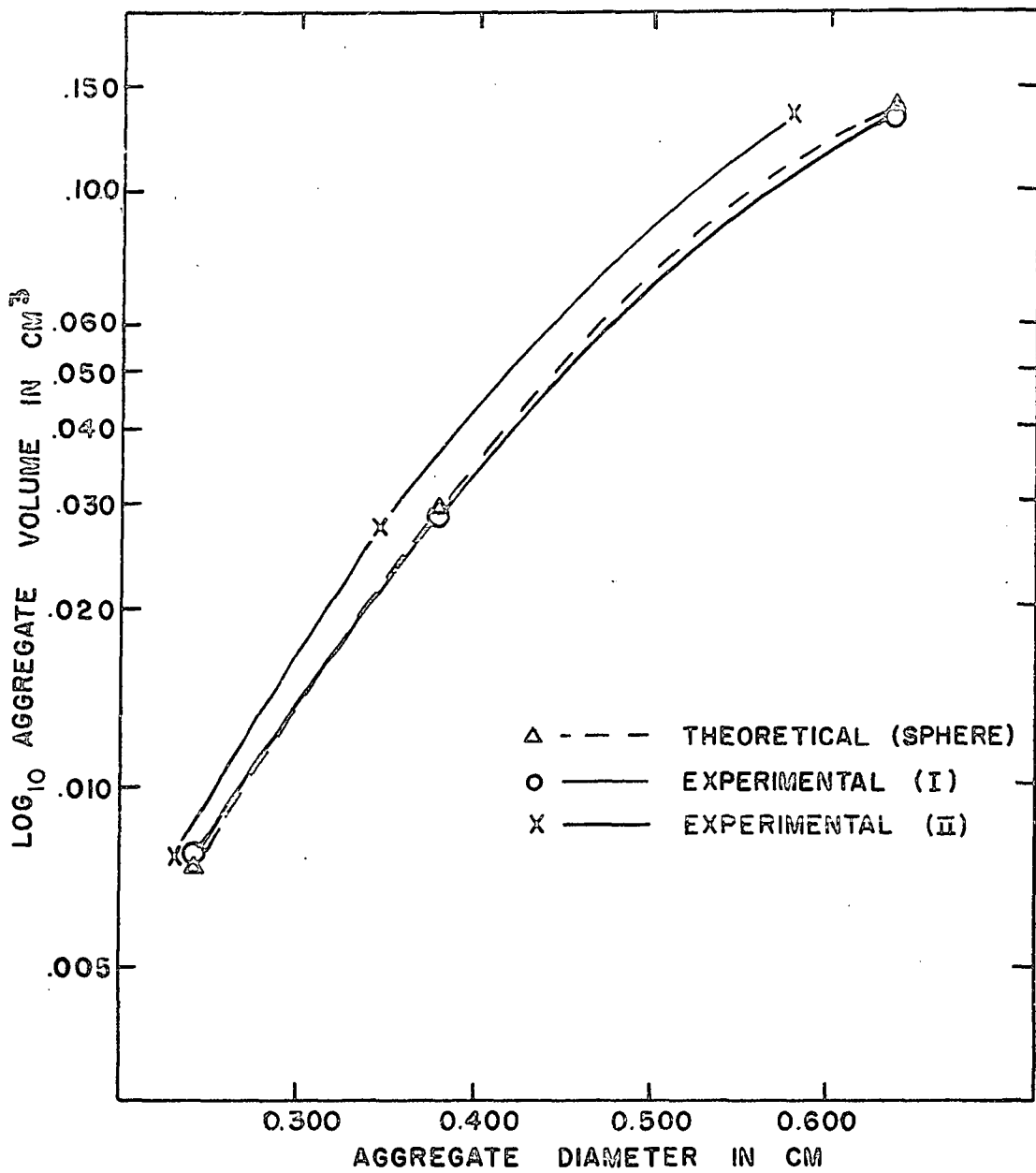


Fig. 5. Same as Fig. 4 except for Webster c.l. aggregates

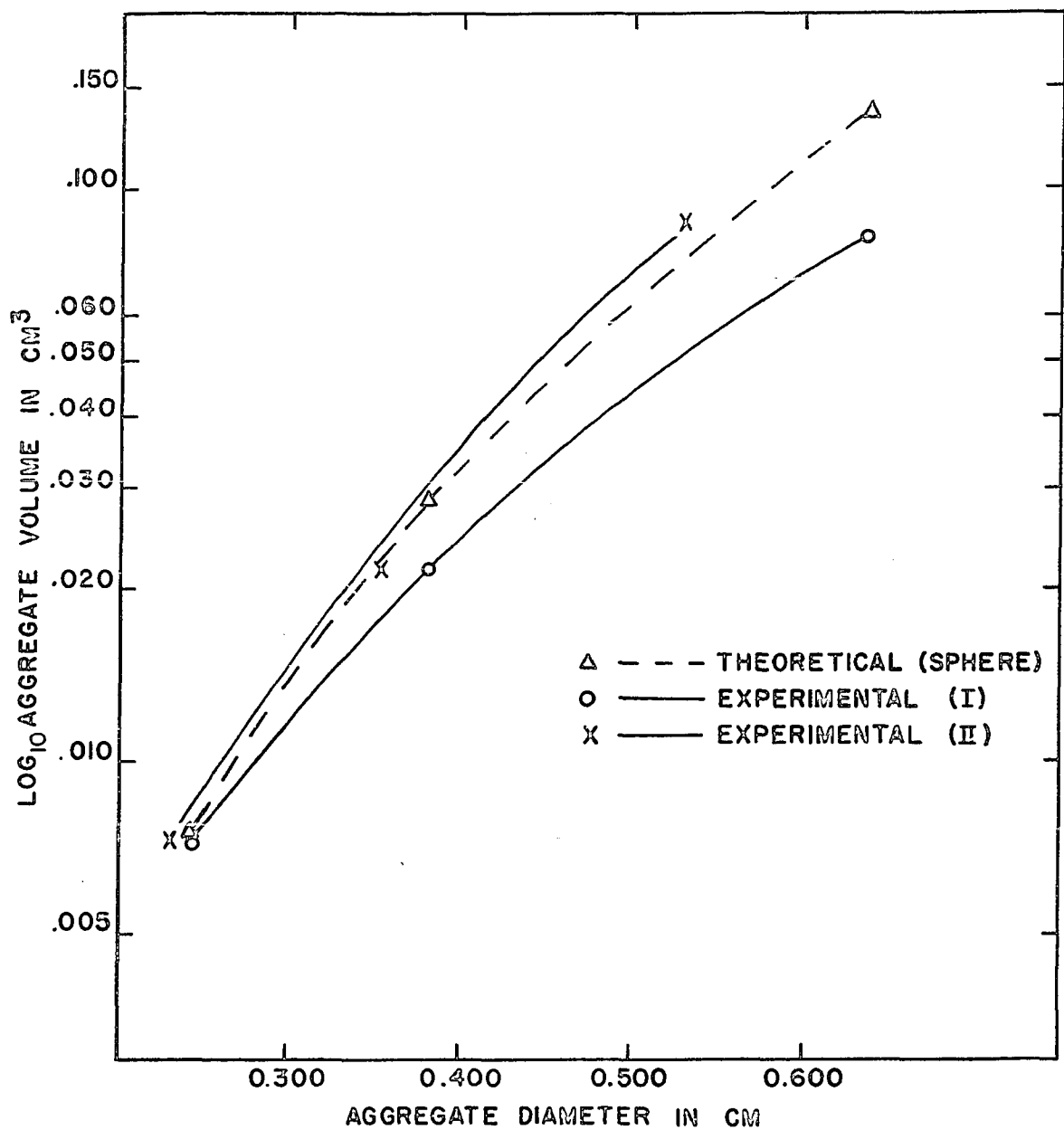


Fig. 6. Same as Fig. 4 except for Luton si.c. aggregates

Table 6. Experimental (I) values of aggregate volume V_e for Clarion s.l., Webster c.l., and Luton si.c. are compared with theoretical values of aggregate volume V_c when aggregate diameter in the equatorial plane d_e is taken as a size parameter

Size group	d_e cm.	V_c	Clarion s.l. V_e	Webster c.l. V_e	Luton si.c. V_e
			cm. ³		
1	0.242	0.0073	0.0067	0.0078	0.0071
2	0.380	0.0286	0.0276	0.0271	0.0219
3	0.638	0.1360	0.0910	0.1352	0.0835

Correction factor

For the purposes of calculations in Table 6 and also for the theoretical curves in Fig. 4, Fig. 5, and Fig. 6, we have chosen d_e (midpoint of a Size group) to represent an average aggregate diameter in the equatorial plane. We reasoned that during a sieving operation aggregates would tend to orient themselves with the longer axis, if a longer axis were to exist, parallel to the screen surface. From data presented in Table 6 and Fig. 4, Fig. 5, and Fig. 6, we can see at a glance that theoretical volume of aggregates was greater than the experimental volume for Clarion s.l. and Luton si.c. and remained about the same for Webster c.l. We might conclude that the average diameter, d_e , chosen was too large.

During the strength measurements we have obtained a polar diameter, d_p , of aggregates. We might suppose that d_p gives a shorter axis of an aggregate. Using d_p as a parameter for experimental volume, V_e we can see from the data in Table 7 and the curves (Experimental II) in Fig. 4, Fig. 5, and Fig. 6 that for Clarion s.l. and Webster c.l. the theoretical volume of

Table 7. Experimental (II) values of aggregate volume V_e for Clarion s.l., Webster c.l., and Luton si.c. are compared with theoretical values of aggregate volume V_c when aggregate diameter in polar plane d_p is taken as a size parameter

Soil	Size group	d_p cm.	V_c	V_e
			cm. ³	
Clarion s.l.	1	0.227	0.0061	0.0067
	2	0.347	0.0219	0.0276
	3	0.507	0.0682	0.0910
Webster c.l.	1	0.233	0.0066	0.0078
	2	0.343	0.0211	0.0271
	3	0.579	0.1016	0.1352
Luton si.c.	1	0.231	0.0065	0.0071
	2	0.353	0.0230	0.0219
	3	0.532	0.0788	0.0835

aggregates was smaller than the experimental volume. On the other hand for Luton si.c. the theoretical and experimental volumes remained about the same. If the results given by computations and curves based on d_e and d_p were identical we could have concluded that aggregates are perfect spheres. This condition is approached as the size of the aggregates decreases and can be seen readily from curves in Fig. 4, Fig. 5, and Fig. 6.

In view of the above discussion, aggregates should be considered to be spheroids rather than spheres. Then the aggregate volume (theoretical) will be given by

$$V_c = \frac{\pi}{6} d_e d_p^2 \quad (29)$$

where d_e is the longer and d_p the shorter aggregate axis^a. For the purposes of this dissertation in our theoretical treatment we assume the aggregates to be spheres, but in the computation of stress in the equatorial plane we introduce a correction factor A. The correction factor A is derived from Equations 26, 29, and the experimental value of aggregate volume. Suppose we write Equation 26 as

$$V_e = \frac{\pi}{6} d_e^3 \frac{V_e}{V_c} \quad (30)$$

in Equation 29 let $d_p = (V_e/V_c)^{0.5} d_e$, then from Equations 29 and 30

$$V_c' = V_e \quad (31)$$

hence

$$d_e = (V_e/V_c)^{-0.5} d_p \quad (32)$$

and

$$A = (V_e/V_c)^{-0.5} \quad (33)$$

Values of A are given in Table 8 for each Size group of every soil used.

^aStrictly speaking, the fact that one of the experimental curves (Experimental I) for Webster c.l. and one for Luton si.c. (Experimental II) did coincide with a theoretical sphere curves (see Fig. 5 and Fig. 6), could indicate the presence of three unequal diameters. Then Equation 29 would be written $V_c' = \frac{\pi}{6} a b c$, where a, b and c are three orthogonal aggregate diameters. If b- and c-diameters happened to be of such a length that their produce was equal to a^2 , a-diameter would behave as if it were an equivalent diameter of a sphere.

Table 8. Correction factor A for the area of equatorial plane

Size group	Clarion s.l. A	Webster c.l. A	Luton si.c. A
1	1.044	1.069	1.014
2	1.018	1.027	1.143
3	1.223	1.001	1.276

THEORY II

Gravity Fractionation of Soil Aggregates

Introduction

Before presenting the mathematical theory of gravity fractionation we shall review the method briefly and shall give a literature review on soil density methods.

Let us suppose we have a single soil aggregate of unknown bulk density. In the first step we saturate it with a liquid B of known density k_2 and determine the densities of the fractionation mixture at which it will float and at which it will sink (two values). In the second step the aggregate is saturated with liquid A of known density k_1 such that $k_1 < k_2$ and the densities of fractionating mixture at which it will float and at which it will sink are again determined (two more values). From these four values we are in a position to determine the range of aggregate bulk density.

The gravity fractionation is a mineralogical technique which aims to divide sand or gravel into fractions of known density. The concept of the gravity fractionation is simple. A material will float if its density is less than the density of a separation liquid, and it will sink if its density happens to be more than that of the separation liquid. This technique has been developed by the ore prospectors and has been applied extensively in the mineralogical studies of soil (Nota and Bakker, 1960; De Leenheer, 1944; and De Leenheer, 1961a).

Pearson and Truog (1937) describe fractionation of minerals, silt, and clay in heavy liquids; Krumbein and Pettijohn (1938) have applied it to the fractionation of silts. Densimetric separation of organic matter

has been carried out by Turc (1949), Henin and Turc (1950), Lein (1940), and more recently by Monnier et al. (1962).

The question of porosity and its effect upon the fractionation does not arise when we are dealing with "solid" particles; it does, however, arise when we turn our attention to porous fractions of sand, silt, clay, and organic matter. Sand, silt, and clay are normally considered as size subdivisions, Baver (1956, p. 10-12). If these fractional subdivisions are composed of solid mineral particles, i.e. quartz, their porosity would essentially be zero. If, on the other hand, they are an aggregate of still smaller particles, they certainly would exhibit porosity which would affect their behavior and give erroneous results during standard gravity fractionation. Effect of porosity has gone unnoticed and unmentioned by researches applying gravity fractionation to sand, silt, and clay particles which could have been porous, and to organic matter which definitely was porous.

Numerous methods have been developed for measuring of bulk density. Some research workers have measured the bulk density of soil in place by weighing a regular sample and determining the volume it occupied, (Curry, 1931; Coile, 1936; Lutz, 1947). More recently bulk density in the field has been measured with a surface radiation probe, (Phillips et al., 1960; Horton, 1962).

Haines (1923) determined the volume of soil clods by immersing them in mercury and assuming that no mercury penetrated the aggregate pores. This assumption is not fully justified, since mercury will penetrate to a certain extent the larger pores in the aggregates forming the clods, to give erroneous results, (Kruger, 1958; Kuipers, 1961).

Shaw (1917), and Perry (1942) covered the clod surface with a protective layer of wax and determined the bulk density by immersion in water or solutions of ZnCl_2 . Sideri (1936) painted the outside of small clods with collodion to prevent slaking and improve stability in his studies of swelling. Chepil (1950) determined the bulk density of dry soil aggregates by comparing a known weight and volume of aggregates with a weight and volume of sand grains of the "same" size and shape. We will discuss Chepil's work further in conjunction with our results.

Russell and Balcerak (1944), and Russell (1948), modified Boyanoff's method^a and proposed the determination of the bulk density of soil clods (100-150 g.) simply by weighing them before and after wetting with a non-polar liquid (kerosene), under standard conditions.

McIntyre and Stirk (1954) have developed a method for determination of the bulk density of soil aggregates greater than 0.200 cm. in diameter. The method consists of evacuating and wetting of the aggregates with a non-polar liquid (kerosene). Aggregates are then drained at a standard tension and their volume is determined by displacement in kerosene. Results obtained have shown that the bulk density of aggregates is measured within 0.03 g. cm.^{-3} (about 2% error).

Grossman (1959) and Kuipers (1961) used McIntyre and Stirk method for the determination of bulk density and porosity of aggregates with satisfactory results.

None of the methods mentioned looked satisfactory for our purposes.

^aNo reference to original work of Boyanoff is listed by the authors.

Since we needed aggregates for further tests, coating them with wax was out of the question. Bulk density values of soil in place or average density values of a group of aggregates would not predict the density of any one individual aggregate.

Use of polar liquids for fractionation

For the purposes of this investigation we were anxious to separate aggregates into density groups with known density ranges, and we were also anxious to be able to run further tests on the same aggregates. It was at this stage that the idea of filling aggregate pores with a pore liquid of known density while accomplishing a gravity fractionation in a heavy liquid bromoform-nitromethane mixture suggested itself. In reviewing the possibilities of this approach, one serious drawback at once became apparent. This drawback can best be illustrated by an example.

Let us suppose that we have a soil aggregate with a bulk density of 1.70 g. cm.^{-3} . Let us further suppose that it has a porosity of 40%; then if we were to saturate it with a pore liquid whose density is 1.60 g. cm.^{-3} , its composite density would become $1.70 + (0.40 \times 1.60) = 2.34 \text{ g. cm.}^{-3}$. Suppose we also have another aggregate, its bulk density is 1.86 g. cm.^{-3} , and its porosity is 30%. This one also would have $1.86 + (0.30 \times 1.60) = 2.34 \text{ g. cm.}^{-3}$ as a composite density and both would sink in a separation mixture whose density was less than 2.34 g. cm.^{-3} .

One way of overcoming this difficulty is to determine composite density two times, the first time using a pore liquid of density 1.60 g. cm.^{-3} which would give a value 2.34 g. cm.^{-3} for both aggregates, and the second time using a pore liquid of some other density. If, the second time, we were to use a liquid with a density of 0.70 g. cm.^{-3} then we would get

1.98 and 2.07 g. cm.⁻³ as composite density values for the two aggregates respectively using now a separation mixture of 2.00 g. cm.⁻³ density, we would have the former one float and the latter one sink. We will show later on in this section that on the basis of two sets of values for composite density of an aggregate we can determine uniquely the bulk density of a porous aggregate.

Criteria of pore liquid selection

There are three criteria governing the selection of an ideal pore liquid for gravity fractionation of porous soil aggregates; the liquid must be readily driven off; the liquid must be non-polar; and the liquid must be immiscible with the liquid in which gravity fractionation is to take place.

Liquid to be readily driven off From the practical standpoint we need a liquid that can be driven off by a moderate heating, at say 110°C., without leaving a residue. Since we have to use two liquids of different densities to effect the true separation of aggregates, it would be very laborious and time consuming if we were to have a long drying cycle between the two fractionations. If we consider ΔH_{298}^V (heat of vaporization at 25°C.) as an index of the above requirement, we can see at a glance from Table 9 that pore liquids listed have ΔH_{298}^V comparable to that of water.

Table 9. Selected properties of fractionation liquids and pore liquids; properties of water are listed for comparison^a

Liquid	Formula	Mol.wt. g.mole ⁻¹	Density g.cm. ⁻³	Dipole moment esu. x10 ⁻¹⁸	ΔH_{298}^V	Vapor pressure at 25°C.; mm of Hg
Bromoform	CHBr ₃	253	2.89	-	-	6
Nitromethane	CH ₃ NO ₂	61	1.13	-	-	34
Isooctane	C ₈ H ₁₈	114	0.70	0	8.40	49
Carbon tetra- chloride	CCl ₄	154	1.60	0	7.81	115
Perfluoro- kerosene	C ₁₂ F ₂₆	645	2.02	0	11.40	< 1
Water	H ₂ O	18	1.00	1.85	9.70	24

^aMol. wt., density and dipole moments are taken from Hodgman (1962); ΔH_{298}^V values are from Hildebrand and Scott (1950 and 1962); properties for C₁₂F₂₆ are estimated from parameters given by Scott (1948); values of vapor pressure are estimated from Jordan (1954).

Liquid to be non-polar Russell (1934) found that clays interact with water and organic liquids containing a polar group by causing a contraction in the volume of a liquid. The interpretation was that cations can orient polar molecules of a dispersion liquid in direct proportion to their surface density of charge. A similar property is also possessed by the free negative charges on a clay particle. On drying, when most of the dispersion liquid has been removed, strongly oriented molecules of polar dispersion liquid bind the negative charges on two clay particles to the cations between them thereby inducing a formation of aggregates. Russell

found no such interaction for non-polar liquids.

Winterkorn (1936) has shown that the swelling of expanding lattice type clays varies directly as the dielectric constant of the polar liquid employed. Waidehlich (1960), working with non-expanding lattice clays, concluded that compression and expansion indices vary as the dipole moment of the liquid used. Thus the use of polar liquid could seriously alter the properties of soil aggregates. It is also likely that a large number of aggregates would break down due to the swelling stresses developed; surviving aggregates could become much stronger on drying. The use of non-polar liquids exclusively would overcome these difficulties; aggregates would remain stable and would be easy to handle even when "wet" during the fractionation. Carbon tetrachloride and isooctane were the non-polar liquids chosen for filling the pores of aggregates.

To see whether or not the use of the carbon tetrachloride or isooctane would change physical properties of aggregates, two physical tests were made: water stability and rupture stress. Three soils were tested.

In Table 10 results for water stability and rupture stress of treated and non-treated aggregates of Clarion s.l., Webster c.l., and Luton si.c. soils are given. Water stability is expressed in terms of the change in mean weight diameter (CMWD) (De Leenheer, 1959), and rupture stress is in dynes cm^{-2} . Treated samples consisted of two groups of randomly selected aggregates which received the same treatment as the rest of the aggregates used in our subsequent studies. Non-treated aggregates also consisted of two groups of aggregates chosen in the same manner as before but not subjected to the influence of liquids used in the gravity fractionation procedures.

Table 10. Average change of mean weight diameter (CMWD) and rupture stress on treated and non-treated aggregates of Clarion s.l., Webster c.l., and Luton si.c. soils. Null hypothesis: "Treated" = "Untreated" is accepted; t values are not significant at 10% level

Soil	CMWD		Rupture stress		t
	Treated	Non-treated	Treated	Non-treated	
	mm.		$\times 10^6$	dyn.cm.^{-2}	
Clarion s.l.	1.37	1.40	9.09 (5.60) ^a	6.61	1.13
Webster c.l.	2.08	1.73 ^b	12.46 (13.64)	12.41	0.54
Luton si.c.	1.46	1.41	37.18 (41.04)	45.11	1.16

^aValues in parentheses give an average value of rupture stress for about 500 aggregates of Clarion and Webster, 250 aggregates of Luton.

^bAn average difference of 0.35 mm. in CMWD for Webster c.l. between treated and non-treated samples is less than the average difference (0.42) within treated and non-treated samples.

Some of the discrepancies observed in Table 10 arise as a result of the small number of aggregates tested. The two groups (treated and non-treated) tested were not significantly different from one another even at the 10 percent level. Since the differences were not significant and only a limited amount of soil was available, further tests with larger samples were not conducted.

Liquid to be immiscible Excellent treatment of solubility of non-electrolytes in general and liquid solubility in particular is presented by Hildebrand and Scott (1950), and in a more recent work by the same authors, Hildebrand and Scott (1962). Solubility parameters (δ) are

listed in the Appendix of both references where

$$\delta = \left(-\frac{E}{V}\right)^{1/2} \quad (34)$$

Here V is the molal volume of the liquid and $(-E)$ is the energy of vaporization to gas at zero pressure. Both E and V change with temperature. When accurate values of the heat of vaporization (ΔH^V) are available for a desired temperature, they represent one of the best methods of calculating δ . At low vapor pressures $(-E)$ can be replaced by the energy of vaporization (ΔE^V) which in turn can be written as $(\Delta H^V - RT)$. Then δ is given by

$$\delta \cong \left(\frac{\Delta H^V - RT}{V}\right)^{1/2} \quad (35)$$

Let us suppose we have a binary solution. At the critical solution temperature (T_c) (with a = activity, and x = mole fraction), $\partial a/\partial x = 0$ and $\partial a^2/\partial x^2 = 0$ for both components, then a general equation can be written (Hildebrand, 1950, p. 253)

$$RT_c = \frac{2X_1X_2V_1^2V_2^2}{(X_1V_1 + X_2V_2)^3} (\delta_1 - \delta_2)^2 \quad (36)$$

Here V_1 and V_2 are molal volumes. When $V_1 \cong V_2$, we can write, assuming $X_1 = X_2 = 1/2$

$$2RT_c = V_{avg} (\delta_1 - \delta_2)^2 \quad (37)$$

and V_{avg} is the average molal volume of the two components.

An approximate criterion of whether the solution will break into two phases is the value of T_c . For the purposes of this discussion values of $T_c < 298^\circ K$ will mean that the pore liquid is miscible with the fractionation

liquid, and the values of $T_c > 298^\circ\text{K}$ will signify separation into two phases, i.e., that the pore liquid is not miscible with the fractionation liquid.

As a basic fractionation liquid we have used bromoform, diluting it to the desired density with nitromethane. Isooctane and carbon tetrachloride were used as pore liquids (1) and (2) respectively. In Table 9 we list some of the properties of these liquids, along with the properties of an "ideal" pore liquid - perfluorokerosene, and properties of water for comparison. With the exception of carbon tetrachloride all liquids have a relatively low vapor pressure at 25°C . This characteristic ensures little change in density resulting from evaporation during fractionation. Values of ΔH_{298}^V listed, as mentioned earlier, describe the heat requirement for pore liquids. We note that with the exception of the value for perfluorokerosene, which is higher, the other two values are lower than the corresponding value for water. Density, molecular weight, and formula complete, in Table 9, the description of the liquids used.

In Table 11 we have computed the critical solution temperature using Equations 36 and 37 from the values of mole fraction X , molal volume V and solubility parameters δ .

The mole fraction is estimated as follows. Separation container had a capacity of 300 cm^3 . On the average, 200 g. of soil aggregates were fractionated at any one time. Average density of soil used was 1.90 g. cm^{-3} , average porosity was 30% . Therefore 200 g. soil has approximately 30 cm^3 of pore space. Let k_1 = density of pore liquid and k_F = density of fractionation liquid; also let W_1 = Mol. Wt. of pore liquid and W_F = Mol. Wt. of fractionation liquid. Then mole fraction of pore liquid x_1 in moles

mole⁻¹ is given by

$$X_1 = \frac{30k_1/W_1}{(30k_1/W_1) + (300k_F/W_F)} \quad (38)$$

and the mole fraction of fractionating liquid in moles mole⁻¹ (X_F or X_2) is given by

$$X_2 = 1 - X_1 \quad (39)$$

In Table 11 the molal volume V and solubility parameters δ are from Hildebrand and Scott (1950 and 1962), values of V and δ for perfluorokerosene are from Scott (1948).

Table 11. Critical solution temperature T_c computed from the values of mole fraction x , molal volume V , and solubility parameter δ (see text).

Liquid	X moles	V cm ³ .mole ⁻¹	δ cal. ^{1/2} cm. ^{-3/2}	T_c deg K°	Equation
Bromoform	0.90	88	10.5	87	37
Carb. tet.	0.10	97	8.6		
Bromoform	0.94	88	10.5	179	36
Isooctane	0.06	166	6.9		
Nitromethane	0.95	54	12.6	138	36
Carb. tet.	0.05	97	8.6		
Nitromethane	0.97	54	12.6	423	36
Isooctane	0.03	166	6.9		
Bromoform	0.97	88	10.5	619	37
Perfluorokerosene	0.03	320	5.8		

We can see at a glance in Table 11 that carbon tetrachloride is soluble both in bromoform and nitromethane; isooctane is soluble in bromoform and not soluble in nitromethane. It was found by experiment, however, that

isooctane is soluble in the mixture of bromoform and nitromethane used by us in the gravity fractionation. We would expect, on the basis of values listed in Table 11, that isooctane would be somewhat less soluble than carbon tetrachloride.

A value of T_c for perfluorokerosene in bromoform is given as an illustration. Since $619 > 298$, we would expect perfluorokerosene to be completely immiscible with bromoform and even more so with nitromethane. Perfluorokerosene would be an ideal pore-filling liquid; however, its prohibitive cost (\$25.00 for 10 g.) precludes its extensive use.

Since both pore liquids used by us were soluble in the fractionation mixture, the separation had to be performed rapidly to counteract any errors that might arise as a result of mixing.

For aggregates saturated with carbon tetrachloride we have allowed 30 seconds from the moment of immersion to the moment when the fraction that floated was separated from the fraction that sank in bromoform-nitromethane mixture of known density. For the aggregates saturated with isooctane the fraction that floated was separated 15 seconds after immersion. These time intervals were selected as a result of visual observation of the time it took the aggregates, which started sinking immediately after immersion, to sink below the level of the separation screen (see Methods). The shorter time allowed for isooctane-saturated aggregates reflects a faster rate of settling. Since both carbon tetrachloride and isooctane were miscible with bromoform-nitromethane mixture, we might suppose that a certain amount of mixing, especially at the surface of soil aggregates could have taken place. Because of its low density value (0.69 g. cm.^{-3}), isooctane combined with a bromoform-nitromethane mixture would tend to lower the density in the

immediate neighborhood of an aggregate more than carbon tetrachloride would. This in turn would cause the aggregates saturated with isooctane to settle faster. We may also assume that because of its low density any replacement of isooctane with bromoform would tend to raise the apparent density of an aggregate more than a corresponding replacement of carbon tetrachloride. This would also contribute to a faster rate of settling.

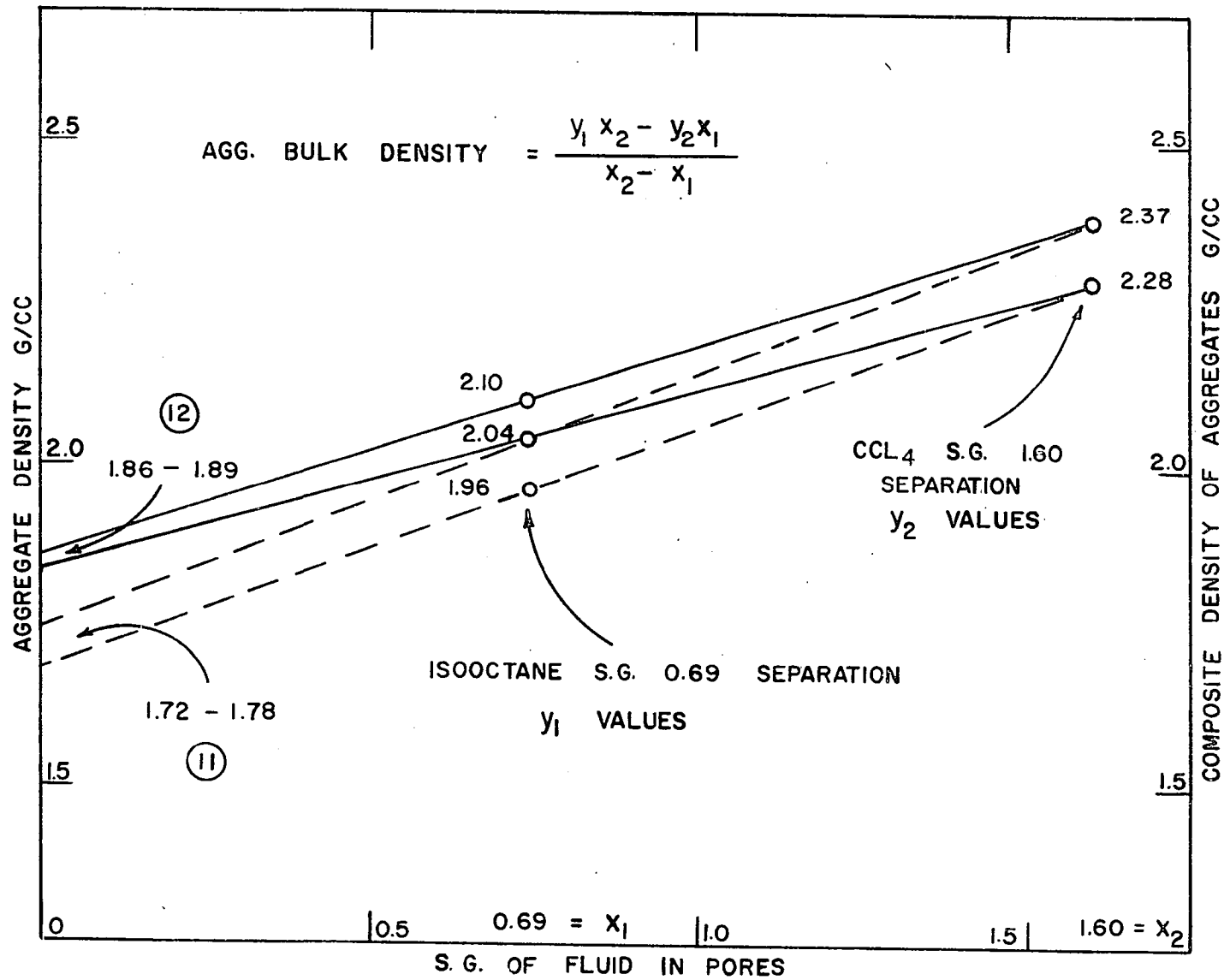
Computation of aggregate bulk density

Straight line equation We wish to illustrate graphically in Fig. 7 how the bulk density range is obtained for aggregates within a given density group. First we need to recall our discussion of Fig. 1 (see Methods: Gravity Fractionation).

In particular we recall that the composite density range (the so-called y_2 -values) for carbon tetrachloride filled aggregates (soil + CCl_4) of encircled group 1 was 2.28-2.37 g. cm.⁻³. In Fig. 7 the vertical scale on the right hand side (the y-scale) gives the composite density of aggregates and the horizontal scale (the x-scale) gives the S.G. of pore filling fluid. We now plot (see Fig. 7) the y-values corresponding to the aggregate composite density of 2.37 and 2.28 g. cm.⁻³ (the y_2 -values) on the vertical scale against the x-value corresponding to the carbon tetrachloride S.G. 1.60 (x_2 -value) on the horizontal scale.

We also recall that encircled group 1 of Fig. 1, after the pore filling carbon tetrachloride was removed and the pores were refilled with isooctane, separated into two groups 11 and 12 whose composite density (soil + C_8H_{18}) ranges (the so-called y_1 -values) were 1.96-2.04 g. cm.⁻³ and 2.04-2.10 g. cm.⁻³, respectively. We now plot (see Fig. 7) the y-values corresponding to the aggregate composite density of 1.96, 2.04 and 2.10 g. cm.⁻³

Fig. 7. Illustration of graphical computation of aggregate bulk density from gravity fractionation data, see text



(the y_1 -values) on the vertical scale against the x -value corresponding to the isooctane S.G. 0.69 (x_1 -value) on the horizontal scale.

The equation of a line through the points x_1, y_1 , i.e., 0.69, 2.10, and x_2, y_2 , i.e., 1.60, 2.37 is

$$\frac{y - y_1}{x - x_1} = \frac{y_2 - y_1}{x_2 - x_1} \quad (40)$$

or

$$y = y_1 + \frac{y_2 - y_1}{x_2 - x_1} (x - x_1) \quad (41)$$

at $x = 0$ when the aggregate pores are filled with a fluid of S.G. 0.00, i.e. air, the composite density y , (soil + air), is equal to aggregate bulk density and is given by

$$y = \frac{y_1 x_2 - y_2 x_1}{x_2 - x_1} \quad (42)$$

We now draw straight lines through the points 2.37, 2.10 and 2.10, 2.04 of Fig. 7. On the left hand side of Fig. 7 the vertical scale (y -axis at $x = 0$) constitutes the aggregate bulk density scale. The points where the lines drawn through 2.37, 2.10 and 2.10, 2.04 intersect the y -axis furnish graphically the density range 1.86-1.89 g. cm.⁻³ for the group 12. Similarly the points where the lines drawn through 2.28, 2.04 and 2.28, 1.96 intersect the y -axis furnish graphically the density range of 1.72-1.79 g. cm.⁻³ for the group 11.

Although in Fig. 7 we have shown graphically how to obtain the bulk densities of the aggregates, we have in practice used Equation 42 above for their calculation.

Algebraic solution If the densities of our two pore liquids are known, and if the composite densities of our porous aggregates when saturated with each pore liquid can be obtained experimentally by gravity fractionation, then bulk density and porosity values can be computed algebraically for our system of porous aggregates---seen as follows:

Let us suppose that k_1 is the density of pore liquid A, and k_2 is the density of pore liquid B. Also let us suppose that the symbols D_A and D_B represent composite densities of aggregates determined experimentally by gravity fractionation. Then if D is the conventional oven dry aggregate bulk density and P is the conventional oven dry aggregate porosity we can write

$$D + k_1 P = D_A \quad (43)$$

$$D + k_2 P = D_B \quad (44)$$

solving for D and P we get

$$D = \frac{k_2 D_A - k_1 D_B}{k_2 - k_1} \quad (45)^a$$

and

$$P = \frac{D_B - D_A}{k_2 - k_1} \quad (46)$$

where D is the aggregate bulk density and P is the aggregate porosity.

Equation 45 gives a unique solution for the bulk density D of the aggregate.

^aEquation 45 is the same as Equation 42 where $D = y$, $D_A = y_1$, $D_B = y_2$, $k_1 = x_1$ and $k_2 = x_2$.

Experimental verification of the theory

Porous ceramics To test the theory experimentally, three types of porous ceramic plates were obtained from Coors Porcelain Co., Golden, Colorado. The three types were Coors P2, Coors P3, and Coors AHP (99% Al_2O_3) 99. On arrival the plates were dried, weighed, and their diameter d and thickness H were carefully measured. The empirical density values D for the porous ceramics were computed from the equation

$$D = (\text{Plate weight})/(\pi d^2 H/4) \quad (47)$$

The plates were broken up and three size fractions (0.200-0.283 cm., 0.283-0.476 cm., and 0.476-0.800 cm.) were obtained by sieving. A fraction passing an 0.02 cm. screen was used for the determination of the particle (solids) density (D_s) by a pycnometer method of the American Society for Testing Materials (1947), where

$$D_s \text{ (at } T^{\circ}) = [W_o / (W_o + W_a - W_b)] T_c \quad (48)$$

Here W_o = weight of oven dried sample

W_a = weight of pycnometer + weight of water at T°

W_b = weight of pycnometer + weight of aggregates + weight of water
at T°

T_c = temperature correction at T°

Values of D_s will not be referred to again until the table after the next.

Using a gravity fractionation technique (see Methods) values of density, D' , were computed using Equation 45. The results for density obtained by gravity fractionation D' and the values D obtained from the empirical data, Equation 47, are presented in Table 12. It was necessary

to use nitromethane, S.G. 1.12 as one of the "pore liquids" for the porous ceramic sample designated AHP 99; when fractionation was attempted with carbon tetrachloride as a pore liquid, apparent density values exceeded the density of pure bromoform (SG. 2.85). Carbon tetrachloride was used as pore liquid B for remaining ceramics, and isooctane was used as a pore liquid A throughout. There was little difference between density values obtained by gravity fractionation for different size fractions. Average values of the three size fractions for density are given in Table 12, and the respective ranges are listed for two methods (gravity fractionation and empirical data) used. Average values obtained by two methods are within 2 percent of one another. A higher degree of precision could undoubtedly be obtained if there was an attempt made to make the ranges narrower. For the purposes of this investigation a range of 0.10 ± 0.05 density units was considered satisfactory.

Table 12. Bulk density values D' obtained from gravity fractionation are compared with empirical values D for "Coors" porous ceramics

Type of Coors	Gravity fractionation ^a			Empirical data ^b		
	D'			D		
Ceramic	Range		Avg.	Range		Ave.
	g cm^{-3}			g cm^{-3}		
AHP 99	2.05	2.09	2.07	2.09	2.10	2.10
P 2	1.62	1.75	1.68	1.64	1.67	1.65
P 3	1.69	1.75	1.72	1.66	1.71	1.69

^a D' determined from experimental data using Equation 45.

^b D determined from Equation 47.

Table 13. Porosity values P' obtained by gravity fractionation are compared with empirical porosity P values for porous ceramics; average pore diameters supplied by the manufacturer are also listed

Coors Ceramic	Gravity fractionation ^a			Empirical values ^b			Diameter of pores in microns
	P'			P			
	Range		Ave.	Range		Avg.	
	%			%			
AHP 99	54.4	71.0	62.6	45.5	45.6	45.5	2.0-3.0
P 2	44.9	62.3	53.4	50.0	50.9	50.5	6.0-8.5
P 3	42.0	58.0	49.5	47.9	49.4	48.7	1.3-2.0

^a P' determined from experimental data using Equation 46.

^b P determined from Equation 49.

Values for porosity P' determined by gravity fractionation and calculated from Equation 46 as well as the values of porosity P calculated from empirical data and Equation 49 below are given in Table 13.

$$P = 1 - \frac{D}{D_s} \quad (49)$$

Here D_s is the particle (solids) density obtained from Equation 48. Average pore diameters in microns supplied by the manufacturer are also listed. It can be seen at a glance in Table 13 that the average values for porosity as determined by gravity fractionation are higher for all ceramics in general and very much higher for AHP 99 in particular. In the next section on the "Sources of error" we will attempt to explain this discrepancy.

Table 14. Range of values of bulk density D' and of average density; range of porosity P' and average porosity P' calculated from gravity fractionation^a; range of porosity P and average porosity P calculated on the basis of empirical data^b; weight percent^c and percent of pores < 0.1 microns in diameter^a for density groups of Clarion s.l., Webster c.l. and Luton si.c. aggregates

Soil group		Gravity fractionation						Empirical				Weight percent	Percent pores < 0.1 micron
		D'			P'			P					
		Range		Avg.	Range		Avg.	Range		Avg.			
		g. cm. ⁻³			%			%					
Clarion s.l.													
1	A	1.74	1.78	1.76	41.1	45.2	43.2	34.0	35.5	34.8	9.5	5.0	
	D	1.87	2.07	1.97	26.9	33.1	30.0	24.5	31.8	28.1	10.6	7.8	
2	B	1.77	1.82	1.80	32.9	36.3	34.6	32.4	34.3	33.3	27.4	5.0	
	C	1.90	1.94	1.92	24.7	28.8	26.8	28.4	29.9	29.2	29.8	5.2	
Webster c.l.													
1	A	1.62	1.81	1.72	27.4	43.5	35.5	32.6	39.7	36.2	14.4	13.6	
	C	1.80	1.94	1.87	21.9	32.9	27.4	28.3	33.5	30.9	6.7	15.2	
2	B	1.71	1.88	1.79	23.3	36.2	29.8	30.1	36.5	33.3	67.8	14.6	
	D	1.86	2.07	1.97	11.0	21.9	16.5	22.2	30.4	26.3	6.6	20.5	
Luton si.c.													
1	A	1.94	2.05	2.00	14.6	16.6	15.5	24.1	28.2	26.2	22.6	26.5	
	B	2.00	2.06	2.03	17.7	19.1	18.4	24.4	26.6	25.5	77.3	28.1	

^a D' calculated using Equation 45; P' calculated using Equation 46.

^b P calculated using Equation 49 and D' values from this table.

^c Weight percent calculated using Equation 50.

^a Percent of pores less than 1 micron in diameter calculated using Equation 53.

Soil aggregates

In Table 14 we present the data for D' and P' for Density groups of three soils as determined by gravity fractionation. Values of P are given for comparison. These values were calculated using Equation 49, and D' values from gravity fractionation. Two other parameters useful in the explanation of results obtained are also included in Table 14. They are: weight percent and percent of pores < 0.1 micron in diameter. The former is computed from Equation 50 below while the latter is given by Equation 53.

$$\text{Weight percent} = \frac{\text{Weight of aggregates for a given density group}}{\text{Weight of all aggregates for a given soil}} \times 100 \quad (50)$$

To obtain a value for percent of pores < 0.1 micron in diameter we need to start with Kelvin equation (Gregg 1961, p. 69). Kelvin equation can be written as

$$RT \ln p/p_0 = (-4\sigma V/d) \cos\theta \quad (51)$$

where p is the vapor pressure above a hemispherical meniscus of diameter d, p_0 is the saturation vapor pressure, V is the molar volume of absorbed liquid, (18 for water), at temperature T, (absolute scale), σ is the surface tension, and we assume contact angle $\theta = 0$.

This equation relates the pore diameter d to the value of p/p_0 at which evaporation would occur. The Kelvin equation can be used to calculate pore diameters down to monolayer conditions (Foster, 1948). In soils the monolayer probably occurs in the vicinity of a relative vapor pressure, $p/p_0 = 0.20$, (Quirk and Panabokke, 1962). Under these conditions we can assume that the occurrence of a monolayer corresponds to the hygroscopic coefficient.

We assume that the water in the soil in an air-dry condition is the so-called hygroscopic water. Then if hygroscopic coefficient F is taken as 3.1×10^7 dyn. cm.⁻² (Lyon et al., 1952) we can write at $p/p_0 = 0.20$

$$F = (RT \ln p/p_0)/V = 3.1 \times 10^7 \text{ dyn. cm.}^{-2} \quad (52a)$$

If σ is the surface tension of water ($\sigma = 72.75$ dyn. cm.⁻¹) and 1×10^4 is the conversion factor from centimeters to microns, using Equations 51 and 52a we have

$$d = 4\sigma \times 10^4 / F = 0.1 \text{ microns} \quad (52b)$$

where d is the pore diameter in microns.

Then the ratio of the volume of pores filled with water in air-dry condition to the total volume of pores should give the fraction of pores < 0.1 micron in diameter or

$$\begin{aligned} &\text{Percent of pores} < 0.1 \text{ micron in diameter} \\ &= \frac{\text{Percent H}_2\text{O by volume in air-dry condition}}{\text{Percent porosity}} \times 100 \quad (53) \end{aligned}$$

Density groups are arranged in Table 14 according to the order of separation during gravity fractionation. Group 1 was found to separate from the Group 2 when the aggregates were saturated with carbon tetrachloride. Subsequently, when aggregates were saturated with isooctane each of these two groups separated into two alphabetical groups (either A, B, C or D). The order A, B, C and D in the alphabetical designation refers to increasing magnitude of the average density. We now examine the ranges of density for each soil in Table 14. It becomes at once apparent that the first separation (Groups 1 and 2 for each soil), produces the aggregates

of essentially similar density range. It is the second separation (alphabetical groups) that produces independent density groups. Combinations A-B, C-D either overlap (Webster) or are included as a narrower range within one another (Luton B in A, Clarion C in D). Alternate combinations A-C, B-D represent distinct ranges for Clarion and Webster soil aggregates. No separation resulted when aggregates of Luton soil were saturated with carbon tetrachloride. Two groups given for Luton si.c. (A and B) were obtained from isooctane saturated aggregates.

Now let us compare porosity P' values as obtained from gravity fractionation by Equation 46 and porosity values P as computed from Equation 49. In general, values of computed porosity P are higher for Webster and Luton and lower for Clarion than the porosity P' determined from gravity fractionation. The observations above that were applied to the density ranges apply also to computed values of porosity P' . Percent of pores < 0.1 micron in diameter is inversely proportional to the porosity P within any given soil and increases directly as the clay content of the soil (see Table 30, results).

Turning our attention now to the relative sizes of density groups (weight percent) we notice that a large fraction of soil is very uniform with respect to density and porosity. The size of this group is largest in Luton si.c., smaller in Webster c.l., and becomes two separate groups in Clarion s.l.

When we compare our values of bulk density for the aggregates of three soils used with those obtained by Perry (1942) for large loam aggregates, the general agreement is remarkably good. Perry's values range from 1.62 g. cm.^{-3} up to 2.04 g. cm.^{-3} . This range covers the values obtained by us.

Similarly the range of bulk densities obtained by McIntyre and Stirk (1954) and by Grossman (1959) agrees well with the values obtained by us.

Chepil's (1950) results Average results for aggregate density given by Chepil (1950) (see Table 15) correspond to the values presented by us here. However, his values for 2.0 - 6.4 mm. aggregates are 20 - 30% lower than ours. We intend to show that Chepil's values for bulk density of aggregates > 1.0 mm. in size are unrealistically low while those in the lower size range are unrealistically high. Chepil determined aggregate density by three methods: the air elutriation method, the threshold velocity method, and the bulk density method.

In the first two methods he computed soil aggregate density from the average air stream velocity required to just lift vertically or just move horizontally a sand grain of comparable size and shape. Chepil concedes that "slight differences between the shape of soil aggregates and sand grains were observed, and the effects of these differences, if any, presumably were reflected in the equivalent apparent density of soil aggregates".

The effect due to size difference within any given size fraction seems to us far from minor. If we examine Chepil's values given in our Table 15, we can see at a glance that for any given size group the size difference between aggregates could have been 40% or even as much as 200%. The shape and size distribution can vary both within the soil size groups and within the sand grain size groups used as standard.

The statement made by Chepil that "for sieve grades above 0.1 mm. in diameter all three methods gave virtually the same values" is questionable. When his results are compared, variations of anywhere from 1% to 30% can be

observed between different methods.

Table 15. Values of bulk density BD and of "aggregate apparent density" AD^a for a bed of aggregates. After Chepil (1950)

Diameter mm.	Difference %	Fine sandy loam		Silt loam		Clay	
		BD	AD	BD	AD	BD	AD
0.1	∞	1.33	2.30	1.32	2.29	1.18	2.04
0.1-0.15	50	1.24	2.15	1.21	2.10	1.04	1.80
0.15-0.25	67	1.22	2.11	1.05	1.82	1.01	1.75
0.25-0.42	68	1.25	2.17	1.01	1.75	1.04	1.80
0.42-0.59	40	1.12	1.94	.99	1.72	1.01	1.75
0.59-0.84	42	1.05	1.82	.93	1.61	1.00	1.73
0.84-1.19	42	1.01	1.75	.97	1.68	.98	1.70
1.19-2.0	68	.91	1.58	.91	1.58	.97	1.68
2.0-6.4	220	.86	1.49	.82	1.42	.86	1.49
Avg.			1.92		1.77		1.75

$$^a \text{Aggregate apparent density} = \frac{\text{BD}}{1.53} \times 2.65.$$

One reason that results for the three methods used are comparable stems from the fact that the same basic erroneous assumption (that the distributions of sizes and shapes of soil and sand grains are the same) was used as a basis of calculation for all three methods.

Let us turn our attention now to the "bulk density method" as proposed by Chepil. The method consists of filling a test tube with aggregates, tapping the test tube, as soil is added, till no increase in weight is observed, then calculating the bulk density of the soil in a test tube. When this value of soil bulk density is multiplied by a fraction 2.65/1.53, the product gives an "average apparent density" (our bulk density) for aggregates within any given size group. The value 2.65 is the particle density (real density) of sand and 1.53 is an average value for bulk density of sand determined in the same manner as the bulk density of the soil before.

Chepil contends that all grain sizes of sand gave approximately the same value for the bulk density, and he correctly assumes that the shape of the grains and the volume of the interstices between the grains are constant for any uniform size of grains. He then assumes the same uniform distribution of size and shape for soil aggregates and calculates soil aggregate density values on the basis of this assumption.

It is our intention to show that his results indicate lack of uniformity in the sand and, furthermore, that his assumptions with regard to the soil aggregates are unjustified. It is unfortunate that the extensive literature in soil mechanics on the subject of packing and internal friction (Taylor, 1948; Terzaghi and Peck, 1948; Jumikis, 1962) as well as the literature in surface chemistry (Gregg, 1961) does not appear to have been consulted. For uniform spheres and uniform packing, porosity value is a constant. Since $\text{Porosity} = 1 - (\text{Bulk density} / \text{Particle (real) density})$, (see Equation 49), it is apparent at once why Chepil's sand bulk density values are constant provided real density for sand is also assumed to be constant. When uniform spheres are piled one upon another vertically in a rectangular arrangement, such packing represents a porosity of 0.477 or bulk density of 1.39 g. cm.^{-3} for sand (S.G. 2.65). This is the most open packing of maximum porosity and the lowest density. If uniform spheres are arranged one above the other rhombically, the porosity is 0.412 and bulk density for sand is 1.56 g. cm.^{-3} . The densest state of packing with uniform spheres is attained when one sphere rests upon three or four others. Then porosity would be 0.260 and the bulk density for sand would give a value of 1.96 g. cm.^{-3} .

An infinite number of packings exists between the rectangular and the

tetrahedral states. Non-uniformity of grain sizes would tend to give higher bulk density and lower porosity, whereas departures from perfectly smooth round spheres would result in higher porosity values and lower bulk density. When we examine Chepil's results for bulk density of quartz sand in Table 15, obtained from various sources, it becomes apparent that Ottawa Standard ASTM sand and Great Bend sand gave the values of bulk density that would indicate rhombic packing arrangement and uniform equivalent shape.

Table 16. Bulk density of sand obtained from different sources. After Chepil (1950)

Source	Bulk density
Ottawa ASTM Standard	1.57
Great Bend, Kansas	1.56
Rolla, Kansas	1.50
St. George, Kansas	1.52

It is felt that lower values quoted for the other two sources reflect an increase in angularity and departure from original spherical shape. We have shown elsewhere (see Theory I) that the soil aggregates can be approximated by spheres. The departure from an ideal sphere is greatest for large aggregates, becoming progressively smaller as the size decreases.

We could reasonably expect that low values of bulk density given by Chepil for his two largest sizes, (Table 15), are a direct result of the increase of angularity. On the other hand, it is argued that as the size decreases, soil aggregates become increasingly more spherical and regular until a point is reached when their shape becomes more smooth and regular

than the corresponding shape of sand grains used as a standard. When that happens, the angle of internal friction for soil aggregates becomes less than for the more angular sand grains. Up and down tapping would tend to promote rhombic packing, as can be seen from the results (a value of 1.57 for bulk density of Ottawa sand). If now the angle of internal friction were to be less for soil aggregates than for sand grains, up and down tapping could result in a certain amount of tetrahedral arrangement of particles, giving bulk density values in excess of the values resulting from rhombic packing. Chepil's inference that larger aggregates were more porous than smaller ones, based on the observation that "apparent density" values increased with the decrease in aggregate size, seems unwarranted since no data are given as to what fraction of each size consisted of sand grains of the same size.

We have found (Table 17a) that there is no increase in density with decrease in size for the sizes we have studied. It should be noted, however, that if the stones are included in the calculation of aggregate density for any given size group, there is a small increase of density with the decrease of size, particularly noticeable for Clarion s.l.. Furthermore, abnormally high values of the aggregate density for Clarion s.l. when stones were included (Yes values) reflect the fallacy of including the sand fraction in the calculation of aggregate density.

Turning our attention back to Chepil's results in Table 15, we note a remarkable constancy of his values for a clay soil > 0.1 and < 2.00 mm. In our studies we have observed very low content of sand in our clay soil. This confirms our belief that the presence of a large number of sand grains (compare values of fine sandy loam in Table 15) is responsible for the

apparent increase in density with decrease in size in Chepil's results.

Table 17a. Average density of three Size groups of Clarion s.l., Webster c.l., and Luton si.c. with and without stones^a

d cm.	Stones	Clarion s.l.	Webster c.l.	Luton si.c.
		Average bulk density		
		g. cm. ⁻³		
0.200-0.283	No	1.88	1.80	2.03
	Yes	2.06	1.83	2.03
0.283-0.476	No	1.87	1.80	2.03
	Yes	2.01	1.81	2.03
0.476-0.800	No	1.85	1.80	2.03
	Yes	2.00	1.81	2.03

^aThe second value, of average bulk density (Yes value), represents average aggregate density for a given size group when the stones (see Methods, Gravity Fractionation) are included in the computation.

Sources of error There are two principal sources of error in the gravity fractionation method. We remember that our pore liquids are soluble in bromoform-nitromethane fractionation mixture; the first source of error arises as a direct result of this. Using Equations 43 and 44 we can rewrite Equation 45 as

$$D = \frac{k_2(D + Pk_1) - k_1(D + Pk_2)}{k_2 - k_1} \quad (54)$$

where k_1 is the density of pore liquid A, k_2 is the density of pore liquid B and $k_2 > k_1$.

For the purposes of clarity we will briefly review the physical picture and assumptions made in the discussion that follows. We recall that an aggregate is saturated with a pore liquid A or pore liquid B and immersed

in a fractionating mixture of bromoform and nitromethane. If it floats, its composite density is less than that of the fractionating mixture; if it sinks, its composite density is more than that of the fractionating mixture. Composite density D_{comp} of an aggregate saturated with a pore liquid has two components. The first one is due to the bulk density D of an aggregate and the second one is due to the product of porosity P and density of the pore liquid k (recall general form of Equations 43 and 44: $D_{\text{comp}} = D + Pk$).

In what follows, we turn our attention to what happens to the product Pk . In particular we consider the change of k within the aggregate. Since density of pore liquids is less than the density of fractionation mixture and both pore liquids are soluble in the fractionation mixture, we assume an increase in the average density of the pore liquid as a result of mixing with the fractionation mixture at the aggregate surface. We assume a random distribution of pores and pore sizes for any one aggregate but stipulate that such distribution be uniform in a statistical sense for any given group.

Considering a large number of aggregates containing a very large number of pores, we feel that the distribution can indeed be considered uniform for any one group. Then a fraction $(k + \Delta k)/k$, the change of density per unit density, will be a measure of respective changes of density within the aggregates as a result of mixing.

Let us now assume that the density of pore liquid k_1 changes by a small amount Δk_1 , and the density of pore liquid k_2 changes by a small amount Δk_2 when aggregates are immersed in a fractionation mixture. We assume that the new determined density D' will be different from the true

density D and we write

$$D' = \frac{k_2[D + P(k_1 + \Delta k_1)] - k_1[D + P(k_2 + \Delta k_2)]}{k_2 - k_1} \quad (55)$$

Equation 55 can be written as

$$D' = D + \frac{k_2 P(k_1 + \Delta k_1) - k_1 P(k_2 + \Delta k_2)}{k_2 - k_1} \quad (56)$$

or

$$D' = D + \frac{Pk_1 k_2 \frac{(k_1 + \Delta k_1)}{k_1} - Pk_1 k_2 \frac{(k_2 + \Delta k_2)}{k_2}}{k_2 - k_1} \quad (57)$$

then

$$D' = D + \frac{Pk_1 k_2}{k_2 - k_1} \left(\frac{k_1 + \Delta k_1}{k_1} - \frac{k_2 + \Delta k_2}{k_2} \right) \quad (58)$$

Let us now examine Equation 58. First let us suppose that $\Delta k_1 = \Delta k_2 = 0$, i.e., pore liquids are immiscible with fractionation mixture. Then the part in brackets becomes 0 and $D' = D$. Suppose Δk_1 and Δk_2 are not zero, then $(k_1 + \Delta k_1)/k_1$ and $(k_2 + \Delta k_2)/k_2$ represent an increase of density of pore liquid per unit density and we have three cases.

Case I: The increase of density per unit density is the same for both pore liquids

$$\frac{k_1 + \Delta k_1}{k_1} = \frac{k_2 + \Delta k_2}{k_2} \quad (59)$$

Then in Equation 58 $D' = D$ the determined density D' remains the same as the true density D .

Case II: The increase of density per unit density for the second pore liquid is larger than for the first.

$$\frac{k_1 + \Delta k_1}{k_1} < \frac{k_2 + \Delta k_2}{k_2} \quad (60)$$

Then in Equation 58 $D' < D$ the determined density D' is less than the true density D .

Case III: The increase of density per unit density for the second pore liquid is less than for the first.

$$\frac{k_1 + \Delta k_1}{k_1} > \frac{k_2 + \Delta k_2}{k_2} \quad (61)$$

Then in Equation 58 $D' > D$ the determined density D' is more than the true density D .

For Case I and Case III the amount of change in bulk density of an aggregate depends on Δk_1 and Δk_2 on the relative magnitudes of k_1 and k_2 , and also on the magnitude of the fraction $k_1 k_2 (k_2 - k_1)$. In general, for this fraction we would wish to minimize the product in the numerator and maximize the difference in the denominator; this suggests that we use a very low density liquid for pore liquid (A) (k_1 low) and a high density liquid for pore liquid (B) (k_2 high). Working with bromoform S.G. 2.85 as a fractionating mixture, k_2 values should not be higher than 2.00 g. cm.⁻³ for practical purposes, and k_1 values below 0.5 g. cm.⁻³ are non-existent. The reader should interpret the remarks made with reference to the density values used.

Let us turn our attention now to the effects of mixing on porosity values. Using Equations 43 and 44 and again assuming small changes Δk_1 and Δk_2 in the densities k_1 and k_2 of pore liquids, we can write Equation 46 as follows

$$P' = \frac{[D + P(k_2 + \Delta k_2)] - [D + P(k_1 + \Delta k_1)]}{k_2 - k_1} \quad (62)$$

where P' the new determined value of porosity is assumed to be different from P , the true porosity. Equation 62 can also be written

$$P' = \frac{P(k_2 + \Delta k_2) - P(k_1 + \Delta k_1)}{k_2 - k_1} \quad (63)$$

or

$$P' = \frac{P[k_2 \frac{(k_2 + \Delta k_2)}{k_2} - k_1 \frac{(k_1 + \Delta k_1)}{k_1}]}{k_2 - k_1} \quad (64)$$

We examine Equation 64 for Case I described earlier by Equation 59.

Case I: $(k_1 + \Delta k_1)/k_1 = (k_2 + \Delta k_2)/k_2$

Then Equation 64 reduces to

$$P' = P(k_1 + \Delta k_1)/k_1 = P(k_2 + \Delta k_2)/k_2 \quad (65)$$

and $P' > P$ the determined porosity P' is greater than the true porosity P by the amount proportional to the change of density per unit density of the pore liquid.

Case II: $(k_1 + \Delta k_1)/k_1 < (k_2 + \Delta k_2)/k_2$ described earlier by Equation

60

or

$$\frac{\Delta k_1}{k_1} < \frac{\Delta k_2}{k_2} \quad (66)$$

since

$$k_1 < k_2 \quad (67)$$

then

$$\frac{1}{k_1} > \frac{1}{k_2} \quad (68)$$

hence

$$\Delta k_1 < \Delta k_2 \quad (69)$$

we rewrite Equation 63 as

$$P' = P \left(1 + \frac{\Delta k_2 - \Delta k_1}{k_2 - k_1} \right) \quad (70)$$

Then $P' > P$, the determined value of porosity P' is greater than the true porosity P . The increase depends on the difference between the respective changes of density of the pore liquid (not on a change of density per unit density as in Case I) and the difference between the densities of two pore liquids. To minimize the effect, we should select pore liquids so that k_2 is much larger than k_1 . Furthermore, if we examine Equation 64 and we suppose that for Case II k_1 , k_2 and $(k_1 + \Delta k_1)/k_1$ stay the same as in Case I, then $P' > P(k_1 + \Delta k_1)/k_1$, the determined porosity P' is greater than the product of true porosity P and the change of density per unit density of the pore liquid.

Case III: $k_1 + \Delta k_1/k_1 > (k_2 + \Delta k_2)/k_2$ described earlier by Equation 61.

Here we have five subcases IIIa, IIIb, IIIc, IIId, and IIIe.

$$\text{IIIa: } k_2 \frac{k_2 + \Delta k_2}{k_2} = k_1 \frac{(k_1 + \Delta k_1)}{k_1} \text{ and } \left(\frac{k_1 + \Delta k_1}{k_1} > \frac{k_2 + \Delta k_2}{k_2} \right)$$

From Equation 64 we have $P' = 0$: the determined porosity P' is equal to zero.

$$\text{IIIb: } k_2 \frac{(k_2 + \Delta k_2)}{k_2} > k_1 \frac{(k_1 + \Delta k_1)}{k_1} \text{ and } \left(\frac{k_1 + \Delta k_1}{k_1} > \frac{k_2 + \Delta k_2}{k_2} \right)$$

From Equation 64 we have $P' > P$: the determined porosity P' is greater than the true porosity P . If we let k_2 , k_1 and $(k_1 + \Delta k_1)k_1$ stay the same as in Case I, then $P' < P(k_1 + \Delta k_1)/k_1$, the determined porosity P' is less than the product of true porosity P and the change of density per unit density of the pore liquid.

$$\text{IIIc: } k_2 \frac{k_2 + \Delta k_2}{k_2} < k_1 \frac{(k_1 + \Delta k_1)}{k_1} \text{ and } \left(\frac{k_1 + \Delta k_1}{k_1} > \frac{k_2 + \Delta k_2}{k_2} \right)$$

From Equation 64 we have $P' < 0$: the determined porosity P' is less than 0. Since P' cannot be less than 0 this situation gives the same answer as IIIa, i.e., $P' = 0$.

In the above three subcases we have considered the inequality $(k_1 + \Delta k_1)/k_1 > (k_2 + \Delta k_2)/k_2$ with reference to the relative magnitude of k_1 and k_2 . In the following two subcases we consider the same inequality with reference to the relative values of Δk_1 and Δk_2 .

IIId: If we take $\Delta k_1 = \Delta k_2$, then since $k_1 < k_2$,

$$\frac{\Delta k_1}{k_1} > \frac{\Delta k_2}{k_2} \quad (71)$$

Adding 1.0 to both sides, we have

$$1 + \frac{\Delta k_1}{k_1} > 1 + \frac{\Delta k_2}{k_2} \quad (72)$$

or

$$\frac{(k_1 + \Delta k_1)}{k_1} = \frac{k_2 + \Delta k_2}{k_2} \quad (73)$$

Then $\Delta k_1 = \Delta k_2$ satisfies initial condition of Case III and we have, from Equation 70 $P' = P$: the determined porosity P' is equal to the true porosity P .

IIIe: Similarly, if we take $\Delta k_1 > \Delta k_2$, the conditions of Case III are satisfied and from Equation 70 we have $P' < P$ if

$[(\Delta k_2 - \Delta k_1)/(k_2 - k_1)] > -1$. The determined porosity P' is less than the true porosity P . This is a special case of Case IIIc. Since $\Delta k_1 > \Delta k_2$ and $k_2 > k_1$ the quantity in square brackets will always be less than zero.

We summarize the three cases discussed for density and porosity in Table 17b.

Both pore liquids used in this study are non-polar liquids. Isooctane is insoluble in water, and carbon tetrachloride is very slightly soluble in water (0.089/100 ml at 20°C.). The second source of error arises as a result of the inability of pore liquids to mix with water. Hygroscopic water in the form of molecular films will line larger pores and essentially block smaller pores. The effective determined porosity P' of an aggregate will be less than the true porosity P .

Turning our attention now to the effect of hygroscopic water on determined density D' values, we would expect the determined density D' to be larger than the true density D .

Table 17b. Summary of relative changes in density and porosity values with respect to the changes of density per unit density for two pore liquids as used in gravity fractionation

Case	Density	Porosity
I. $(k_1 + \Delta k_1)/k_1 = (k_2 + \Delta k_2)/k_2$ ^a	$D' = D$ ^b	$P' > P$ ^c $P' = P(k_1 + \Delta k_1)/k_1$
II. $(k_1 + \Delta k_1)/k_1 < (k_2 + \Delta k_2)/k_2$	$D' < D$	$P' > P$ $P' > P(k_1 + \Delta k_1)/k_1$
III. $(k_1 + \Delta k_1)/k_1 > (k_2 + \Delta k_2)/k_2$	$D' > D$	
a. $k_1 + \Delta k_1 = k_2 + \Delta k_2$	$D' > D$	$P' = 0$
b. $k_1 + \Delta k_1 < k_2 + \Delta k_2$	$D' > D$	$P' > P$ $P' < P(k_1 + \Delta k_1)/k_1$
c. $k_1 + \Delta k_1 > k_2 + \Delta k_2$	$D' > D$	$P' = 0$
d. $\Delta k_1 = \Delta k_2$	$D' > D$	$P' = P$
e. $\Delta k_1 > \Delta k_2$	$D' > D$	$P' < P$ $P' > 0$

^a k_1 = density of pore liquid (A)

k_2 = density of pore liquid (B)

k_1 = change in density of pore liquid (A)

k_2 = change in density of pore liquid (B)

^b D = true density of porous aggregates

D' = determined density of porous aggregates

^c P = true porosity of porous aggregates

P' = determined porosity of porous aggregates

Let us suppose that w , ($0 \leq w < 1$), is a fraction of total aggregate porosity P occupied by hygroscopic water. Then $(1 - w)$ represents that fraction of the pore space which is not filled with water. Furthermore we assume that the density of hygroscopic water is equal to unity. Then Equation 43 can be written

$$D + wP + (1 - w)k_1P = D_A \quad (74a)$$

where D is aggregate bulk density, P is aggregate porosity, k_1 is the density of pore filling liquid A (other than water), and D_A is the aggregate composite density (see Equation 43). Similarly Equation 44 can be written

$$D + wP + (1 - w)k_2P = D_B \quad (74b)$$

where D and P are as defined above and k_2 and D_B refer to the pore liquid density and aggregate composite density for a pore filling liquid B (see Equation 44).

Solving for D and P we get

$$P = \frac{1}{1-w} \left(\frac{D_B - D_A}{k_2 - k_1} \right) \quad (74c)$$

$$D = \frac{k_2 D_A - k_1 D_B}{k_2 - k_1} - w \left(\frac{D_B - D_A}{k_2 - k_1} \right) \quad (74d)$$

Comparing Equation 74c (true porosity P) with Equation 46 (determined porosity P') we can see at a glance that

$$P = \frac{1}{1-w} P' \quad (74e)$$

True porosity P is greater than determined porosity P' ($w < 1$). Also comparing Equation 74d (true density D) with Equation 45 (determined density D') we can see that

$$D = D' - wP'$$

(74f)

True density D is less than the determined density D' .

Since $0 \leq w < 1$ the correction for porosity is greater than the corresponding correction for density. For example if we assume that for Density Group B of Luton si.c. in Table 14 percent of pores less than 0.1 micron in diameter represents the fraction w of total porosity that is filled with hygroscopic water ($w = 0.281$). Then $(1-w)$ equals 0.719 and $1/(1-w)$ equals 1.39 or 32.7% error between the values of average determined porosity P' and average true porosity P . On the other hand calculating the corrected value of density from the data given for Luton si.c. Density Group B in Table 14 we find that wP' equals 0.05 or 2.5% error between the values of determined and true density.

The aggregates used in density fractionation were oven dried (at 110°C.) prior to separation therefore we would expect a much smaller fraction of pore space to be filled with hygroscopic water. Although the porosity correction might still be considerable the determined density values should be well within the allowable experimental error.

Let us examine our results in the light of the two sources of error discussed above. First let us turn our attention to the values of density and porosity for Porous Ceramics in Table 12 and Table 13. For P2 and P3 we have $D' > D$ and $P' > P$. Hence we conclude that this must be Case IIIb.

On the basis of results in Table 12 and with $k_1 = 0.69 \text{ g. cm.}^{-3}$ (k_1 for isooctane) and $k_2 = 1.60 \text{ g. cm.}^{-3}$ (k_2 for carbon tetrachloride), we would expect from Equation 58 for ceramic P2, the relation

$$\left(\frac{k_1 + \Delta k_1}{k_1} - \frac{k_2 + \Delta k_2}{k_2} \right) = 0.04 \quad (74g)$$

and again from equation 58 the correction for density would be

$$D = D' - P(0.05) < 2\% \quad (75)$$

Using Equation 65 and values of P and P' (for ceramic P2) in Table 13, we would have under conditions of Case IIIb

$$P' < P (1.06) \quad (76)$$

if we assume

$$\frac{k_1 + \Delta k_1}{k_2} = 1.06 \quad (77)$$

then from Equation 74g we would have

$$\frac{k_2 + \Delta k_2}{k_2} = 1.02 \quad (78)$$

Equations 76, 77 and 78 satisfy the conditions of Case IIIb, i.e., $1.06 > 1.02$ and $1.06 \times 0.69 < 1.02 \times 1.60$.

Turning our attention now to the values for AHP99 in Table 12 and Table 13, we notice $D' < D$ and $P' > P$, and Case II applies. Density of AHP99 is high; when an attempt was made to use carbon tetrachloride as a pore liquid, no separation could be made since the composite density of aggregates was larger than 2.85 g. cm.^{-3} density of pure bromoform. Ceramic aggregate pores were filled with nitromethane and separation effected on that basis. Nitromethane mixes very readily with bromoform. We would expect $k_1 + \Delta k_1/k_1$ for isooctane $<< k_2 + \Delta k_2/k_2$ for nitromethane. The results for this determination agree well with theory $D' < D$ and $P' > P$.

Furthermore, the results illustrate the point made earlier that when

a difference $(k_2 - k_1)$ is small, discrepancies become larger. For isooctane $k_1 = 0.69 \text{ g. cm.}^{-3}$, for nitromethane $k_2 = 1.12 \text{ g. cm.}^{-3}$, then $(k_2 - k_1)$ equals 0.42. Contrast this value with $(k_2 - k_1) = 0.91$ when $k_1 = 0.69 \text{ g. cm.}^{-3}$ for isooctane and $k_2 = 1.60 \text{ g. cm.}^{-3}$ for carbon tetrachloride.

Let us examine the results of gravity fractionation for the three soils in Table 14. The pore liquids were carbon tetrachloride and isooctane. On the basis of tests on Porous Ceramics we would expect $P' > P$. However, the results point to the presence of the second source of error discussed. The low values of determined porosity P' for Webster and Luton follow the relative percent values of pores less than 0.1 micron in diameter, with lowest determined porosity P' corresponding generally to the highest percent of pores less than 1 micron in diameter. The values of determined porosity P' for Clarion s.l. are in general higher than values of true porosity P . This is an expected result (see Table 18, Case IIIb) particularly if we consider a relatively low percent of pores < 0.1 micron in diameter.

In view of these results we conclude that the average values of determined density D' for Clarion s.l., Webster c.l. and Luton si.c. density groups should approximate closely the true value of density D . The values of D' as given should be within 2% or better of the true density D value of a given group.

We have attempted to explain the discrepancies encountered in the determination of porosity. In the Results section we have used the computed value of porosity P listed in Table 14 and calculated from Equation 49.

Conclusions

We have demonstrated that density D and porosity P of porous aggregates can be determined uniquely by gravity fractionation using two pore

liquids whose densities are k_1 and k_2 ($k_1 \ll k_2$) respectively. Then if D_A is the composite density of an aggregate filled with pore liquid A and D_B is the composite density of an aggregate filled with pore liquid B,

$$D = \frac{k_2 D_A - k_1 D_B}{k_2 - k_1}$$

and

$$P = \frac{D_B - D_A}{k_2 - k_1}$$

Ideally pore liquids should have low value of the quantity ΔH_{298}^V , (see Table 9), low vapor pressure, (see Table 9), be non-polar, (see Table 9), and immiscible with fractionation liquid, (see Table 11).

If the liquids are miscible with the fractionation liquid, then we have to make a choice. If we want exact D values, we should choose a pore liquid so that $\frac{k_1 + \Delta k_1}{k_1} = \frac{k_2 + \Delta k_2}{k_2}$ where Δk_1 and Δk_2 are small changes in densities k_1 and k_2 when aggregates are immersed in fractionation mixture. On the other hand, if exact values of P are required, then $\Delta k_1 = \Delta k_2$ should be the criterion of pore liquid selection. Finally, when applying the method of soils, hygroscopic water should be taken into account.

In particular, heavy clays and loams will give lower values for porosity. This will not affect the density determination.

Finally we might point out that the analysis of the sources of error suggests two studies that could be conducted. A refined and sophisticated version of this method could well be used in : (a) determination of the solubility rates of non-electrolytes (b) microporosity analysis of soils with reference to hygroscopic water.

THEORY III

Theoretical Treatment of Soil Aggregate Rupture

General concepts

We wish to consider a rupture of an individual soil aggregate. We have shown earlier (see Theory I) that aggregates of the soils tested approximate spheres. For the purposes of this dissertation we assume these aggregates to be brittle spheres. We also assume that the relationship between stresses and strains remains reasonably constant in any arbitrarily chosen direction. This statement should not be interpreted to mean that the relationship is the same in all directions.

The term regular as used in connection with the soil aggregates shall have the following meaning: if it is assumed that a stress of arbitrarily chosen magnitude and direction is uniformly distributed throughout a certain volume, then the probability that the rupture will start within this volume shall be the same irrespective of the volume's relative position within the individual specimen. Let us consider, for instance, an individual soil aggregate. Rupture will not occur within those volume elements which are filled with sand grains. In the strict sense we might be inclined to regard such a material as anisotropic^a. This could be true from the standpoint of a single aggregate but need not be so from the statistical point of view. From the statistical point of view a single aggregate is of no importance, and it is only the properties of a group of aggregates that really matter. Suppose we investigate a large number of

^aThe material is considered anisotropic if its characteristics at every point are not the same in all directions.

aggregates and are in a position to determine the points in which the formation of cracks has begun. Then, for each aggregate, cracking may be imagined to have started at any point within a certain volume of that aggregate. The last statement takes into account that sand grains in different aggregates can be distributed in any possible way (Weibull, 1939b). From visual observation we have concluded that occurrence of cracks is almost entirely confined to the load axis of a spherical soil aggregate. Furthermore, cracking is assumed to originate in the neighborhood of the center of a spherical aggregate.

The concept of homogeneity in the soil is difficult to apply. To attain a degree of homogeneity we have attempted three groupings of soil aggregates: (a) we have grouped aggregates of each soil with respect to size; (b) we have grouped the aggregates of each soil with respect to density, and finally (c) we have grouped all aggregates of each soil together without respect for size or density. It is furthermore assumed that each individual aggregate, particularly in the neighborhood of its center, is homogeneous in composition when compared with the soil as a whole. The reader is advised to examine the theory and results presented in the light of these remarks and to take into consideration the design of our experiment (see Methods: Experimental Design). The theory and results given, although lacking in accuracy when applied to a single individual aggregate, present a sound interpretation of facts when considered from a statistical point of view and applied to a large group of aggregates.

Statement of a problem and assumptions

We wish to consider a spherical soil aggregate under point loads applied at the poles.

The aggregate is homogeneous and regular. The load is symmetrically distributed about the load axis throughout its volume, and the value of the stress at the center of the spherical soil aggregate describes adequately the strength of the soil. The aggregate is considered to be a brittle solid with little if any plastic deformation taking place when the stress is applied. The fracture occurring in the polar plane along the load axis is considered to be a brittle fracture due to the tension generated within the aggregate as a result of diametral loading. Propagation of an elliptical crack in the neighborhood of the center is assumed to be the mechanism responsible for fracture. Soil strength is considered to be a function of void ratio, porosity, size, carbon, and clay contents. It is furthermore assumed that the decrease in strength of soil aggregates at higher moisture contents is a function of change in void ratio, porosity, and size.

Elementary concepts of elastic theory

The mathematical theory of elasticity follows an orderly prescribed course. Firstly the notions of stress and strain are developed, secondly a stress-strain relationship between these quantities is assumed, and finally, using this relationship, equations of motion or equilibrium are set up which enable the state stress or strain to be calculated when a body is acted upon by external forces. It is beyond the scope of this work to delve deeply into the complex ramifications of the theory. Certain aspects of the theory will be presented in so far as they pertain to the problem studied. For an extensive theoretical treatment, the original sources listed later may be consulted.

Stress To specify the forces acting at a point within a body we

proceed as follows: at some point, O , we take a definite direction OK and a circular surface area ∂a perpendicular to OK and containing O (Fig. 8a). Line OK is called the normal to the surface ∂a . The right-hand side of the surface ∂a in the direction OK will be called "positive side", and the left-hand side of the surface ∂a in the opposite direction will be called the "negative side". At each point of the surface ∂a the material on the right-hand side exerts a definite force upon the material on the left-hand side and if we were to make a cut across the surface ∂a and insert these forces, the conditions in a solid as a whole would not be altered. The resultant of all the forces exerted by the material on the right-hand side upon the material on the left-hand side will be a force ∂F and a couple G about a definite axis. Since the area ∂a is supposed to be infinitesimally small, the couple G is negligible compared to the force ∂F .

To clarify the last statement made we recall from elementary physics that the resultant of any two forces which are not parallel can be found by moving them along their lines of action to a common point and then using the parallelogram law. The line of action of the resultant of two parallel forces, \overline{F}_1 and \overline{F}_2 , divides the distance between them inversely in the ratio of the forces, internally if the forces are like and externally if they are unlike. If $\overline{F}_1 = \overline{F}_2$, this method breaks down. No single force can replace a pair of equal, unlike parallel forces whose lines of action do not coincide. Such a combination is called a couple. The torque exerted by a couple is equal to the product $\overline{F}_1 \times L$, where L is the distance between \overline{F}_1 and \overline{F}_2 (Marshall and Pounder, 1957, pp. 80-81).

The limit of the ratio $\partial F/\partial a$ as ∂a tends to zero is called the stress at the point O across the plane whose normal is in the direction OK (Love,

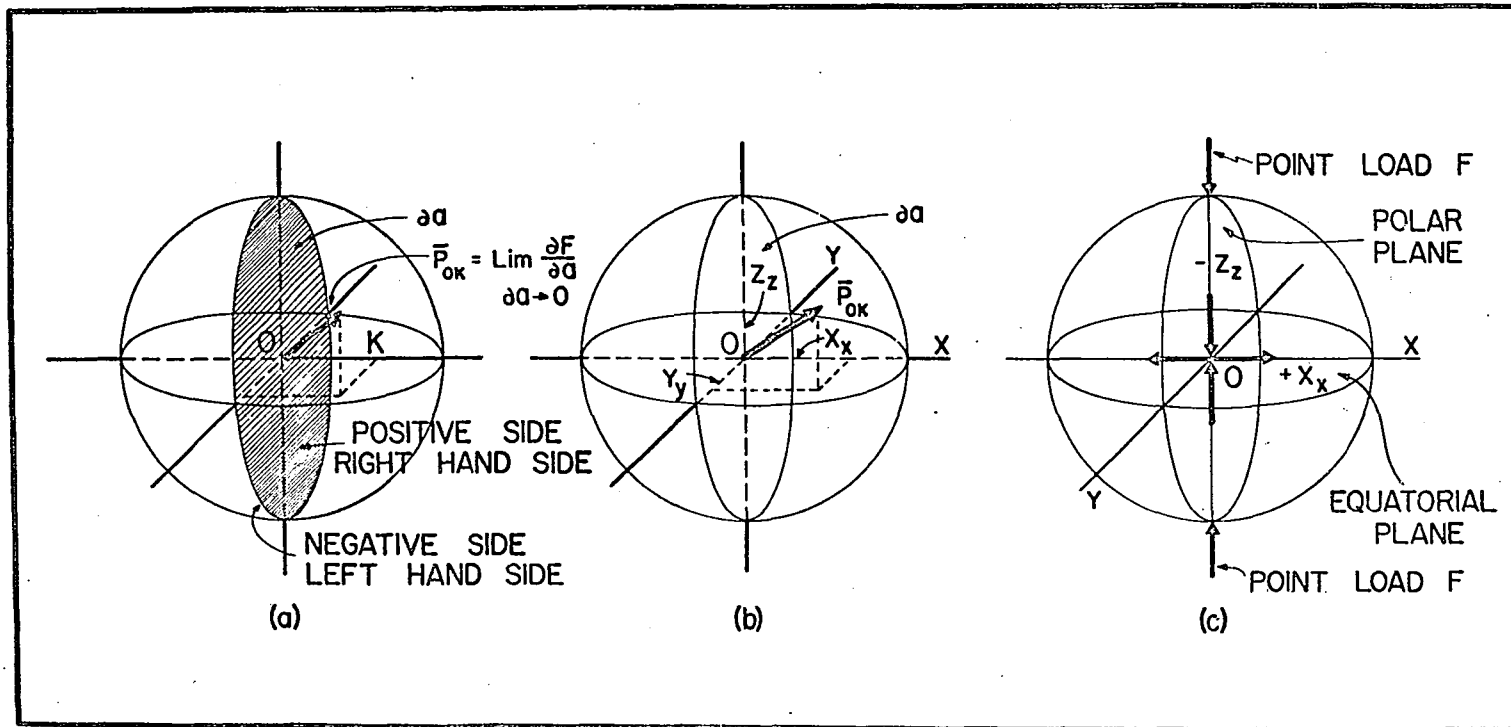


Fig. 8. Forces acting at a point within a body: (a) resultant vector \bar{P}_{ok} (b) components of \bar{P}_{ok} in rectangular coordinate system (c) component stress vectors at the center of a diametrically loaded sphere

1927, p. 74). Suppose \bar{P}_{OK} is a vector whose magnitude has dimensions of force per unit area then

$$\bar{P}_{OK} = \lim_{\partial a \rightarrow 0} \frac{\partial F}{\partial a} \quad (79)$$

In general the direction of the stress vector \bar{P}_{OK} is inclined at an angle to the area ∂a on which it acts. Let us suppose that we now describe a sphere with the center located at the point O of the area ∂a , and the radius equal to the radius of the area ∂a (see Fig. 8a). We now set up a rectangular coordinate system in such a manner that the origin is located at the point O, line OK normal to the surface ∂a is in the direction of the x-axis and the area ∂a becomes the YZ polar plane (see Fig. 8b). We assume that this system describes a spherical soil aggregate.

In this discussion we also assume that area ∂a for a single soil aggregate is infinitesimally small. The reader should bear in mind, in what follows that a polar plane (YZ-plane in Fig. 8b) or equatorial plane (YX-plane in Fig. 8b) for a 0.200-0.800 cm. in diameter soil aggregate is indeed infinitesimally small when compared with a large block of soil aggregates under natural field conditions.

The vector \bar{P}_{OK} can now be resolved into components along the X, Y and Z axes. Using notation given by Love (1927, p. 79), the stress at O, across the polar YZ-plane whose normal is in the direction OX (OK in Fig. 8a), will have the components

$$X_x, Y_x, Z_x \quad (80)$$

Components Y_x and Z_x (not shown in Fig. 8b), which are in the plane of the area ∂a , are called transverse or shear stresses. The component X_x acting along OX in Fig. 8b (OK in Fig. 8a) is called the normal component of

stress. This component is oriented towards the right-hand side and is subsequently referred to as a tensile stress on the polar YZ-plane.

In the same way the stress at O, across the XZ-plane whose normal is in the direction OY will have the components

$$X_y, Y_y, Z_y \quad (81)$$

Components X_y and Z_y (again not shown in Fig. 8b) which are in the plane XZ are called transverse or shear stresses. The component Y_y acting along OY in Fig. 8b is called the normal component of stress.

Finally the stress at O, across the equatorial YX-plane whose normal is in the direction OZ will have the components

$$X_z, Y_z, Z_z \quad (82)$$

Components X_z and Y_z (again not shown in Fig. 8b) which are in the equatorial XY-plane are called transverse or shear stresses. The component Z_z acting along OY in Fig. 8b is called the normal component of stress. The stress components at the point O at the center of the sphere can then be written using the notation in Love (1927, p. 79).

$$\begin{array}{ccc} X_x & Y_x & Z_x \\ X_y & Y_y & Z_y \\ X_z & Y_z & Z_z \end{array} \quad (83)$$

We also note (Jaeger, 1956, p. 6) that $Z_y = Y_z$, $X_z = Z_x$, $X_y = Y_x$, thus only six quantities are needed to specify the stress at a point.

We recall here the assumption we have made in the statement of the problem that the spherical soil aggregate is under concentrated load at the poles and that the stress at the center of this aggregate describes adequately enough for practical purposes the properties of the soil

aggregates studied. Under these conditions, Z_z (see Fig. 8c) the normal stress component in the z direction is negative, pertains to pressure, and is subsequently referred to as a crushing stress on the equatorial XY -plane. The problem of a diametrically loaded sphere is by its nature axially symmetric, so X_x should be equal to Y_y at the center, thus in Fig. 8c only X_x is shown. From now on we will speak about X_x , which is positive, and refer to it as a tensile stress on the polar plane.

The axis of symmetry Z is taken along the line of action of the point loads. It is now assumed that X_x , perpendicular to Z_z in an arbitrarily chosen direction X , is uniformly distributed on the polar plane in the neighborhood of the center of the sphere. It is also assumed that the probability that rupture will start in the polar plane shall be the same irrespective of the relative direction of X_x within the aggregate. Mutually orthogonal stresses X_x , Y_y and Z_z oriented along the coordinate axes intersecting at O form a system of principal stresses. As we have mentioned before at the center of the sphere $X_x = Y_y$; we choose to call a YZ -plane across which the fracture occurs, "the polar plane" and designate X_x , acting along OX on YZ -plane as the tensile stress in X -direction. By symmetry, the shear stresses in polar and equatorial plane vanish at the center of the sphere (Timoshenko, 1934, p. 309). Therefore, our problem resolves itself into a consideration of only the principal crushing stress Z_z and the principal tensile stress X_x at the center of the sphere.

The exact solution for the stress distribution in an elastic sphere

^aIf equatorial plane is thought of as a 360° circle X_x may be thought of as directed along its radius in any direction between 0° and 360° .

under two equal and opposite loads applied at the end points of a diameter was given by Sternberg and Rosenthal (1952). The solution is based on a Boussinesq stress-function approach to axially symmetric problems and is represented as a sum of two solutions. The first, a singular solution, is in closed form, and the second, a series solution, corresponds to surface tractions which are finite and continuous on the surface of the sphere. At the center of the sphere the series solution terminates and the complete value of the crushing stress Z_z in the equatorial plane Z_z is represented by the closed formula:

$$Z_z = - \frac{3F(14 + 5u)}{2\pi r^2(7 + 5u)} \quad (84)$$

Here F is the load, r is the radius of the sphere, and u is the Poisson ratio.

Poisson ratio u may be defined as the ratio of transverse to longitudinal strain, estimated per unit length, produced by the longitudinal stress. Let us suppose that for an ideal elastic solid p is the normal stress in longitudinal direction, e_L is the longitudinal strain in the direction of p and e_T is the transverse strain or strain at right angles to the direction of p , then

$$u = \left| \frac{e_T}{e_L} \right| \quad (85a)$$

Poisson ratio u is a constant independent of the state of stress in the material (Terzaghi and Peck, 1948, p. 106).

Furthermore if p_1 , p_2 and p_3 represent the three principal stresses, the ratio of the change of volume ΔV to original volume V , or the unit volume change produced by the application of these stresses to an elastic

material, can be written

$$\frac{\Delta V}{V} = \frac{1 - 2u}{E} (p_1 + p_2 + p_3) \quad (85b)$$

where E is the modulus of elasticity defined by $E = p/e_L$. For $u = 0.5$ the volume change is zero and the material can be thought of as incompressible.

Examining stress-strain characteristics of unconfined clay samples Terzaghi and Peck (1948, p. 107) found that the volume of the sample of clay subjected to the unconfined compression test remained constant throughout the entire test. Hence the Poisson ratio would be equal to 0.5 throughout the entire test.

For a diametrically loaded spherical aggregate the volume change at the instant of rupture will certainly be zero. Hence we assume that for our aggregates at rupture Poisson ratio $u = 0.5$.

Frocht and Guernsey (1952) developed a new general method of three-dimensional photoelastic stress analysis and applied it to a sphere subjected to diametral compressive loads. Their results show possibilities of high accuracy. Working with fosterite ($u = 0.48$) the authors reported that although relatively large deformations were developed in the loaded zones, the sphere was not significantly distorted from its original shape. They also reported that the stress pattern of the whole sphere was rotationally symmetrical.

In Fig. 9 the location of load axis D-D, the location of equatorial diameter A-A, and the location of the line B-B are given. Along these lines Frocht and Guernsey (1952) determined photoelastically the stress distributions in a fosterite sphere. The stress distributions of normal stresses Z_z , X_x and Y_y along the lines D-D, A-A, and B-B, after Frocht

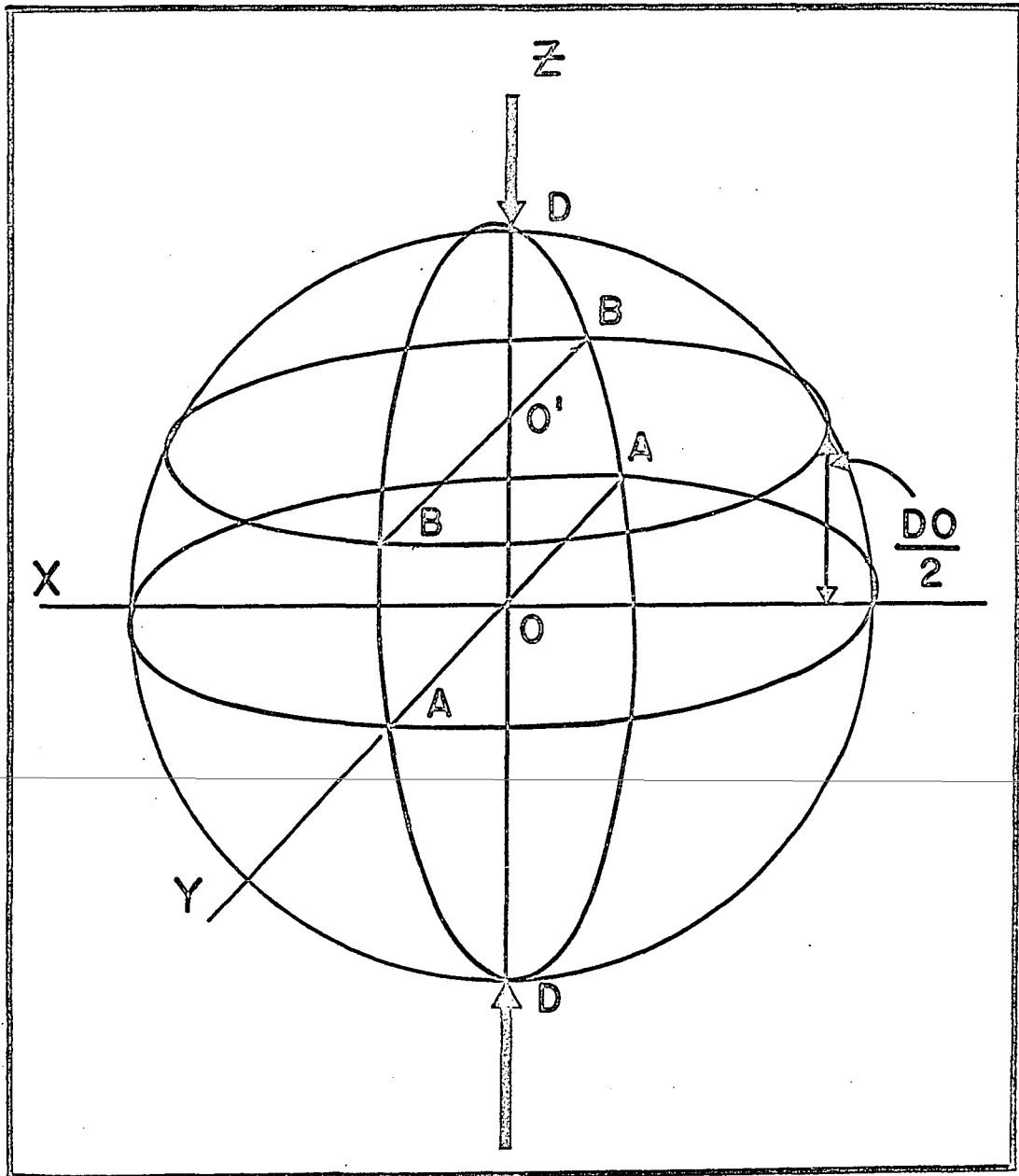


Fig. 9. Location of lines D-D, A-A and B-B for a diametrically loaded sphere. After Frocht and Guernsey (1952). See discussion of the next three figures

and Guernsey (1952), are shown in Fig. 10, Fig. 11, and Fig. 12. In these figures owing to the rotational symmetry only the stress distribution along half the distance, i.e., DO, AO and BO is shown. On the vertical axis the dimensionless stress values (stress/(F/a)) are listed and on the horizontal axis the dimensionless fractions of the distance from the sphere center are shown, i.e., at the center of the sphere in Fig. 10 Z/DO equals zero and stress/(F/a) for $X_x = Y_y$ is 0.45 and for Z_z is -2.59. It is well to remember when examining Fig. 10, Fig. 11 and Fig. 12 that the minus values represent compressive stress whereas plus values represent tensile stress.

If we assume that the fracture of a sphere along the polar plane will result when the tensile strength of the material is exceeded, we can see in Fig. 10 that the tensile component of stress X_x along the load line D-D (of Fig. 9) is greatest at the center of the sphere ($Z/DO = 0$). Along the line A-A (Fig. 11) X_x remains constant for about 40% of the distance ($Y/AO = 0.4$) from the center and along the line B-B (Fig. 12) X_x decreases in value slightly as we go from the surface ($Y/BO = 1$) towards the load line D-D. We might then expect a fracture in a form of an elliptical crack oriented on either side of load line D-D when the tensile stress component X_x at the center of the sphere exceeds the tensile strength of soil. The tensile stress component X_x and the crushing strength component Z_z at the center of the sphere as computed by Frocht and Guernsey (1952) are

$$X_x = 0.45 F/a \quad (85c)$$

$$Z_z = - 2.59 F/a \quad (86)$$

where F is the load and a the area of the equatorial plane.

When the theoretical results of Sternberg and Rosenthal (1952) are

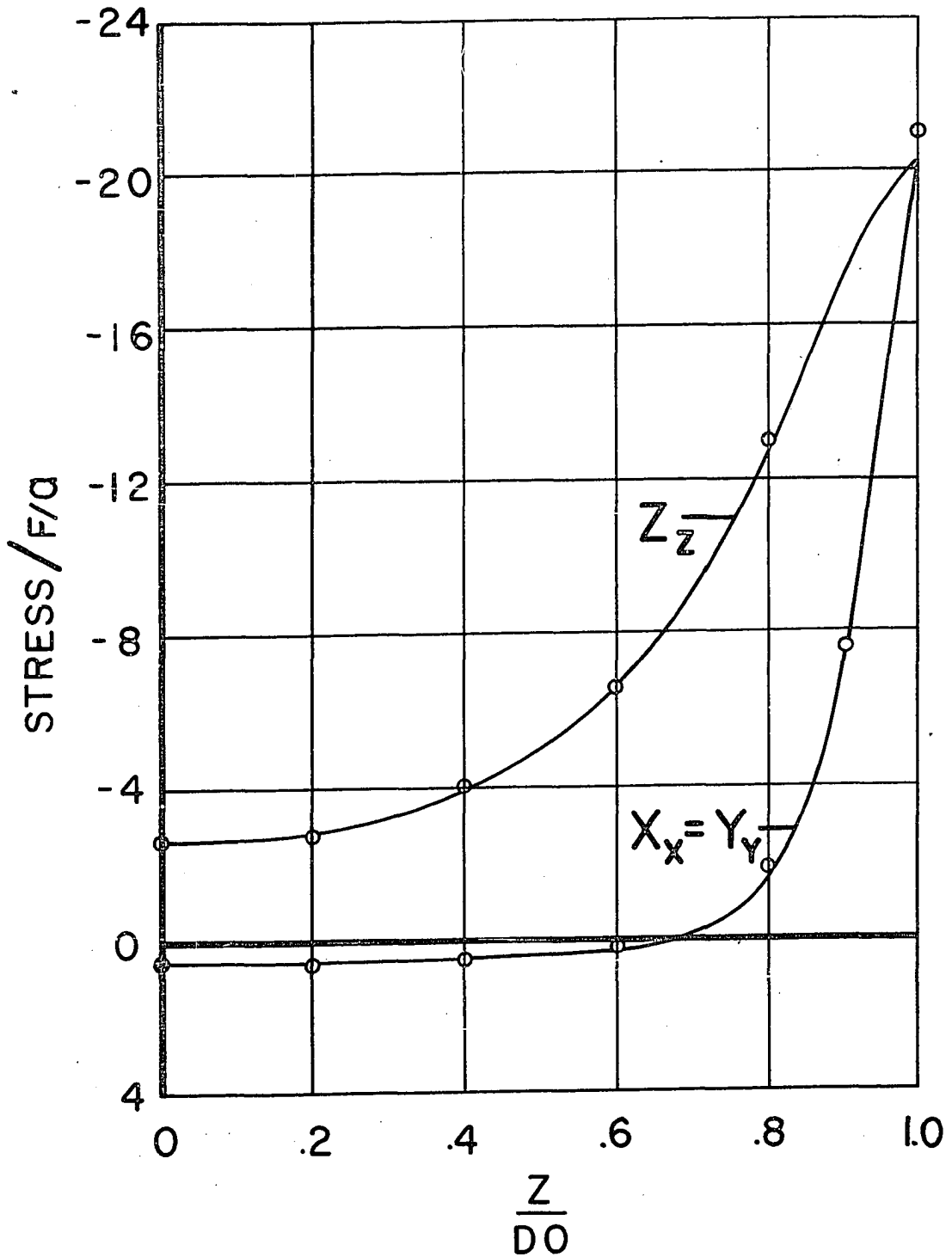


Fig. 10. Distribution of normal stresses Z_z , X_x , Y_y along polar diameter D-D of Fig. 9. Because of rotational symmetry only the portion D0 is considered. After Frocht and Guernsey (1952)

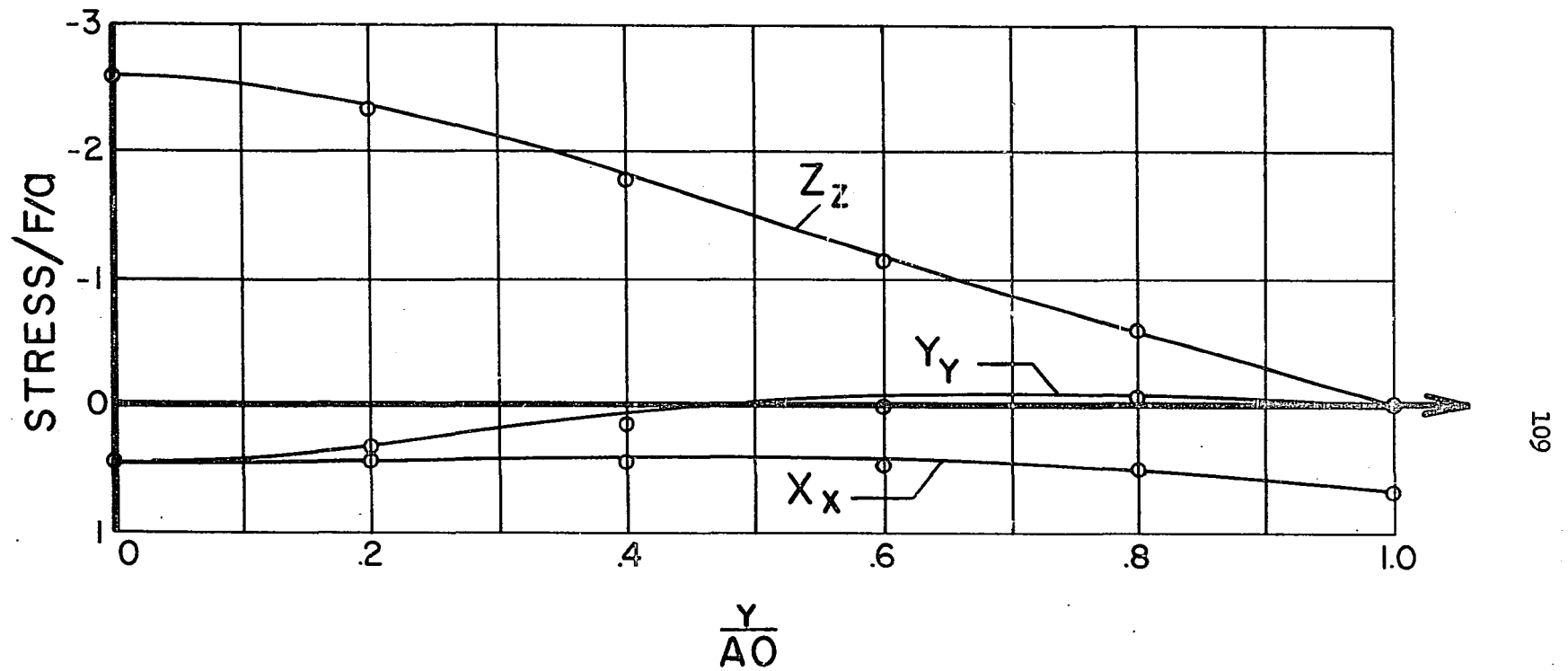


Fig. 11. Distribution of normal stresses along equatorial diameter A-A of Fig. 9. Because of rotational symmetry only the portion AO is considered. After Frocht and Guernsey (1952)

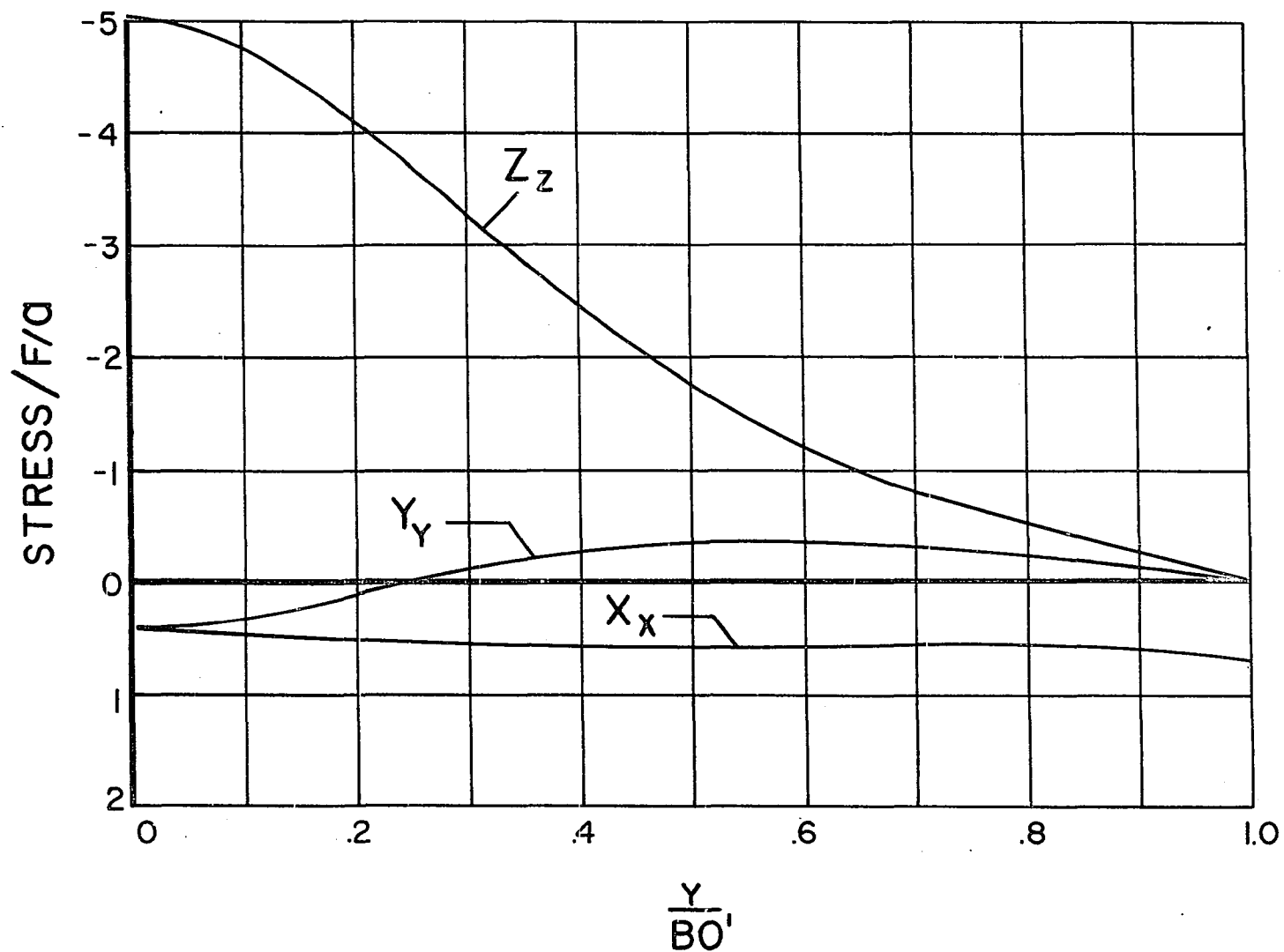


Fig. 12. Distribution of normal stresses along line B-B of Fig. 9. Because of rotational symmetry only the portion BO' is considered. After Frocht and Guernsey (1952)

compared with experimental values obtained by Frocht and Guernsey there is some discrepancy in equatorial plane near the surface of the sphere where the stress is relatively low, but in the neighborhood of the center of the sphere the agreement between theoretical and experimental values is remarkably good. Substituting our previously described (Equation 85a) u -value of 0.5 in Equation 84, rearranging the terms, and remembering that πr^2 represents an area of the equatorial plane (a), we obtain the following equation

$$Z_z = - \frac{3(14 + 2.5)}{2(7 + 2.5)} \left(\frac{F}{a} \right) = - 2.61 \frac{F}{a} \quad (87)$$

which has essentially the same value as Equation 86.

From Equation 85 and Equation 86 we have at the center of the sphere

$$X_x = - \frac{0.45}{2.59} (-Z_z) = 0.1737 Z_z \quad (88)$$

$$Z_z = - \frac{2.59}{0.45} X_x = - 5.7556 X_x \quad (89)$$

Strain

When a body is distorted so that the relative configuration of its component particles is changed in any way, it is said to be strained. Suppose that point 0 represents an initial or "unstrained" position of an element within a body, and 0' represents the final or "strained" position of an element, then vector 00' is called the displacement of the point 0. If the relative displacement can be specified for every point of a body, the state of strain is completely known.

The purpose of any analysis of strain is to define the quantities which give the measure of strain and to discuss the way in which they vary in a neighborhood of a point 0. Two measures of strain that are at once apparent are, first, the change in length of a line or extension and second,

the change of an angle between any two lines, or shear. Let us suppose that d is the distance in the unstrained state between neighboring points O and P and d' is the distance in the strained state between the corresponding points O' and P' . We define e_{OP} as the unit extension corresponding to the points O and P in the unstrained state; that is, we have

$$e_{OP} = \frac{d - d'}{d} \quad (90)$$

The value e_{OP} is the ratio of the change of length to the original length. If a line and plane in three dimensions are perpendicular to one another in the unstrained state and make an angle of $\frac{1}{2} \pi - \theta$ with one another in the strained state, then the amount of shear γ is

$$\gamma = \tan \theta \quad (91)$$

The general theory of strain (Love, 1927) is so complicated as to be beyond the scope of this work. The difficulty results from the fact that straight lines in the unstrained state become curves on straining. We recall here the remarks made earlier concerning the tensile stress distribution X_x along the load axis D-D in Fig. 10. Since the tensile stress X_x is highest at the center of the sphere, we would expect relative displacements around the axis D-D to be in a form of an ellipsoid, assuming homogeneity in the medium.

For practical purposes we can assume a homogeneous strain distribution in the axially loaded sphere. The strain can certainly be taken as homogeneous in a small enough neighborhood around the center of the sphere. The strain is considered homogeneous if, in general, the component displacements can be expressed as linear functions of coordinates (Love, 1927, p. 36). Under these conditions a sphere would be transformed into an

ellipsoid, and any three orthogonal diameters of the sphere would be transformed into three conjugate diameters of the ellipsoid.

The three orthogonal diameters as applied to the problem of a sphere subjected to diametral compressive loads represent the three mutually orthogonal directions of principal strains. These principal strains are oriented along the coordinate axes of the sphere in the same direction as the corresponding principal stresses. At the center of the sphere shear strains vanish and the problem resolves itself into the principal crushing strain e_z in the equatorial plane and the principal tensile strain, e_x , in the polar plane.

Hooke's law The relationship between the components of stress and the components of strain has been established experimentally and is known as the generalized Hooke's law (Timoshenko, 1934, p. 7). If we imagine a sphere subjected to the diametral compressive loads as described before, then the neighborhood of the center of the sphere is subjected to the normal compressive stress Z_z and the tensile stress X_x . It has been shown experimentally that for an isotropic material these normal stresses do not produce any distortion of angles in the equatorial plane. We have assumed that a spherical soil aggregate is regular and homogeneous (see General Concepts section at the beginning of Theory III). Composition may vary between aggregates but each individual member may be considered reasonably uniform, especially in the neighborhood of the center. This neighborhood can be made as small as we please. Then we have

$$E_z = - \frac{Z_z}{e_z} \quad (92)$$

where E_z is the average modulus of elasticity in compression in the

equatorial plane, and e_z is the principal strain normal to the equatorial plane. In the discussion that follows, Z_z is the average crushing stress and e_z is the average crushing strain. When crushing stress exceeds the crushing strength of the material, fracture results. The value of crushing stress at rupture Z_{zr} is the measure of crushing strength. The values for Z_{zr} , Z_z and e_z , e_{zr} (crushing e_{zr} strain at rupture) have been determined experimentally and are presented in the section on results.

The meaning of the term average is not to be taken as representing the average E_z over the area of the equatorial plane. The meaning of average is this: for each aggregate we have a set of values for strain e_z and stress Z_z obtained from readings at equal intervals of time under the conditions of constant diametral loading (see Methods). Strain e_z and stress Z_z are averaged for each aggregate. Average strains and stresses for each aggregate are then averaged for a Size-density subgroup. Their ratio gives an E_z value for a subgroup.

Strains and stresses are also averaged for each Size or Density group consisting of several subgroups (see Methods) giving the values of e_z and Z_z referred to here. Then a ratio of these average values of Z_z and e_z gives the average E_z described. In this sense, values of e_z and Z_z are an average of about 500-800 separate readings for air-dry aggregates. The values e_{zr} and Z_{zr} listed are the average values of strain and stress at rupture averaged as before for each group.

From Equation 88 it follows that

$$X_{xr} = 0.1737Z_{zr} \quad (93)$$

where X_{xr} is called the experimental tensile rupture stress in the polar plane.

The modulus of elasticity in tension E_x can be written

$$E_x = \frac{X_{xr}}{e_{xr}} \quad (94)$$

and

$$E_x = -u \frac{X_{xr}}{e_{zr}} \quad (95)$$

where e_{xr} is the rupture strain in the polar plane, e_{zr} is the rupture strain in the equatorial plane, and u is the Poisson ratio. From Equation 94 and Equation 95 above it follows that

$$u = \left| \frac{e_{zr}}{e_{xr}} \right| \quad (96)$$

We also assume that

$$\frac{X_{xr}}{e_{xr}} = \frac{X_x}{e_x} \quad (97)$$

and

$$-u \frac{X_{xr}}{e_{zr}} = -u \frac{X_x}{e_z} \quad (98)$$

Then using Equations 88, 92, and 98, we obtain

$$0.1737 u \frac{Z_z}{e_z} = 0.1737 u E_z \quad (99)$$

and from Equations 88, 95, and 99, we obtain

$$E_x = 0.1737 u E_z \quad (100)$$

From Equation 94 we have

$$e_{xr} = \frac{X_{xr}}{E_x} \quad (101)$$

or from Equations 100 and 101

$$e_{xr} = \frac{X_{xr}}{0.1737 u E_z} \quad (102)$$

We assume (see discussion below Equation 85b) that at rupture $u = 1/2$. Also we consider E_x to be a function of void ratio (v), porosity (P), size (d), carbon (C) and clay and some constant K . Therefore we may write for computed modulus of elasticity in tension (E_{xc})

$$E_{xc}(v, P, d, C, \text{clay}) = \frac{1}{(v)^a} \times \frac{1}{(P)^b} \times \frac{1}{(d)^c} \times (\text{clay})^d \times (C)^e \times K \dots \quad (103)$$

Void ratio v can be defined as the ratio of the volume of voids V_{voids} , to the volume of solids V_{solids} . Porosity P (see Equation 46) can be defined as the ratio of the volume of voids V_{voids} , to the total volume of a soil aggregate V_{total} , where V_{voids} refers to that portion of the soil aggregate which is not occupied by mineral particles (Terzaghi and Peck, 1948, pp. 25-26). Then we can write

$$P = V_{\text{voids}}/V_{\text{total}} \quad (104a)$$

and

$$v = V_{\text{voids}}/(V_{\text{total}} - V_{\text{voids}}) \quad (104b)$$

or

$$v = V_{\text{voids}}/V_{\text{solids}} \quad (104c)$$

Let us now define aggregate bulk density D (see Equation 45) and aggregate particle density D_s (see Equation 48), in similar terms. Then if W_{solids} represents the weight of the solid material within a soil aggregate we can write

$$D = W_{\text{solids}}/V_{\text{total}} \quad (104d)$$

and

$$D_s = W_{\text{solids}} / V_{\text{solids}} \quad (104e)$$

where V_{total} and V_{solids} are as in Equations 104a and 104c above.

Then from Equations 104a, 104c, 104d and 104e we have

$$v = D_s P / D \quad (104f)$$

Equation 104f can be written

$$v = D_s / (D/P) \quad (104g)$$

and the reciprocal of the quantity in the right hand side of Equation 104g, i.e., $(D/P)/D_s$ will represent the reciprocal of the void ratio, i.e., $1/v$.

Then we can compare computed value from Equation 103, E_{xc} , with experimental value, E_{xe} , given by Equation 100. The percent error will be

$$\frac{E_{xc} - E_{xe}}{0.5(E_{xc} + E_{xe})} \times 100 = \text{percent error} \dots \quad (104h)$$

Similarly for computed tensile stress, X_{xrc} we have

$$X_{xrc}(v, P, d, C, \text{clay}) = \frac{1}{(v)^f} \times \frac{1}{(P)^g} \times \frac{1}{(d)^h} \times (\text{clay})^i \times (C)^j \times K \quad (105)$$

We can compare X_{xrc} (computed) from Equation 105 with X_{xre} (experimental) from Equation 93. The percent error is given by

$$\frac{X_{xrc} - X_{xre}}{0.5(X_{xrc} + X_{xre})} \times 100 = \text{percent error} \dots \quad (106)$$

Finally if we assume that a computed value of rupture strain e_{xrc} is also a function of void ratio porosity, aggregate diameter, carbon and clay contents we can also write

$$e_{xrc}(v, P, d, C, \text{clay}) = \frac{1}{(v)^K} \times \frac{1}{(P)^1} \times \frac{1}{(d)^m} \times (\text{clay})^n \times (C)^q \times K \quad (107)$$

Using Equation 102 we can obtain e_{xre} (experimental rupture strain) and compare it with rupture strain computed (e_{xrc}) from Equation 107 above in the same manner as before (Equations 104h and 106)

$$\frac{e_{xrc} - e_{xre}}{0.5(e_{xrc} + e_{xre})} \times 100 = \text{percent error} \quad (108)$$

Equations 103, 105 and 107 represent the general form of equations for E_{xc} , X_{xrc} and e_{xrc} . We note that the exponents of void ratio v , porosity P , aggregate size d , carbon C and clay can vary. Furthermore the constant K may assume any necessary values provided these values remain the same for each soil tested at a given moisture content. Equation 103 is used in the analysis of aggregate Size groups and in the analysis of a Soil as a whole averaged over Size and Density groups. Equations 105 and 107 are used in the analysis of Density groups. The quantities v , P , d , C , and clay may have different values for the Size groups, Density groups and Soil as a whole. Except for the general similarity of form we should not expect an exact correspondence between respective functions for E_{xc} , X_{xrc} and e_{xrc} .

In conclusion, to test the assumption that $u = 1/2$ at rupture and the assumptions made in Equations 97 and 98 write the expression

$$\left| \frac{e_{xr}}{e_{xrc}} \right| = u \quad (109)$$

then from Equations 96, 97 and 98 we should have

$$\left| \frac{e_z}{e_x} \right| = \left| \frac{e_{zr}}{e_{xr}} \right| = "u" = 1/2 \quad (110)$$

The computed values of "u" testing the assumption that $u = 1/2$ are presented in the Results.

Griffith theory of brittle rupture (Griffith 1921 and 1924)

The attempts to calculate the tensile strength of crystals usually give higher results than those observed experimentally. This kind of discrepancies attracted the attention of Griffith (1921 and 1924) and led him to formulate his crack hypothesis. According to this hypothesis, fine cracks in the surface of the material result in building up of local stresses at the apex of each crack^a. When a value of the stress at the apex reaches the tensile strength of the material, fracture takes place. It should be pointed out that Griffith also stated that tensile stresses are developed in a specimen undergoing compression, this fact is of fundamental importance both in this section and the preceeding section (see General Concepts of elastic theory) and can be readily seen from photo-elastic results of Frocht and Guernsey (1952) (see Fig. 10, Fig. 11 and Fig. 12). Griffith considers a crack of the length L to be a very narrow elliptical hole with the major axis perpendicular to the direction of the tensile force. For a plate of unit thickness this "Griffith crack" results in the reduction of initial strain energy (Timoshenko, 1934, p. 144) U

^aWe assume fine cracks to exist in the neighborhood of the center of a spherical aggregate. This view is more consistant with the geometry of the sphere and tensile stress distribution along the load axis (see Fig. 10).

$$\frac{dU}{dL} dL = \frac{\pi L X_x^2}{4E_x} dL \quad (111)$$

Here L is the length of the crack, i.e., its major axis. The loaded edges of the plate are fixed, the body forces can be neglected, external forces do not produce work, and the potential energy of the system remain unchanged. Then the critical value of the tensile stress X_{xr} is that value of stress at which the reduction of strain energy resulting from the spreading of the crack is equal to the increase of surface energy (T) due to fracture. Using Equation 111, we have

$$\frac{dU}{dL} dL = \frac{\pi L X_{xr}^2}{2E_x} dL = 2 dLT \quad (112)$$

or

$$X_{xr} = \left(\frac{4E_x T}{\pi L} \right)^{1/2} \quad (113)$$

It follows directly from this result that in a uniformly and increasingly stressed specimen one of the largest and most suitably oriented cracks will be the first to spread. The rupture stress X_{xr} will then depend on the size of this crack. If we suppose that the largest cracks are equal to the size of the specimen, then the applied stress per unit area at rupture would vary inversely as the square root of specimen size (Millard et al., 1955).

We have noted previously the distribution of tensile stress (X_x) about the load axis D-D (Fig. 10) for a diametrically loaded sphere, after Frocht and Guernsey (1952). We postulate an existence of an elliptical crack in the polar plane with the major axis oriented along the load axis D-D. In

particular in the immediate neighborhood of the center of the sphere, the conditions outlined above are assumed to exist, i.e., the neighborhood of the center of the sphere is subjected to plane tensile stress. If we further assume the length of the crack to be equal to the soil aggregate diameter d , we can write Equation 113 as

$$X_{xr} = \left(\frac{4E_x T}{\pi d} \right)^{1/2} \quad (114)$$

where T is equal to energy of rupture in ergs cm^{-2} ; rupture stress X_{xr} , modulus of elasticity in tension E_x and d have been defined before.

Suppose we write Equation 114 as

$$X_{xr} = E_x A/d^{0.5} \quad (115)$$

where A is a constant characteristic of the soil and moisture content.

From Equations 114 and 115 we have

$$T = \frac{\pi E_x A^2}{4} \quad (116)$$

Also using Equation 101 and Equation 115, we obtain for a computed value (e_{xrc}) of rupture strain

$$e_{xrc} = A/d^{0.5} \quad (117)$$

Then the value of " u " can be computed from Equation 110.

Influence of moisture on soil aggregate strength

Equation 103 describes E_x as a function of void ratio (v), porosity (P), size (d), carbon (C) and clay content. On contact with water, soil aggregates expand. As a result of expansion we would expect a change in volume ΔV for a spherical aggregate to be given by

$$\Delta V = 0.1667 \pi (d_2^3 - d_1^3) \quad (118)$$

where d_1 is the aggregate diameter at the initial moisture content (here air-dry) and d_2 is the aggregate diameter at the final moisture content (here 15 atm. moisture tension). Change of volume equals the new pore space created on swelling; then we can write ΔP as a change in pore space per unit volume

$$\Delta P = \Delta V / 0.1667\pi d_1^3 \quad (119)$$

or using Equation 118

$$\Delta P = (d_2^3 - d_1^3) / d_1^3 \quad (120)$$

Corresponding to d_1 and d_2 we will have P_1 , P_2 , and D_1 , D_2 where here the P's and D's refer to initial and final states of porosity and bulk density respectively. Pertinent equations are

$$P_2 = P_1 + \Delta P \quad (121)$$

$$D_2 = (1 - P_2) D_s \quad (122)$$

Here Equation 122 has the same form as Equation 49 and D_s is particle density of a given group of aggregates. Using the experimental values of d_1 and d_2 and Equations 121 and 122, we assume the relation

$$E_x(2) = E_x(1) \times \left(\frac{D_2 P_1}{D_1 P_2} \right)^a \times \left(\frac{P_1}{P_2} \right)^b \times \left(\frac{d_1}{d_2} \right)^c \quad (123)$$

Here again $E_x(1)$ and $E_x(2)$ refer to the modulus of elasticity in tension at initial and final moisture contents respectively. Corresponding to Equations 115, 116 and 117 we will have

$$X_{xr}(2) = E_x(2) A_2 / d_2^{0.5} \quad (124)$$

$$T_2 = \frac{\pi E_x A_2^2}{4} \quad (125)$$

$$e_{xr}(2) = A_2/d_2^{0.5} \quad (126)$$

then

$$\Delta T = \frac{\pi}{4} (A_{2E_x}^2(2) - A_{1E_x}^2(1)) \quad (127)$$

or

$$\Delta T = T_2 - T_1 \quad (128)$$

and for "u"₂ we have (compare with Equation 110)

$$"u"_2 = |e_{zr}(2)/e_{xrc}(2)| \quad (129)$$

From the change in size ($d_2 - d_1$) we can compute the strain induced by swelling e_{zi} where

$$e_{zi} = (d_2 - d_1)/d_1 \quad (130)$$

Finally we can express as the "percent of stable aggregates" that fraction of the total number tested (aggregates at 15 atm. moisture tension) which gives non-zero stress values

$$\text{Percent stable aggregates} = \frac{N - N_0}{N} \times 100 \quad (131)$$

Here N is the total number of aggregates in a given group; and N_0 is a number of aggregates that gave zero stress values.

Statistical theory of the strength of materials (Weibull, 1939a and 1939b)

Ultimate strength of a material can be determined, according to the classical theory, by the internal stresses at a point. We assume that a suitable combination of the three principal stresses (for example see Equation 83) or strains will result in a value of strength that is characteristic for a given material. Experimental values give results which often do not agree with theory. Weibull assumes that the probability of rupture

S, at any given distribution of stresses Z^a over the volume V is determined by the equation

$$\log(1 - S) = - \int_V f(Z) dV \quad (132)$$

Here $f(Z)$ is a function characteristic of each particular material.

Equation 132 can be written

$$S = 1 - \exp[- \int_V f(Z) dV] = 1 - \exp [-Vf(Z)] \quad (133)$$

consequently

$$\log \log \frac{1}{1-S} = \log f(Z) + \log V \quad (134)$$

It follows that if $\log \log \frac{1}{1-S}$ (log to the base 10 is taken for convenience) is plotted as an ordinate against arbitrary function $f(Z)$ as an abscissa in the system of rectangular coordinates, the variation of volume V of the test specimen will imply parallel displacement but no deformation of the distribution function. The characteristic function $f(Z)$ is assumed to have the form

$$f(Z) = \left(\frac{Z - Z_u}{Z_o} \right)^m \quad (135)$$

Taking $f(Z) = (Z - Z_u)$ as abscissa, the distribution function will be linear since

$$\log \log \frac{1}{1-S} = m \log(Z - Z_u) - m \log Z_o + \log V \quad (136)$$

In applying this method we have to solve graphically for Z_u . When $\log \log \frac{1}{1-S}$ is plotted against $\log Z$ and the figures happen to follow a straight line then we have $Z_u = 0$. If on the other hand the test data

^aHere we consider crushing stress Z_{zr}

are located on a curved line we have $Z_u \neq 0$, a test value is taken for Z_u until a plot of $\log \log \frac{1}{1-S}$ against $\log (Z - Z_u)$ gives a straight line. It should be mentioned that our values of Z are negative, hence a negative value of Z_u is subtracted and a positive value of Z_u is added in $(Z - Z_u)$.

We then proceed to determine the two remaining constants Z_0 and m . To determine Z_0 we observe that $\log \log \frac{1}{1-S} = 0$ when $S = 0.90$. If the plot is made on a log log paper, the value of Z_0 is read off directly at the ordinate $\log \frac{1}{1-S} = 1$. The value of Z_0 at the probability of rupture $S = 0.90$ will be referred to subsequently as aggregate ultimate crushing strength. We can then compute the slope m from the equation

$$m = (\log \log 1/(1-S)) / [\log(Z - Z_u) - \log Z_0] \quad (137)$$

Having presented the general outline of Weibull's theory, we refer the reader to the Equation 132 and outline briefly how the function specified by Equations 132 through 135 arises in the first place. If N is the number of individual measurements of rupture stress Z_{zr} the ordinate S (probability of rupture) between 0 and 1 is divided into N equal intervals, and N values of rupture stress are arranged in the order of increasing magnitude. The centers of N intervals determine the ordinates for corresponding values of Z_{zr} . This results in an s-shaped curve in rectangular coordinates which can be described by $S = 1 - \exp(-f(Z))$. The specialization of the function $f(Z)$ in Equation 135 completes the calculations.

Weibull regards the slope m of the line computed from Equation 137 as characteristic of the material. Weibull lines offer the simplest method of obtaining any b-size distribution curve from any a-size distribution curve (Evans and Pomeroy, 1958). For example, suppose we have a distribution curve for our Clarion s.l. Size-group 1 (0.227 cm in diameter) we

label it "a-size distribution". Then from Size group 1 distribution curve (a-size distribution) the distribution curve for any other size group (b-size distribution) can be obtained from Weibull's theory by computing the shift of Weibull lines described by Equations 134 and 136.

The calculated shift CS on Weibull lines at $S = 0.5$ parallel to the horizontal axis, can be written

$$CS = (1/m) \log (d_b/d_a) \quad (138)$$

where d_a and d_b represent aggregate diameter of an a-size and b-size distribution.

If more than one distribution is known and plotted the observed shift OS at $S = 0.5$ in cycles of logarithms can be read off directly from respective plots of the distributions concerned and compared with the calculated shift CS.

Finally we observe that since S is the probability of rupture, $1 - S$ is the probability of survival. By extrapolation we can determine the size of an aggregate that has a 0.90 chance of survival (referred to as an ultimate aggregate) at the average value of rupture stress, $\text{ave. } Z_{zr}$, for a given soil. The computation is carried on in a following manner. We draw a straight line through $S = 0.90$ ordinate with the same slope as the average slope for the soil as a whole. At $S = 0.5$ the observed shift OS in cycles of logarithms between that line (a-size line), and a line of b-size line is measured. Letting the size of the ultimate aggregate be d_u , from Equation 138 we have

$$d_u = d_b / \text{antilog}(m(OS)) \quad (139)$$

Presentation of Weibull's theory completes our theoretical treatment

of aggregate rupture. The detailed computed values of strength parameters in Appendix I, Appendix II and Appendix III as well as the principal values of strength parameters abstracted from the appendices and presented in the Results are calculated on the basis of Equations 84 through 139 discussed and derived in this section.

RESULTS

Experimental data for Clarion sandy loam (s.l.), Webster clay loam (c.l.) and Luton silty clay (si.c.) are presented in the tables and figures which follow. The data deal separately with three aspects of the problem. First, the influence of soil aggregate size on the soil aggregate strength is examined. Second, the effect of soil aggregate density on soil aggregate strength is studied. Third, the influence of the type of soil on the soil aggregate strength is considered. In each of the above three aspects, effects of carbon and clay content are evaluated, and the relations between the strength in the air-dry state and at 15 atm. moisture tension as well as water stability figures are examined.

Detailed results and calculations based on the equations derived in Theory III section are presented in Appendix I (for aggregate Size groups), in Appendix II (for aggregate Density groups), and in Appendix III (for the Soils as a whole). Finally, in Appendix IV the analyses of variance for the variables studied are given.

In the presentation that follows we have attempted to summarize the results presented in the appendices emphasizing the most important aspects of this research.

We recall here that density, porosity, void ratio, moisture content, carbon content, clay content, and water stability pertain to a given Size group or Density group of aggregates as a whole. On the other hand, strength measurements represent average values of measurements on individual aggregates. We also recall that experimental results for Z_{zr} , Z_z , e_{zr} and e_z are for the values of these quantities (see Appendix V, List of

symbols) in the equatorial plane at the center of a spherical soil aggregate. Directionally these quantities are oriented along the z-axis (for location of z-axis see Fig. 8c). The values thus given are associated with crushing strength of a soil.

We have observed experimentally that the plane of fracture is the polar plane. Making use of the proportionality constant 0.1737 (see Theory III), the values of Z_{zr} and E_z ($E_z = Z_z/e_z$) in equatorial plane (see Appendix V, List of symbols) are converted into the values of rupture stress, X_{xr} , and stress/strain ratio, E_x , in the polar plane at the center of an aggregate. The values thus obtained represent tensile strength of the soil and lend themselves more easily to the theoretical treatment proposed by Griffith (1921 and 1924). Furthermore, the connection established between tensile strength of soil and void ratio, porosity, clay, and carbon contents can be more readily understood and explained.

Influence of Aggregate Size on Aggregate Strength

The presentation of results in this section falls into six distinct phases. In the first phase for each size group of every soil tested: (1) we give the values for aggregate diameter (Table 18); (2) we establish what percentage of the total soil it constitutes (Table 19); (3) we test the theoretical assumption that the stress/strain ratio remains constant as the load is applied (Table 20), and (4) we present results for rupture stress and rupture strain in equatorial plane at the center of the aggregate (Table 21).

In the second phase for each size group of every soil: (1) we establish the relationship between modulus of elasticity in tension and void

ratio, porosity, size, clay, and carbon contents (Table 22), and (2) we test the assumption that a change in void ratio, porosity, and size resulting from an increased moisture content is a measure of reduction in the modulus of elasticity in tension (Table 23).

In the third phase for each size group of every soil tested: (1) we use Griffith crack theory to compute tensile strength of soil in air-dry condition (Table 24) and at 15 atm. moisture tension (Table 25); (2) we use Griffith crack theory to compute the values of rupture strain in polar plane and we test the assumption (see Theory III, below Equation 85b) that $u = 1/2$ (Table 26) and (3) we use Griffith crack theory to compute the change in energy of rupture (Table 27).

In the fourth phase for each size group of every soil tested: (1) we compare the strain induced by swelling with average strain (Table 28) and (2) we compare the percent of stable aggregates with the percent of water stable aggregates (Table 29).

In the fifth phase for each size group of every soil tested: (1) we use Weibull theory to obtain slopes of Weibull lines and an absolute value for an aggregate crushing strength (Table 30); (2) we use Weibull theory to compute the shift of Weibull lines with size (Table 31), and (3) we compute the size of ultimate aggregate (Table 32).

Finally in the sixth phase for each size group of every soil we present (Table 33) the values of tensile strength and crushing strength in psi.

Table 18a. Experimental values of average aggregate size (diameter d)^a for Size groups of Clarion s.l., Webster c.l. and Luton si.c. aggregates in air-dry condition (diameters d_1) and at 15 atm. moisture tension (diameters d_2)^b

Size group	Clarion s.l.		Webster c.l.		Luton si.c.	
	d_1	d_2	d_1	d_2	d_1	d_2
1	0.227	0.222	0.233	0.228	0.231	0.249
2	0.347	0.369	0.343	0.386	0.353	0.399
3	0.507	0.511	0.579	0.616	0.532	0.615

^aArithmetic mean of measured sizes using the ring strain gauge described in the Methods section.

^bData abstracted from Appendix I, Table 52.

Table 18b. The arithmetic, geometric and harmonic means of aggregate sizes as computed from sieve openings for the three Size groups of Table 18a

	Group number	1	2	3
	Sieve opening	0.200-0.283	0.283-0.476	0.476-0.800
Mean				
Arithmetic mean		0.242 ^a	0.380	0.638
Geometric mean		0.238 ^b	0.367	0.617
Harmonic mean		0.234 ^c	0.355	0.595

$$^a(.200 + .283)/2 = .242$$

$$^b(.200 \times .283)^{1/2} = .238$$

$$^c(((.200)^{-1} + (.283)^{-1})/2)^{-1} = .234$$

Table 19. Weight percent, WP, of the three size groups of Clarion s.l., Webster c.l. and Luton si.c.^a

Size group	Clarion s.l.	Webster c.l.	Luton si.c.
	%		
1	18.4	18.2	17.3
2	38.2	42.1	47.5
3	20.7	35.2	35.1
Other	23.3	5.9	0.0

^aData abstracted from Appendix I, Table 52.

Table 20. Modulus of elasticity in compression (average value of stress/strain ratio) E_z^a , and value at rupture E_{zr}^b , for the respective Size groups of Clarion s.l., Webster c.l. and Luton si.c. aggregates in air-dry condition and at 15 atm. moisture tension^c

	Clarion s.l.		Webster c.l.		Luton si.c.	
Size group	E_z	E_{zr}	E_z	E_{zr}	E_z	E_{zr}
	$\times 10^8 \text{ dyn. cm.}^{-2}$		$\times 10^8 \text{ dyn. cm.}^{-2}$		$\times 10^8 \text{ dyn. cm.}^{-2}$	
Aggregates in air-dry condition						
1	0.73	0.74	1.67	1.59	4.87	5.40
2	1.09	1.07	1.78	1.71	3.81	4.18
3	0.91	0.87	1.62	1.56	3.12	3.25
Aggregates at 15 atm. moisture tension						
2	0.17	0.19	0.13	0.13	0.21	0.23
3	0.23	0.25	0.08	0.08	0.09	0.09

$$^a E_z = Z_z / e_z$$

$$^b E_{zr} = Z_{zr} / e_{zr}$$

^cFor values of Z_z , e_z , Z_{zr} , and e_{zr} see Appendix I, Table 53.

Table 21. Rupture stress (crushing strength) Z_{zr} and rupture strain e_{zr} on the equatorial plane, for the respective Size groups of Clarion s.l., Webster c.l., and Luton si.c. aggregates in the air-dry condition and at 15 atm. moisture tension^a

Size group	Clarion s.l.		Webster c.l.		Luton si.c.	
	Z_{zr}	e_{zr}	Z_{zr}	e_{zr}	Z_{zr}	e_{zr}
	dyn.cm. ⁻²	cm.cm. ⁻¹	dyn.cm. ⁻²	cm.cm. ⁻¹	dyn.cm. ⁻²	cm.cm. ⁻¹
	$\times 10^6$	$\times 10^{-2}$	$\times 10^6$	$\times 10^{-2}$	$\times 10^6$	$\times 10^{-2}$
Aggregates in air-dry condition						
1	5.68	7.64	16.26	10.22	60.96	11.24
2	6.45	6.01	13.47	7.87	35.49	8.50
3	4.66	5.33	11.18	7.16	26.65	8.21
Aggregates at 15 atm. moisture tension						
2	1.09	5.68	1.21	9.31	3.76	16.33
3	1.10	4.44	0.69	8.25	0.98	11.03

^aData abstracted from Appendix I, Table 53.

Table 22. Modulus of elasticity in tension given by the stress/strain ratio on the polar plane: computed E_{xc}^a values are compared with experimental E_{xe} values for the respective Size groups of Clarion s.l., Webster c.l., and Luton si.c. aggregates in air-dry condition^b

Soil	Size group	E_{xc}	E_{xe}	Error %
		$\times 10^6$	dyn. cm. ⁻²	
Clarion s.l.	1	6.34	6.34	0.0
	2	9.43	9.47	-0.3
	3	7.91	7.91	0.0
Webster c.l.	1	14.66	14.51	+1.1
	2	15.27	15.46	-1.2
	3	14.31	14.07	+1.7
Luton si.c.	1	43.94	42.30	+3.8
	2	31.66	33.09	-4.4
	3	28.00	27.10	+3.3

$$E_{xc}^a (\text{Clarion}) = (v)^{-0.5} \times P^{-2.0} \times d^{-0.25} \times (\text{clay}/C^{2.0})^{3.0} \times K,$$

$$\text{where } K = 0.08 \times 10^2 \text{ dyn. cm.}^{-2}$$

$$E_{xc} (\text{Webster}) = (v)^{-0.5} \times P^{-2.0} \times d^{-0.25} \times (\text{clay}/C)^{2.0} \times K,$$

$$\text{where } K = 8.30 \times 10^3 \text{ dyn. cm.}^{-2}$$

$$E_{xc} (\text{Luton}) = (v)^{-0.5} \times P^{-2.0} \times d^{-0.375} \times (\text{clay} \times C) \times K,$$

$$\text{where } K = 5.80 \times 10^7 \text{ dyn. cm.}^{-2}$$

^bFor detailed computations see Appendix I, Table 54, Table 56, and Table 58.

Table 23. Modulus of elasticity in tension given by the stress/strain ratio on the polar plane: computed values E_{xc}^a are compared with experimental values E_{xe} for the respective Size groups of Clarion s.l., Webster c.l., and Luton si.c. aggregates at 15 atm. moisture tension^b

Soil	Size group	E_{xc}	E_{xe}	Error
		<hr/>		
		$\times 10^6 \text{ dyn. cm.}^{-2}$		
Clarion s.l.	2	1.79	1.48	18.9
	3	6.41	2.00	-
Webster c.l.	2	1.08	1.13	4.5
	3	3.29	0.70	-
Luton si.c.	2	1.69	1.83	8.0
	3	0.81	0.78	3.8

$$^a E_{xc}(2) = E_{xc}(1) \times (v_1/v_2)^{0.5} \times (P_1/P_2)^{2.0} \times (d_1/d_2)^c$$

where $c = 0.250$ for Clarion and Webster and 0.375 for Luton.

^bFor detailed calculations see Appendix I, Table 60.

Table 24. Rupture stress X_{xrc}^a on the polar plane (tensile strength) computed using Griffith crack theory and compared with experimental values X_{xre} , for the respective Size groups of Clarion s.l., Webster c.l., and Luton si.c. aggregates in the air-dry condition^b

Soil	Size group	X_{xrc}	X_{xre}	Error %
$\times 10^6 \text{ dyn. cm.}^{-2}$				
Clarion s.l.	1	0.96	0.99	-2.5
	2	1.16	1.12	+3.8
	3	0.79	0.81	-2.2
Webster c.l.	1	2.82	2.82	0.0
	2	2.48	2.34	+5.8
	3	1.74	1.94	-11.0
Luton si.c.	1	10.46	10.59	-1.2
	2	6.63	6.16	+7.6
	3	4.42	4.63	-4.6

$$^a X_{xrc} = AE_x/d^{0.5}$$

^bFor detailed calculations see Appendix I, Table 55, Table 57, and Table 59.

Table 25. Rupture stress $X_{xrc}(2)^a$ on the polar plane (tensile strength) computed using Griffith crack theory and compared with experimental values X_{xre} , for the respective Size groups of Clarion s.l., Webster c.l., and Luton si.c. aggregates at 15 atm. moisture tension^b

Soil	Size group	$X_{xrc}(2)$	$X_{xre}(2)$	Error
		<hr/>		
		$\times 10^6 \text{ dyn. cm.}^{-2}$		
Clarion s.l.	2	0.177	0.189	-6.6
	3	0.204	0.191	+6.6
Webster c.l.	2	0.226	0.210	+7.3
	3	0.111	0.120	+7.8
Luton si.c.	2	0.564	0.653	-13.0
	3	0.193	0.170	+12.6

$$^a X_{xrc}(2) = A_2 E_x(2) / d_2^{0.5}$$

^bFor detailed calculations see Appendix I, Table 61.

Table 26. Rupture strain e_{xrc}^a values on the polar plane computed using Griffith crack theory and values of " u "^b, for the respective Size groups of Clarion s.l., Webster c.l., and Luton si.c. aggregates in air-dry condition (1), and at 15 atm. moisture tension (2)^c

Soil	Size group	$e_{xrc}(1)$ cm.cm. ⁻¹	" u " ₁	$e_{xrc}(2)$ cm.cm. ⁻¹	" u " ₂
	1	0.1517	0.50	-	-
Clarion s.l.	2	0.1228	0.49	0.1203	0.47
	3	0.1001	0.53	0.1021	0.43
	1	0.1946	0.53	-	-
Webster c.l.	2	0.1604	0.49	0.2013	0.46
	3	0.1235	0.58	0.1592	0.52
	1	0.2470	0.46	-	-
Luton si.c.	2	0.2000	0.43	0.3085	0.53
	3	0.1632	0.50	0.2487	0.44

$$^a e_{xrc} = A/d^{0.5}$$

$$^b "u" = |e_{zr}/e_{xrc}|$$

^cData abstracted from Appendix I, Table 55, Table 57, Table 59, and Table 61.

Table 27. Change in the energy of rupture ΔT^a resulting from the change in moisture content (air-dry to 15 atm. moisture tension), for the respective Size groups of Clarion s.l., Webster c.l., and Luton si.c. aggregates^b

Soil	Size group	T_1	T_2	ΔT
		$\times 10^4 \text{ ergs cm.}^{-2}$		
Clarion s.l.	1	2.65	-	-
	2	3.96	0.62	3.34
	3	3.31	0.84	2.47
Webster c.l.	1	10.09	-	-
	2	10.75	1.40	9.35
	3	9.79	0.86	8.93
Luton si.c.	1	47.06	-	-
	2	36.83	5.49	31.34
	3	30.15	2.27	27.88

$$^a \Delta T = T_1 - T_2$$

$$T_1 = \pi A_1^2 E_x(1)/4 \text{ (air-dry)}$$

$$T_2 = \pi A_2^2 E_x(2)/4 \text{ (15 atm.)}$$

^bData abstracted from Appendix I, Table 55, Table 57, Table 59 and Table 61.

Table 28. Strain induced by swelling e_{zi}^a as a result of increased moisture content at 15 atm. moisture tension compared with the average strain e_z (aggregates in air-dry condition) in equatorial plane for the respective Size groups of Clarion s.l., Webster c.l., and Luton si.c. aggregates^b

Size group	Clarion s.l.		Webster c.l.		Luton si.c.	
	e_{zi}	e_z	e_{zi}	e_z	e_{zi}	e_z
cm. cm. ⁻¹						
2	0.0634	0.0443	0.1253	0.0509	0.1303	0.0780
3	0.0078	0.0358	0.0639	0.0451	0.1560	0.0579

$$^a e_{zi} = (d_2 - d_1)/d_1$$

^bFor detailed calculations see Appendix I, Table 62.

Table 29. Percent stable aggregates SA^a compared with percent water stable aggregates WS for the respective Size groups of Clarion s.l., Webster c.l., and Luton si.c. aggregates^b

Size group	Clarion s.l.		Webster c.l.		Luton si.c.	
	SA	WS	SA	WS	SA	WS
%						
2	54.2	60.1	28.8	47.8	72.5	63.7
3	63.5	59.2	46.9	39.6	60.5	55.3

$$^a \% SA = \frac{N - N_0}{N} \times 100$$

^bFor detailed calculations see Appendix I, Table 62.

Table 30. Slope m of Weibull lines in Fig. 13 and values of the ultimate crushing strength Z_0 at the probability of rupture $S = 0.90$ for Size groups of Clarion s.l., Webster c.l., and Luton si.c. aggregates in air-dry condition and at 15 atm. moisture tension^a

Size group	Clarion s.l.		Webster c.l.		Luton si.c.	
	m	Z_0	m	Z_0	m	Z_0
		dyn.cm. ⁻² x 10 ⁶		dyn.cm. ⁻² x 10 ⁶		dyn.cm. ⁻² x 10 ⁶
Aggregates in air-dry condition						
1	1.42	14.8	0.98	29.0	1.42	112.0
2	1.74	10.2	1.25	26.5	1.60	76.0
3	1.47	8.5	0.82	21.0	1.66	58.0
Aggregates at 15 atm. moisture tension						
2	0.92	2.5	1.36	1.4	0.51	7.0
3	0.84	2.1	1.08	1.0	0.84	1.7

^aData abstracted from Appendix I, Table 63.

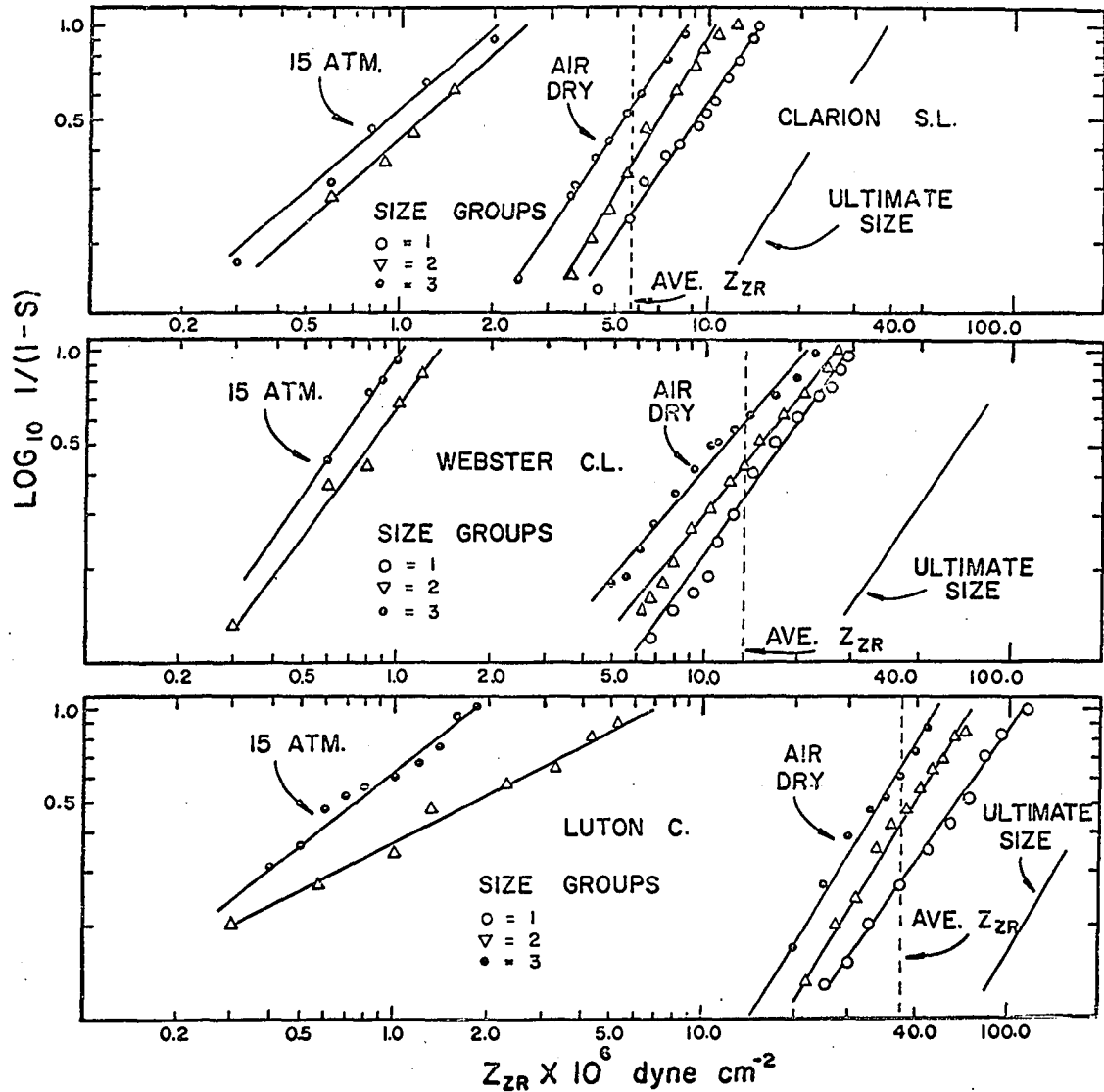


Fig. 13. Weibull lines for Size groups of Clarion s.l., Webster c.l., and Luton si.c. aggregates in air-dry condition and at 15 atm. moisture tension and Weibull lines for ultimate sized aggregates, see text

Table 31. Shift of Weibull lines CS with size of aggregates at the probability of rupture $S = 0.50$ calculated using the footnoted equation below^a and compared with the shift observed, OS, from Fig. 13 for Clarion s.l., Webster c.l., and Luton si.c. aggregates in air-dry condition (1) and at 15 atm. moisture tension(2)^b

Soil	Size range		(1)		Size range		(2)	
	d_a	d_b	OS	CS	d_a	d_b	OS	CS
			unit: one cycle	log scale			unit: one cycle	log scale
	cm.				cm.			
Clarion s.l.	0.227	0.347	0.14	0.12	--	--	--	--
	0.227	0.507	0.26	0.23	--	--	--	--
	0.347	0.507	0.12	0.11	0.369	0.511	0.15	0.16
Webster c.l.	0.233	0.343	0.22	0.16	--	--	--	--
	0.233	0.579	0.46	0.39	--	--	--	--
	0.343	0.579	0.25	0.22	0.386	0.616	0.15	0.17
Luton si.c.	0.231	0.353	0.12	0.12	--	--	--	--
	0.231	0.532	0.20	0.23	--	--	--	--
	0.353	0.532	0.08	0.11	0.399	0.615	0.26	0.28

^a $CS = (1/m) \log (d_b/d_a).$

^bFor discussion of CS see Theory III, Equation 138.

Table 32. Size of ultimate aggregates d_u in microns for Size groups of Clarion s.l., Webster c.l. and Luton si.c. aggregates calculated from the footnoted equation below^a and data from Fig. 13 and Table 30^b.

Size group	Clarion s.l.		Webster c.l.		Luton si.c.	
	(1-S) ^c	d microns	(1-S)	d microns	(1-S)	d microns
Ultimate	0.90	297	0.90	1042	0.90	241
1	0.58	2270	0.46	2270	0.56	2270
2	0.44	3470	0.36	3430	0.40	3530
3	0.29	5070	0.25	5790	0.24	5320

$$^a d_u = d_b / \text{antilog } (m \times OS).$$

^bFor discussion of ultimate size see Theory III, Equation 139.

^cThe quantity (1-S) denotes the probability of survival.

Table 33. Tensile strength X_{xr} and crushing strength Z_{zr} in psi^a for the respective Size groups of Clarion s.l., Webster c.l., and Luton si.c. aggregates in air-dry condition and at 15 atm. moisture tension

Size group	Clarion s.l.		Webster c.l.		Luton si.c.	
	X_{xr}	Z_{zr}	X_{xr}	Z_{zr}	X_{xr}	Z_{zr}
psi						
Aggregates in air-dry condition						
1	14.3	82.4	41.0	235.8	153.5	883.9
2	16.2	93.5	33.9	195.3	89.4	514.6
3	11.8	67.8	17.7	102.1	67.1	386.4
Aggregates at 15 atm. moisture tension						
2	2.7	15.8	3.0	17.5	9.5	54.5
3	2.8	16.0	1.7	10.0	2.5	14.2

^aConversion factors are

$$1 \text{ dyne cm.}^{-2} = 1.45 \times 10^{-5} \text{ lb. in.}^{-2} \text{ (psi)}$$

$$1 \text{ dyne cm.}^{-2} = 1.02 \times 10^{-6} \text{ Kg. cm.}^{-2}$$

$$1 \text{ dyne cm.}^{-2} = 1.00 \times 10^{-3} \text{ millibars}$$

$$1 \text{ dyne cm.}^{-2} = 1.04 \times 10^{-6} \text{ tons ft.}^{-2}$$

$$1 \text{ dyne cm.}^{-2} = 0.99 \times 10^{-6} \text{ atm.}$$

Influence of Aggregate Density on Aggregate Strength

The presentation of results in this section falls into six distinct phases.

The first phase for each density group for every soil tested: (1) we give the values of aggregate bulk density and size (Table 34); (2) we test the theoretical assumption that the stress/strain ratio remains constant

as the load is applied (Table 35), and (3) we present results for rupture stress and rupture strain in an equatorial plane at the center of an aggregate (Table 36).

In the second phase for each density group for every soil tested:

(1) we establish the relationship between tensile strength (Table 37) and void ratio, porosity, size, carbon, and clay contents and between the same variables and the tensile strain, (Table 38); we also test the assumption (see Theory III, below Equation 85b) that $u = 1/2$ (Table 38) and compute the value of modulus of elasticity in tension; (2) we test the assumption that a change in void ratio, porosity, and size resulting from an increased moisture content is a measure of reduction in the magnitude of the modulus of elasticity in tension (Table 39).

In the third phase for each density group for every soil tested: (1) we use the Griffith crack theory to compute the change in the energy of rupture (Table 40).

In the fourth phase for each density group for every soil tested: (1) we compare the percent of stable aggregates with the percent of water stable aggregates (Table 41).

In the fifth phase for each density group for every soil tested: (1) we use the Weibull theory to present slope of Weibull lines and an absolute value for an aggregate crushing strength (Table 42).

Finally, the sixth phase for each density group of every soil we present (Table 43) the values of tensile strength and crushing strength in psi.

Table 34. Density range, D_{range} , and average bulk density, D_{avg} , of aggregates for respective Density groups of Clarion s.l., Webster c.l., and Luton si.c. aggregates in air-dry condition^a

Density group	Clarion s.l.		Webster c.l.		Luton si.c.	
	D_{range}	D_{avg}	D_{range}	D_{avg}	D_{range}	D_{avg}
g. cm.^{-3}						
A	<u>1.74-1.78</u>	1.76	<u>1.62-1.81</u>	1.72	1.94-2.05	2.00
B	<u>1.77-1.82</u>	1.80	<u>1.71-1.88</u>	1.79	2.00-2.06	2.03
C	<u>1.90-1.94</u>	1.92	1.80-1.94	1.87		
D	<u>1.87-2.07</u>	1.97	<u>1.86-2.07</u>	1.97		

^aData abstracted from Theory II, Table 14, and Appendix II, Table 64.

^bThe quantities contained between each set of parallel vertical lines indicate distinct bulk density values for each group. Comparisons are made between groups contained within different sets of parallel vertical lines for every soil. The underlined numbers give a range of aggregate bulk density for a given group.

Table 35. Modulus of elasticity in compression (average^a value of stress/strain ratio), E_z^a , and value of rupture, E_{zr}^b , for the respective Density groups of Clarion s.l., Webster c.l., and Luton si.c. aggregates in air-dry condition and at 15 atm. moisture tension

Density group	Clarion s.l.		Webster c.l.		Luton si.c.	
	E_z	E_{zr}	E_z	E_{zr}	E_z	E_{zr}
	$\times 10^8 \text{ dyn.cm.}^{-2}$		$\times 10^8 \text{ dyn.cm.}^{-2}$		$\times 10^8 \text{ dyn.cm.}^{-2}$	
Aggregates in air-dry condition						
A	0.68	0.69	1.54	1.41	3.93	4.15
B	0.88	0.85	1.33	1.31	4.23	4.67
C	1.03	1.06	1.95	1.92		
D	0.98	0.97	1.99	1.86		
Aggregates at 15 atm. moisture tension						
A	0.22	0.24	0.11	0.10	0.16	0.19
B	0.15	0.21	0.10	0.11	0.15	0.15
C	0.19	0.14	0.12	0.13		
D	0.23	0.28	0.12	0.11		

$$^a E_z = Z_z / e_z$$

$$^b E_{zr} = Z_{zr} / e_{zr}$$

^cFor values of Z_z , e_z , Z_{zr} , and e_{zr} see Appendix II, Table 65.

Table 36. Rupture stress Z_{zr} (crushing strength) and rupture strain e_{zr} in the equatorial plane, for the respective Density groups of Clarion s.l., Webster c.l., and Luton si.c. aggregates in air-dry condition and at 15 atm. moisture tension^a

Density group	Clarion s.l.		Webster c.l.		Luton si.c.	
	Z_{zr}	e_{zr}	Z_{zr}	e_{zr}	Z_{zr}	e_{zr}
	dyn.cm. ⁻²	cm.cm. ⁻¹	dyn.cm. ⁻²	cm.cm. ⁻¹	dyn.cm. ⁻²	cm.cm. ⁻¹
	$\times 10^6$	$\times 10^{-2}$	$\times 10^6$	$\times 10^{-2}$	$\times 10^6$	$\times 10^{-2}$
Aggregates in air-dry condition						
A	4.55	6.60 ^b	12.38	8.76	39.26	9.46
B	5.58	6.59	11.09	8.49	42.82	9.17
C	5.90	5.57	16.67	8.66		
D	6.36	6.53	14.40	7.76		
Aggregates at 15 atm. moisture tension						
A	1.14	4.68	0.82	8.48	3.12	16.82
B	0.91	4.27	0.77	6.98	1.62	10.55
C	0.84	5.98	1.08	8.09		
D	1.50	5.33	1.04	9.17		

^aData abstracted from Appendix II, Table 65.

^bComparisons are made between groups contained within different sets of parallel vertical lines for every soil (see Table 34 footnote b).

Table 37. Rupture stress X_{xrc} on the polar plane (tensile strength) computed for the respective Density groups and compared with the experimental values X_{xre} , for Density groups of Clarion s.l., Webster c.l., and Luton si.c. aggregates in air-dry condition^a

Soil	Density group	X_{xrc}	X_{xre}	Error
		$\times 10^6 \text{ dyn.cm.}^{-2}$		%
Clarion s.l. ^c	A	0.80	0.79	+1.4 ^b
	B	0.99	0.97	+1.8
	C	1.01	1.03	-1.8
	D	1.12	1.11	+1.4
Webster c.l. ^d	A	2.08	2.15	-3.3
	B	1.98	1.93	+2.6
	C	2.68	2.90	+1.4
	D	2.39	2.50	-4.5
Luton si.c. ^e	A	6.80	6.82	-0.3
	B	7.44	7.44	0.0

^aFor detailed calculations see Appendix II, Table 66, Table 68, and Table 70.

^bComparisons are made between groups contained within different sets of parallel vertical lines for every soil (see Table 34 footnote b).

^c X_{xrc} (Clarion) = $(v)^{-1.0} \times d^{-0.75} \times (C/\text{clay}) \times K$
 where $K = 1.77 \times 10^6 \text{ dyn.cm.}^{-2}$

^d X_{xrc} (Webster) = $(v)^{-0.75} \times (\text{clay}/C)^{2.0} \times K$
 where $K = 1.40 \times 10^4 \text{ dyn.cm.}^{-2}$

^e X_{xrc} (Luton) = $(v)^{-1.0} \times d^{-1.0} \times K$
 where $K = 0.92 \times 10^6 \text{ dyn.cm.}^{-2}$

Table 38. Computed rupture strain e_{xrc} on the polar plane is compared with experimental e_{xre} for the respective Density groups of Clarion s.l., Webster c.l., and Luton si.c. aggregates in air-dry condition; respective values of "u"^a are also listed^b

Soil	Density group	e_{xrc} cm.cm. ⁻¹	e_{xre}	Error %	"u"
Clarion s.l. ^d	A	0.1370	0.1338	+2.3	0.48 ^c
	B	0.1206	0.1266	-5.0	0.55
	C	0.1198	0.1146	+4.5	0.47
	D	0.1304	0.1298	+0.5	0.50
Webster c.l. ^e	A	0.1650	0.1608	+2.6	0.53
	B	0.1594	0.1670	-4.5	0.53
	C	0.1664	0.1711	-2.7	0.52
	D	0.1420	0.1445	-2.0	0.55
Luton si.c. ^f	A	0.2004	0.1997	+0.2	0.47
	B	0.2018	0.2023	-0.3	0.45

$$^a \text{"u"} = |e_{xr}/e_{xrc}|$$

^bFor detailed calculations see Appendix II, Table 67, Table 69, and Table 71.

^cComparisons are made between groups contained within different sets of parallel vertical lines for every soil (see Table 34 footnote b).

$$^d e_{xrc} = (v)^{-0.5} \times P^{2.0} \times d \times (C)^{-1} \times K$$

$$\text{where } K = 2.38 \times 10^{-2}$$

$$^e e_{xrc} = (v)^{-1.0} \times P^{1.5} \times (\text{clay})^{3.0}/C^{0.5} \times K$$

$$\text{where } K = 6.254$$

$$^f e_{xrc} = (v) \times d^{-0.5} \times \text{clay} \times K$$

$$\text{where } K = 0.6774$$

Table 39. Modulus of elasticity in tension (stress/strain ratio in polar plane): computed values E_{xc}^a compared with experimental values E_{xe} for Density groups of Clarion s.l., Webster c.l., and Luton si.c. aggregates at 15 atm. moisture tension^b

Soil	Density group	E_{xc}	E_{xe}
		$\times 10^6 \text{ dyn.cm.}^{-2}$	
Clarion s.l.	A	2.93	1.91 ^c
	B	2.96	1.30
	C	8.47	1.65
	D	4.97	2.00
Webster c.l.	A	2.37	0.96
	B	2.14	0.85
	C	1.07	1.04
	D	3.58	1.04
Luton si.c.	A	1.30	1.39
	B	0.77	1.30

$$^a E_{xc}(2) = E_{xe}(1) v_1/v_2 \times P_1/P_2 \times d_1/d_2$$

^bFor detailed calculations see Appendix II, Table 72.

^cComparisons are made between groups contained within different sets of parallel vertical lines for every soil (see Table 34 footnote b).

Table 40. Change in the energy of rupture ΔT^a resulting from a change in moisture content (air-dry to 15 atm. moisture tension) for the respective Density groups of Clarion s.l., Webster c.l., and Luton si.c. aggregates

Soil	Density group	T_1	T_2	ΔT
		$\times 10^4 \text{ ergs cm.}^{-2}$		
Clarion s.l.	A	2.88	0.80	2.08 ^b
	B	3.35	0.54	2.81
	C	4.90	0.69	4.21
	D	3.89	0.84	3.05
Webster c.l.	A	9.00	1.18	7.82
	B	8.79	1.04	7.75
	C	12.46	1.28	11.18
	D	11.05	1.28	9.77
Luton si.c.	A	31.71	4.15	27.56
	B	40.35	3.88	36.47

$$^a \Delta T = (\pi/4)(A_1^2 E_{xe}(1) - A_2^2 E_{xe}(2)) = T_1 - T_2$$

where $A_1 = 0.073$ (Clarion) $A_2 = 0.073$

$A_1 = 0.094$ (Webster) $A_2 = 0.125$

$A_1 = 0.119$ (Luton) $A_2 = 0.195$

and E_x values are taken from Appendix II, Table 72.

^b Comparisons are made between groups contained within different sets of parallel vertical lines for every soil (see Table 34 footnote b).

Table 41. Percent stable aggregates SA computed from the footnoted equation below^a is compared with the percent of water stable aggregates WS^b, for the respective Density groups of Clarion s.l., Webster c.l., and Luton si.c. aggregates

Soil	Density group	Density g. cm. ⁻³	SA	WS
			%	
Clarion s.l.	A	1.76 ^c	66.4	52.4
	B	1.80	60.6	63.9
	C	1.92	53.9	63.1
	D	1.97	54.1	54.5
Webster c.l.	A	1.74	12.5	49.5
	B	1.79	26.3	39.1
	C	1.87	46.5	51.1
	D	1.97	66.5	55.5
Luton si.c.	A	2.00	65.3	63.9
	B	2.03	67.7	55.3

$$^a_{SA} = \frac{N - N_o}{N} \times 100 \text{ (see Theory III, Equation 131)}$$

^bData abstracted from Appendix II, Table 65.

^cComparisons are made between groups contained within different sets of parallel vertical lines for every soil (see Table 34 footnote b).

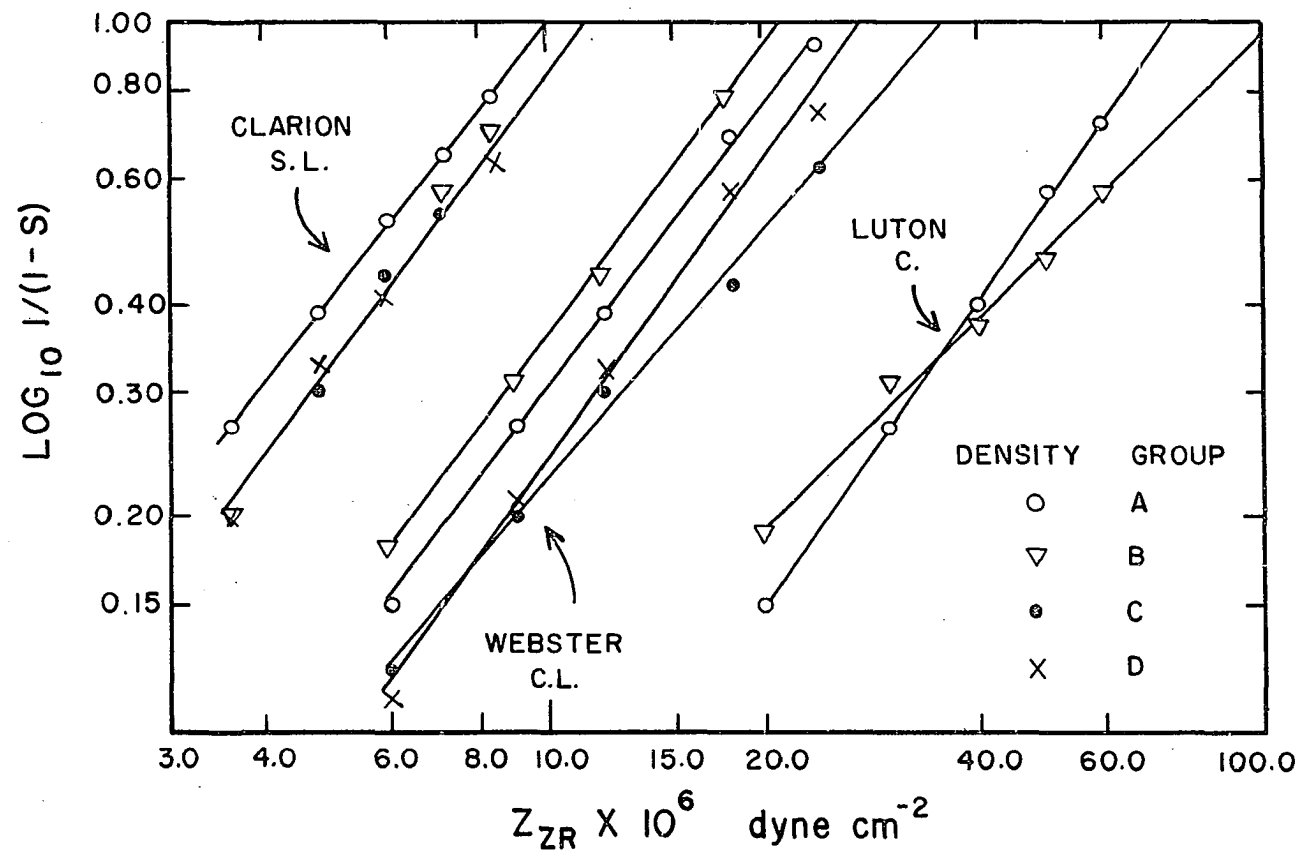


Fig. 14. Weibull lines for Density groups of Clarion s.l., Webster c.l., and Luton si.c. aggregates in air-dry condition, see text

Table 42. Slope m of Weibull lines in Fig. 14 and values of the ultimate crushing strength Z_o at the probability of rupture $S = 0.90$ calculated using Equation 137^a and data in Fig. 14 for the respective Density groups of Clarion s.l., Webster c.l., and Luton si.c. aggregates in air-dry condition

Density group	Clarion s.l.		Webster c.l.		Luton si.c.	
	m	Z_o	m	Z_o	m	Z_o
		dyn.cm. ⁻² x 10 ⁶		dyn.cm. ⁻² x 10 ⁶		dyn.cm. ⁻² x 10 ⁶
A	1.27	10.1 ^b	1.32	24.6	1.42	76.0
B	1.46	10.5	1.32	21.5	0.97	107.0
C	1.36	11.3	1.16	36.0		
D	1.29	11.8	1.39	27.5		

^a $Z_u = 0$ for all Density groups (see Theory III, Equation 137).

^bComparisons are made between groups contained within different sets of parallel vertical lines for every soil (see Table 34 footnote b).

Table 43. Tensile strength X_{xr} and crushing strength Z_{zr} in psi for the respective Density groups of Clarion s.l., Webster c.l., and Luton si.c. aggregates in air-dry condition and at 15 atm. moisture tension

Density group	Clarion s.l.		Webster c.l.		Luton si.c.	
	X_{xr}	Z_{zr}	X_{xr}	Z_{zr}	X_{xr}	Z_{zr}
	psi		psi		psi	

Aggregates in air-dry condition

A	11.5	66.0	31.2	179.5	98.9	569.3
B	14.1	80.9	27.9	160.8	107.9	620.9
C	14.9	85.6	42.0	241.7		
D	16.0	92.2	36.3	208.8		

Table 43. Continued

Density group	Clarion s.l.		Webster c.l.		Luton si.c.	
	X_{xr}	Z_{zr}	X_{xr}	Z_{zr}	X_{xr}	Z_{zr}
	psi ^a		psi		psi	
Aggregates at 15 atm. moisture tension						
A	2.9	16.5 ^b	2.1	11.9	7.9	45.2
B	2.3	13.2	2.0	11.2	4.1	23.5
C	2.1	12.2	2.7	15.7		
D	3.8	21.8	2.6	15.1		

^aConversion factors are listed below Table 33.

^bComparisons are made between groups contained within different sets of parallel vertical lines for every soil (see Table 34 footnote b).

Influence of the Type of Soil on the Aggregate Strength

The arrangement of the data for the soils as a whole follows a general outline similar to that used for Size and Density groups.

In the first phase for every soil we again test the theoretical assumption that the stress/strain ratio remains constant as the load is applied (Table 44), and we present the results for rupture stress and rupture strain in an equatorial plane at the center of the aggregate (Table 45).

In the second phase we evaluate for every soil the effect of void ratio, porosity, size, clay, and carbon contents on modulus of elasticity in tension (Table 46), and we test the assumption that the change in void

ratio, porosity and size resulting from an increased moisture content (air-dry to 15 atm.) is a measure of reduction in the magnitude of the modulus of elasticity in tension (Table 47).

In the third phase for every soil we compute tensile strength using the Griffith crack hypothesis, for air-dry condition (Table 48), and at 15 atm. moisture tension (Table 49); we also present results for the change in energy of rupture (Table 50).

Finally, in the fourth phase for every soil we present (Table 51a) the values of tensile strength and crushing strength in psi.

Table 44. Modulus of elasticity in compression (average value of stress/strain ratio), E_z^a , and value at rupture E_{zr}^b for Clarion s.l., Webster c.l., and Luton si.c. aggregates in air-dry condition (1) and at 15 atm. moisture tension (2)^c

Soil	(1)		(2)	
	E_z	E_{zr}	E_z	E_{zr}
	$\times 10^8 \text{ dyn. cm.}^{-2}$			
Clarion s.l.	0.89	0.89	0.20	0.18
Webster c.l.	1.69	1.62	0.11	0.11
Luton si.c.	4.08	4.40	0.15	0.17

$$^a E_z = Z_z / e_z$$

$$^b E_{zr} = Z_{zr} / e_{zr}$$

^cFor values of Z_z , e_z , Z_{zr} , and e_{zr} see Appendix III, Table 74.

Table 45. Percent clay, rupture stress Z_{zr} (crushing strength) and rupture strain e_{zr} in the equatorial plane for Clarion s.l., Webster c.l., and Luton si.c. aggregates in air-dry condition (1) and at 15 atm. moisture tension (2)^a

Soil	Clay	(1)		(2)	
		Z_{zr}	e_{zr}	Z_{zr}	e_{zr}
		dyn.cm. ⁻²	cm.cm. ⁻¹	dyn.cm. ⁻²	cm.cm. ⁻¹
		$\times 10^6$	$\times 10^{-2}$	$\times 10^6$	$\times 10^{-2}$
Clarion s.l.	15.1	5.60	6.32	1.10	6.06
Webster c.l.	31.4	13.64	8.42	0.95	8.71
Luton si.c.	52.0	41.04	9.32	2.37	13.68

^aData abstracted from Appendix III, Table 74.

Table 46. Modulus of elasticity in tension (stress/strain ratio in polar plane): computed values E_{xc} ^a are compared with experimental values E_{xe} for Clarion s.l., Webster c.l., and Luton si.c. aggregates in air-dry condition^b

Soil	E_{xc}	E_{xe}	Error %
	$\times 10^6 \text{ dyn.cm.}^{-2}$		
Clarion s.l.	7.59	7.96	-4.7
Webster c.l.	15.65	14.66	+6.5
Luton si.c.	34.50	35.43	-2.7

$$^a E_{xc} = (v)^{-1.0} \times \text{clay} \times K_r$$

$$\text{where } K_r = 2.30 \times 10^7 \text{ dyn.cm.}^{-2}.$$

^bFor detailed calculations see Appendix III, Table 75.

Table 47. Modulus of elasticity in tension (stress/strain ratio in polar plane): computed values $E_{xc}(2)^a$ are compared with experimental values $E_{xe}(2)$ for Clarion s.l., Webster c.l., and Luton si.c. aggregates at 15 atm. moisture tension^b

Soil	E_{xc}	E_{xe}
	$\times 10^6 \text{ dyn.cm.}^{-2}$	
Clarion s.l.	4.03	1.74
Webster c.l.	2.09	0.96
Luton si.c.	1.05	1.30

$$^a E_{xc}(2) = E_{xe}(1) \times v_1/v_2 \times P_1/P_2 \times d_1/d_2$$

^bFor detailed calculations see Appendix III, Table 76.

Table 48. Rupture stress X_{xrc}^a in the polar plane (tensile strength) computed using Griffith crack theory and compared with experimental values X_{xre} for Clarion s.l., Webster c.l., and Luton si.c. aggregates in air-dry condition^b

Soil	X_{xrc}	X_{xre}	Error %
	$\times 10^6 \text{ dyn.cm.}^{-2}$		
Clarion s.l.	0.92	0.97	-5.4
Webster c.l.	2.41	2.37	+1.8
Luton si.c.	6.73	7.13	-5.8

$$^a X_{xrc} = AE_x/d^{0.5}$$

where $A = 0.073 \text{ cm.}^{0.5}$ for Clarion s.l.

$A = 0.094 \text{ cm.}^{0.5}$ for Webster c.l.

$\lambda = 0.119 \text{ cm.}^{0.5}$ for Luton si.c.

^bFor detailed calculations see Appendix III, Table 75.

Table 49. Rupture stress $X_{xrc}(2)^a$ in the polar plane (tensile strength) computed using Griffith crack theory and compared with experimental values X_{xre} for Clarion s.l., Webster c.l., and Luton so.c. aggregates at 15 atm. moisture tension^b

Soil	X_{xrc}	X_{xre}	Error %
	$\times 10^6 \text{ dyn.cm.}^{-2}$		
Clarion s.l.	0.191	0.191	0.0
Webster c.l.	0.169	0.165	+2.4
Luton si.c.	0.356	0.411	-14.3

$$^a X_{xrc}(2) = A_2 E_x(2) / d_2^{0.5}$$

where $A_2 = 0.073$ for Clarion s.l.

$A_2 = 0.125$ for Webster c.l.

$A_2 = 0.195$ for Luton si.c.

^bFor detailed calculations see Appendix III, Table 76.

Table 50. Change in energy of rupture ΔT^a resulting from the change in moisture content (air-dry to 15 atm. moisture tension) for Clarion s.l., Webster c.l., and Luton si.c. aggregates^b

Soil	T_1	T_2	ΔT
	$\times 10^4 \text{ ergs cm.}^{-2}$		
Clarion 2.l.	3.69	0.73	2.96
Webster c.l.	10.29	1.18	9.11
Luton si.c.	36.00	4.54	31.46

$$^a \Delta T = T_1 - T_2 = (\pi/4)[A_1^2 E_{xe}(1) - A_2^2 E_{xe}(2)].$$

^bValues $E_{xe}(1)$ and $E_{xe}(2)$ are taken from Appendix III, Table 76 and are the average values for Size group 2 and Size group 3, see note (d) below Table 72 in Appendix II.

Table 51a. Tensile strength X_{xr} and crushing strength Z_{zr} in psi^a of Clarion s.l., Webster c.l., and Luton si.c. aggregates in air-dry condition (1) and at 15 atm. moisture tension (2)

Soil	(1)		(2)	
	X_{xr}	Z_{zr}	X_{xr}	Z_{zr}
	psi		psi	
Clarion s.l.	14.1	81.2	2.8	16.0
Webster c.l.	34.4	197.8	2.4	13.8
Luton si.c.	103.4	595.1	6.0	34.4

^aConversion factors are listed below Table 33.

Statistical

Analysis of variance

In Table 51b below a summary of the analysis of variance over Size and Density treatments is presented. The detailed analysis of variance for each of the variables listed in Table 51b is given in Appendix IV, Table 78 through Table 83.

Table 5lb. Significance level^a for variables of carbon C, clay, water stability WS, crushing strength at rupture Z_{zr} , average crushing strength Z_z , and average strain e_z as obtained from analysis of variance over Size and Density treatments^b for Clarion S.l., Webster c.l. and Luton si.c. aggregates in air-dry condition

Variables	Soils					
	Clarion s.l.		Webster c.l.		Luton si.c.	
	Treatments					
	Size	Density	Size	Density	Size	Density
	Significance level					
C	**	**	NS	**	**	**
clay	NS	*	NS	*	NS	NS
WS	NS	NS	*	NS	*	**
Z _{zr}	**	*	**	**	**	NS
Z _z	**	*	**	**	**	NS
e _z	**	NS	**	NS	**	NS

^aSignificance level: ** significant at 1% level; * significant at 5% level; NS non-significant.

^bTreatments: Three (1,2,3) Size groups and four (A,B,C,D) Density groups.

The analysis of variance tells us that there exists a difference or differences which are significant. Duncan's multiple range test (Duncan, 1955) shows which of the differences are significant. We have used analysis of variance and Duncan's multiple range test for variables listed in Table 5lb. For rupture stress Z_{zr} , average stress Z_z and average strain analysis of variance and Duncan's multiple range test is on aggregates in air-dry

condition only. The reasons for not analyzing data at 15 atm. moisture tension statistically have been given earlier (see Methods: Experimental Design).

In Table 51c Duncan's multiple range test is applied to the Size groups of Clarion s.l., Webster c.l., and Luton si.c., for variables tested by analysis of variance (see Table 51b). Similarly in Table 51d Duncan's multiple range test is applied to Density groups for the same variables as in Table 51c, of the same three soils.

Size groups

Applying Duncan's multiple range test to the respective Size groups of the three soils tested, we have found (see Table 51c) that all values of carbon content for Luton si.c. were significantly different from one another. On the other hand, no significant differences in carbon content between Size groups were observed for Webster c.l., and the value for Size group 1 (1.06%) for Clarion s.l. was significantly greater at 5% level than the other two groups.

We have found no significant differences in clay within the three Size groups of soils tested. Water stability was significantly higher on Size group 2 of Luton si.c. (63.7). Rupture stress was significantly different for each Size group within Luton si.c. and Webster c.l. soils, but on Clarion s.l. only Size group 3 (4.66) was significantly smaller than the other two. The values for average strain were significantly different from one another for all size groups within each soil.

Density groups

Applying Duncan's multiple range test to the respective Density groups of soils tested, we have found (see Table 51d) the values for carbon on

Table 51c. Duncan's multiple range test applied to Size groups, averaged over densities for percent carbon C, percent clay, percent water stable aggregates WS, rupture stress Z_{Zr} , average stress Z_z , and average strain e_z of Clarion s.l., Webster c.l., and Luton si.c. aggregates in air-dry condition. The test is applied to each soil separately

Soil Property	Units of Soil Property	Soil								
		Clarion s.l.			Webster c.l.			Luton si.c.		
		1	2	3	1	2	3	1	2	3
		Values of indicated soil property								
C	%	1.06	<u>0.96</u>	<u>0.95</u> ^a	<u>3.36</u>	<u>3.23</u>	<u>3.18</u>	3.11	2.93	2.84
clay	%	<u>15.7</u>	<u>15.1</u>	<u>14.4</u>	<u>31.2</u>	<u>31.7</u>	<u>31.3</u>	<u>51.8</u>	<u>52.2</u>	<u>52.0</u>
WS	%	<u>56.0</u>	<u>60.1</u>	<u>59.2</u>	<u>56.7</u>	<u>47.8</u>	<u>39.6</u> ^b	<u>59.7</u>	63.7	<u>52.2</u>
$Z_{Zr} \times 10^6$	dyn.cm. ⁻²	<u>5.68</u>	<u>6.45</u>	4.66	16.26	<u>13.47</u>	<u>11.18</u>	60.96	35.49	26.65 ^c
$Z_z \times 10^6$	dyn.cm. ⁻²	<u>4.88</u>	<u>4.85</u>	3.26	12.48	9.06	7.30	38.00	22.04	15.10
$e_z \times 10^{-2}$	cm.cm. ⁻¹	6.70	4.43	3.58	7.47	5.09	4.51	7.80	5.79	4.84

^aUnderlined numbers are not significantly different from one another at 5% level, i.e., 0.96 is not significantly different from 0.95.

^bWhen more than one tier of lines is present interpret each underlining separately, i.e., in this case we would read that 56.7 and 47.8 are not significantly different from one another, also 47.8 and 39.6 are not significantly different from one another, but 56.7 and 39.6 are significantly different from one another at the 5% level.

^cNumbers not underlined by the same line are significantly different from one another at 5% level, i.e., 60.96, 35.49 and 26.65 are all significantly different; in footnote a 1.06 is significantly different from 0.96 and 0.95 at 5% level.

Table 51d. Duncan's multiple range test applied to Density groups averaged over sizes for percent carbon C, percent clay, percent water stable aggregates WS, rupture stress Z_{zr} , average stress Z_z , and average strain e_z of Clarion s.l., Webster c.l., and Luton si.c. aggregates in air-dry condition. The test is applied to each soil

Soil Property	Units of Soil Property	Soil									
		Clarion s.l.				Webster c.l.				Luton si.c.	
		Density group									
		A	B	C	D	A	B	C	D	A	B
		Values of indicated soil property									
C	%	<u>1.00</u>	1.17	<u>0.98</u>	0.80	<u>3.23</u>	<u>3.43^a</u>	2.96	<u>3.43</u>	3.12	2.79
clay	%	<u>16.3</u>	<u>15.6</u>	<u>15.7</u>	12.7	<u>31.8</u>	<u>31.5</u>	<u>31.9</u>	30.4	<u>51.7</u>	<u>52.3</u>
WS	%	<u>52.4</u>	<u>63.9</u>	<u>63.1</u>	<u>54.5^b</u>	<u>49.5</u>	<u>51.1</u>	39.1	<u>55.5</u>	63.9	55.3
$Z_{zr} \times 10^6$	dyn.cm. ⁻²	<u>4.55^c</u>	<u>5.58</u>	<u>5.90</u>	<u>6.36</u>	<u>12.38</u>	<u>11.09</u>	16.67	14.40	<u>39.26</u>	<u>42.82</u>
$Z_z \times 10^6$	dyn.cm. ⁻²	3.65	<u>4.33</u>	<u>4.43</u>	<u>4.92</u>	8.99	7.86	11.42	10.17	<u>23.89</u>	<u>26.20</u>
$e_z \times 10^{-2}$	cm.cm. ⁻¹	<u>5.34</u>	<u>4.94</u>	<u>4.30</u>	<u>5.01</u>	<u>5.84</u>	<u>5.93</u>	<u>5.87</u>	5.12	<u>6.08</u>	<u>6.20</u>

^aUnderlined values are not significantly different from one another at 5% level, i.e., 3.23 and 3.43 are not significant.

^bWhen more than one tier of lines is present, interpret each underlining separately, i.e., 63.9, 63.1, and 54.5 are not significantly different from one another, also 52.4, 63.1, and 54.5 are not significantly different from one another, but 52.4 and 63.9 are significantly different from one another at 5% level.

^cNumbers not underlined by the same line are significantly different from one another at 5% level, i.e., 4.55 is significantly different from 5.58, 5.90 and 6.36 at 5% level.

Luton si.c. to be significantly different from one another. For Webster c.l. the Density group C (2.96) was significantly lower in carbon than the other two. For Clarion s.l. the Density group B (1.17) was significantly higher in carbon while the Density group D (0.80) was significantly lower in carbon than the other groups.

With respect to clay we have found no significant differences between the values of clay for Luton si.c., while the Density group D on both Webster c.l. (30.4) and Clarion s.l. (12.7) gave a significantly lower value for clay than the remaining three groups. Water stability was significantly higher on Density group A of Luton si.c. There were no significant differences between the rupture stress values for Luton si.c. Density groups C and D on Webster c.l. (16.67 and 14.40) gave significantly higher rupture stress values and were also significantly different from one another. Density group A for Clarion s.l. (4.55) was significantly lower in rupture stress than the other three groups. Values of strain for Luton si.c. were not significantly different. On Webster c.l. and Clarion s.l. strain for Density groups D and C, respectively, was significantly lower than for the remaining three Density groups of each soil.

Soil as a whole

The differences observed between the three soils used are so obvious for certain properties that no statistical analysis is necessary to interpret the results. The differences that stand out most clearly are the differences in clay content and average rupture stress. Compare, for example, the values of clay content and the values of rupture stress Z_{2r} for Clarion s.l., Webster c.l. and Luton si.c. in either the Table 51c or Table 51d. We feel that it is the obvious large differences in certain properties

(like for example the differences in clay content) that have a most definite bearing on the strength of soil aggregates of different soils. This viewpoint is demonstrated in the preceding three sections of Results and will be discussed in detail in the Discussion of Results section that follows.

DISCUSSION OF RESULTS

In the discussion of our results we will first consider our findings and, second, we will review the findings of other research workers and compare our results with the results obtained by others. We will follow the same general scheme of presentation as outlined in the results section. Since the results section is a summary of findings presented in detail in Appendix I, Appendix II, Appendix III, and Appendix IV, it will be necessary at times to refer to a specific information contained in the appendix sections as well as other sections of this thesis.

Influence of Aggregate Size on Aggregate Strength

General information

Aggregate size (Table 18a and Table 18b). The average size of aggregates (arithmetic mean) is given in Table 18a for each of the Size groups of every soil. There is a general agreement in size from soil to soil the soils of Size group 1 and Size group 2 in air-dry conditions, but the average sizes for the Size group 3 vary from soil to soil with largest aggregates being found in Webster c.l. and smallest in Clarion s.l. Turning now our attention to the aggregates at 15 atm. moisture tension, we notice (except for decreases for the Size group 1 of Clarion s.l. and Webster c.l.) an increase in aggregate size over the size in air-dry condition. The increase is the smallest for Clarion s.l. and the largest for Luton si.c. The decreases for Clarion s.l. and Webster c.l. ($0.227 - 0.222 = 0.005$ cm. and $0.233 - 0.228 = 0.005$ cm.) are within the experimental error. But the general conclusion remains that the sizes of moist aggregates were larger than the sizes of the air-dry.

In Table 18b we present the arithmetic geometric and harmonic mean values expected for sizes of aggregates based on the diameters of the sieve openings used in separating the aggregates. Comparing the values in Table 18b with our experimental values presented in Table 18a we observe that for aggregates in the air-dry condition (diameters d_1) the sizes of Groups 1 and 2 (0.227, 0.347), (0.233, 0.343), and (0.353), (0.231, 0.353) of all soils most closely approximate the harmonic means (0.234, 0.355) of Table 18b. The Size group 3 values (0.579) for Webster c.l. in air-dry condition is close to the value (0.595) expected as a harmonic mean of that group, but values of Group 3 on both Luton si.c. (0.532) and Clarion s.l. (0.507) are far below it.

For aggregates at 15 atm. moisture content (diameters d_2) the diameter 0.369 cm. of Size group 2 for Clarion s.l. approximates the sieve geometric mean 0.367 cm. The values for Size group 3 of Webster c.l. and Luton si.c. also approximate closely the sieve geometric mean. The values of Size group 1 for Luton si.c. as well as the values of Size group 2 for Webster c.l. and Luton si.c. most closely approximate the sieve arithmetic mean value.

We see from the discussion above that the average size distribution of aggregates varies as the moisture content. In air-dry condition the sizes < 0.476 cm. but > 0.200 cm. in diameter can be reasonably well described by a harmonic mean value of sieving class. For aggregates at 15 atm. moisture tension the size distribution is a function of change in volume and will vary from soil to soil as well as from Size group to Size group, as we have seen above.

It has been shown (Mellor, 1910) that the arithmetic mean is not the

correct representative value for a group containing a large number of aggregates between two limiting diameter values x_1 and x_2 . On the other hand, a harmonic mean of the weight distribution (Herdan, 1960, pp. 32-35) is equal to the mean volume-surface diameter. Since the sieving operation yields weight distribution of aggregate sizes, we might reasonably expect that a harmonic mean of size limits, x_1 and x_2 , should give the average value of the aggregate diameter.

Weight percent, (Table 19). If we examine the results in Table 19 it becomes apparent that the second size group was the largest by weight of all the size groups examined while the first one was the smallest for all soils. For example, on Clarion s.l. compare 38.2 (Group 2) with 18.4 and 20.7 (Groups 1 and 3). Percent of "other" indicates mostly stones. A sandy Clarion soil contained the largest percent of stones while a clay Luton soil contained none. This observation is of great importance in the determination of soil bulk density as we have pointed out earlier (see Theory II, discussion below Table 16).

Early research workers measured the aggregate distributions by sieving soil samples in the field under natural conditions (Keen, 1933). Volkov (1933) first proposed sieving of dry material. Chepil (1951), working with dry aggregate distributions, found that the size fraction > 0.64 cm. in diameter increase for loams and silt loams to around 50% of the total by weight. But for fine sandy loam that size fraction constituted only 17.7%, while for silty clay it was 28.0% of the total. The size of the 0.084 to 0.64 cm. fraction varied in a manner generally similar to that of the > 0.64 cm. fraction but was less than the > 0.64 cm. fraction at all times.

In another study (Chepil, 1952), the size of the 0.238-0.635 cm. fraction of loam and silty clay aggregates (which is comparable to our 0.283-0.476 cm. fraction) was larger than the size fractions above it (0.635-1.270 cm.) or below it (1.19-2.38 cm.). On the other hand, for a sandy loam, silt loam, and silty clay loam the 0.238-0.635 cm. fraction was about midway in size between the other fractions mentioned above.

In view of the discussion above we conclude that on some soils the size fraction 0.283-0.476 cm. may be larger than other fractions. In the following sections we attempt to explain this behavior in terms of results obtained in relation to crushing strength as well as the water stability.

Constancy of the stress/strain ratio, (Table 20) In Table 20 we compare the average value of a stress/strain ratio E_z for a given Size group with a value of stress/strain ratio E_{zr} at rupture. We have assumed in our theoretical development (see Theory III, Equations 97 and 98) that the value of a stress/strain ratio is a constant. On the basis of our experimental results we see that it does indeed remain reasonably constant, particularly for Clarion s.l. and Webster c.l. aggregates, i.e., for Size group 1 of Clarion s.l. in air-dry condition compare 0.73 and 0.74. The greatest departures from constancy are observed for Luton si.c. aggregates in air-dry condition.

Elastic theory is used by soil engineers for estimating stresses caused with a soil by externally applied loads. According to the elastic theory, constant ratios exist between the stresses and strains. If the theory is to be applicable, the real requirement is not necessarily that the material be elastic but that the ratios between the stresses and corresponding strains remain constant. We can therefore apply the so-called

elastic theory to the non-elastic soil material for any cases in which stresses and strains adhere to reasonable constant ratios (Taylor, 1948).

The values of stress/strain ratios obtained by us remain reasonably constant for the Size groups of the respective soils. We will show later that these ratios remain reasonably constant for Density groups and for the Soils as a whole as well. Therefore we feel that the use we have made of elastic theory in the derivation of equations based on Hooke's law is justified.

The possibility that the modulus of elasticity for the soil (stress/strain ratio) might be different in tension from what it is in compression seems to have been overlooked by most research workers. We have derived our theoretical equations (see Theory III) and have calculated our experimental data on the basis of the assumption that the modulus of elasticity in tension for soil aggregates was different from the modulus of elasticity in compression.

When working with slurries or compacting the soil into briquettes, preferential orientation of clay can be induced, affecting the results obtained (Vomocil, 1963). We have found no mention in soils literature, other than indications from Vomocil's (1963) work, that the modulus of elasticity in tension and compression are different from one another. Since the results obtained by us on the basis of this assumption seem to correspond to the independent studies made by others (Grossman and Cline, 1957; Kirkham et al., 1958; Moldenhauer and Long, 1964; Taylor and Gardner, 1963; Gill, 1959) we feel reasonably confident that in so far as the soil aggregates are concerned the assumption is correct.

Crushing strength, (Table 21)

Results for the crushing strength Z_{zr}

of aggregates are presented in Table 21. In general the crushing strength (rupture stress in equatorial plane) decreased as the aggregate size increased, i.e., 16.26, 13.47 and 11.18 for Groups 1, 2 and 3 of Webster c.l. in air-dry condition. The value of crushing strength Z_{zr} for Size group 1 of Clarion s.l. seems to contradict the statement made above. Included in this value however are values of zero stress ($Z_{zr} = 0$) obtained for some aggregates in this group. Were the aggregates exhibiting zero stress excluded, the value for Size group 1 of Clarion would have been 7.10×10^6 dyn.cm.⁻². To obtain a complete description of a soil we have felt that the values of zero stress for aggregates in air-dry condition should be included in the average value for a given sizegroup.

We should note that the values of stress for aggregates at 15 atm. moisture tension are very much lower than for the aggregates in air-dry condition, compare 13.47 with 1.21 for Size group 2 of Webster c.l., and although large differences exist among the soils in air-dry condition, there is little difference between the values of crushing strength at 15 atm. moisture tension. For example, compare the values of Size group 2 on all soils. In air-dry condition we have 6.45, 13.47 and 35.49 while at 15 atm. we have 1.09, 1.21 and 3.76 for Clarion s.l., Webster c.l. and Luton si.c.

Corresponding to the increase in the crushing strength with the decrease in size there is also an increase in strain e_{zr} with the decrease in size, i.e., see the values of 10.22, 7.87 and 7.16 for Webster c.l. in air-dry condition. Comparing the values of strain in air-dry condition and at 15 atm. moisture tension, we notice that the difference between the two is the largest for Luton si.c. (8.50 vs 16.83 for Group 2). On the

other hand, there is little change in strain for a Clarion s.l. (6.01 vs 5.68 for Group 2).

Hooghoudt (1950), in a very extensive study has determined the modulus of rupture by pressure, by smash, by tear, and by bend in an attempt to elucidate the binding forces within the soil.

His research differs from ours in that where we have worked with natural soil aggregates, Hooghoudt employed reworked, puddled and then dried specimens and shaped them into definite geometric shapes. Furthermore, where we have derived our theoretical assumptions and treatment from the theory of elasticity, photoelastic results (Frocht and Guernsey, 1952) and Griffith crack theory, Hooghoudt employed the methods developed by the porcelain and pottery industries and gave no theoretical treatment of his assumptions.

Working with a clay and loam soil, Hooghoudt first destroyed organic matter and CaCO_3 . Controlling the quantity of clay, silt, fine, and coarse sand fractions, he was able to obtain the values of moduli of rupture for samples ranging from 15 to 80% clay. Furthermore, he studied the influence of Ca^{++} , H^+ , Li^{++} , Na^+ , K^+ , Rb^+ , Cs^+ , Mg^{++} , Sr^{++} , Ba^{++} , and La^{++} ions. Finally Hooghoudt made a series of comparisons employing additions of artificial humus.

Hooghoudt found that the moduli of rupture increased directly with clay content and were higher in fine sand samples than in coarse sand samples. The difference between the samples saturated with divalent or trivalent cations was not great. Generally, Mg^{++} gave highest values of the moduli of rupture and Cs^{++} the lowest (about 1/6 the value for Mg^{++}). In the study made with artificial humus additions, Hooghoudt found that it either

decreases the magnitudes or has no influence on the magnitudes of the moduli of rupture.

To measure the modulus of rupture by pressure, Hooghoudt prepared half-balls of three different diameters, sanding the flat surface down to obtain a perfectly smooth contact area between the half-ball and the base plate. Placing the half-balls face down on a base plate, he applied pressure to the curved part with an inverted T shaped stamp. The stamp, driven by a motor, was coupled to a scale and the resistance to fracture was registered directly on a dial in grams. Hooghoudt found that initially as the pressure was applied a curved portion of the half-ball became flattened, giving a contact area that was parallel to the equatorial plane of the half-ball. Following the initial flattening, the scale dial began registering an increase in pressure. Maximum pressure at rupture was recorded by a tell-tale hand that registered the scale reading.

In this way Hooghoudt found that the modulus of rupture by pressure, given as a load in kg. at rupture, was independent of the diameter of half-balls used. These findings are contrary to our results which indicate that the modulus of rupture is size dependent. We feel that Hooghoudt's results for the modulus of rupture by pressure are unrealistic. In the first place his presentation of results in terms of load alone is meaningless. His modulus of rupture by pressure would have been inversely proportional to the area of the surface of contact (Timoshenko, 1934, p. 346) which is not taken into account in his computations. Secondly, Hooghoudt's area of contact would vary not only with the size of the half-balls but also with their relative consistency. These two effects, we feel, are responsible for the lack of any influence due to size of the half-balls and render the

values of the modulus of rupture by pressure questionable. If we were to assume that Hooghoudt's area of contact was within the range of from 1 to 3 cm^2 (1/5 of the area of equatorial plane of half-balls), his results for the modulus of rupture by pressure would be comparable to our values.

Hooghoudt's average values for the modulus of rupture by tear (our tensile strength) are generally higher than the values obtained by us. Where our values range from 1 to $7 \times 10^6 \text{ dyn.cm}^{-2}$ (see values of X_{xr} in Table 48) Hooghoudt's values vary between $4.5 - 18.0 \times 10^6 \text{ dyn.cm}^{-2}$. One possible reason for this is that Hooghoudt used reworked, puddled and then dried soil pastes with no organic matter or CaCO_3 , whereas our aggregates were in a natural state. Also, Hooghoudt's samples were oven dried with 0.5-2.0% moisture content at rupture whereas our values are in air-dry condition, (2-7% moisture content). Finally, if we multiply our values of aggregate ultimate crushing strength Z_o (values of crushing stress at 0.90 probability of rupture), in Table 30 by a constant 0.1737, we get the values of X_o , which correspond to the ultimate tensile strength of the soil aggregates. Using Size group 1, we would get the values of the ultimate tensile strength of 2.57, 5.03, and $19.5 \times 10^6 \text{ dyn. cm}^{-2}$ for Clarion s.l., Webster c.l., and Luton si.c., respectively, which would compare favorably with the range of values ($4.5-18.0 \times 10^6 \text{ dyn. cm}^{-2}$) obtained by Hooghoudt.

On the basis of these comparisons we might expect fair agreement between the work done on reworked, puddled and then dried soil and individual aggregates. Provided the puddled reshaped soil can be treated as a single unit much in the same way as we treat individual aggregates, the agreement will probably be satisfactory. On the other hand, we would expect no agreement if a soil tested were composed of distinct aggregates

which would each have its own characteristics.

It is for these reasons that we disagree with statements made by some research workers (McMurdie, 1963) who state that since deformation by tri-axial compression test of a soil was found to be non-linear, finite, irreversible, and that since Young's modulus and Poisson ratio were not found to be constant during deformation process, the theory of elasticity is not generally applicable to soils. We feel that in a medium that is being tested the results depend largely on the scale effect and moisture content.

Taking an individual aggregate, we might assume homogeneity of structure within, related to relative homogeneity in a larger puddled dry clod which in turn is related to a soil as a whole in air-dry condition, when viewed from a standpoint of a large stratum. On the other hand, any tests which are relatively speaking on a small scale will fail to give satisfactory results. In the tests like the one described above by McMurdie, in which the individual aggregates are a relatively major portion of the total, their individual physical characteristics will affect adversely the over-all results.

Finally, as the saturation process increases, the individual aggregates lose their identity and the soil assume different characteristics of behavior as a result of the change of porosity and density. Hence any generalizations regarding the soil might be inaccurate unless they specify precisely the moisture content, porosity, and density values at which they are carried out.

A widely accepted method of soil strength determination is a method for the so-called modulus of rupture as proposed by Richards (1953). The

exact nature of the forces involved is somewhat obscure. Richards claims that his modulus of rupture furnishes the parameter which is between the values of tensile and crushing strength. Richards prepared soil briquets by placing screened dry soil (< 0.200 cm. in diameter) in brass molds wetting for one hour by subbing and drying at 50°C . The force required to break a briquet when loaded as a horizontal beam is given as a so-called modulus of rupture calculated from the equation

$$\text{Modulus of rupture} = \frac{3}{2} \frac{FL}{bd} \quad (140)$$

where F is the force, L is the distance between two lower supports, b is the width of the briquet, and d is the depth of the briquet.

Essentially this is the modulus of rupture by bend giving the inter-aggregate strength for a given soil. This explains low values obtained by Richards (i.e., 0.3×10^6 dynes cm^{-2} air-dry strength) as compared with our results and with the values obtained by Hooghoudt (1950).

We do not feel that this so-called modulus of rupture constitutes a valid parameter of soil strength except perhaps in a special case when we wish to study the inter-aggregate bonds formed during a single wetting and drying cycle.

Gerard et al. (1962) reported that the modulus of rupture of dry fine sandy loam briquets tested, using Richards (1953) method, ranged from 0.2 to 0.3×10^6 dynes cm^{-2} , depending on drying temperature and relative humidity. These values are again much lower than the values obtained by us or by Hooghoudt (1950) for the reasons outlined above.

We feel that the values of the so-called modulus of rupture, calculated from Richards (1953) method may furnish a measure of surface crust

resistance. Richards method further stipulates a single wetting and drying cycle. It is likely that the results obtained by this method give a value of the natural crust strength, provided the soil is moistened without being compacted. We do not think that the method would give satisfactory results under conditions of intense rainfall when the soil surface is compacted by falling rain drops.

Relationship of strength measurements to other variables tested

Aggregates in air-dry condition (Table 22) In Appendix I, Table 54, Table 56, and Table 58, we have attempted to compute the value of modulus of elasticity in tension from other known variables. These other variables treated as dimensionless quantities are: void ratio, porosity, size, clay, and carbon content. The results of this analysis are presented in Table 22. On the whole the agreement between the experimental and computed values is very satisfactory. For example, compare the values of 9.43 and 9.47 obtained for Group 2 of Clarion s.l.

It can be seen from the equations listed below Table 22 (Appendix I, Equations 147, 148 and 149) that the modulus of elasticity in tension is inversely proportional to the square root of void ratio, square of porosity, and approximately the fourth root of size. It can also be seen that it is directly proportional to some function of clay and carbon contents. We have chosen the clay-carbon functions listed for the best fit of our results.

Turning our attention to the specific results in Appendix II, Table 54, we note that for Clarion s.l. the size (column 2) and clay-carbon functions (column 6) determine the value of E_{xc} (column 8); void ratio (column 3) and porosity (column 4) introducing only minor corrections. Similarly for

Webster c.l. in Table 56 and for Luton si.c. in Table 58, size and clay-carbon functions are the principal variables.

We should emphasize that it is the carbon-clay relationship that has to be considered, and not each of these variables separately. In Table 51c we note a limited significance of carbon results and observe that no clay values were significant for any other soils. Yet a clay-carbon function gave exact values of E_{xc} when used with the appropriate function of size.

Aggregates at 15 atm. moisture tension (Table 23) The carbon and clay contents remain constant irrespective of the change of volume for a given aggregate resulting from an increase of moisture content, because the values for carbon and clay are calculated as percentages on the dry weight basis. However, the quantities pertaining to size will increase in magnitude as the moisture content is increased.

If we assume that equations below Table 22 do indeed give correct values for the modulus of elasticity in tension $E_{xc}(1)$ then the modulus of elasticity in tension for aggregates at 15 atm. moisture tension $E_{xc}(2)$ should be given by the equation below Table 23 (Appendix I, Equation 150).

From the results in Table 23 we can see that there is reasonable agreement between computed, E_{xc} , and experimental values of E_{xc} for both Size groups on Luton si.c., i.e., 0.81 and 0.78 for Luton si.c. Group 3, and the Size group 2 of Webster c.l. There is, however, no agreement for other Size groups listed. The groups that show best agreement also exhibit largest measurable swelling. For example (Appendix I, Table 60) the swelling expressed as a change in aggregate diameter d for Group 3 of Luton si.c. would be 0.083 cm. (0.615-0.532), and for Group 3 of Clarion s.l. it would

be 0.004 cm. (0.511-0.507). We may conclude that the lack of agreement on the Size group 3 of Webster c.l. and both Size groups of Clarion s.l. can perhaps be attributed to internal swelling that does not show up as an increase in over-all size.

The strength of a brittle solid is frequently much diminished by the presence of gas or vapor which is capable of being adsorbed on the solid, (Dollimore and Gregg, 1958). Moreover, since absorption is known in representative cases to produce swelling (Bangham, 1947), it would certainly bring about an increase in strain energy at a distance of several molecular diameters from the edge of the adsorbed film. Thus a strain would be introduced into as yet unfractured solid, thereby reducing the amount of externally supplied stress at rupture.

The importance of swelling in reducing the externally applied stress has been emphasized by Guerney and Borysowski (1948). They found that polymethyl methacrylate exposed to carbon tetrachloride decreased in strength from 28×10^7 dyn. cm.⁻² to 5.2×10^7 dyn. cm.⁻².

Dollimore and Gregg (1958) suggest that polar adsorbates such as water cause swelling and reduction in strength in ionic solids such as clays.

In an extensive study, Sideri (1936) has formulated the effect of swelling process on porosity. According to Sideri the water in the soil may be absorbed in two ways: (a) it may be absorbed in capillaries and pores (capillary imbibition water), or (b) it may be absorbed in the lattices of clay minerals (swelling water). Setting the amount of water calculated as a percentage of swollen soil to be K_{Δ} , Sideri introduces a correction (r) where $r = K_{\Delta} \Delta V / 100$ (ΔV = volume increase). If K is the amount of non-polar liquid absorbed by the soil, expressed as a percent of air-dry

soil then for $K_{\Delta} - r = K$ there is only capillary imbibition. On the other hand, if $K_{\Delta} - r > K$, there is swelling. Then a ratio $S = K/(K_{\Delta} - r)$ gives an expression of the changes in structure during absorption of water and is termed structure coefficient. The smaller this coefficient the greater the change in soil structure. Sideri found that for a fine loamy sand S was equal to 1 with merely capillary absorption and no change in structure. For an alkali soil S was about 0.60, indicating considerable swelling and structure deterioration.

Sideri's research suggests that not all the changes in volume in the soils as a result of water absorption are due to swelling of clay. Admittedly if any amounts of clay are present and oriented in a form of a stable matrix, changes will largely be due to swelling. On the other hand, if no structure as such is present and an aggregate is a loose combination of primary particles, volume changes need not be related to swelling of clay but will be a result of capillary imbibition of water.

The forces developed by capillary imbibition are larger than the corresponding forces due to measured swelling of soil clay (Davidson and Page, 1956). We may assume the presence of trapped air in the pores and capillaries of a soil aggregate. Considering a capillary as a tube with both ends in water, the water will try to penetrate it with a pressure of $2\sigma/r$ where r is the tube radius and σ is the surface tension of water. For pores with 0.1 micron radius we would have the pressure of the walls of capillary in excess of $15.0 \times 10^6 \text{ dyn. cm.}^{-2}$. Compare this to $0.7 \times 10^6 \text{ dyn. cm.}^{-2}$ for a swelling pressure of montmorillonitic clay (Davidson and Page, 1956). It is not surprising that we find the strength values for our Clarion s.l. at 15 atm. moisture tension to be comparable to the strength values for Luton

si.c. also at 15 atm. moisture tension. For example, compare (see Table 21) a 1.10 value of Z_{zr} for Size group 3 of Clarion s.l. at 15 atm. moisture tension with 0.98 values for the same Size group of Luton si.c. The reason for the above situation becomes apparent when we consider the nature of the pores in the sandy and clay soil. We would expect the smaller pores to be far more numerous in a clay soil (see Theory II, Table 16) resulting in higher imbibitional pressures. Coupled to the swelling pressure of clay the forces developed would be of sufficient magnitude to rupture or considerably lower the strength of strong clay soil aggregates.

Mattson (1932) investigates the effect of hygroscopic water, water of osmotic imbibition and capillary rise water on the swelling of soil colloid. The intake of hygroscopic water of molecular attraction as well as the water of osmotic imbibition results in colloidal swelling. Mattson considers molecular films to be about 10 molecular layers thick. This situation would give rise to disjoining pressures between primary particles (Deryagin and Melnikova, 1958).

The water of osmotic imbibition can be thought of as a function of ionic condition of soil colloid (Mattson, 1932). On the other hand, the water of capillary rise, assuming no "explosions" due to trapped air result, would tend to counteract any swelling tendencies by bringing the particles closer together. This water would be oriented in the form of pendular rings and in the soil capillaries.

Although experimental values of swelling pressures for montmorillonite as given by Davidson and Page (1956) are relatively low, we would suspect that, in view of the discussion above, they represent the over-all effect of the three kinds (hygroscopic, osmotic imbibition and capillary) of water.

On the microscopic scale we would expect much higher forces than quoted by Davidson and Page to be developed locally as a result of clay swelling giving rise to Griffith cracks.

The situation appears rather complex. In view of our results and the discussion above we might conclude that the results at 15 atm. moisture tension represent the equilibrium strength of pendular water rings between the component parts of the aggregates tested. The component parts might be primary particles of sand silt and clay or they might be the ultimate aggregates presented in Table 32 and discussed later (see Shift of Weibull lines). The nature of this equilibrium is beyond the scope of this work, particularly if an additional effect due to trapped air within the capillaries is taken into account.

Koenigs (1961) examined the influence of moisture content on soil cohesion. He concluded that intra-aggregate cohesion will have a maximum value in the dry state, decreasing progressively until a minimum is reached at saturation. He states that swelling is a result of difference in energy level of intra- and inter-aggregate moisture. At a certain critical energy level of the exterior moisture, a net swelling pressure will develop resulting in the uptake of moisture. The ensuing increase of distance between the component particles will cause a rapid drop in cohesion. Swelling will be accompanied by shear stresses and fracture planes will arise leading to a strong decrease in cohesion of the individual aggregates.

The inter-aggregate cohesion follows a different pattern when examined in its relation to moisture content. At a very low moisture content the cohesion between aggregates is at the minimum. Only at a few points of contact is the distance small enough to come within the range of cohesion

forces. Pendular rings of water develop as the moisture content increases with surface tension of water contributing to the cohesion of soil. The binding forces will increase until the individual pendular rings coalesce. From that point on to saturation the cohesion will decrease.

Furthermore, as the moisture content increases the friction between the aggregates will increase if any deformation is attempted. Any deformation will result in points of contact being changed into planes of contact. The increase in the area of contact would account for friction increases.

Graecen (1959) suggests that the concept of soil strength might be used for describing soils on the basis of their resistance to deformation in saturated state. In view of the discussion of Mattson (1932) and Koenigs (1961) work, there seems to be little merit in this approach.

Griffith crack theory

Tensile strength in air-dry condition (Table 24). In Table 24 we present the tensile strength X_{xr} of aggregates in air-dry condition computed using Griffith crack theory (see Theory III). The agreement between the computed X_{xrc} and experimental X_{xre} values is reasonably good, (compare for example 0.96 and 0.99 for Group 1 of Clarion si.c.). As we have shown before (see equations below Table 22), the values of E_{xc} for any size of the three soils used can be computed from empirical data on porosity, density, size, carbon, and clay contents. Then, as we demonstrate now in Table 24, using Griffith crack theory we can compute the values of tensile strength X_{xrc} for a given size group with reasonable accuracy.

Millard et al. (1955) have broken coal specimens in crushing tests. They found that the crushing loads varied as the half-power of the specimen weight. They have proposed the use of Griffith crack theory to account

for experimental facts. They have stipulated that the theory could be applied provided the specimen was extensively cracked. Using Griffith correction factor that crushing strength should equal eight times the tensile strength, they were able to account successfully for the experimental values obtained. They have used the theory to compute the energy of rupture of coal (Llandebie) and have obtained a value of 3×10^4 ergs cm.⁻².

From theoretical considerations, Griffith (1924) has proposed that the crushing strength should be eight times the tensile strength. Griffith, however, conceded that in practice this value may vary, i.e., the crushing strength of steel is 5.5 times the tensile strength, and, in such materials as stone, the crushing strength is 7 to 11 times the tensile strength.

We have applied the Griffith crack theory to our experimental data on spherical soil aggregate. The theory as proposed predicts that the apparent crushing strength of aggregates will continue to increase with decreasing aggregate size, the upper limit being set by the tensile strength of uncracked material. On the basis of the photoelastic considerations of Frocht and Guernsey (1952) we felt justified in using a factor of 0.1737 to compute the tensile strength values from our experimental crushing strength results. Under these conditions we may note that the crushing strength would equal 5.76 times the tensile strength ($5.76 = 1/0.1737$). The agreement between the experimental results and the results obtained by the use of the Griffith crack theory justifies the use of the above-mentioned factor for soils.

Evans and Pomeroy (1958), working with coal, report that their experimental results do not support the deductions of the Griffith crack theory. They have also observed that the theory does not concern itself with great

variations of strength among the specimens of the same size. Commenting on their objections J. W. Phillips (Millard et al. 1955) pointed out that the Griffith crack theory concerns itself with extensively cracked material and, furthermore, if a large number of specimens is tested over a wide range of sizes, the variation of strength within a size is insignificant by comparison with the variation between sizes.

As we have mentioned earlier (see Theory III) porous nature of soil is synonymous with extensive cracking. To overcome variations within a given size, we have used a large number of aggregates for our tests on soil. Therefore, we feel reasonably certain that the use of the Griffith crack theory as proposed by us is justifiable in so far as the soil aggregates are concerned.

Tensile strength at 15 atm. moisture tension (Table 25) Turning our attention to Table 25, we note that the Griffith crack theory predicts with a reasonable degree of accuracy the tensile strength values at 15 atm. moisture tension also. The agreement between computed and experimental values, for example compare 0.177 and 0.189 for Group 2 of Clarion sl.l. is not quite as good as for the corresponding values in air-dry condition (Table 24). In particular the computed values for Luton si.c. differ by as much as 13% from the experimental values.

The lack of sensitivity in the apparatus at this moisture content (very low readings on ring dial) and fewer aggregates per group (see Methods) are chiefly responsible for larger values of discrepancies. We should also take into account the fact that as the percent of clay increases the soils tend to become more plastic than brittle at the higher moisture contents. This perhaps is reflected by the fact that our error

values are smallest on Clarion s.l. and largest on Luton si.c.

Tetelman (1963), working with the hydrogen embrittlement of ferrous alloys, has shown that hydrogen introduced in excess of lattice solubility can produce sufficient stress to cause cracking. Furthermore, he has shown that if hydrogen collects in microcracks and exerts an internal pressure, p , this pressure may be added directly to the external stress, Z , to produce a required total stress ($p + Z$) necessary to satisfy the Griffith criterion of crack propagation.

Considering the case of soil aggregates, we might draw up a parallel hypothesis concerning the relationship of moisture to aggregate rupture. We may suppose that the action of water on soil is analogous to the action of hydrogen on ferrous alloy. The action of water is such that the internal pressures developed might very well exceed the rupture stress value and satisfy the Griffith criterion for crack propagation. When that happens the aggregate will rupture prior to any external application of stress.

For other aggregates the values of external stress required to effect rupture will be greatly lowered. Under these conditions the difference between the rupture stress in air-dry condition and at 15 atm. moisture tension can be taken to represent the magnitude of internal stress produced by water.

Rupture strain (Table 26) In Table 26 rupture strain values e_{xrc} in the polar plane are presented. These values are calculated from the Griffith crack theory. Using the values of rupture strain in equatorial plane from Table 21, the value of Poisson ratio (see Equation 85a) is computed. We have assumed in our theoretical treatment that " u " at rupture should be equal to 0.50. In Table 26 this assumption is tested. We put

u in quotation marks since under normal conditions Poisson ratio does not exceed 0.50. Since we are interested in how closely the value of u approximate 0.50, both higher and lower values are admissible with the stipulation that they give an index of dispersion around 0.50 rather than an absolute value of u .

For example, the values of " u " for Groups 1, 2, and 3 for Clarion s.l. in air-dry condition are 0.50, 0.49 and 0.53. These values are close enough to 0.50 to support our assumption that Poisson ratio u equals 0.50 for aggregates tested.

Change in energy of rupture (Table 27) In Table 27, using Griffith crack theory we have computed the energy of rupture for aggregates in air-dry condition and at 15 atm. moisture tension. Comparing the values of the energy of rupture for aggregates in air-dry condition in Table 27 with the weight percent WP presented in Table 19 for each respective size group, we note that the second group which was the largest for Clarion s.l. and Webster c.l. exhibits also the highest energy of rupture in air-dry condition for both soils respectively. For example, compare T of 3.96×10^4 ergs cm^{-3} for Group 2 of Clarion s.l. ($3.96 > 2.65$ of Group 1, $3.96 > 3.31$ of Group 3) in Table 27 with relative magnitude of weight percent value WP of 38.2% also for Groups 2 of Clarion s.l. ($38.2 > 18.4$ of Group 1, $38.2 > 20.7$ of Group 3) in Table 19. However, this trend does not continue on Luton si.c. The large differences due to size influences in Luton si.c. most probably overshadow any other differences present.

The difference in the energies of rupture for aggregates in air-dry condition and at 15 atm. moisture tension reflects the differences in swelling among the three soils tested. For Clarion s.l. the change in the energy

of rupture was small, i.e., 3.34×10^4 ergs cm^{-2} for Group 2, likewise the change of size due to swelling was small ($0.369 - 0.347 = 0.022$ cm. also for Group 2, see Table 18). On the other hand, a larger change in size due to swelling for Luton si.c. gave a very high change in the energy of rupture.

Examining the results in Table 27, we note that the change in energy is considerable and similar in magnitude for all groups within any one soil (for example, for Webster c.l. ΔT values are 9.35, 8.93). We would suspect then that the increase in moisture content, particularly for the three soils tested by us, is a primary mechanism of breakdown for soil aggregates. The change in energy of rupture although similar in magnitude within any one soil tends to increase as the aggregate size is decreased, i.e., 8.93 value above is for Webster group 3, 9.35 value is for Group 2. This finding supports the commonly held view that fine-grained soils are much harder to work with in the field than coarser or more granulated ones.

Griffith (1921 and 1924) considers that the energy of rupture is the surface energy of the material. Orowan (1948) has pointed out that, considering metals, this energy is to a large extent the energy of plastic deformation. Millard et al. (1955) observed that their value of the energy of rupture is too high to be the surface energy and seems to indicate that plastic deformation occurs around the apex of cracks at rupture. Our values for the energy of rupture are even higher than the values obtained by Millard et al. We might therefore consider our values as the energy of plastic deformation rather than the surface energy of the material.

Day and Holmgren (1952) have found that in a moist soil, during the application of pressure, the volume changes are attributable largely to the

plastic deformation of the aggregates. Using a microscope, they were able to observe and record on a series of photomicrographs that deformation occurring readily at the lower plastic limit caused progressive closing of inter-aggregate spaces as the pressure was increased. Although we have worked at lower moisture contents than Day and Holmgren, we feel that the energy of plastic deformation could account satisfactorily for the high values of rupture energy obtained by us.

McMurdie and Day (1958), using a triaxial compression apparatus, found that moist soil aggregates compress in a manner similar to that expected of a pack of perfectly plastic grains. However, there is an important difference. Soil aggregate packs expand greatly when the applied pressure is released. The authors suggest that the translocation of water within the specimen tested is the most satisfactory explanation for this behavior. Soil aggregates are capable of shrinking and swelling under the influence of varying conditions of mechanical stress, and they differ in this respect from perfectly plastic bodies which are not subject to differential translocations of components.

We might suggest that the behavior described by McMurdie and Day, i.e., that packs expand greatly when pressure is released, is also characteristic of elastic materials. However, the soil aggregates packs do not recover their shape completely and in that they differ from the perfectly elastic materials.

When two solids are brought in contact, provided the force of adhesion is sufficient to bring about appreciable plastic deformation of one of the solids, the process is likely to be cumulative and irreversible (Bangham, 1947). We would expect sand-clay contacts to behave in the manner described

above. On the other hand, clay-clay contacts might behave like elastic solids. Both kinds of contacts present within the soil could account for the behavior observed experimentally by McMurdie and Day (1958).

Water stability

Induced strain (Table 28) Strain induced by swelling, i.e., as a result of increased moisture content at 15 atm. moisture tension, is compared with an average strain e_z for aggregates in air-dry condition in Table 28 on two size groups of three soils tested. We can see at a glance that induced strain by far exceeds the average strain with the exception of the size group 3 on Clarion s.l. (for example in Group 2 of Luton si.c. $0.1303 > 0.0780$).

In fact if we compare the results for induced strain e_{zi} in Table 28 with the strain at rupture e_{zr} in Table 21, i.e., for the same Group 2 of Luton si.c. we would have $0.1303 > 0.1124$, we note that only for size group 3 on Clarion and size group 3 on Webster was the induced strain lower. We might therefore expect that on the soils tested the rupture due to swelling of clay and imbibition water would be the principal mechanism of soil aggregate breakdown.

Aggregate stability (Table 29) Rupture due to swelling is illustrated by the percent of stable aggregates as compared with percent of water stable aggregates in Table 29. The percent of stable aggregates SA is given by that fraction of aggregates at 15 atm. moisture tension that exhibited a non-zero value of rupture stress. The percent of water stable aggregates WS is obtained from the set sieving analysis (see Methods). Considering a diverse character of the methods used to determine stability, we observe a remarkably good agreement between the two sets of values, i.e.,

for Group 3 of Clarion s.l. SA was 63.5% as compared with 59.2% WS.

None of the values of water stability for Clarion s.l. and Webster c.l. were significantly different from one another (see Table 51c). The only values that were significantly different were the water stability values for Luton si.c. For that soil the order of magnitude of stable aggregates SA was the same as the order of magnitude for water stable aggregates WS.

The fact that the second size group on Luton si.c. was significantly more water stable than the third group might perhaps help to explain why the second size group on Luton si.c. was also the largest of the three size groups tested (see Table 19).

Weibull theory

Parameters (Table 30 and Fig. 13) In Fig. 13 Weibull lines are presented for the respective size groups of Clarion s.l., Webster c.l., and Luton si.c. in air-dry condition and at 15 atm. moisture tension. In Table 30 the slopes of Weibull lines and the values of crushing strength at 0.90 probability of rupture are given for aggregates in air-dry condition and at 15 atm. moisture tension.

According to the Weibull theory (see Theory III) the slope, m , is the characteristic of the material. We observe that Weibull lines for Clarion s.l. and Luton si.c. exhibit similar slopes, i.e., for Group 1 we have $m = 1.42$ for both Clarion and Luton. The slope of lines for Webster c.l. is less than for the other two ($m = 0.98$ for Group 1) for aggregates in air-dry condition. In practical terms it means that as we increase the load the probability of rupture increases faster for Clarion s.l. and Luton si.c. than it does for Webster c.l. We recall that in the Methods section

we have pointed out that Webster is the most mature and developed soil of the three soils tested.

Weibull lines and their respective slopes for aggregates at 15 atm. moisture tension exhibit a trend opposite to that found for aggregates in air-dry condition. Here again the slopes of Weibull lines for Clarion s.l. and Luton si.c. are similar but they are less than the slope of Weibull lines for Webster c.l. For example, compare the values of m for Group 3, we have $m = 0.84$ for Clarion and Luton and $m = 1.08$ for Webster. In practical terms it means that as we increase the load, the probability of rupture increases slower for Clarion s.l. and Luton si.c. than it does for Webster c.l. The slope of the second size group on Luton si.c. is particularly low indicating a likelihood of plastic behavior in that soil.

The values of the ultimate crushing strength Z_0 at 0.90 probability of rupture follow the same pattern as the average values of Z_{zr} described in Table 21. The highest values are obtained on the smallest aggregates, the lowest on the largest. Comparing for example the values of Z_0 for Clarion s.l. in air-dry condition we have $Z_0 = 14.8$ for Size group 1 and 8.5 for Size group 3.

Weibull lines provide a visual description of the probability of rupture and a means of outright comparison between different soils used. Considering an over-all picture in Fig. 13 we note that the soils in air-dry condition exhibit similar slopes and vary with respect to the load. On the other hand, the soils at 15 atm. moisture tension are all grouped essentially around the same load but vary in slopes. If we recall the values for water stability (see Table 29), we note that the lowest value for a slope for aggregates at 15 atm. moisture tension was observed on size

group 2 of Luton si.c. (0.51) which exhibited a significantly higher value of water stability (WS = 63.7%) and the highest values of slope ($m = 1.36$ and $m = 1.08$) were obtained on Group 2 and 3 Webster c.l., exhibiting lowest values of water stability (WS = 47.8 and 39.6%).

Shift of Weibull lines (Table 31 and Table 32) According to the Weibull theory (see Theory III), the computed and observed shifts of Weibull lines taken in the neighborhood of 0.50 probability of rupture should be the same. Provided the lines are parallel to one another, the lateral displacements are indicative of the change in size for respective distributions.

In Table 31 we have assumed the lines in Fig. 13 to be approximately parallel to one another. We see that computed (CS) and observed (OS) shifts are reasonably close. The greatest discrepancies are observed for Webster c.l. For example, on Clarion s.l. observed shift OS of 0.347 cm. diameter Weibull line from 0.227 cm. diameter line is 0.14 log units, the calculated shift CS is 0.12 log units.

If we extrapolate from this information, we can compute the size of the smallest aggregate (ultimate aggregate) found in each soil. This is done in Table 32. The data indicate that the smallest aggregates for Clarion s.l. (297 microns) and Luton si.c. (241 microns) are about the same size but the smallest aggregate for Webster c.l. (1042 microns) is about four times larger. These results would fit the general description of the three soils used (see Methods). Webster c.l., being the most mature of the three, would certainly have the largest, best-developed aggregates.

Evans and Pomeroy (1958) have applied the Weibull form of strength distribution function to their experimental data on coal. Their results

were satisfactory. A different slope was exhibited by the different kinds of coal, and the values of observed and calculated shifts of Weibull lines agreed reasonably well. The authors were able to compute the ultimate size of coal domain that showed a reasonable agreement with theoretical predictions.

In our use of Weibull distribution we have found a satisfactory agreement between observed and calculated shifts of Weibull lines as pointed out earlier in Table 31. However, the distribution functions for different sizes had to be corrected to a different extent (see values of Z_u in Table 63). We do not feel that such corrections are entirely justified. In his subsequent work Weibull (1939b) considers more complex phenomena than the elementary approach of his original statement of the theory (Weibull, 1939a). In particular this treatment of anisotropic, irregular, and heterogeneous material could be of value in the study of soils. We have only considered the simplest approach and found a fair agreement with the theory. The prohibitive number of computations involved to test every possibility has prevented us from delving more deeply into the subject.

We feel that the use of Weibull's theory could be valuable in the study of differences between respective soils at different moisture contents. In so far as we know, the theory is unique in its capability of predicting the ultimate size of aggregates for soils studied, as we have demonstrated graphically in Fig. 13.

Essentially no differences in slope for the different soils in Fig. 13 might be taken as an indication that all aggregate sizes are similar in composition. On the other hand, it is equally informative that soil density groups significantly low in carbon exhibit lower slopes (Fig. 14 will be

discussed further in the discussion of Density groups).

Tensile and crushing strength values in psi (Table 33)

The data summarized in Table 33 have been computed and presented before. Various units for expressing soil strength and interaction of plants with the soil environment, as well as the interaction of soil and weather, have been used by different research workers. We have included this summary to facilitate the interpretation of our values in the light of their findings.

Influence of Aggregate Density on Aggregate Strength

General information

Aggregate density (Table 34) The density range and the average density for respective density groups are presented in Table 34. The detailed information is given in Table 14 (see Theory II).

To analyze the influence of aggregate density on aggregate strength in a meaningful way we need to recall the discussion of Table 14 presented in Theory II. In particular we have mentioned there that ranges of the density groups A-B and C-D either overlap or are included in one another completely.

Surveying the density ranges for Clarion s.l. Density groups in Table 34 the situation mentioned above becomes apparent. Therefore, to make sure that the comparisons are made between distinct density groups we will treat density groups A and B combined as well as C and D combined for Clarion s.l. as a unit in the discussion that follows. In this way for example a combined Density group AB (contained within parallel vertical lines in Table 34) will have a density range 1.74-1.82 g. cm.⁻³ and a combined group CD

will have a density range 1.87-2.07 g. cm.⁻³.

Examining the density ranges for Webster c.l. Density groups in Table 34, we note that the range for density group A and B combined (1.62-1.88), as compared with the range for density group D (1.86-2.07) form two distinct density groups, while the range of density group C overlaps them both. With that in view, in our discussion we will compare the results for Webster c.l. density group A and B taken as a unit with those obtained for group D, leaving out for the time being the results for density group C. This procedure will again insure that we are dealing with distinct density groups. It is felt that in this way we will most certainly deal with the strength measurements that are significantly different from one another (see Results, Table 51d), although the values for carbon, clay, and water stability are not likely to be so in all cases.

Since there are only two density groups for Luton si.c., with one included in the other and since the values obtained for strength measurement on Luton si.c. although different are not significantly different from one another (see Table 51d) we will treat the results presented for Luton si.c. as indicators of trends.

The results for density group D of Clarion s.l., for density group C of Webster c.l., and for density group B of Luton si.c. are informative from the standpoint of carbon. These groups will be discussed separately at the end of this section.

Grossman (1959) determined the bulk density of soil aggregates from a B horizon of some Illinois soils using a modified McIntyre and Stirk (1954) method for determination of porosity. His procedure was briefly as follows:

About 20 gms of air-dry 0.635 cm. to 0.953 cm. aggregates were weighed on a cheese cloth tare. The aggregates were saturated under vacuum with kerosene. They were then transferred to sintered glass desorption apparatus covered with kerosene, and equilibrated through step-wise desorption over approximately 2 hours to 3 cm. kerosene tension. Under these conditions the largest pores drained free from kerosene would be .040 to .050 cm. in diameter. Next the aggregates were transferred to a graduated cylinder that had been calibrated to a volume of 50 cc. at 20°C. with the burette used throughout the experiment to deliver and measure the kerosene. Kerosene at 20°C. was then added from the burette to bring the volume of aggregates plus kerosene to 50 cc. The difference between 50 cc. and the volume of kerosene added to the graduate cylinder equaled the volume of the aggregates. Moisture corrections were obtained from separate samples.

Using this procedure, Grossman (1959) obtained the values of aggregate bulk density ranging from 1.63 to 1.80 gms cm.⁻³ as compared to the range of 1.22-1.56 g. cm.⁻³ for the core samples of the same soils. We note that the bulk density range for aggregates as obtained by Grossman is essentially the same as the range obtained by us. Furthermore, we note that the bulk density of the core samples is much lower than that of the aggregates.

In the discussion of the sections that follow we have to remember that the values of bulk density for a soil as quoted by other researchers usually (unless otherwise specified) refer to the bulk density of a sample as a whole, and should not be confused or compared directly with our values. We emphasize very strongly that the bulk density as given by us in this dissertation refers to the bulk density of the individual aggregates.

On the other hand, we feel justified in making general comparisons

that relate the aggregate bulk density or soil bulk density to the strength measurements obtained. High values of soil bulk density as obtained by compaction at a high moisture content or high values as obtained by preparation of test samples from slurries should approximate closely the conditions of bulk density within individual aggregates as discussed by us.

Weight percent Comprehensive discussion on this subject is presented in Theory II, Table 14. In view of the groupings discussed above, we should mention that on Clarion s.l. we will be comparing two groups of approximately equal size (36.9% of total for AB and 40.4% of total for CD).

On Webster c.l. AB group, which accounts for 82.2% of all aggregates by weight, will be compared with a D group which constitutes only 6.6% of the total. On Luton si.c. the B density group constitutes 77.3% of the total with the A density group accounting for the remainder.

Considering these results, we observe that the densities of soil aggregates fall within a narrow density range and that the majority of the aggregates within a given range have essentially constant density (see Theory II, Table 14). Suppose we assume for a given soil, that the density of any aggregate is the same as the average density of the soil value. Then if we apply the methods developed in the previous section for dealing with the aggregate size, we will have at our disposal a very useful way of characterizing strength behavior of any soil.

Constancy of the stress/strain ratio (Table 35) In Table 35 we compare the average stress/strain ratio E_z for a given density group with the value of the stress/strain ratio E_{zr} at rupture. We observe that results similar to those obtained for size groups of corresponding soils are also obtained here, justifying our theoretical assumption (see Theory III).

Equations 97 and 98) that the stress/strain ratio remains constant.

As before largest discrepancies are observed for the Luton si.c. aggregates in air-dry condition, i.e., compare 3.93 and 4.15 for Luton si.c. Density group A. Also, aggregates of Clarion s.l. at 15 atm. moisture tension show very poor agreement between the average values of stress/strain ratio and the values of stress/strain ratio at rupture, which was not the case when the values for Clarion s.l. size groups were compared. Some of the discrepancies might be due to the smaller number of aggregates averaged to give respective density groups (see Methods).

Crushing strength (Table 36) Results for crushing strength Z_{zr} of aggregates are presented in Table 36. The groupings compared are those discussed before (see discussion of Table 34) and are indicated by parallel vertical lines. Comparing the crushing strength values for different density groups both on aggregates in air-dry condition and at 15 atm. moisture tension we note that the crushing strength Z_{zr} was higher on the denser aggregates of Clarion s.l. and Webster c.l. For example, compare Z_{zr} values of the Group CD (5.90 and 6.36) on Clarion s.l. with the Z_{zr} values of the Group AB (4.55 and 5.58) for aggregates in air-dry condition. The same trend was observed on Luton si.c. aggregates in air-dry condition. These results support our original hypothesis, i.e., that the denser aggregates should be stronger (see Introduction).

We have remarked earlier (see discussion of Table 21) that for Size groups the values of crushing strength for aggregates at 15 atm. moisture tension were very much lower than the crushing strength values of aggregates in air-dry condition. The same situation prevails for Density groups in Table 36. For example, for Clarion s.l. at 15 atm. moisture tension we

have for Density group AB crushing strength values of 1.14 and 0.91. We have pointed out above the same group AB has the crushing strength values of 4.55 and 5.58 in air-dry condition.

There was little difference between the values of Z_{zr} in aggregates at 15 atm. moisture tension for size groups in Table 21. However for density groups the differences observed in air-dry condition extend to the aggregates at 15 atm. moisture tension. With the exception of Group B on Luton si.c. at 15 atm. moisture tension higher density group also exhibit higher Z_{zr} values as was the case for air-dry material before.

There is little difference between the values of strain e_{zr} at rupture obtained for different density groups. In general the values of strain e_{zr} are higher for aggregates of lower density, i.e., compare 6.60 and 6.59 for Group AB with 5.57 and 6.53 for Group CD on air-dry Clarion s.l. This is an expected result. Aggregates of lower density should contain fewer internal points of contact and permit larger displacements per unit of length. Comparing the values of strain in air-dry condition and at 15 atm. moisture tension we find that there is little consistent difference between the two.

Taylor and Gardner (1963) have measured the effects of soil bulk density, moisture content, and strength on penetration of cotton seedling tap roots into Amarillo fine sandy loam. They have used five different bulk densities (1.55-1.85 g. cm.⁻³) and 4 different moisture contents (2/3- 1/5 atm.). They found that although moisture content-root penetration and bulk density-root penetration relationships were significant, the highest correlation coefficient (- 0.96) was obtained for the relationship between soil strength (as measured with a static penetrometer) and tap root

penetration. They concluded that soil strength and not soil bulk density was the main factor controlling root penetration.

The values of soil strength obtained by Taylor and Gardner increased with the increasing bulk density of the samples tested. The values ranged from 0.9×10^6 dyn. cm.⁻² for the lowest bulk density sample (1.55 g. cm.⁻³) to 29.0×10^6 dyn. cm.⁻² for the highest bulk density sample (1.85 g. cm.⁻³). Their moisture content by weight ranged from 5.5% at 2/3 atm. to 8.0% at 1/5 atm.

In general we have also found the soil strength to decrease with an increasing moisture content and increase with a bulk density of soil aggregates. The values of soil strength, however, obtained by Taylor and Gardner are higher than the values obtained by us at a comparable moisture content, i.e., for Clarion s.l. at 15 atm. moisture tension (8% moisture content by weight) our highest value was 1.50×10^6 dyn. cm.⁻².

The reasons for the possible discrepancy may be found in the terminology used by Taylor and Gardner. Their values for soil strength actually represent the so-called soil resistance R (Jumikis, 1962). Furthermore, the use of a penetrometer on the strength studies of soils is closely related to the pile-driving formulas employed extensively in soil engineering (Jumikis, 1962, p. 661).

We may consider a penetrometer needle to be a special case of a pile and compute the soil resistance R using the equation given by Jumikis

$$R = Wh/s \quad (141)$$

Here W is the weight that falls on the top of the pile, h is the distance of fall, and s is the depth of penetration. The units of h and s cancel.

If we consider W as a force and divide through by the area of the needle tip, we obtain the soil resistance in units of force per unit area.

To overcome the inconsistency that if $s = 0$, $R = \infty$, this formula is usually written as

$$R = Wh/(s + 1) \quad (142)$$

following the reasoning that R cannot be greater than the total energy of the weight (Wh). Here 1 in the denominator has the same units as s . Furthermore, the soil engineers use a factor of safety η , ($\eta = 6$), then we have

$$R/\eta = Wh/[\eta(s+1)] = Wh/[6(s+1)] \quad (143a)$$

If we assume a spherical soil aggregate to be present in a close packing arrangement within the soil mass, it will have six points of contact. We might suppose that use of $\eta = 6$ could be related to the confining resistance pressure of surrounding aggregates. Under these circumstances the above formula might be considered equivalent to the soil crushing strength, Z_{zr} , then

$$Z_{zr} = (1/\eta)R = Z_B \quad (143b)$$

where Z_B is the safe bearing capacity of a pile.

Taylor and Gardner calculated the penetrometer stress (equivalent to Z_B here) from the maximum force (W here) required for the 0.48 cm. diameter penetrometer tip to be forced 0.5 cm. ($s = 0.5$) into the soil. There are no indications that the corrections of s and η mentioned above have been taken into account. If we were to apply these corrections to the values of

soil strength given by Taylor and Gardner, we would get the values of soil strength (Z_{zr} here) equal to about 1/18 of their original values listed. These new values would be within the range of values obtained by us and would not affect the general conclusions and correlations originally found by the above authors. We have to remember that η is a safety factor as used by the soil engineers; but as we have pointed out above (below Equation 143a) there could be a valid theoretical basis for the use of η with reference to packings of spherical aggregates. Furthermore, we feel that average crushing strength Z_{zr} as used by us and safe pile bearing capacity Z_{B} as given by Jumikis are equivalent.

The importance of the paper presented by Taylor and Gardner lies in the fact that they have successfully demonstrated that the most frequently published explanations for poor root growth in compacted zones are relatively minor as compared to the major influence of soil strength. The explanations usually given are: (a) aeration was inadequate within or below the compact zones (Gill and Miller, 1956; Meredith and Patrick, 1961), (b) soil pores were too small for root caps to enter (Meredith and Patrick, 1961; Wiersum, 1957) and (c) some critical soil bulk density was exceeded (Trowse and Humbert, 1961; Veihmeyer and Hendrickson, 1946; Veihmeyer and Hendrickson, 1948; Horton, 1962).

If we assume that the values of Z_{zr} at 15 atm. moisture tension (or any other appropriate tension) will yield the values of soil resistance offered to the penetration of plant roots, a significant relationship between soil crushing strength, compaction, and root penetration studies would be available. Then the relation between the soil resistance per unit area, R , as obtained from the penetrometer readings and soil crushing

strength, Z_{zr} , would be

$$Z_{zr} = R/6 \quad (144)$$

where R is given by Equation 142.

Phillips and Kirkham (1962) studied mechanical impedance of corn seedling roots using the depth of penetration of a needle penetrometer as a measure of soil resistance to root penetration. They found that the rate of corn seedling root elongation decreased linearly with decreased penetration of a needle penetrometer into artificially compacted samples of Colo clay.

Gill and Bolt (1955) reviewed Pfeffer's studies of the root growth and pressures exerted by plants. The axial pressures exerted by roots at its tip or near the vicinity of the root tip ranged from 19×10^6 dyn. cm.⁻² for *Faba vulgaris* (broad bean) to 24×10^6 dyn. cm.⁻² for *Zea mais* (corn). Values of 13×10^6 dyn. cm.⁻² for *Viciasativa* (common vetch) and 7×10^6 dyn. cm.⁻² for *Aesculus hippocastanum* (horse chestnut) were also recorded.

Comparing these results with the values of crushing strength of the soils tested by us, it becomes apparent that Luton si.c. (Z_{zr} of 42.82×10^6 dyn. cm.⁻²) is the only soil that is likely to present problems in the air-dry condition. None of the soils tested would present any real barrier to the root development at 15 atm. moisture tension; however, the increased resistance of Luton si.c. with decreasing moisture as the wilting point is approached would probably slow down root growth.

It is a common saying among farmers that roots grow to water. The truth of the matter probably is that since the roots follow the path of

least resistance, they would be more likely to grow in the less resistant, relatively wetter soil provided, of course, aeration does not become limiting.

Relationship of strength measurements to other variables tested

Aggregates in air-dry condition: tensile strength (Table 37) In

Table 37 we compare computed values of tensile strength X_{xrc} with the values of tensile strength obtained experimentally X_{xre} for Clarion s.l., Webster c.l., and Luton si.c. respectively. The values of tensile strength computed from the equations listed below Table 37 (Appendix II, Equations 151, 153 and 155) show very good agreement with the values obtained experimentally. Compare the values of 0.80 and 0.79, 0.99 and 0.97 for Clarion s.l. Group AB as an example.

As we have done with the corresponding treatment of results for size groups in Table 22 we turn our attention now to the influence of specific variables on respective density groups. Detailed computations for Clarion s.l. are presented in Appendix II Table 66. We note that void ratio (column 3) and clay-carbon function (column 5) determine the value of X_{xrc} with the size function (column 2) introducing only a minor correction. Similarly for Webster c.l. in Appendix II Table 68, void ratio and clay-carbon function are the principal variables. No significant differences were observed between the values of tensile strength for Luton si.c. This is reflected in the computations (see Appendix II, Table 70) where the principal variable appears to be the function of size (column 2).

Values of tensile strength in Table 37 follow the same pattern as we have already described for the crushing strength in Table 36. Again the tensile strength increases as the aggregate density increases, provided we

consider the grouping (indicated by brackets) which we have outlined in connection with Table 34.

Vomocil et al. (1961) applied tensile stress to soil samples by a body force developed as the samples were rotated in a specially designed centrifuge head. Cylinders or briquettes of soil were positioned in the centrifuge head with their long axes normal to the axis of rotation. Vomocil calculated the magnitude of applied stress from sample dimensions, sample mass, and angular velocity of the centrifuge. Tensile strength tests were made on samples from five different soil types at moisture contents ranging from oven-dry to approximately 1/3 atm. and bulk densities ranging from 1.1 to 1.7 g. cm.⁻³.

Vomocil found that reducing the aggregate size from 0.300 cm. to 0.050 cm. reduced the variability. This observation supports our contention (see Theory I) that as the aggregate size decreases, the shapes of the aggregates approximate regular spheres more closely. Under these conditions, variability due to packing and arrangement of aggregates should decrease as the size decreases.

Vomocil also found that in general the tensile strength varied as the sample bulk density within each respective soil tested. Examining his results we may conclude that the increase in strength also varied inversely as the moisture content of the samples tested. Finally the tensile strength values for samples within the similar ranges of density generally varied as the respective clay content of the soil. However, no conclusive evidence for the last statement can be found since the particle size distribution analysis was done on a size fraction smaller than the size of aggregates used in tensile strength measurements. Furthermore, there are indications

that the variability of bulk density between the soils and the size of respective sand fractions might have been partly responsible for differences of soil tensile strength observed.

Vomocil's results in general support our findings. His values for tensile strength, however, are lower in magnitude than the values obtained by us (our values range from 0.79×10^6 dyn. cm.⁻² for Group A Clarion s.l. to 7.44×10^6 dyn. cm.⁻² for Group B Luton si.c. while his values are between 0.167 and 0.478×10^6 dyn. cm.⁻² for Yolo loam). The principal reason for the low values obtained by Vomocil lies in his pretreatment procedure. Since his air-dry soil aggregates were equilibrated to required moisture tension or saturated by soaking up moisture and then oven dried, the measurement of tensile strength, essentially, gave only the inter-aggregate tensile strength values. These values, even in the air-dry condition, are therefore understandably low. On the other hand, Vomocil's values for the samples of Yolo loam (19% clay) that were subjected to compression prior to the determination of tensile strength are more in line with our results. These samples are lower by about 0.4×10^6 dyn. cm.⁻² than our values for Clarion s.l. (15.1% clay). Taking into account the fact that these values were measured at a higher moisture content than the values obtained by us on Clarion s.l., we feel that they can be considered to be within the true range of soil strength.

Experiments by Vomocil et al. (1961), Richards (1953), and Gerard et al. (1962), as contrasted with the experiments of Hooghout (1950), Gill (1959), Grossman and Cline (1957), and the results obtained by us, illustrate the difference between the inter-aggregate soil strength and true soil strength. Furthermore, the correspondence between the results

obtained by Hooghout, Gill, Grossman and Cline, and our results supports the assumption, made by us at the beginning of this section, that the values of strength obtained for individual soil aggregates can be extended to the soil as a whole.

Kirkham et al. (1958) determined the modulus of rupture of undisturbed soil cores 6.9 cm. in diameter and 2 and 5 cm. long. They used the so-called Brazilian test (Peltier, 1954), to determine the modulus of rupture (here tensile strength) of cylindrical soil cores from the formula

$$\text{Modulus of rupture} = 2F/(\pi dL) \quad (145)$$

where F is the load in kg, d is the diameter in cm., and L is the length of the core.

Kirkham et al. found that their values for the modulus of rupture correlated well with the number of blows it took to force a sampling can to 8 cm. depth into the soil. They also found a significant correlation between modulus of rupture and bulk density on a silty clay loam soil; however, there was no correlation between modulus of rupture and bulk density on a silt loam soil.

The values obtained for the modulus of rupture (tensile strength) in air-dry condition by Kirkham et al. are about 1×10^6 dyn. cm.⁻². This value corresponds to the tensile strength of our sandy loam soil (Clarion group C) but is lower than what we would expect on the basis of results for the clay loam Webster soil.

We find the procedure as it was applied to undisturbed soil cores unsatisfactory for several reasons.

The theoretical approach to the Brazilian test is based on the two-

dimensional problem of a concentrated load. The applied load per unit length of application appears as a force at a point of a straight boundary (Timoshenko, 1934, pp. 82-93). One can show that circles tangent to the point of the load application represent the points of simple radial stress, $X = -2F/(\pi d)$, where d is a given cord of the circle.

In a circular disk problem there are no forces acting on the diameter of the disk. Therefore, if we add normal compressive stresses of magnitude $2F/(\pi d)$ to the circumference of the disk, then the stress distribution in the disk would be that obtained by superposing the stress distribution arising from two concentrated forces.

This is equivalent to saying that if we superpose a uniform tension in the polar plane of the disk of magnitude $2F/\pi d$ on the two simple radial stress distributions, we will obtain the stress distribution of a disk. Since the radial distribution problem shows that the normal force acting on the polar plane through the point of application of the two forces is zero, then in the disk problem this normal force is equal to the applied tension. J. L. McMurdie, Riverside, California. Private communication.

Examining the physical picture presented by the theoretical approach and contrasting it with the procedure used by Kirkham et al. (1958), we would suggest the following modifications. The sample core should be taken horizontally and not vertically as was done by the authors. In this way a correspondence to the forces applied at the soil surface by compaction machinery could be established. Furthermore, driving in of sample tubes by blows should if possible be avoided as it can produce both compaction (sample surface), and shattering (sample interior), leading to erroneous results. We would suggest use of an auger that cuts around a sample without

affecting the properties of a core. However the lubricated, thin-wall, cans used by Kirkham et al. reduced compaction effects of sampling, as compared with core samplers conventionally used. If horizontal cores are taken, possible horizontal soil anisotropy would need to be considered in applying rupture stresses and in possible modifications of Equation 145 to account for anisotropy.

We recall (see discussion of Table 21) that when Hooghoudt(1950) applied pressure to half-balls of soil he found that initially the curved portion of the half-ball became flattened giving a contact area that was parallel to the equatorial plane of the half-balls. Only following the initial flattening the scale dial began registering an increase in pressure. Similar situation should arise when soil cores such as those used by Kirkham et al. are compressed laterally.

In theory (Timoshenko, 1934, p. 84), the stress at the point of load application is infinitely large because a finite force is acting over an infinitely small area. In practice, at the point of application there is always a certain yielding of material, and as a result of this the load will become distributed over a finite area of contact. If this contact area varies between the different specimens tested, the resulting tensile strength values will not be comparable since the rupture will start at different points within the disk.

In our research, assuming a point contact and a brittle solid, we have attempted to minimize the above effect by adopting a spherical aggregate as an experimental unit, by computing the forces at the center of the sphere, and by taking a very large number of samples. This effect will increase on highly plastic soils particularly as the moisture content is increased.

Peltier (1954), in his theoretical development of the Brazilian test, has computed the so-called safety factor for the tests to make sure that the rupture starts at the center of concrete disks. He stipulated that to obtain appropriate values of tensile strength of concrete the ratio $2a/d$, where $2a$ is the width of the area of contact and d the diameter, should be larger than 0.15 but less than 0.25. Based on his values and the ratio of crushing to tensile strength of soil obtained by us (approx. 6.0), we estimate that the width of the contact area of test specimens used by Kirkham et al. should have been in the neighborhood of 2.00 cm. Peltier (1954) suggests the use of thin plates between the specimen and the load. In this way, the imprint left by the test specimen on the plate records the width of contact area $2a$. These considerations have not been taken into account by Kirkham et al. (1958).

According to Peltier (1954), satisfactory results were obtained with a cylinder whose length (but length of the cylinder does not occur in the factor $2a/d$) was twice the diameter (2:1). For the use on soils a length to diameter ratio 1:1 would probably be satisfactory. Kirkham et al. (1958) have found that oven drying of cores with a ratio of 1:4 caused 60% of the samples tested to breakdown prematurely before a load could be applied while 1:1.14 ratio gave only 23% breakdown.

As pointed out in the discussion of Table 23, the oven-dried values of tensile strength for natural soil cores might be lower than the strength values of the same soil under a certain optimum moisture content (Koenigs, 1961). We feel that the air-dry condition which we have tried to approximate in our studies should furnish the closest approximation to the soil strength under natural conditions.

The procedure proposed by Kirkham et al. might be applicable to artificially prepared cylindrical briquettes where a premature fracture due to oven drying would be less likely since more controlled conditions would prevail. As we point out in the discussion of Table 21, results from briquettes artificially prepared from slurries or from compacted moist material give the results that correspond closely to the range of values obtained by us for natural aggregates. This is not surprising since the compacted bulk densities that can be attained correspond closely to the bulk densities of individual aggregates.

We point out, by comparing our results with the work of others (Taylor and Gardner, 1963; Barley, 1963; and Horton, 1962), that the soil resistance as offered to the penetrating plant roots is a function of soil intra-aggregate strength rather than the inter-aggregate strength as obtained by (Richards, 1953; Gerard et al. 1962; Vomocil, 1961). A reasonable approach to the study of compaction and plant root penetration therefore would seem to be four-fold: (a) determination of aggregate densities from known levels of compaction, (b) preparation of appropriate test disks of the same degree of compaction as that of the soil aggregates, using slurries or compaction, (c) measuring the strength of cylinders by a suggested Brazilian test, (d) comparing these values with the values of strength for undisturbed cores and individual aggregates.

Having obtained soil tensile strength, an appropriate factor of $1/0.1737$ suggested by us could be used to obtain the crushing strength. From the values of tensile and crushing strength, in the discussion of Table 43, reasonably accurate maximum values of shear strength for a given soil could be obtained.

It is felt that these proposed studies could be conducted for different textural classes of soils as well as for different moisture contents, provided that in cases where the natural stability of a test disk was low, an ambient pressure similar to that used by soil engineers in the triaxial test (Jumikis, 1962, pp. 488-503) should be incorporated.

Aggregates in air-dry condition: tensile rupture strain (Table 38)

In Table 38 we compare computed values of rupture strain e_{xrc} in polar plane with the values of rupture strain e_{xre} obtained experimentally for Clarion s.l., Webster c.l., and Luton si.c. respectively. Furthermore, the values of "u" are given which test the theoretical assumption that $u = 0.50$ (see Equation 85a). As can be seen, the values of "u" are clustered around the 0.5 value. The remarks we made earlier with reference to values of "u" in Table 26 also apply here.

The values of rupture strain computed e_{xrc} from the equations listed below Table 38 (Appendix II Equations 152, 154, 156) show very good agreement with the values obtained experimentally (e_{xre}). For example, for group AB of Clarion s.l. in air-dry condition we compare 0.1370 with 1.338 and we compare 0.1206 with 0.1266. Proceeding as we have done before, we now turn our attention to the influence of specific properties on rupture strain e_{xrc} , for our Density groups.

Detailed computations for Clarion s.l. are presented in Appendix II Table 67. We observe that the porosity (column 4) and carbon function (column 6) determine the value of e_{xrc} with the size (column 5) and void ratio (column 3) introducing only a minor correction. Similarly for Webster c.l. in Appendix II Table 69 the void ratio and porosity are the principal variables, with size and clay-carbon function introducing only

a minor correction. No significant differences were observed between the values of rupture strain on Luton si.c. (see Table 51d). This is reflected in the computations (see Appendix II, Table 71) where the principal variable appears to be the function of size (column 4).

Values of rupture strain in the polar plane in Table 38 follow the same pattern as we have already described for the rupture strain in the equatorial plane in Table 36. Again the rupture strain decreases as the density increases if we consider the grouping (indicated by vertical lines) which we have outlined in connection with Table 34.

To summarize our discussion of Tables 37 and 38 four short paragraphs follow.

The results of Table 37 indicate that for density groups the tensile strength is inversely proportional to the void ratio. In practical terms it means that if we increase the volume of solids (void ratio = $V_{\text{voids}} / V_{\text{solids}}$), the tensile strength and consequently the crushing strength will increase.

On the other hand, Table 38 shows that the rupture strain in the polar plane of an aggregate appears to be directly proportional to the porosity. In practical terms the direct proportionality means that as we increase the volume of voids (porosity = $V_{\text{voids}} / V_{\text{total}}$) the value of rupture strain in the polar plane and consequently the value of rupture strain in the equatorial plane will increase, with the soil becoming progressively more plastic.

In a previous section (discussion of Table 22) we found that the modulus of elasticity in tension for the respective size groups is inversely proportional to the diameter of an aggregate. Since the modulus of

elasticity in tension is the ratio of tensile strength to rupture strain in the polar plane, we would expect this ratio to be proportional to the product $(V_{\text{solids}}/V_{\text{voids}}) \times (V_{\text{voids}}/V_{\text{total}})$ or $V_{\text{solids}}/V_{\text{total}}$, which is a spatial description of size.

Finally, the above mentioned quantities are proportional to some clay-carbon function in so far as it affects the volume of solids, the volume of voids, and the size.

Aggregates at 15 atm. moisture tension (Table 39) In Table 39 we assume, as we have done earlier (see the discussion of Table 23), that the value of the modulus of elasticity in tension at 15 atm. moisture content can be approximated by a product of the modulus of elasticity for aggregates in air-dry condition and a correction factor involving the change in void ratio, porosity, and size due to swelling. We have computed the values of E_{xc} from the equation listed below Table 39 (Appendix II, Equation 157).

In general there is no agreement between computed E_{xc} and experimental E_{xe} values. The reasons for the lack of agreement are three-fold. First, the error due to a limited amount of measurable swelling was compounded by averaging over size groups. Second, only two larger sizes could be used in computations for reasons explained before (see discussion of aggregate size in the previous section). Third, a small amount of aggregates tested for the density groups at 15 atm. moisture tension was not enough to give a representative value (see Methods: Experimental design and methods of averaging).

Change in energy of rupture (Table 40) In Appendix II, Table 67, Table 69, and Table 71, we have computed the values of e_{xrc} using the

the Griffith crack theory for respective density groups, i.e., column 1 and 2 in Table 67. Although the Griffith crack theory is directly applicable where differences in size exist, we have found that reasonably good approximations for the values of e_{xrc} , for density groups, could be obtained if we used the constants A previously computed for the size groups of soils tested in the air-dry condition and at 15 atm. moisture tension (see Appendix I, Table 55, i.e., $A = 0.073$ for Clarion s.l., Table 57, Table 59, and Table 61).

On the basis of these findings we felt justified in computing the values for the energy of rupture in air-dry condition (T_1) and at 15 atm. moisture tension (T_2), as well as the change in the energy of rupture, $\Delta T = T_1 - T_2$. The results obtained are presented in Table 40. The energy of rupture increases as the aggregate density increases (comparing the groupings indicated by vertical lines) both for aggregates in air-dry condition and at 15 atm. moisture tension, i.e., T_1 for Group AB on Clarion s.l. is 2.88 and 2.35, but on Group CD T_1 is 4.90 and 3.89. The change in energy of rupture is largest for the most dense aggregates. For example, compare the value of 9.77 for Webster c.l. Group D with 7.82 and 7.75 obtained for Group AB.

No relationship between the weight percent WP (Table 14) for a Group and higher values of rupture energy could be observed on Webster c.l. However, on both Clarion c.l. and Luton si.c. the groups constituting a larger weight percent (see discussion on weight percent in Table 14) also display higher rupture energy values. For example, for the Group CD of Clarion s.l. weight percent is 40.4 ($40.4 > 36.9$) and T_1 is 4.90 and 3.89 which is greater than 2.88 and 3.55 for Group AB:

If we consider the energy of rupture as a measure of the surface tension for the soil (Griffith, 1924), we could expect the aggregates of higher density (lower specific surface) to exhibit higher energy values.

Water stability (Table 41) In Table 41 the percent of stable aggregates SA (aggregates exhibiting non-zero value of rupture stress) is compared with water-stable aggregates WS (see Methods) for Density groups of Clarion s.l., Webster c.l., and Luton si.c. As we remarked earlier (see discussion of Table 29), considering the divergent character of methods used, the agreement is good. For the AB group of Clarion s.l. compare 66.4 and 60.6 with 52.4 and 63.9.

We may suppose that the water stability analysis (de Leenheer and de Boodt, 1959) measures the fraction of aggregates that are resistant to slaking and dispersion. It can say nothing about absolute strength of the fraction that is considered stable; neither can it say anything about the strength characteristics of the fraction that is dispersed. Since the values of water stability will depend largely on the state of dispersion at the particular time of sampling, we would expect to obtain satisfactory reproducible values only in regions where no extreme wet or dry conditions prevail.

Weibull parameters (Table 42, Fig. 14) In Fig. 14, Weibull lines are presented for the Density groups of Clarion s.l., Webster c.l., and Luton si.c. in the air-dry condition. In Table 40 the slope of those lines and the values of crushing strength at 0.90 probability of rupture are given. We recall as was the case with the Griffith crack theory that the Weibull lines are generally useful in comparing size distributions. However, according to the Weibull theory, the slope, m , is also a characteristic

of the material.

Comparing the slopes of lines indicated by groups (quantities within vertical lines) we do not observe any great differences in slopes. For example, a slope m is equal to 1.32 on Webster c.l. Group AB while a slope on the Group D of the same soil is equal to 1.39. This indicates that although the soils vary in strength among themselves, and the groups vary in density within each soil, the soil materials as measured by the values m of Weibull lines is essentially the same.

Three anomalous Density groups; the influence of carbon

At the beginning of this section in the discussion of aggregate density (Table 34) we mentioned that the results for Density group D on Clarion s.l., Density group C for Webster c.l., and Density group B for Luton si.c. would be discussed separately.

Each one of the above-mentioned groups is distinct from the others within a given soil in that it contains a significantly lower amount of carbon (see Table 51d). If we make an assumption that the behavior of these groups is related to their respective carbon contents, we can draw some conclusions regarding the influence of carbon on the soils studied.

We note, in Table 34, that all three groups span similar density ranges (ca. 1.80-2.07 g. cm.⁻³) and observe (Appendix II, Table 64) that their size (ca. 0.355 cm.) particle density (ca. 2.72 g. cm.⁻³) and porosity (ca. 28.0%) values are very close together. Of the three, only the Clarion s.l. group has a significantly lower clay content (Appendix II, Table 65), while the Webster c.l. and Luton si.c. groups display the lowest values for water stability. Values for water stability agree quite well (particularly for Clarion s.l. and Webster c.l. groups) with the percent of stable

aggregates (see Table 41).

In terms of strength measurements all three groups furnish the highest values of crushing strength (6.36, 16.67 and 42.82 for the Clarion s.l., Webster c.l. and Luton si.c., see Table 36) and tensile strength (1.11, 2.90 and 7.44 for Clarion s.l., Webster c.l. and Luton si.c., see Table 37) soils. The values of rupture strain both in the polar plane (Table 38) and in the equatorial plane (Table 36) are, relatively speaking, the same for all groups (ca. 8.00×10^{-2}). However, the values of rupture stress Z_{zr} (Table 36) and X_{xr} (Table 37) are relatively lower for Clarion s.l. group than they are for the Webster c.l. and Luton si.c. groups. This observation is related to the significantly lower clay content on Clarion s.l. adversely affecting the value of size (0.347 cm. for Clarion vs 0.367 cm. and 0.361 cm. for Webster and Luton, respectively)^a. As a result of this situation, the values of E_{zr} , E_z , and E_x and the quantities related to them are relatively lower for the Clarion s.l. group than they are for Webster c.l. and Luton si.c. groups. We still observe good correspondence between the values of E_{zr} and E_z for these groups (Table 35), if for Group D on Clarion s.l. we compare 0.97 and 0.98..

Turning our attention to Fig. 14 and Table 42, we note that both the Webster c.l. group and Luton si.c. group display much lower values of slope than do the other groups of the respective soils. In practical terms it means that these groups are more plastic in air-dry condition than the groups that have a higher carbon content. This might mean that for aggregates in air-dry condition a lower carbon content reflects a lower number

^aSee discussion of Table 38.

of brittle organic matter bonds which are weaker than the corresponding clay bonds.

Finally, in Table 40 we note that both Webster c.l. and Luton si.c. groups discussed above are characterized by the highest energy of rupture in air-dry condition (12.46 and 40.35×10^4 ergs cm^{-2} respectively). The same observation holds true for the change in the energy of rupture values.

In summarizing our discussion of three anomalous Density groups and the influence of carbon on the strength of aggregates we might conclude that if the influence of carbon alone on strength of soil aggregates is examined, we might expect to find stronger soil aggregates at lower carbon contents.

In absolute terms higher carbon values decrease the aggregate strength by increasing the volume of voids and decreasing the volume of solids ($\text{Stress} \propto V_{\text{solids}}/V_{\text{voids}}$). Higher carbon values also increase the rupture strain by increasing the volume of voids ($\text{Strain} \propto V_{\text{voids}}/V_{\text{total}}$). The over-all effect on the modulus of elasticity is an increase in aggregate size ($E \propto V_{\text{solids}}/V_{\text{total}}$).

To clarify the meaning of the ration $V_{\text{solids}}/V_{\text{total}}$, consider first the possible changes in V_{total} . As V_{total} increases, i.e., as the aggregate size increases, the value of E will decrease, which corresponds to our findings that smaller aggregates are stronger. One characteristic of organic matter is that it has a very small volume of solids as compared to the total volume (V_{total}). Hence a high value of carbon would go along with larger aggregate size.

Some research workers express the "strength" of soil aggregates in terms of crushing load (Martinson, 1949) or in terms of crushing load per unit weight (Chepil, 1951). Others, (De Leenheer and De Boodt, 1959;

van Bavel, 1949; Gardner, 1956) use water stability values as an index of aggregate "strength". We would expect larger aggregates to require greater crushing load if the crosssectional area is not taken into account. We might expect larger more porous aggregates to give relatively higher values of crushing strength per unit weight. We would also expect larger aggregates to appear more water stable.^a If we assume that carbon promotes a formation of larger aggregates, it is not surprising that high carbon soils are considered "stronger".

Kuipers (1958), applying confined compression tests to aggregates of different clay and carbon content, concluded that at pF 1.9 (1/10 atm. of water suction) organic matter raises soil strength. However, he found that at pF 4.2 (15 atm.) the soils high in organic matter are less hard than those with normal carbon contents. His findings for pF 4.2 are in agreement with our results. Since Kuiper's samples were confined within metal cylinders at pF 1.9, we would expect that excessive swelling of organic matter within the soil would offer additional resistance. This additional resistance would most certainly be absent if these samples were in the unconfined condition.

We can appreciate the preoccupation of agricultural research workers with the high carbon soils. Being more porous and weaker, aggregates of these soils provide a superior medium for root development. Their high porosity and, relatively speaking, larger size makes them more resistant

^aWater stability analyses are based usually on cumulative weight percentages. Larger aggregates could account for greater weight for a given group.

to erosion. Furthermore, being weaker, high organic matter soils are easier to work and are favored by farm operators.

Tensile and crushing strength in psi (Table 43)

Tensile X_{xr} and crushing Z_{zr} strength of aggregates in air-dry condition and at 15 atm. tension for each density group of every soil is presented in Table 43. According to Timoshenko (1934, pp. 187-188) the maximum shearing stress τ_{max} can be taken as one half the difference of the principal tensile X_{xr} and the crushing stress Z_{zr} at a point. In the section that follows we will attempt to show how our results correspond to the work done by Barley (1963), Taylor et al. (1962) and Horton (1962).

Barley (1963) has found that corn radicles were prevented from elongating by an initial shearing strength of 4.35 psi in a fine-grained cohesionless material. The results suggest that small negative pressures in the pore water may increase the shearing strength of certain soils sufficiently to reduce the growth of roots. Barley has also found that the radius of the root tips became greater as the strength of the medium increased. With this in mind we have to exercise caution in extending the results of soil resistance to the root pressures developed.

Taylor et al. (1962) found that when soil strength at field capacity is excessive [10 psi vane shear strength (Jumikis, 1962, pp. 507-510) 400 psi penetrometer pressure or higher] the root growth is restricted severely. Since the same penetrometer as described previously (Taylor and Gardner, 1963), was used, we may want to apply the same correction factor as before (1/18). Then the value of soil crushing strength would be 22.2 psi. This value would again be within the range obtained by us for other soils, as can be seen in Table 33, Table 43, and Table 51.

If we suppose that 22.2 psi is the crushing strength of Armarillo fine sandy loam, then the tensile strength would be 3.9 psi.^a Then the maximum shearing strength can be taken as 9.2 psi [$\tau_{\max} = (1/2)(Z_{\text{zr}} - X_{\text{xr}})$, Timoshenko, 1934, pp. 187-188]. We note that this value agrees fairly well with the value of 10 psi as obtained independently by Taylor et al. (1962).

Horton (1962, pp. 112-116), using a torsion shear test method (Schafer, 1961), investigated briefly the shearing strength of a Webster c.l. compacted to different bulk densities. Computing approximate mean maximum value of shear strength (from Horton's Fig. 21, p. 115) we get a value of 7.75 psi (maximum 13.4 psi). Mean maximum shear strength for our Webster c.l. (calculated as before from Timoshenko, 1934, pp. 187-188) at 15 atm. moisture tension is 5.56 psi. This value compares favorably with Horton's value, both sets of values having been obtained at approximately the same moisture content (20% moisture content by weight).

From the results of shear strength obtained by Barley, Taylor et al. and Horton, for the cohesionless beads (0% clay), sandy loam (8.2% clay), and clay loam (31.4% clay), respectively, it appears that as the clay

^aWe assume a proportionality factor of 0.1737 (Frocht and Guernsey, 1952); we also assume that strength values are given at the center of a hypothetical spherical aggregate.

content increases, the seedling roots are able to overcome increasingly higher resistance forces within the soil mass (4.35, 10.0, and 13.9 psi, respectively). This behavior could be related to the decline in the rigidity of pore structure (Wiersum, 1957) or it could be related to the increase in available water (Taylor and Gardner, 1963). We feel that the increase in available water provides a more satisfactory explanation.

Influence of the Type of Soil on the Aggregate Strength

General information

Constancy of the stress/strain ratio (Table 44) In previous sections dealing with the aggregate size and density groups we have shown that the stress/strain ratio remains constant. In Table 44 we demonstrate the constancy of the stress/strain ratio for soils as a whole. As before, the agreement between the average values E_z and values of the ratio at rupture E_{zr} is good. Again largest discrepancies are observed on Luton si.c. in the air-dry condition. To illustrate: compare the values of 4.08 and 4.40 on air-dry aggregates of Luton si.c. with 0.89 obtained for both E_z and E_{zr} on Clarion s.l. air-dry aggregates.

Crushing strength (Table 45) Results for the crushing strength Z_{zr} of aggregates for our soils considered as a whole are presented in Table 45. Along with the values of crushing strength we have included the percent values of clay. We note that for aggregates in air-dry condition the values of crushing strength are directly proportional to clay for the soils. We note that for Clarion s.l. the clay was 15.1% and Z_{zr} was 5.60×10^6 dyn. cm.⁻², as the clay increased to 31.4% for Webster c.l. Z_{zr} increased to 13.64×10^6 dyn. cm.⁻². There is little difference between Clarion s.l.

and Webster c.l. strengths at 15 atm. moisture tension (1.10 vs 0.95) while the Luton si.c. appears to be the strongest (2.37). The large differences that existed between the values for the soils in the air-dry condition do not appear at 15 atm. moisture tension.

In general the values of rupture strain e_{zr} also presented in Table 45 increase as the percent of clay increases, i.e., 6.32 for Clarion s.l. but 9.32 for Luton si.c. This observation holds true for values of strain both in air-dry condition and at 15 atm. moisture tension. We note that there is little difference between the values of strain e_{zr} for aggregates in the air-dry condition and at 15 atm. moisture tension of Clarion s.l. and Webster c.l. soils. On the other hand, the value of strain e_{zr} for Luton si.c. increases from 9.32 to 13.68 at 15 atm. moisture tension. We recall that a similar observation was consistently true also for the size and density groups of Luton si.c.

Relationship of strength measurements to other variables tested

Aggregates in air-dry condition (Table 46) In Appendix III, Table 75, we have computed the value of modulus of elasticity in tension E_{xc} in terms of other variables for each soil. We have found that E_{xc} the equation listed below Table 46 (Appendix III, Equation 158) most closely approximates our experimental values of E_{xe} . For example, for Clarion s.l. E_{xc} is 7.59 and E_{xe} is 7.96, the two values differ by less than 5%. Similar results could have been obtained if some function of porosity, i.e., P^{-2} , were used in place of the void ratio.

We recall that in our previous computations of a similar nature, both size (see discussion of Table 22) and carbon content (see discussion of Table 22, Table 37, and Table 38) were included in the empirical equations

derived. In the consideration of a soil as a whole presented here, the effects due to size average out. Since the carbon content is likely to be on the "per aggregate basis", varying between aggregates, as is the size, the influence of either one does not show up when we consider the soil as a whole. On the other hand, the values of void ratio, porosity, and clay are characteristic of aggregates in a soil as a whole, since, as we have shown before, (see discussion of Table 14), most aggregates fall within a narrow density range.

The values of modulus of elasticity in tension, computed from the equation shown below Table 46, are presented in Table 46. The agreement between computed and experimental values is good. The modulus of elasticity in tension follows the same pattern as that presented in Table 44 for the modulus of elasticity in compression, that is the magnitude of E_x varies directly as the clay.

Turning our attention to the equation listed below Table 46, we note that the value of the proportionality constant K_r is equal to 2.30×10^7 dyn. cm.⁻². The modulus of rupture for kaolin can be taken as 7.5×10^6 dyn. cm.⁻² (Dollimore and Gregg, 1958) while selected values of the modulus of rupture for pottery clays passing 30 mesh (0.6 mm) sieve range from 2.34×10^7 dyn. cm.⁻² to 4.19×10^7 dyn. cm.⁻² (Beech and Holdridge, 1954). We feel that the value of the constant K_r as obtained by us represents the modulus of rupture for clay in the soils we have used. We recall that the void ratio can be replaced by some function of porosity, which in turn (see discussion of Table 38) is directly proportional to the strain at rupture. Hence Equation 158 presented also below Table 46 gives a method of calculating the modulus of elasticity for aggregates of any soil in

air-dry condition from the easily measurable parameters, bulk density, particle density, porosity^a, and clay content.

Stauffer (1927) reports that the relationship between the clay content and soil strength appears to be linear. Working with synthetic soils, Stauffer prepared short cylinders by forcing the soil in a wet plastic state through a tube of constant diameter, cutting it into sections, and allowing the sections to dry. Using the apparatus and computations similar to those later developed by Richards (1953), Stauffer found that modulus of rupture at 50% clay content was 32×10^6 dyn. cm.⁻². This value corresponds to our results for the crushing strength of Luton si.c. (41.04×10^6 dyn. cm.⁻²) if our interpretation of his figures is correct.

Grossman and Cline (1957) studied 24 fragipan horizons^b to determine the relationship between crushing strength and particle size distribution. Crushing strength measurements of unaltered natural clods were related to various textural components. The natural clods were shaped by hand into rough cylinders (4.0 cm. long and 2.5 cm. in diameter). The upper and lower ends of these cylinders were encased in plaster of paris to form smooth, parallel bearing surfaces. The crushing strength per unit of crosssectional area was determined by application of axial stress using a

^aWe recall that the void ration equals $D_s P/D$.

^bA fragipan horizon is a natural subsurface horizon with high bulk density, seemingly cemented when dry but when moist showing a moderate to weak brittleness. It is low in carbon, mottled, slowly permeable to water and it shows bleached cracks forming polygons.

proving ring assembly. This procedure is similar to that used by us in this study, the main differences being the shape of the sample (cylinders as compared to spheres used by us) and the fact that apparently no strain values were recorded. Mean values of 25 to 40 clods from each horizon were used in the analysis of data (40 aggregates were used for each size-density group by us).

Grossman and Cline have found that the crushing strength was highly correlated with percent of clay. They concluded that clay was a principal bonding agent among primary particles and that very fine sand or silt may be equally effective as a matrix within which such clay bonding may occur. They suggest that clay may act either as a bonding agent or as an agent of structural development, i.e., part of the matrix. Consequent weakness of the specimens would depend upon its amount and distribution within the soil mass. Their data do not suggest any special role for ultra-fine clay.

All the soil series studied by Grossman and Cline, with one exception, were derived from glacial till just as were the three soils used by us. The mean value of crushing strength was 17×10^6 dyn. cm.⁻² and the median clay content was 13%. The mean values obtained by us for Clarion s.l., Webster c.l., and Luton si.c. can be seen in Table 45 and are 5.60, 13.64 and 41.04×10^6 dyn. cm.⁻² respectively. We observe that in general the value of a crushing strength obtained by Grossman and Cline is within the range of values obtained by us. The value of crushing strength on Clarion s.l., however, which has a clay content comparable to the clay content of the soils used by Grossman and Cline, is lower than the values obtained by Grossman and Cline. The discrepancy most probably is related to the moisture content at testing time. Our values are for aggregates

equilibrated for two weeks or more at about 25°C. and 40% relative humidity. Values obtained by Grossman and Cline are for clods oven-dried at 42°C. for two days.

Another source of error could possibly be the sensitivity of the ring employed by Grossman and Cline. The proving rings used by us had 10 and 25 lbs. capacity; the proving ring used by Grossman and Cline had 1,000 lbs. capacity. Furthermore, since the fragipan horizons studied by Grossman and Cline are in a sense more compact and oriented than the surface aggregates studied by us, we feel that the differences between the results obtained are justified.

Knox (1957) reports that the very fine-grained material, apparently holding sand and silt particles together was identified as illite by the method of x-ray diffraction. Further experiments, based on selective removal and destruction of possible bonding material, indicate that illite is responsible for a major part of fragipan strength and that both illite and colloidal silica are involved in the strength of an extreme pan. Comparison of natural clods and artificial briquettes compacted at 50 psi showed that the briquettes were about one-half as strong (crushing strength) as natural clods. The additional strength of the natural clods may be due to the better organization of the particles or to the presence of some other material in addition to clay.

In our earlier work, using water stability as an index of strength (Rogowski and Kirkham, 1962), we have found that artificially prepared 0.200 cm. to 0.800 cm. soil aggregates were not as water stable as the natural soil aggregates for all values of compacting pressure used. The water stability of the artificially prepared soil aggregates, however,

increased as the value of compacting pressure increased. At a compacting pressure of 1,000 psi, artificial aggregates were obtained that were as water stable as the natural aggregates compacted at the same pressure. We have also found that the water stability of natural aggregates decreased as the pressure was raised to about 200 psi. Further increments of pressure had little effect on the water stability of natural aggregates. In view of our results and those reported by Knox (1957) we may assume that (a) a compacting pressure as high as 1,000 psi is not sufficient to restore natural strength, (b) compacting pressures applied to a briquette will decrease the strength of natural aggregates. Since the soil tested by us in the above study was Webster c.l. and since the results obtained in this dissertation indicate higher water stability values for stronger aggregates of Webster c.l., we feel justified in drawing the conclusions (a) and (b) above.

The results reported by Stauffer (1927), Grossman and Cline (1957) and Knox (1957) justify inclusion of the term for clay in our empirical relations describing soil strength.

Our earlier work (Rogowski, 1960) illustrates one of the reasons for the low results for soil strength obtained by Richards (1953), Vomocil et al. (1961) and Gerard et al. (1962). Since even a high degree of compaction failed to restore completely the natural strength, no applied compaction would give little information about true soil strength.

Aggregates at 15 atm. moisture tension (Table 47) In Table 47 we test the assumption made previously (see discussion of Table 22, Table 39, and Theory III) that the modulus of elasticity in tension for aggregates at the moisture content other than air-dry, is given by the product of E_x

in air-dry condition and a correction factor. The correction factor is assumed to be a function of change in the void ratio, porosity, and size resulting from swelling.

The results of Table 47 for the soils considered as a whole show that, again, the computed and experimental values of E_x exhibited fair agreement on Luton si.c. (1.05 vs 1.30) and poor agreement on Clarion s.l. (4.03 vs 1.74). These findings are related to the change of volume measurements on respective soils. On Luton si.c. we assume the swelling was largest and the change of volume most measurable. Thus, best agreement of computed and experimental values of E_x was obtained. On the other hand little change of volume on Clarion s.l. is reflected by lack of agreement in the E_x values.

Our change of volume measurements lacked in sensitivity and accuracy. At the time the measurements were taken they were not intended for the purpose for which they were ultimately employed. The fact, demonstrated in this dissertation, that the expansion on an aggregate (and the resulting changes in volume, porosity, density, and size) considerably reduces strength of an aggregate, is in itself of great importance. A series of more refined studies oriented towards the precise measurement of the swelling of clay within an aggregate is needed to shed more light on the strength problem.

Griffith crack theory

Tensile strength in air-dry condition (Table 48) We have shown previously (see discussion of Table 24) that the Griffith crack theory can be used satisfactorily on different size groups of a given soil to compute the tensile strength. Using the values of the proportionality constant A obtained previously, and given below Table 48, we show in Table 48 that the

Griffith crack theory can also be used to calculate the tensile strength of a soil as a whole. Computed and experimental values of X_{xr} agree reasonably well for all soils tested, i.e., the values 0.92 and 0.97 for Clarion s.l. differ from one another by 5.4% only.

We have shown in the discussion of Table 46 that satisfactory values of E_x can be obtained from easily measurable parameters of clay and void ratio $D_s P/D$. The importance of the Griffith crack theory for soils is on the basis of computed values of E_{xc} the tensile strength as well as the crushing strength^a for any size group can readily be calculated.

Tensile strength at 15 atm. moisture tension (Table 49) In Table 49 the computed and experimental values for tensile strength X_{xr} of the soils at 15 atm. moisture tension are presented. The computed values are calculated using the Griffith crack theory and the constants A obtained previously and listed below Table 49 (see discussion of Table 25).

Although the computed values X_{xrc} for Clarion s.l. and Webster c.l. approximate the experimental X_{xre} values very closely (less than 3% difference), a large discrepancy exists between computed and experimental values on Luton si.c. (14.3% difference). We recall that a similar situation prevailed for the tensile strength values of the size groups of the soils (see Table 25). We might expect that in the soils of lower clay content a brittle fracture takes place, but as the amount of clay increases, a plastic deformation, which is not accounted for by the Griffith crack theory, sets in. Furthermore, the values given are for aggregates at 15

^aWe recall that $X_{xr} = 0.1737 Z_{xr}$ (see Equation 93) therefore $Z_{xr} = (1/0.1737)X_{xr}$.

atm. moisture tension, hence their relative moisture contents by volume are not the same (see Table 74).

Gill (1959), working with Lloyd clay, has found that increases in tensile strength were associated with moisture losses which occurred during the aging period of his test samples. His test apparatus consisted of an hour-glass shaped mold into which soil, passing a 0.200 cm. sieve and moistened to approximately 25% moisture content by weight, was compressed at 54 psi using a pneumatically operated plunger. In one series of tests, moisture contents were adjusted to the levels obtained for other samples by aging. On these samples, following the addition of required amounts of water and compression, the tensile strength tests were run immediately.

Gill's results indicate that although the strength varied inversely as the moisture content, the maximum tensile strength values were obtained at about 20% moisture content and amounted to about 8×10^6 dyn. cm.⁻². On further drying there was a slight decrease in tensile strength. It is possible that the decrease occurred as a result of the shattering of some previously formed bonds. We would expect that under the conditions of aging where moisture loss is slow, the surface of a briquette could be in an air-dry condition while the center was still moist. This would result in stresses on the surface as the drying continued and would very likely cause some shattering of the previously formed bonds. We feel that the explanation given above could account for lower values obtained in the air-dry conditions [see also the discussion of Koenigs (1961) work below Table 23].

The values of tensile strength for samples on which the moisture

content was adjusted just prior to tensile strength determination (Gill, 1959) were much lower than the corresponding values for samples on which the same moisture content was obtained by aging. If we assume that on aging the orderly redistribution of stresses and strains within and among the clay particles accounts for the soil strength, it should be quite obvious that in samples that are moistened and tested immediately no orderly redistribution of stress and strains within clay can occur.

As we mentioned above, the maximum value of tensile strength of Lloyd clay was found by Gill to be $8.0 \times 10 \text{ dyn. cm.}^{-2}$. This value compares favorably with the value of $7.13 \times 10^6 \text{ dyn. cm.}^{-2}$ obtained by us for Luton si.c. (Table 48). Gill's initial values of tensile strength are somewhat higher than the values of tensile strength for our aggregates at 15 atm. moisture tension.

Change in energy of rupture (Table 50) The values for energy of rupture in the air-dry condition T_1 and at 15 atm. moisture tension T_2 and the values of the change in energy of rupture $\Delta T = T_1 - T_2$ again reflect the respective clay contents of the given soils. The highest energy of rupture ($36.00 \times 10^4 \text{ ergs cm.}^{-2}$) and the highest change in the energy of rupture ($31.46 \times 10^4 \text{ ergs cm.}^{-2}$) was obtained on Luton si.c.; the lowest values are given by Clarion s.l. This is an expected result. In terms of clay content Luton si.c. soil would exhibit the highest surface area. If T is taken as a measure of the surface tension of soil, the higher clay contents would undoubtedly give higher values of surface tension. If T is taken as a measure of the energy of plastic deformation, the highest clay content would likewise give highest values.

According to the Griffith crack theory (see Theory III), the tensile

strength of the soil would be that value of stress at which the reduction of strain energy resulting from the spreading of the crack is equal to the increase of surface energy T due to fracture. Then the change in energy of rupture would give the amount of work done by water or outside forces on the aggregates of the soils. Schofield (1938) and Payne (1954) have related the work of desorption to the pore size distribution and surface area of aggregates respectively. We suspect that the rate of water movement in the unsaturated state for a given soil could be related to the rate of change with moisture in the energy of rupture.

Much of the theory of unsaturated flow (Philip, 1957); Nielsen et al., 1961; Hanks and Bowers, 1963) centers around the concept of diffusivity^a where $K(\theta)$ and $D(\theta)$ are assumed to be the functions of the moisture content by volume. We feel in view of our discussion that the rate of change in the rupture energy might be a more meaningful parameter relating the change of moisture content by volume to the geometry change of the medium.

Moldenhauer and Long (1964), using a rainfall simulator, have determined the amount of energy (T_i) in terms of rainfall, intensity, and duration necessary to initiate a runoff on the 1300 cm.² test sample of some Iowa soils. In particular their results show that a rainfall of 3.43 cm. hr.⁻¹ intensity on a Luton si.c. soil composed of aggregates less than 0.800 cm. in diameter started the runoff after 56 minutes, when the total energy input was 66.9×10^4 ergs cm.⁻². On Haegner sand (s) soil composed of the

^aDiffusivity, $D(\theta)$, is taken as $D(\theta) = [K(\theta)\partial\psi/\partial\theta]$ where θ is the moisture content by volume and ψ is the capillary potential.

same size aggregates the rainfall of the same intensity started the runoff after 90 minutes, while the total energy input was 121.0×10^4 ergs cm^{-2} . Doubling the rainfall intensity decreased the time for a runoff to start by one-half, but the total energy input remained essentially constant for respective soils.

Evaluating the results of Moldenhauer and Long in terms of the results obtained by us, there seems to be little correspondence between the energy necessary to initiate runoff, T_i , and the energy of rupture of soil aggregates, T_r , for Luton si.c.^a This impression however is deceptive. To understand clearly the relationship between our results and those obtained by Moldenhauer and Long we need first to analyze the variables involved in the process of runoff and erosion.

We may assume that the amount of energy necessary to initiate a runoff, T_i , should be proportional to the energy of rupture, T_r , of the soil aggregates in air-dry condition. Our results indicate that all but a small fraction of this energy is dissipated by wetting and equilibration of aggregates at 15 atm. moisture tension. Similarly we would expect most of this energy to be given off when aggregates are subjected to wetting by a steady rainfall.

As the energy of rupture T_r is lowered, as a result of wetting, at some time (t) it will be low enough for an aggregate to be ruptured by the impacting water drops. For the sake of simplicity we will assume that the energy of rupture in air-dry condition, T_r , represents the total amount of energy necessary to rupture the aggregate by raindrop impact.

^aLuton si.c. was the only soil used by us that has also been used by Moldenhauer and Long in their study.

Furthermore, we would expect the amount of energy required for initiation of runoff, T_i , to vary with the respective porosity of the soil and its slope. In the studies of Moldenhauer and Long the slope was constant for all soils studied. On the other hand, the porosity, or rather the change in macro-porosity (assuming similar initial packing of aggregates), would vary considerably. The change in porosity would depend on (a) amount of swelling of individual soil aggregates and (b) the rate at which the macropores would become clogged with fine material from ruptured surface aggregates. When the porosity becomes limiting, i.e., when the rainfall rate exceeds the infiltration rate, the runoff will start.

Both (a) and (b) above would depend to a very large extent on the amount of clay in the respective soils. We therefore assume that the difference between the energy necessary to initiate runoff, T_i , and the energy of rupture, T_r , for aggregates in air-dry condition should be inversely proportional to the clay content of the soil. That is, we should have

$$(T_i - T_r) \times \% \text{ clay} = K_i \quad (146)$$

where K_i is a constant for a given moisture content.

Our value for T_r on Luton si.c. is 39×10^4 ergs cm^{-2} and for clay is 52.0% (for both of these values see Appendix III, Table 75) using Moldenhauer and Long value for T_i of 66.9×10^4 ergs cm^{-2} and Equation 146 we have obtained K_i equal to 14.6×10^4 ergs cm^{-2} .

To establish how Equation 146 applied to a number of soils over a range of texture, Moldenhauer¹ using our apparatus and procedure determined

¹Moldenhauer, W. C. USDA ARS., Ames, Iowa. Data from rupture stress analysis. Private communication. 1964.

the energy of rupture T_r on the soils studied before (Moldenhauer and Long, 1964). Moldenhauer's preliminary results are shown in Table 51e.

The values of K_i in Table 51e appear reasonably constant for all soils except for IDA. This suggests that a very fine silt fraction (IDA is 88.4% silt) could have the same effect as that produced by clay alone on the values of K_i in Equation 146. Since we consider clay as smaller than 2 microns in size any larger particles (i.e., 2 to 5 microns) would not be measured as clay by a conventional pippette analysis. These particles, classified as fine silt would have a similar effect on sealing of pores according to Moldenhauer as the smaller clay particles. Thus if these particles (2 to 5 microns) were taken into account and added to the 0.116 factor for clay a new higher factor would result giving higher K_i values for IDA. The above discussion illustrates the inadequacies of conventional particle analysis where continuous particle distribution curves are needed.

The discrepancy that exists between the K_i values for Luton si.c. as obtained by us (14.6×10^4 ergs cm^{-2}) can be traced to the difference in moisture content (3.55 for ours vs 4.75 for Moldenhauer's). Since higher moisture content would result in lower crushing strength and consequently lower values of T_r the values of K_i obtained from Equation 146 would be higher (as illustrated). This suggests that K_i values are dependent on the moisture content by weight and might be equal to approximately 9.8×10^4 ergs cm^{-2} provided moisture content by weight is around 2.50%.

If the values of K_i are indeed constant for all soils, provided the slope, the aggregate size and initial packing and moisture content, are comparable, the Equation 146 could be of great use in the study of erosion

Table 51e. Preliminary values of K_i as computed by Moldenhauer^a from Equation 146 for selected Iowa soils over a wide range of texture^b

Soil	Texture	Moisture by weight %	d cm.	T_i $\times 10^4$	T_r $\times 10^4$	$(T_i - T_r)$ ergs cm. ⁻²	Clay g.g. ⁻¹	K_i $\times 10^4$ ergs cm. ⁻²
Luton	si.c.	4.75	0.484	66.9	23.5	43.4	0.530	23.0
IDA	si.	2.47	0.514	43.8	11.6	32.2	0.116	3.7
Marshall	si.c. l.	2.76	0.538	63.8	40.1	23.7	0.364	8.6
Moody	si.c. l.	2.91	0.555	46.2	17.4	28.8	0.320	9.2
Grundy	si.c. l.	3.74	0.486	55.4	18.8	36.6	0.320	11.7
Seymour	si.c. l.	2.65	0.509	58.8	21.5	37.3	0.284	10.6
Kenyon	l.	1.80	0.532	64.6	16.8	47.8	0.225	10.8
Haegner	s.	2.13	0.457	121.0	1.0	120.0	0.069	8.3

^aMoldenhauer, W. C. Ames, Iowa. Data from rupture stress analysis. Private communication. 1964.

^bTexture: si. = silt

si.c. l. = silty clay loam

l. = loam

s. = sand

problems. Measurement and computation of T_r and percent of clay are relatively simple, easy, fast, and cheap as compared with the equipment and procedure for current runoff studies; however, more experimental data are needed before any final conclusions are made.

Tensile and crushing strength values in psi (Table 51)

Tensile and crushing strength values in psi for the soils as a whole in air-dry condition and at 15 atm. moisture tension are given in Table 51. These values are listed for reference and have been discussed in terms of cgs units in the discussion of Table 45, Table 48, and Table 49. Conversion factors are listed below Table 33.

SUMMARY AND CONCLUSIONS

This dissertation deals with the strength of individual soil aggregates. Aggregates from the plow layer of Clarion sandy loam (s.l.), Webster clay loam (c.l.), and Luton silty clay (si.c.), 0.200 to 0.800 cm. in diameter were studied. The 0.200-0.800 cm. aggregates of each soil were separated into groups of known density range by a specially developed heavy liquid fractionation method. Following density fractionation the aggregates in each Density groups were further subdivided into three Size groups (0.200-0.283, 0.283-0.476, 0.476-0.800).

Percent of carbon (organic matter), percent of clay, and percent of water stable aggregates was determined on each Size-density group of every soil. The data were averaged with respect to aggregate Size groups, with respect to aggregate Density groups, and with respect to the Soils as a whole. Analysis of variance was performed on the data and the results for Size and Density groups were compared by Duncan's multiple range test.

Aggregate size, crushing strength at rupture, and strain at rupture were obtained on 40 aggregates of each Size-density group in air-dry condition and at 15 atm. moisture tension^a. The data were averaged with respect to aggregate Size groups, with respect to aggregate Density groups, and with respect to Soils as a whole. Analysis of variance was performed on the data and the results for Size and Density groups were compared by Duncan's multiple range test. All the size and strength measurements were obtained with a modified unconfined compression test apparatus as used in soil engineering, employing 10 and 25 lbs. capacity proving rings and strain

^aFewer than 40 aggregates were measured at 15 atm. moisture tension.

gauges with a sensitivity of 1/10000 inch.

The assumption that surface soil aggregates are spherical in shape was tested. The gravity fractionation of aggregates is analyzed in detail and the possible sources or error are given.

The theoretical treatment of aggregate strength is based on the elementary theory of elasticity. From the equation for a sphere under the concentrated loads at the poles (Sternberg and Rosenthal, 1952) and the photoelastic considerations (Frocht and Guernsey, 1952), the values of crushing and tensile stress on the equatorial and on the polar plane respectively are computed.

It is assumed that modulus of elasticity in tension is not equal to the modulus of elasticity in compression. Strain on equatorial plane is obtained experimentally, strain on polar plane, modulus of elasticity in tension, and modulus of elasticity in compression are computed. The ratio of transverse to longitudinal strain (Poisson ratio) of the material of the aggregates was established to be about 0.5, a value used in all calculations.

The Griffith crack theory of rupture (Griffith, 1924) is applied to soils. According to this theory the tensile strength of the material is inversely proportional to the square root of the length of a suitable worst-oriented crack. It is assumed that the length of the crack will be equal to the polar diameter of a soil aggregate. Using the Griffith crack theory, values of the energy of rupture are obtained.

Empirical equations are derived relating the influence of carbon (organic matter), clay, void ratio, and porosity to the strength measurements on the Size groups, Density groups, and Soils as a whole. An

assumption that the modulus of elasticity in tension varies as a change in void ratio, porosity, and size due to the change of moisture content is tested.

Weibull's theory of brittle rupture is applied to soils studied (Weibull, 1939a). Weibull assumes that the probability of rupture, S , at any given distribution of stresses, Z , over the volume, V is given by: $\log (1-S) = - \int_V f(Z) dV$. The differences between the Size and Density groups are examined and the ultimate aggregate size is computed.

The data are compared with the results obtained for soil strength by other research workers. A relationship between the penetrometer method (Taylor and Gardner, 1963) and soil strength as given by us is suggested. Values of shear strength computed from our data are compared with values obtained by others. The concept of inter- and intra-aggregate strength is examined and a correspondence between the energy of rupture and the amount of energy required to initiate runoff (Moldenhauer and Long, 1964) is shown.

In Table 51f principal results obtained for aggregates of Clarion s.l., Webster c.l., and Luton si.c. are shown. In Table 51g principal levels of significance for selected properties averaged over size (diameter) and density are given.

From our results it is concluded that for Clarion s.l., Webster c.l., and Luton si.c. soils tested:

- 1) We have demonstrated that density D and porosity P of porous aggregates can be determined uniquely by gravity fractionation using two pore liquids whose S.G. is k_1 and k_2 ($k_1 < k_2$) respectively. Then if D_A is the composite density (soil + pore liquid) of an aggregate

Table 51f. Summary of the results obtained for aggregates of Clarion s.l., Webster c.l. and Luton si.c. in air-dry condition

Property	Units ^a	Soils		
		Clarion s.l.	Webster c.l.	Luton si.c.
		Average values		
Size	cm.	0.361	0.372	0.372
Density	g. cm. ⁻³	1.86	1.84	2.02
Porosity	%	31.4	31.6	25.8
Void ratio		0.457	0.461	0.346
Carbon	%	0.99	3.26	2.96
Clay	%	15.1	31.4	52.0
WS	% ^b	58.4	48.0	59.6
SA	%	58.8	38.0	66.5
$Z_{zr}^c \times 10^6$	dyn.cm. ⁻²	5.60	13.64	41.04
$X_{xr}^c \times 10^6$	dyn.cm. ⁻²	0.92	2.41	6.73
$T_r \times 10^4$	ergs cm. ⁻²	3.33	10.19	39.43
$E_x \times 10^6$	dyn.cm. ⁻²	7.96	14.66	35.43
A	cm. ^{0.5}	0.073	0.094	0.119

^aConversion factors:

$$1 \text{ dyn.cm.}^{-2} = 1.45 \times 10^{-5} \text{ lbs/sq. inch (psi)}$$

$$1 \text{ ergs cm.}^{-2} = 6.9 \times 10^{-4} \text{ ft.-lb./sq.ft.}$$

^bWS = water stability

SA = stable aggregates exhibiting non-zero stress at rupture when moist

^c Z_{zr} = crushing strength

X_{xr} = tensile strength

T_r = energy of rupture

E_x = modulus of elasticity in tension

A = constant, moisture and soil dependant

Table 5lg. Significance levels^a for selected properties averaged over size (diameter) and density of Clarion s.l., Webster c.l. and Luton si.c. aggregates in air-dry condition

Property	Soils					
	Clarion s.l.		Webster c.l.		Luton si.c.	
	Size	Density	Size	Density	Size	Density
	Significance level					
Carbon	**	**	NS	**	**	**
Clay	NS	*	NS	*	NS	NS
WS	NS	NS	*	NS	*	**
Z _{zr}	**	*	**	**	**	NS

^aSignificance levels:

** = significant at 1%

* = significant at 5%

NS = non-significant

filled with pore liquid A and D_B is the composite density of an aggregate filled with pore liquid B,

$$D = \frac{k_2 D_A - k_1 D_B}{k_2 - k_1}$$

and

$$P = \frac{D_B - D_A}{k_2 - k_1}$$

Ideally pore liquids should have low heat of vaporization, low vapor pressure, should be non-polar, and should be immiscible with

fractionation liquid.

If the liquids are miscible with fractionation liquid, then we have to make a choice. If we want exact D values, we should choose a pore liquid so that $\frac{k_1 + \Delta k_1}{k_1} = \frac{k_2 + \Delta k_2}{k_2}$, where Δk is the change of pore liquid density as a result of mixing with fractionation liquid.

On the other hand, if exact values of P are required, then

$\Delta k_1 = \Delta k_2$ should be the criterion of selection. Finally, when applying the method to soils, hygroscopic water should be taken into account.

In particular, heavy clays and loams will give lower values for porosity if there is hygroscopic water present. But this water will not affect the density separation.

- 2) The plow layer soil aggregates can be considered as spheres; however, more closely they approximate spheroids. The mean aggregate diameter for aggregates greater than 0.200 cm. but less than 0.476 cm. in size is equal to the harmonic mean of the sieving class.
- 3) Aggregates when considered in a statistical sense obey Hooke's law, i.e., that the stress is proportional to strain, both in air-dry condition and at 15 atm. tension. But the modulus of elasticity in tension does not equal the modulus of elasticity in compression.
- 4) Water stability values WS do not vary from soil to soil in the same manner as does soil strength. Water stability values WS for Clarion s.l., Webster c.l., and Luton si.c. are related to the percent of stable aggregates SA (aggregates exhibiting non-zero strength after moistening).
- 5) Crushing strength Z_{zr} at the center of spherical aggregate under

concentrated loads at the poles is given by

$$Z_{zr} = 3F(14+5u)/2\pi r^2(7+5u)$$

where F is the load, u is the ratio of transverse to longitudinal strain (Poisson ratio), and r is aggregate radius.

- 6) Aggregate tensile strength X_{xr} is given by

$$X_{xr} = 0.1737 Z_{zr}$$

- 7) The Griffith crack theory of rupture can be applied to soils studied both in air-dry condition and at 15 atm. moisture tension. The tensile strength X_{xr} of the soil aggregates varies inversely as the square root of their diameter, d .

$$X_{xr} = AE_x/d^{0.5}$$

where A is a constant characteristic of soil and moisture content.

- 8) The energy of rupture T_r is given by

$$T_r = (\pi A^2 E_x)/4$$

and is related to the amount of energy required to initiate runoff, T_i on selected Iowa soils, by

$$(T_i - T_r) \times \% \text{ clay} = K_i$$

where $K_i = 9.8 \times 10^4 \text{ ergs cm.}^{-2}$ is an approximate value of the constant K_i . The values of K_i appear to be very sensitive to changes in moisture content.

- 9) The modulus of elasticity in tension for Size groups is inversely proportional to the aggregate diameter, d . For Density groups the

tensile strength is inversely proportional to the void ratio v whereas the strain is found to be proportional to porosity P . All the quantities above are directly proportional to some clay-carbon function. For the Soils as a whole the modulus of elasticity in tension E_x is given by

$$E_x = v^{-1} \times \% \text{ clay} \times K_r$$

where $K_r = 2.30 \times 10^7 \text{ dyn. cm.}^{-2}$ is thought to represent the modulus of rupture for clay in the soil.

- 10) The over-all effect of a significantly lower carbon content is to increase aggregate strength by decreasing aggregate size. Aggregates with low carbon content are also observed to have lower values of water stability.
- 11) The value of the modulus of elasticity in tension, after correcting for volume expansion does not approximate the modulus of elasticity in tension at 15 atm. moisture tension. The only exception is Luton si.c. which expanded more than the other two soils when the moisture content was increased from the air-dry to 15 atm. condition. Little difference was observed among the crushing strength of all soils (ca. $1.5 \times 10^6 \text{ dyn. cm.}^{-2}$) when moist. Decrease in strength of moist aggregates cannot be explained by swelling alone but is thought to be related to the equilibrium between hygroscopic imbibitional and capillary water within soil aggregates.
- 12) Weibull's theory shows that the aggregates of the soils studied are composed of basically similar material. In air-dry condition a more mature soil (Webster c.l.) can be distinguished from the other

two (Clarion s.l. and Luton si.c.) Likewise, when the Density groups are examined, the groups with a significantly lower carbon content can be differentiated.

- 13) The size of an ultimate aggregate (smallest aggregate whose probability of survival at average rupture stress is 0.90) according to Weibull's theory is 1042 microns on Webster c.l., 297 microns on Clarion s.l., and 241 microns on Luton si.c.
- 14) The relationship between soil resistance per unit area R , to crushing strength Z_{zr} should be given by

$$Z_{zr} = R/6$$

- 15) The value of maximum shear strength τ_{max} of Webster c.l. is given by

$$\tau_{max} = (1/2)(Z_{zr} - X_{xr})$$

- 16) Since in the studies of Pfeffer (Gill and Bolt, 1955) the roots of selected plants were found to exert axial pressures as high as 166 psi and the values of soil crushing strength obtained by us vary between 13.8 to 595.1 psi depending on the soil and moisture content, the values of soil strength should be of great use and interest in soil and root studies.

These values are given in terms of units that can easily be understood and compared with the values of other research workers. Furthermore, these values can be related to the energy relationships of plants and environment.

LITERATURE CITED

- American Society for Testing Materials. Procedures for testing soils.
1947 2nd ed. Philadelphia, Pa. Author.
- Bangham, D. H. Physical processes involved in sintering. Soc. Glass
1947 Tech. J. 31:264-266.
- Bangham, D. H., Fakhoury, N. and Mohamed, A. F. The swelling of charcoal.
1932 II. Roy. Soc. (London) Proc. Ser. A, 138:162-183.
- Barley, K. P. Influence of soil strength on growth of roots. Soil Sci.
1963 96:175-180.
- Baver, L. D. Soil Physics. 3rd ed. New York, N.Y. John Wiley and Sons,
1956 Inc.
- Beech, D. G. and Holdridge, D. A. Some aspects of the testing of clays
1954 for the pottery industry. Brit. Ceram. Soc. Trans. 53:103-133.
- Bowen, H. J. M. Tables of interatomic distances and configurations in
1958 molecules and ions. Chem. Soc. London Spec. Pub. No. 11.
- Chepil, W. S. Apparent density of soil particles. Soil Sci. 70:351-362.
1950
- Chepil, W. S. Properties of soil which influence wind erosion: V.
1951 Mechanical stability structure. Soil Sci. 72:465-478.
- Chepil, W. S. Improved rotary sieve for measuring state and stability of
1952 dry soil structure. Soil Sci. Soc. Am. Proc. 16:113-117.
- Coile, T. S. Soil samplers. Soil Sci. 42:139-142.
1936
- Curry, A. S. A comparison of methods for determining the volume weight of
1931 soils. J. Agric. Res. 42:765-772.
- Daniels, F. and Alberty, R. A. Physical chemistry. New York, N.Y., John
1958 Wiley and Sons, Inc.
- Davidson, S. E. and Page, J. B. Factors influencing swelling and shrinkage
1956 in soils. Soil Sci. Soc. Am. Proc. 20:320-324.
- Day, P. R. and Holmgren, G. G. Microscopic changes in soil structure
1952 during compression. Soil Sci. Soc. Am. Proc. 16:73-77.
- De Leenheer, K. Introduction a l'etude minearalogique des sols du Congo
1944 Belge. Inst. Nat. Et. Agron. Congo, Public. No. 25.

- De Leenheer, L. Soil mineralogy. Unpublished set of lectures on soil
1961a mineralogy. Ames, Iowa. Department of Agronomy. Iowa State
University of Science and Technology.
- De Leenheer, L. Soil structure. Unpublished set of lectures on soil
1961b texture and structure (soil physics). Ames, Iowa. Department
of Agronomy. Iowa State University of Science and Technology.
- De Leenheer, L. and De Boodt, M. Determination of aggregate stability
1959 by change in mean weight diameter. Medel. Landbouwhogeschool,
Gent. 24:290-300.
- Deryagin, B. V. and Melnikova, N. K. Mechanism of moisture equilibrium
1958 and migration in soils. Highway Res. Board Spec. Rep. 40:43-54.
- Dollimore D. and Gregg, S. J. The strength of brittle solids. Research
1958 Applied in Industry 11:180-184.
- Duncan, D. B. Multiple range and multiple t-tests. Biometrics 11:1-42.
1955
- Emerson, W. W. The structure of soil crumbs. J. Soil Sci. 10:235-244.
1959
- Evans, I. and Pomeroy, C. D. The strength of cubes of coal in uniaxial
1958 compression. In Walton, W. H., ed. Mechanical properties of non-
metallic brittle materials. pp. 5-28. New York, N.Y. Inter-
science Publishers, Inc.
- Fitts, J. W., Lyons, E. S. and Rhoades, H. F. Chemical treatment of
1943 "slick spots". Soil Sci. Soc. Proc. 8:432-436.
- Foster, A. G. Pore size and pore distribution. Farad. Soc. Disc. 3:41-51.
1948
- Frocht, M. M. and Guernsey, Jr., F. A special investigation to develop
1952 a general method for three-dimensional photoelastic stress analysis.
Nat. Adv. Comm. for Aeronautics Technical Note 2822.
- Gardner, W. R. Representation of soil aggregate size distribution by a
1956 logarithmic normal distribution. Soil Sci. Soc. Am. Proc. 20:
151-153.
- Gerard, C. J., Cowley, W. R., Burleson, C. A. and Bloodworth, M. E. Soil
1962 hardpan formation as affected by rate of moisture loss, cyclic
wetting and drying and surface applied forces. Soil Sci. Soc.
Am. Proc. 26:601-605.
- Gill, W. R. The effect of drying on the mechanical strength of Lloyd clay.
1959 Soil Sci. Soc. Proc. 23:255-257.

- Gill, W. R. and Bolt, G. H. Pfeffers' studies of the root growth pressure
1955 exerted by plants. Agron. J. 47:166-168.
- Gill, W. R. and Miller, R. D. A method for study of the influence of
1956 aeration on growth of seedling roots. Soil Sci. Soc. Am. Proc.
20:154-157.
- Graecen, E. L. The strength of cultivated soil. J. Agric. Eng. Res.
1959 4:60-61.
- Gregg, S. J. The surface chemistry of solids. 2nd ed. New York, N.Y.
1961 Reinhold Publishing Corp.
- Griffith A. A. The phenomena of rupture and flow in solids. Roy. Soc.
1921 (London) Phil. Trans. Ser. A, 221:163-198.
- Griffith, A. A. The theory of rupture. First International Congress
1924 for Applied Mechanics Proc.
- Grossman, R. B. Characterization of ped surfaces in contrast to ped
1959 interiors from B horizons of some major great soil groups in
Illinois. Unpublished Ph.D thesis. Urbana, Illinois. Library,
University of Illinois.
- Grossman, R. B. and Cline, M. G. Fragipan horizons in New York soils. II.
1957 Relationship between rigidity and particle size distribution. Soil
Sci. Soc. Am. Proc. 21:322-325.
- Guerney, C. and Borysowski, Z. Delayed fracture of materials under ten-
1948 sion, torsion and compression. Phys. Soc. (London) Proc. 61:
446-452.
- Haines, W. B. The volume changes associated with variations of water con-
1923 tent in soil. J. Agric. Sci. 13:296-310.
- Hanks, R. J. and Bowers, S. A. Influence of variations in the diffusivity
1963 water content relation on infiltration. Soil Sci. Soc. Am. Proc.
27:263-265.
- Hardesty, J. O. and Ross, W. H. Factors influencing granulation of ferti-
1938 lizer mixtures. J. Ind. and Eng. Chem. 30:668-672.
- Henin, S. and Turc, L. Essais de fractionnement des matieres organiques
1950 du sol. Fourth Int. Cong. Soil Sci. Trans. 1:152.
- Herdan, G. Small particle statistics. 2nd ed. New York, N.Y. Academic
1960 Press.
- Hildebrand, J. H. and Scott, R. L. The solubility of nonelectrolytes. 3rd
1950 ed. New York, N.Y. Reinhold Publishing Corporation.

- Hildebrand, J. H. and Scott, R. L. Regular solutions. Englewood Cliffs, 1962 N. J. Prentice-Hall, Inc.
- Hildebrand, W. F. A danger to be guarded against in making mineral
1913 separations by means of heavy solutions. Am. J. Sci. Ser. 4,
35:439-440.
- Hooghoudt, S. B. Bijdragen tot de kennis van enige natuur kundige
1950 grootheden vande grond. No. 10. The modulus of rupture by
pressure, by bend, by smash and by tear, and the hardness of
soils in a dried state. Groningen, Netherlands. Vers.
Landbouwk. Onderz. No. 56.3.
- Hodgman, C. D. Handbook of chemistry and physics. 45th ed. Cleveland,
1962 Ohio. Chemical Rubber Publishing Company.
- Horton, M. L. Soil compaction and corn growth under controlled moisture
1962 conditions. Unpublished Ph.D thesis. Ames, Iowa, Library, Iowa
State University of Science and Technology.
- Jaeger, J. C. Elasticity fracture and flow. New York, N.Y. John Wiley
1956 and Sons, Inc.
- Jordan, T. E. Vapor pressure of organic compounds. New York, N.Y. Inter-
1954 science publishers.
- Jumikis, A. R. Soil mechanics. Princeton, N.Y. D. Van Nostrand Company.
1962
- Keen, B. A. Experimental methods for the study of soil cultivation. Emp.
1933 J. Exp. Agric. 1:97-102.
- Kirkham, Don. Advanced soil physics. A set of 20 lectures. Soil Sci.
1960 Inst. Ghent, Belgium. Mimeo. Revised 1960. Ames, Iowa. Depart-
ment of Agronomy. Iowa State University of Science and Technology.
- Kirkham, Don, De Boodt, M. and De Leenheer, L. Modulus of rupture determin-
1958 ation on cylindrical soil samples. International Symposium on Soil
Structure, Ghent, Belgium, Proc. 369-376.
- Knox, E. G. Fragipan horizons in New York soils. III. The basis of
1957 rigidity. Soil Sci. Soc. Am. Proc. 21:326-330.
- Koenigs, F. F. R. The mechanical stability of clay soils as influenced by
1961 the moisture conditions and some other factors. Vers. Landbouwk.
Onderz. 67, No. 7.
- Kruyer, S. The penetration of mercury and capillary condensation in packed
1958 spheres. Farad. Soc. Trans. 54:1758-1767.

- Krumbein, W. C. and Pettijohn, F. J. Manual of sedimentary petrography.
1938 New York, N.Y. Appleton Century Co.
- Kuipers, H. Confined compression tests on soil aggregate samples. Inter-
1958 national Symposium on Soil Structure, Ghent, Belgium, Proc. 349-
357.
- Kuipers, H. Preliminary remarks on porosity of soil aggregates in air-
1961 dry state and at pF 2. Neth. J. Agric. Sci. 9:168-173.
- Lein, Z. Y. K voprosu o formah svyazu gumusa s mineralnoy chastiu pochvy.
1940 Pochvovedenie. 10:41-57.
- Love, A. E. H. A treatise on the mathematical theory of elasticity.
1927 4th ed. Cambridge, England. University Press.
- Lutz, J. F. Apparatus for collecting undisturbed soil samples. Soil
1947 Sci. 64:399-401.
- Lyon, T. L., Buckman, H. O. and Brady, N. C. 5th ed. New York, N.Y.
1952 Macmillan Company.
- Marshall, J. S. and Pounder, E. E. Physics. New York, N.Y. Macmillan
1957 Company.
- Martinson, D. C. and Olmstead, L. B. Crushing strength of aggregated
1949 soil materials. Soil Sci. Soc. Am. Proc. 14:34-38.
- Mattson, S. Laws of soil colloidal behavior: VIII. Forms and functions
1932 of water. Soil Sci. 33:301-323.
- Mebius, L. J. Determination of organic carbon. Anal. Chim. Acta 22:120.
1960
- Mellor, J. W. Jackson's and Purdy's surface factors. Cer. Soc. Trans.
1910 9:94-113.
- Meredith, H. L. and Patrick, W. H., Jr. Effect of soil compaction on sub-
1961 soils root penetration and physical properties of three soils in
Louisiana. Agr. J. 53:163-167.
- McClelland, J. E., White, E. M. and Riecken, F. F. Causes of differences
1950 in soil series of the Missouri River bottomland of Monona County
Iowa. Acad. of Sci. 57:253-260.
- McIntyre, D. S. and Stirk, G. C. A method for determination of apparent
1954 density of soil aggregates. Aust. J. Agric. Res. 5:291-296.
- McMurdie, J. L. Some characteristics of soil deformation process. Soil
1963 Sci. Soc. Proc. 27:251-254.

- McMurdie, J. L. and Day, P. R. Compression of soil by isotropic stress.
1958 Soil Sci. Soc. Am. Proc. 22:18-21.
- Millard, D. J., Newman, P.C., and Phillips, J. W. Apparent strength of
1955 extensively cracked materials. Phys. Soc. (London) Proc. Ser.
B, 68:723-728.
- Moldenhauer, W. C. and Long, D. C. Influence of rainfall, energy on soil
ca. loss and infiltration effect over range of texture. [Presented
1964 for publication to Soil Sci. Soc. Proc.]
- Monnier, G., Turc, L., Jeanson, C., and Vusinang, L. Fractionation of
1962 soil organic matter by centrifugation. Ann. Agron. 13:55-63.
- Nielsen, D. R., Kirkham, Don, and Van Wijk, W. R. Diffusion theory
1961 calculations of field soil water infiltration profiles. Soil
Sci. Soc. Am. Proc. 25:165-168.
- Nota, D. J. G. and Bakker, A. M. G. Identification of soil minerals using
1960 optical characteristics and specific gravity separation. Medel.
Landbouwkogeschool, Wageningen, Nederland, 60, No. 11:1-11.
- Orowan, E. Fracture and strength of solids. Phys. Soc. (London) Repts.
1949 on Prog. in Physics 12:186-231.
- Payne, D. The determination of approximate surface area of soil crumbs.
1954 Fifth Int. Cong. Soil Sci. Trans. 2:46-52.
- Pearson, R. W. and Truog, E. Procedure for the minearalogical subdivision
1937 of soil separate by means of heavy liquid specific gravity
separation. Soil Sci. Soc. Am. Proc. 2:109-114.
- Peltier, R. Theoretical investigation of the Brazilian test. Int. Assoc.
1954 Test. Res. Lab. Paris. Bul. 19:31-69.
- Perry, P. A simple rapid method of determining the apparent density of
1942 soil aggregates. Soil Sci. Soc. Am. Proc. 7:409-411.
- Philip, J. R. The theory of infiltration. I. The infiltration equation
1957 and its solution. Soil Sci. 83:345-357.
- Phillips, R. E. and Kirkham, Don. Soil compaction in the field and corn
1962 growth. Agr. J. 54:29-34.
- Phillips, R. E. Soil compaction and corn growth. Unpublished Ph.D thesis.
1959 Ames, Iowa. Library, Iowa State University of Science and
Technology.
- Phillips, R. E., Jensen, C. R. and Kirkham, D. Use of radiation equipment
1960 for plow-layer density and moisture. Soil Sci. 89:2-7.

- Quirk, J. P. and Panabokke, C. R. Pore volume-size distribution and swelling of natural soil aggregates. *J. Soil Sci. (Oxford)* 13:71-81. 1962
- Richards, L. A. Pressure membrane apparatus, construction and use. *Agr. Engr.* 28:451-454. 1947
- Richards, L. A. Modulus of rupture as an index of crusting in soil. *Soil Sci. Soc. Proc.* 17:321-323. 1953
- Rogowski, A. S. Stability of soil aggregates as affected by moisture and forming pressure. Unpublished M.S. thesis. Ames, Iowa. Library, Iowa State University of Science and Technology. 1960
- Rogowski, A. A. and Kirkham, Don. Moisture, pressure and formation of water stable soil aggregates. *Soil Sci. Soc. Am. Proc.* 26:213-216. 1962
- Russell, E. W. The interaction of clay with water and organic liquids as measured by specific volume changes and its relation to the phenomena of crumb formation in soil. *Roy. Soc. London Phil. Trans. Ser. A*, 233:361-389. 1934
- Russell, E. W. Soil structure. *Imp. Bur. Soil Sci. Tech. Comm.* 37. 1938
- Russell, E. W. The laboratory determination of the volume weight and air space of stony soils. *2nd. Int. Conf. Soil Mech. Proc.* 3:94-96. 1948
- Russell, E. W. and Balcerak, W. The determination of the volume and air space of soil clods. *J. Agric. Sci.* 34:123-132. 1944
- Schafer, R. L. A technique for measuring shear forces of agricultural soils. Unpublished M.S. thesis. Ames, Iowa. Library, Iowa State University of Science and Technology. 1961
- Schofield, R. K. Pore-size distribution as revealed by the dependance of suction (pF) on moisture content. *First Comm. Int. Soc. Soil Sci. Trans. A*:38-45. 1938
- Scott, R. L. The solubility of fluorocarbons. *Am. Chem. Soc. J.* 70:4090-4092. 1948
- Shaw, C. F. A method for determining volume weight of soils in field condition. *Am. Soc. Agron. J.* 9:38-42. 1917
- Sideri, D. T. Soil swelling. I. The swelling of soil in water considered in connection with the problem of soil structure. *Soil Sci.* 41:135-151. 1936
- Snedecor, G. W. Statistical methods. 5th ed. Ames, Iowa. Iowa State College Press. 1957

- Stauffer, L. H. Measurement of physical characteristics of soils.
1927 Soil Sci. 24:373-379.
- Sternberg, E. and Rosenthal, F. The elastic sphere under concentrated
1952 loads. J. Appl. Mech. 19:413-421.
- Sullivan, J. D. Heavy liquids for mineralogical analyses. U. S. Bureau
1927 of Mines Tech. Paper 381.
- Taylor, D. W. Fundamentals of soil mechanics. New York, N.Y. John Wiley
1948 and Sons, Inc.
- Taylor, H. M. and Gardner, H. R. Penetration of cotton seedling tap roots
1963 as influenced by bulk density, moisture content, and strength of
soil. Soil Sci. 96:153-156.
- Taylor, H. M., Burnnett, E., and Welch, N. H. Influence of soil strength
ca. on root growth habits of plants. Unpublished paper presented at
1962 Am. Soc. Agr. Eng. meeting, Washington, D.C., June, 1962. Mimeo.
S.W. Great Plains Field Sta., Bushland, Texas. U. S. Dept. of Agr.
- Terzaghi, K. and Peck, R. B. Soil mechanics in engineering practice. New
1948 York, N.Y. John Wiley and Sons.
- Tetelman, A. S. Hydrogen embrittlement of ferrous alloys. Metallurgical
1963 Society Conferences. 20:671-708.
- Timoshenko, S. Theory of elasticity. New York, N.Y. McGraw-Hill Book
1934 Company.
- Trouse, A. C., Jr. and Humbert, R. P. Some effect of soil compaction on
1961 the development of sugar cane roots. Soil Sci. 91:208-217.
- Turc, L. Sur la matiere organique du sol fractionnee par densite. Acad.
1949 Sci. Comp. Rend. (Paris) 229:427-428.
- van Bavel, C. H. M. Mean weight-diameter of soil aggregates as a statisti-
1949 cal index of aggregation. Soil Sci. Soc. Am. Proc. 14:20-23.
- van Bavel, C. H. M. Report of the committee on physical analyses. Soil
1953 Sci. Soc. Am. Proc. 17:416-418.
- van Schuylenborgh, J. On study of soil structure. Ph.D thesis, Library,
1947 Wageningen State University. Wageningen, Netherlands, Ponsen
and Looijen.
- Veihmeyer, F. J. and Hendrickson, A. H. Soil density as a factor in deter-
1946 mining the permanent wilting percentage. Soil Sci. 62:451-456.

- Veihmeyer, F. J. and Hendrickson, A. H. Soil density and root penetration.
1948 Soil Sci. 65:487-493.
- Volkov, M. I. On the methods for determination of soil structure. (translated title) Pochvovedenie:52-58. Original not available; cited in Russell, E. W., Soil structure. Imp. Bur. Soil Sci. Tech. Comm. 37:8. 1938.
- Vomocil, J. A. Degradation of the structure of Yolo sandy loam by compaction. Am. Soc. of Agron. Agron. Abst. 55:68.
1963
- Vomocil, J. A., Waldron, L. J. and Chancellor, W. J. Soil tensile strength
1961 by centrifugation. Soil Sci. Soc. Am. Proc. 25:176-180.
- Waidelich, W. C. Physico-chemical factors influencing the consolidation
ca. of soils. Unpublished M.S. thesis. Princeton, New Jersey,
1960 Library, Princeton University.
- Weibull, W. Statistical theory of the strength of materials. Ingeniors
1939a Vetenskaps Akademien Stockholm Handligar 151.
- Weibull, W. The phenomenon of rupture in solids. Ingeniors Vetenskaps
1939b Akademien Stockholm Handligar 153.
- Wiersum, L. K. The relationship of the size and structural rigidity of
1957 pores to their penetration by roots. Plant and Soil 9:75-78.
- Winterkorn, H. F. Surface-chemical factors influencing the engineering
1936 properties of soils. High. Res. Board Proc. 16:293-300.
- Yoder, R. E. A direct method of aggregate analysis of soils and study
1936 of physical nature of erosion losses. Am. Soc. Agron. J.
28:337-351.

ACKNOWLEDGEMENTS

The author wishes to express his appreciation for guidance, suggestions, comments and in particular for the thorough review of this thesis to Dr. Don Kirkham, Professor of Soils and Physics at the Iowa State University of Science and Technology.

The author wishes to thank Dr. R. S. Hansen, Professor of Chemistry at the Iowa State University of Science and Technology for his suggestions, comments and review of this work and for inspiring the chain of thought that led to this study.

The author wishes also to thank Dr. H. J. Weiss, Professor of Mathematics at the Iowa State University of Science and Technology for his assistance with the mathematical approach to this study and Dr. J. B. Sheeler of the Civil Engineering Experiment Station Laboratory at the Iowa State University of Science and Technology for his suggestions regarding certain soil engineering aspects of this work.

The author wishes to express his appreciation to Dr. W. C. Moldenhauer of the U.S.D.A. A.R.S. at the Iowa State University of Science and Technology for his encouragement and assistance in some aspects of this problem.

The author also wishes to thank Dr. J. M. Bremner and Dr. W. E. Larson of the Agronomy Department at the Iowa State University of Science and Technology for their comments during the course of this study and for their review of this thesis.

The author furthermore wishes to acknowledge Mary A. Clem and Norman Hutton of the Iowa State University Computation Center for their assistance in the computation of data; James Lyon, Alfredo O. Bernal and Dennis Anderson of Ames for their assistance with routine experimental studies

and preparation of drawings; Mrs. Kay Havick of Ames for typing the rough draft; Mrs. Kathryn Lapp of Ames for proof reading the original, and Mrs. Natalie Skola of Ames for typing the final copy.

Finally the author wishes to acknowledge the financial assistance of the Iowa Agricultural Experiment Station for support of this work.

APPENDIX I

Detailed Results and Calculations Pertaining to Strength Measurements
for Respective Size Groups of Clarion s.l., Webster c.l., and Luton
si.c. Aggregates.

Table 52. Average values of size d, of bulk density D, of particle density D_s , of percent porosity P, and of weight percent WP for three size groups of Clarion sandy loam (s.l.), Webster clay loam (c.l., and Luton silty clay (si.c.)^a

	1	2	3	4	5	6	7	8	9	10	11	12	13	14	15
	Clarion s.l.					Webster c.l.					Luton si.c.				
Size group	d ^b	D	D_s	P	WP	d	D	D_s	P	WP	d	D	D_s	P	WP
	cm.	g.cm. ⁻³	g.cm. ⁻³	%		cm.	g.cm. ⁻³	g.cm. ⁻³	%		cm.	g.cm. ⁻³	g.cm. ⁻³	%	
1	.227	1.86	2.72	31.6	18.4	.233	1.84	2.70	32.0	18.2	.231	2.02	2.70	25.2	17.3
2	.347	1.86	2.70	31.2	38.2	.343	1.84	2.69	31.7	42.1	.353	2.02	2.74	26.3	47.5
3	.507	1.86	2.71	31.3	20.7	.579	1.84	2.66	31.0	35.2	.532	2.02	2.71	25.7	35.1
Other ^b	-	-	-	-	23.3	-	-	-	-	5.9	-	-	-	-	0

^aColumns 2, 6 and 11 are average measured values of aggregate diameter as obtained from strain/gauge measurements. Columns 3,7,12 are average values of aggregate bulk density as obtained by gravity fractionation. Columns 4,8,13 are average values of particle density as obtained by pycnometer method. Columns 5,9,14 are average values of porosity as obtained from Equation 48. Columns 6,10,15 are average values of weight percent that each fraction constitutes of the soil as a whole. For details on procedures see section on Methods.

^bOther refers to aggregates heavier (mostly stones) or lighter (very few) than the highest and lowest density group for a given soil respectively.

Table 53. Average size (diameter) d , percent of carbon C , clay, water-stable aggregates WS , average rupture stress Z_{zr} , average stress Z_z , rupture strain e_{zr} and average strain e_z in equatorial plane for three size groups of Clarion s.l., Webster c.l., and Luton si.c. Values of d , Z_{zr} , Z_z , e_{zr} and e_z are given for aggregates in air-dry condition (diameter d_1) and at 15 atm. moisture tension (diameter d_2); moisture contents by weight and by volume are listed^a

Soil				
Size group	d_1	C	clay	WS
	cm.		%	
Clarion s.l.				
1	0.227	1.06	15.7	56.0
2	0.347	0.96	15.1	60.1
3	0.507	0.95	14.4	59.2
Webster c.l.				
1	0.233	3.36	31.2	56.7
2	0.343	3.23	31.7	47.8
3	0.579	3.18	31.3	39.6
Luton si.c.				
1	0.231	3.11	51.8	59.7
2	0.353	2.93	52.2	63.7
3	0.532	2.84	52.0	55.3

^aFor detailed procedures see section on Methods.

Table 53. Continued

Aggregates in air-dry condition				Moisture content	
Z_{zr}	Z_z	e_{zr}	e_z	by wt.	by vol.
$\times 10^6$	dyn.cm. ⁻²	$\times 10^{-2}$	cm.cm. ⁻¹	%	
5.68	4.88	7.64	6.70	1.27	2.36
6.45	4.85	6.01	4.43	0.78	1.45
4.66	3.26	5.33	3.58	0.83	1.53
16.26	12.48	10.22	7.47	2.84	5.20
13.47	9.06	7.87	5.09	2.43	4.28
11.18	7.30	7.16	4.51	2.97	5.44
60.96	38.00	11.24	7.80	3.07	6.18
35.49	22.04	8.50	5.79	3.74	7.64
26.65	15.10	8.21	4.84	3.85	7.76

Table 53. Continued

Aggregates at 15 atm. tension					Moisture content	
d_2	Z_{zr}	Z_z	e_{zr}	e_z	by wt.	by vol.
cm.	$\times 10^6$	cyn.cm. ⁻²	$\times 10^{-2}$	cm.cm. ⁻¹	%	
0.222	-- ^b	--	--	--	--	--
0.369	1.09	0.93	5.68	5.46	8.4	15.7
0.511	1.10	0.86	4.44	3.67	7.5	13.9
0.228	--	--	--	--	--	--
0.386	1.21	1.05	9.31	7.82	18.6	33.9
0.616	0.69	0.51	8.25	6.05	19.6	36.0
0.249	--	--	--	--	--	--
0.399	3.76	2.61	16.33	12.69	21.5	43.0
0.615	0.98	0.81	11.03	9.00	21.0	42.0

^bAggregates at 15 atm. moisture tension for Size group 1 gave inconsistent and zero readings so are not listed.

Table 54. Stress/strain ratio E_{xc} as computed for the polar plane using Equation 147^a for three size groups of Clarion s.l. and as compared with experimental values E_{xe} ^b for aggregates in air-dry condition

1	2	3	4	5	6	7	8	9	10
Size group	d^c	$(\frac{D/P}{D_s})^{0.5}$	$\frac{1}{p^{2.0}}$	$\frac{1}{d^{0.25}}$	$(\frac{\text{clay}}{c^{2.0}})^{3.0}$	$\frac{K}{\text{dyn.cm.}^{-2}}$	$\frac{E_{xc}}{x 10^6 \text{ dyn.cm.}^{-2}}$	$\frac{E_{xe}}{x 10^6 \text{ dyn.cm.}^{-2}}$	Error ^d
	cm.	dimensionless ^e				$x 10^2$			%
1	0.227	1.471	10.0	1.448	2756	1.08	6.34	6.34	0.0
2	0.347	1.484	10.2	1.302	4427	1.08	9.43	9.47	-0.3
3	0.507	1.481	10.2	1.184	4096	1.08	7.91	7.91	0.0

$$E_{xc} = \left(\frac{D/P}{D_s}\right)^{0.5} \times \frac{1}{p^{2.0}} \times \frac{1}{d^{0.25}} \times \left(\frac{\text{clay}}{c^{2.0}}\right)^{3.0} \times K \quad (147)$$

^aSee Equation 103.

^bSee Equation 100.

^cSee List of Symbols.

^dSee Equation 104b.

^eDimensionless for decimal units, i.e., percent can be represented as a fraction of 100, centimeters can be represented as a fraction of one centimeter.

Table 55. Average rupture stress X_{xrc} as computed for the polar plane using Griffith crack theory^a for three size groups of Clarion s.l., and as compared with experimentally determined values of X_{xre} ^b. computed values of T^c , e_{xrc}^d , and " u "^e are given; aggregates are in air-dry condition

Size group	d^f	T	$d^{0.5}$	AE_{xe}	X_{xrc}	X_{xre}	Error ^g	e_{xrc}	"u"
	cm.	$\times 10^4$ ergs cm. ⁻²	cm. ^{0.5}		$\times 10^6$ dyn.cm. ⁻²		%	cm.cm. ⁻¹	
1	0.227	2.65	0.481	0.463	0.962	0.987	-2.5	.1517	0.50
2	0.347	3.96	0.594	0.691	1.164	1.120	+3.8	.1228	0.49
3	0.507	3.31	0.729	0.577	0.792	0.809	-2.2	.1001	0.53

^aSee Equation 115 where $A = 0.073 \text{ cm.}^{0.5}$.

^bSee Equation 93.

^cSee Equation 116.

^dSee equation 117.

^fSee list of symbols.

^gSee Equation 106.

Table 56. Stress/strain ration E_{xc} on the polar plane for three size groups of Webster c.l. computed from Equation 148^a below and compared with experimental values of E_{xe} ^b for aggregates in air-dry condition

1	2	3	4	5	6	7	8	9	10
Size group	d^c	$(\frac{D}{P})^{0.5}$	$\frac{1}{p^{2.0}}$	$\frac{1}{c^{0.25}}$	$(\frac{clay}{C})^{2.0}$	K	E_{xc}	E_{xe}	Error ^d
	cm.	dimensionless ^e				dyn.cm. ⁻² x 10 ³	x 10 ⁶ dyn.cm. ⁻²		
1	0.233	1.458	9.77	1.439	86.21	8.30	14.66	14.51	+1.1
2	0.343	1.468	9.95	1.307	96.34	8.30	15.27	15.46	-1.2
3	0.579	1.492	10.40	1.146	96.90	8.30	14.31	14.07	+1.7

$$E_{xc} = \left(\frac{D}{P}\right)^{0.5} \times \frac{1}{p^{2.0}} \times \frac{1}{c^{0.25}} \times \left(\frac{clay}{C}\right)^{2.0} \times K \quad (148)$$

^aSee Equation 103.

^bSee Equation 100.

^cSee list of symbols.

^dSee Equation 104h.

^eSee footnote - Table 54.

Table 57. Average rupture stress X_{xrc} on the polar plane for three size groups of Webster c.l. computed using Griffith crack theory^a, and compared with experimentally determined values of X_{xre} ^b; computed values of T^c , e_{xrc}^d , and " u "^e are given; aggregates are in air-dry condition

Size group	d^f cm.	T ergs cm. ⁻² $\times 10^4$	$d^{0.5}$ cm. ^{0.5}	AE_{xe} $\times 10^6$	X_{xrc} dyn.cm. ⁻²	X_{xre}	Error ^g %	e_{xrc} cm.cm. ⁻¹	"u"
1	0.233	10.09	0.483	1.364	2.824	2.824	0	.1946	0.53
2	0.343	10.75	0.586	1.453	2.481	2.340	+5.8	.1604	0.49
3	0.579	9.79	0.761	1.323	1.739	1.942	-11.0	.1235	0.58

^aSee Equation 115 where $A = 0.094 \text{ cm.}^{0.5}$.

^bSee Equation 93.

^cSee Equation 116.

^dSee Equation 117.

^eSee Equation 110.

^fSee list of symbols.

^gSee Equation 106.

Table 58. Stress/strain ratio E_{xc} on the polar plane for three size groups of Luton si.c. computed from Equation 149^a below and compared with experimental values of E_{xe} ^b for aggregates in air-dry condition

1	2	3	4	5	6	7	8	9	10
Size group	d^c	$(\frac{D/P}{D_s})^{0.5}$	$\frac{1}{p^{2.0}}$	$\frac{1}{d^{0.375}}$	clay x C	K	E_{xc}	E_{xe}	Error ^d
	cm.	dimensionless ^e				$\frac{\text{dyn.cm.}^{-2}}{x 10^7}$	$x 10^6 \text{ dyn.cm.}^{-2}$		%
1	0.231	1.724	15.74	1.733	0.01611	5.80	43.94	42.30	+3.8
2	0.353	1.676	14.45	1.474	0.01529	5.80	31.66	33.09	-4.4
3	0.532	1.702	15.15	1.267	0.01477	5.80	28.00	27.10	+3.3

$$E_{xc} = \left(\frac{D/P}{D_s}\right)^{0.5} \times \frac{1}{p^{2.0}} \times \frac{1}{d^{0.375}} \times (\text{clay} \times C) \times K \quad (149)$$

^aSee Equation 103.

^bSee Equation 100.

^cSee list of symbols.

^dSee Equation 104h.

^eSee footnote - Table 54.

Table 59. Average rupture stress X_{xrc} on the polar plane for three size groups of Luton si.c. computed using Griffith crack theory^a, and compared with experimentally determined values of X_{xre} ^b; computed values of T ^c, e_{xrc} ^d and "u"^e are given; aggregates are in air-dry condition

Size group	d^f cm.	T ergs cm. ⁻² $\times 10^4$	$d^{0.5}$ cm. ^{0.5}	AE_{xe} $\times 10^6$	X_{xrc} dyn.cm. ⁻²	X_{xre}	Error ^g %	e_{xrc} cm.cm. ⁻¹	"u"
1	0.231	47.06	0.481	5.034	10.46	10.59	-1.2	0.2470	0.46
2	0.353	36.83	0.594	3.938	6.63	6.16	+7.6	0.2000	0.43
3	0.532	30.15	0.729	3.225	4.42	4.63	-4.6	0.1632	0.50

^aSee Equation 115 where $A = 0.119 \text{ cm.}^{0.5}$.

^bSee Equation 93.

^cSee Equation 116.

^dSee Equation 117.

^eSee Equation 110.

^fSee list of symbols.

^gSee Equation 106.

Table 60. Stress/strain ratio $E_{xc}(2)$ on the polar plane computed from Equation 150^a below for two size groups of Clarion s.l., Webster c.l. and Luton si.c., respectively, and compared with experimental value E_{xe}^b ; aggregates are at 15 atm. moisture tension

Size group	d_1^c	d_2	$(\frac{D_2 P_1}{D_1 P_2})^{0.5}$	$(\frac{P_1}{P_2})^{2.0}$	$(\frac{d_1}{d_2})^c$	$E_{xc}(1)$	$E_{xc}(2)$	$E_{xe}(2)$
	cm.		dimensionless			$\times 10^6 \text{ dyn.cm.}^{-2}$		
Clarion s.l.								
2	0.347	0.369	0.608	0.321	0.985	9.43	1.79	1.48
3	0.507	0.511	0.943	0.863	0.998	7.91	6.41	2.00
Webster c.l.								
2	0.343	0.386	0.400	0.183	0.971	15.27	1.08	1.13
3	0.579	0.616	0.648	0.364	0.985	14.31	3.29	0.70
Luton si.c.								
2	0.353	0.399	0.387	0.138	0.955	31.66	1.69	1.83
3	0.532	0.615	0.300	0.103	0.947	28.00	0.81	0.78

$$E_{xc}(2) = E_{xc}(1) \times \left(\frac{D_2 P_1}{D_1 P_2}\right)^{0.5} \times \left(\frac{P_1}{P_2}\right)^{2.0} \times \left(\frac{d_1}{d_2}\right)^c \quad (150)$$

$c = 0.250$ for Clarion and Webster

$c = 0.375$ for Luton

^aSee Equations 118 through 123.

^bSee Equations 100.

^cSee list of symbols.

Table 61. Average rupture stress X_{xrc} on polar plane for two size groups of aggregates at 15 atm. moisture tension computed using Griffith crack theory and compared with experimentally determined values of X_{xre} for Clarion s.l., Webster c.l., Luton si.c.; computed values of T , e_{xrc} , and " u " are also given for each soil, respectively^a

Size group	d_1	d_2	T_2	$d_2^{0.5}$	$A_2 E_x(2)$	$X_{xrc}(2)$	$X_{xre}(2)$	Error	$e_{xrc}(2)$	" u_2 "
	cm.		ergs cm. ⁻² x 10 ⁴	cm. ^{0.5}		x 10 ⁶ dyn.cm. ⁻²		%	cm.cm. ⁻¹	
Clarion s.l.										
2	0.347	0.369	0.62	0.607	0.108	0.177	0.189	-6.6	0.1203	0.47
3	0.507	0.511	0.84	0.715	0.146	0.204	0.191	+6.6	0.1021	0.43
Webster c.l.										
2	0.343	0.386	1.40	0.621	0.141	0.226	0.210	+7.3	0.2013	0.46 ^a
3	0.579	0.616	0.86	0.785	0.088	0.111	0.120	-7.8	0.1592	0.52
Luton si.c.										
2	0.353	0.399	5.49	0.632	0.339	0.564	0.653	-13.0	0.3085	0.53
3	0.532	0.615	2.27	0.784	0.144	0.193	0.170	+12.6	0.2487	0.44

^aSee Equation 124 where $A_2 = 0.073 \text{ cm.}^{0.5}$ for Clarion s.l., $A_2 = 0.125 \text{ cm.}^{0.5}$ for Webster c.l., $A_2 = 0.195 \text{ cm.}^{0.5}$ for Luton si.c.; also see Equations 93, 125, 126, 129, list of symbols, and Equation 106.

Table 62. Strain induced by swelling e_{zi}^a is compared with average strain e_z in equatorial plane; percent stable aggregates^b SA is compared with percent water stable aggregates WS for two size groups of Clarion s.l., Webster c.l., and Luton si.c. aggregates

Size group	d_1^c	d_2	e_{zi}	e_z	N	N_o	SA	WS
	cm.		cm.cm. ⁻¹				%	
Clarion s.l.								
2	0.347	0.369	0.0634	0.0443	72	33	54.2	60.1
3	0.507	0.511	0.0078	0.0358	84	19	63.5	59.2
Webster c.l.								
2	0.343	0.386	0.1253	0.0509	76	55	28.8	47.8
3	0.579	0.616	0.0639	0.0451	63	31	46.9	39.6
Luton si.c.								
2	0.353	0.399	0.1303	0.0780	29	8	72.5	63.7
3	0.532	0.615	0.1560	0.0579	38	15	60.5	55.3

^aSee Equation 130.

^bSee Equation 131.

^cSee list of symbols.

Table 63. Slope m of Weibull lines in Fig. 13 calculated from Equation 137 and data in Fig. 13 for three size groups of aggregates in air-dry condition and two size groups of aggregates at 15 atm. tension for Clarion s.l., Webster c.l., and Luton si.c. soils

Size group	Aggregates in air-dry condition				Aggregates at 15 atm. tension			
	<u>d₁</u>	<u>Z_o(1)</u>	<u>Z_u(1)</u>	<u>m(1)</u>	<u>d₂</u>	<u>Z_o(2)</u>	<u>Z_u(2)</u>	<u>m(2)</u>
	cm.	x 10 ⁶ dyn. cm. ⁻²			cm.	x 10 ⁶ dyn.cm. ⁻²		
Clarion s.l.								
1	0.227	14.8	+2.0	1.42	--	--	--	--
2	0.347	10.2	0.0	1.74	0.369	2.5	+0.3	0.92
3	0.507	8.5	0.0	1.47	0.511	2.1	0.0	0.84
Webster c.l.								
1	0.233	29.0	-1.0	0.98	--	--	--	--
2	0.343	26.5	0.0	1.25	0.386	1.4	0.0	1.36
3	0.579	21.0	-1.0	0.82	0.616	1.0	+0.3	1.08
Luton si.c.								
1	0.231	112.0	-5.0	1.42	--	--	--	--
2	0.353	76.0	+7.0	1.60	0.399	7.0	-0.7	0.51
3	0.532	58.0	+5.0	1.66	0.615	1.7	0.0	0.84

APPENDIX II

Detailed Results and Calculations Pertaining to Strength Measurements
for Respective Density Groups of Clarion s.l., Webster c.l., and Luton
si.c. Aggregates.

Table 64. Average bulk density D , particle density D_s , size d , percent porosity P , and weight percent WP for four density groups of Clarion s.l., Webster c.l., and two density groups of Luton si.c.^a

Density group	Clarion s.l.					Webster c.l.					Luton si.c.				
	D	D_s	d	P	WP	D	D_s	d	P	WP	D	D_s	d	P	WP
	$\frac{\text{g. cm.}^{-2}}$	$\frac{\text{g. cm.}^{-3}}$	cm.	%		$\frac{\text{g. cm.}^{-2}}$	$\frac{\text{g. cm.}^{-3}}$	cm.	%		$\frac{\text{g. cm.}^{-2}}$	$\frac{\text{g. cm.}^{-3}}$	cm.	%	
A	1.76	2.70	0.347	34.8	9.5	1.72	2.69	0.384	36.2	14.4	2.00	2.70	0.382	26.2	22.6
B	1.80	2.69	0.377	33.3	27.4	1.79	2.69	0.393	33.3	67.8	2.03	2.73	0.361	26.5	77.3
C	1.92	2.71	0.371	29.2	29.8	1.87	2.71	0.367	30.9	6.7					
D	1.97	2.74	0.347	28.1	10.6	1.97	2.66	0.396	26.2	6.6					

^aSee footnote a in Table 52 and Methods section.

Table 65. Average density percent carbon C, clay, water stable aggregates WS, average rupture stress Z_{zr} , average stress Z_z , rupture strain e_{zr} and average strain e_z for aggregate of the four Density groups A, B, C, D of Clarion s.l., Webster c.l., and two Density groups A, B or Luton si.c.; values of Z_{zr} , Z_z , e_{zr} and e_z are given for aggregates in air-dry condition and at 15 atm. moisture tension; respective moisture contents by weight and by volume are listed^a

Soil				
Density group	D	C	clay	WS
	g. cm. ⁻³		%	
Clarion s.l.				
A	1.76	1.00	16.3	52.4
B	1.80	1.17	15.6	63.9
C	1.92	0.98	15.7	63.1
D	1.97	0.80	12.7	54.4
Webster c.l.				
A	1.74	3.23	31.8	49.5
B	1.79	3.43	31.5	51.1
C	1.87	2.96	31.9	39.1
D	1.97	3.43	30.4	55.5
Luton si.c.				
A	2.00	3.12	51.7	63.9
B	2.03	2.79	52.3	55.3

^aSee section on Methods.

Table 65. Continued

Aggregates in air-dry condition				Moisture content	
Z_{zr}	Z_z	e_{zr}	e_z	by wt.	by vol.
$\times 10^6$	dyn.cm.^{-2}	$\times 10^{-2}$	cm.cm.^{-1}	%	
4.55	3.65	6.60	5.34	0.99	1.75
5.58	4.33	6.59	4.94	0.93	1.67
5.90	4.43	5.57	4.30	0.80	1.53
6.36	4.92	6.53	5.01	1.11	2.18
12.38	8.99	8.76	5.84	2.87	4.93
11.09	7.86	8.49	5.93	2.71	4.85
16.67	11.42	8.66	5.87	2.52	4.70
14.40	10.17	7.76	5.12	2.74	5.40
39.26	23.89	9.46	6.08	3.47	6.94
42.82	26.20	9.17	6.20	3.67	7.44

Table 65. Continued

Aggregates at 15 atm. moisture tension				Moisture content	
Z_{zr}	Z_z	e_{zr}	e_z	by wt.	by vol.
$\times 10^6$ dyn. cm. ⁻²		$\times 10^{-2}$ cm.cm. ⁻¹		%	
1.14 ^b	.93	4.68	4.18	7.14	12.6
0.91	0.73	4.27	4.93	9.26	16.7
0.84	0.78	5.98	4.11	8.13	15.1
1.50	1.14	5.33	5.03	7.23	14.2
0.82	0.74	8.48	6.87	19.6	33.6
0.77	0.66	6.98	6.73	21.9	39.1
1.08	0.90	8.09	7.25	16.9	31.5
1.04	0.82	9.17	6.88	18.1	35.6
3.12	2.08	16.82	12.81	20.9	41.7
1.62	1.34	10.55	8.88	21.7	43.3

^bFor aggregates at 15 atm. moisture tension density groups are averaged over two size groups only (see footnote b of Table 53).

Table 66. Average rupture stress X_{xrc} on the polar plane for four density groups of Clarion s.l. compared from equation 151^a below and compared with experimentally determined values of X_{xre} ^b for aggregates in air-dry condition

1	2	3	4	5	6	7	8	9
Density group	D^c	$\frac{D/P}{D_s}$	$\frac{1}{d^{0.75}}$	$\frac{C}{\text{clay}}$	K	X_{xrc}	X_{xre}	Error ^d
	g.cm.^{-3}	dimensionless ^e			$\times 10^6 \text{ dyn. cm.}^{-2}$			%
A	1.76	1.875	3.937	0.0613	1.77	0.80	0.79	+1.4
B	1.80	2.009	3.690	0.0752	1.77	0.99	0.97	+1.8
C	1.92	2.429	3.745	0.0625	1.77	1.01	1.03	-1.8
D	1.97	2.557	3.937	0.0629	1.77	1.12	1.11	+1.4

$$X_{xrc} = \frac{D/P}{D_s} \times \frac{1}{d^{0.75}} \times \frac{C}{\text{clay}} \times K \quad (151)$$

^aSee Equation 105, note that exponent of P is zero.

^bSee Equation 93.

^cSee list of symbols.

^dSee Equation 106.

^eSee footnote - Table 54.

Table 67. Rupture strain e_{zrc}^a on the polar plane is computed from Equation 152 below and compared with experimental values of e_{xre}^b , for four Density groups of Clarion s.l. aggregates in air-dry condition; values of u^c and values of e_{xr} computed from Griffith crack theory^d are also given

1	2	3	4	5	6	7	8	9	10	11	12
Density group	D^e	$(\frac{D/P}{D_s})^{0.50}$	$P^{2.0}$	d	$\frac{1}{C}$	$K \times 10^{-2}$	e_{xrc}	e_{xre}	Error ^f	u	e_{xr} Griffith
	$g.cm.^{-3}$	dimensionless					$cm.cm.^{-1}$		%		$cm.cm.^{-1}$
A	1.76	1.369	0.1211	0.347	100.0	2.38	0.1370	0.1338	+2.3	0.48	0.1239
B	1.80	1.418	0.1109	0.377	85.4	2.38	0.1206	0.1266	-4.96	0.55	0.1188
C	1.92	1.559	0.0853	0.371	102.0	2.38	0.1198	0.1146	+4.5	0.47	0.1198
D	1.97	1.599	0.0790	0.347	125.0	2.38	0.1304	0.1298	+0.5	0.50	0.1239

$$e_{xrc} = \left(\frac{D/P}{D_s}\right)^{0.5} \times P^{2.0} \times d \times \frac{1}{C} \times K$$

(152)

^aSee Equation 107.

^bSee Equation 102.

^cSee Equation 110.

^d $e_{xr} = 0.073/d^{0.5}$ - see Equation 117 and Table 55.

^eSee list of symbols.

^fSee Equation 108.

Table 68. Average rupture stress on the polar plane X_{xrc} for four Density groups of Webster c.l. computed from Equation 153 below^a and compared with experimentally determined values of X_{xre} ^b for aggregates in air-dry condition

1	2	3	4	5	6	7	8
Density group	D^c	$(\frac{D/P}{D_s})^{0.75}$	$(\frac{\text{clay}}{C})^{2.0}$	K	X_{xrc}	X_{xre}	Error ^d
	g.cm.^{-3}	dimensionless			$\times 10^6 \text{ dyn.cm.}^{-2}$		%
A	1.74	1.532	97.023	0.014	2.08	2.15	-3.3
B	1.79	1.682	84.272	0.014	1.98	1.93	+2.6
C	1.87	1.827	116.640	0.014	2.98	2.90	+1.4
D	1.97	2.179	78.500	0.014	2.39	2.50	-4.5

$$X_{xrc} = \left(\frac{D/P}{D_s}\right)^{0.75} \times \left(\frac{\text{clay}}{C}\right)^{2.0} \times K \quad (153)$$

^aSee Equation 105, note that exponents of P and D are zero.

^bSee Equation 93.

^cSee list of symbols.

^dSee Equation 106.

Table 69. Rupture strain e_{xrc}^a on the polar plane is computed from Equation 154 below and compared with experimental values of e_{xre}^b for four density groups of Webster c.l. aggregates in air-dry condition; values of "u"^c and values of e_{xr} computed from Griffith crack theory^d are also given

1	2	3	4	5	6	7	8	9	10	11	12
Density group	D^e	$\frac{D/P}{D_s}$	$P^{1.50}$	d	$\frac{\text{clay}^{3.0}}{C^{0.5}}$	K	e_{xrc}	e_{xre}	Error ^f	"u"	e_{xrc} Griffith
	g.cm.^{-3}		dimensionless ^g				cm.cm.^{-1}		%		cm.cm.^{-1}
A	1.74	1.768	0.218	0.384	0.1785	6.254	0.1650	0.1608	+2.6	0.53	0.1516
B	1.79	1.999	0.192	0.393	0.1688	6.254	0.1594	0.1670	-4.5	0.53	0.1499
C	1.87	2.234	0.172	0.367	0.1888	6.254	0.1664	0.1711	-2.7	0.52	0.1551
D	1.97	2.825	0.134	0.396	0.1515	6.254	0.1420	0.1445	-2.0	0.55	0.1494

$$e_{xrc} = \frac{D/P}{D_s} \times P^{1.50} \times d \times \frac{\text{clay}^{3.0}}{C^{0.5}} \times K \quad (154)$$

^aSee Equation 107.

^bSee Equation 102.

^cSee Equation 110.

^d $e_{xrc} = 0.094/d^{0.5}$ - see Equation 117 and Table 57.

^eSee list of symbols.

^fSee Equation 108.

^gSee footnote - Table 54.

Table 70. Average rupture stress in the polar plane X_{xrc} for two density groups of Luton si.c. is computed from Equation 155 below^a and compared with experimentally determined values of X_{xre} ^b for aggregates in air-dry condition

1	2	3	4	5	6	7	8
Density group	D^c	$\frac{D/P}{D_s}$	$\frac{1}{d}$	K_a	X_{xrc}	X_{xre}	Error ^d
	$g.cm.^{-3}$	dimensionless ^e			$\times 10^6 \text{ dyn.cm.}^{-2}$		%
A	2.00	2.824	2.617	0.92	6.80	6.82	-0.3
B	2.03	2.920	2.770	0.92	7.44	7.44	0.0

$$X_{xrc} = \frac{D/P}{D_s} \times \frac{1}{d} \times K \quad (155)$$

^aSee Equation 105 note that exponents of P, C, and clay are zero.

^bSee Equation 93.

^cSee list of symbols.

^dSee Equation 106.

^eSee footnote - Table 54.

Table 71. Rupture strain e_{xrc}^a in the polar plane is computed from Equation 156 below and compared with experimental values of e_{xre}^b for two density groups of Luton si.c., aggregates in air-dry condition. Values of " u "^c and values of e_{xr} computed from Griffith crack theory^d are also given

1	2	3	4	5	6	7	8	9	10	11
Density group	D^e	$(\frac{D/P}{D_s})^{-1.0}$	$\frac{1}{d^{0.5}}$	clay	K	e_{xrc}	e_{xre}	Error ^f	"u"	e_{xr} Griffith
	g.cm.^{-3}	dimensionless				cm.cm.^{-1}		%		cm.cm.^{-1}
A	2.00	0.3541	1.618	0.517	0.6774	0.2004	0.1997	+0.2	0.47	0.1925
B	2.03	0.3424	1.663	0.523	0.6774	0.2018	0.2023	-0.3	0.45	0.1980

$$e_{xrc} = \left(\frac{D/P}{D_s}\right)^{-1.0} \times \frac{1}{d^{0.5}} \times \text{clay} \times K \quad (156)$$

^aSee Equation 107.

^bSee Equation 102.

^cSee Equation 110.

^d $e_{xr} = 0.119/d^{0.5}$ - see Equation 117 and Table 59.

^eSee list of symbols.

^fSee Equation 108.

^gSee footnote - Table 54.

Table 72. Stress/strain ratio $E_{xc}(2)$ on the polar plane computed from Equation 157 below for four Density groups of Clarion s.l. and Webster c.l. and for two Density groups of Luton si.c. and compared with experimental value of $E_{xe}(2)$ for aggregates at 15 atm. moisture tension^a

Density group	D	d_1^b	d_2	$\left(\frac{D_2 P_1}{D_1 P_2}\right)$	$\left(\frac{P_1}{P_2}\right)$	$\left(\frac{d_1}{d_2}\right)$	$E_{xe}(1)$	$E_{xc}(2)$	$E_{xe}(2)$
	g.cm.^{-3}	cm.		dimensionless			$\times 10^6 \text{ dyn.cm.}^{-2}$		
Clarion s.l.									
A	1.76	0.407	0.423	0.60	0.74	0.96	6.87	2.93	1.91
B	1.80	0.451	0.471	0.55	0.70	0.96	8.00	2.96	1.30
C	1.92	0.443	0.449	0.83	0.88	0.99	11.71	8.47	1.65
D	1.97	0.408	0.418	0.70	0.78	0.98	9.29	4.97	2.00
Webster c.l.									
A	1.74	0.461	0.498	0.34	0.58	0.93	12.90	2.37	0.96
B	1.79	0.472	0.511	0.33	0.55	0.93	12.66	2.14	0.85
C	1.87	0.439	0.494	0.16	0.42	0.89	17.94	1.07	1.04
D	1.97	0.473	0.502	0.42	0.57	0.94	15.91	3.58	1.04
Luton si.c.									
A	2.00	0.455	0.516	0.14	0.37	0.88	28.51	1.30	1.39
B	2.03	0.429	0.498	0.08	0.31	0.86	36.28	0.77	1.30

$$E_{xc}(2) = E_{xe}(1) \times \left(\frac{D_2 P_1}{D_1 P_2}\right) \times \left(\frac{P_1}{P_2}\right) \times \left(\frac{d_1}{d_2}\right) \quad (157)$$

^aSee Equations 118 through 123, Equation 100 and list of symbols. Average size is for two size groups only (2.83 to .476 cm. and .476 to .800 cm.). Values for 0.200 to 0.283 cm. size group gave inconsistent and zero readings of stress and are not included in Table 72. $E_{xe}(1)$ values in air-dry condition calculated from exp. data for the Density groups of the two size groups in footnote b above.

Table 73. Average rupture strain e_{xrc} on the polar plane for respective Density groups of Clarion s.l., Webster c.l. and Luton si.c. aggregates computed from Griffith crack theory and compared with experimental values of e_{xre} ; values presented are for two size groups (.283 to 0.476 and 0.476 to 0.800 cm.) and aggregates are at 15 atm. moisture tension; computed values of "u" and ΔT values are also listed^a

Density group	D	$\frac{d_1}{d_2}$	d_2	$d_2^{0.5}$	$\frac{E_{xe}(2)}{x \cdot 10^6 \text{ dyn.cm.}^{-2}}$	$\frac{e_{xrc}(2)}{\text{cm.cm.}^{-1}}$	$\frac{e_{xre}(2)}{\text{cm.cm.}^{-1}}$	"u"	$\frac{\Delta T}{x \cdot 10^4 \text{ ergs cm.}^{-2}}$
Clarion s.l.									
A	1.76	0.407	0.423	0.650	1.91	0.112	0.104	0.42	2.08
B	1.80	0.451	0.471	0.686	1.30	0.106	0.122	0.40	2.81
C	1.92	0.443	0.449	0.670	1.65	0.109	0.088	0.55	4.21
D	1.97	0.408	0.418	0.647	2.00	0.113	0.131	0.47	3.05
Webster c.l.									
A	1.74	0.461	0.498	0.706	0.96	0.177	0.148	0.48	7.82
B	1.79	0.472	0.511	0.715	0.85	0.174	0.158	0.40	7.75
C	1.87	0.439	0.494	0.703	1.04	0.177	0.181	0.46	11.18
D	1.97	0.473	0.502	0.709	1.04	0.176	0.174	0.52	9.77
Luton si.c.									
A	2.00	0.455	0.516	0.718	1.39	0.272	0.390	0.62	27.56
B	2.03	0.429	0.498	0.706	1.30	0.276	0.216	0.38	36.47

^aSee Equations 124 and 126 and Table 61; $A_2 = 0.073 \text{ cm.}^{0.5}$ for Clarion s.l.; $A_2 = 0.125 \text{ cm.}^{0.5}$ for Webster c.l.; $A_2 = 0.195 \text{ cm.}^{0.5}$ for Luton si.c.; see Equation 102, Equation 110, Equation 127 and Table 72; see also list of symbols.

APPENDIX III

Detailed Results and Calculations Pertaining to Strength Measurements
for Soil as a Whole for Clarion s.l., Webster c.l., and Luton si.c.
Aggregates.

Table 74. Average size d , bulk density D , particle density D_s , percent porosity P , carbon C , clay water stable aggregates WS , rupture stress Z_{zr} on equatorial plane, average stress Z_z , rupture strain e_{zr} , average strain e_z , percent moisture content by weight and by volume for Clarion s.l., Webster c.l., and Luton si.c. aggregates in air-dry condition and at 15 atm. moisture tension^a

Soil	d	D	D_s	P	c	clay	WS
	cm.	g. cm. ⁻³			%		
Clarion s.l.	0.361	1.86	2.71	31.4	0.99	15.1	58.4
Webster c.l.	0.372	1.84	2.69	31.6	3.26	31.4	48.0
Luton si.c.	0.372	2.02	2.71	25.8	2.96	52.0	59.6

^aSee section on Methods.

Table 74. Continued

Aggregates in air-dry condition				Moisture content	
Z_{zr}	Z_z	e_{zr}	e_z	by wt.	by vol.
$\times 10^6 \text{ dyn.cm.}^{-2}$		$\times 10^{-2} \text{ cm.cm.}^{-1}$		$\%$	
5.60	4.33	6.32	4.89	0.96	1.78
13.64	9.61	8.42	5.69	2.75	4.97
41.04	25.05	9.32	6.14	3.55	7.19

Table 74. Continued

Aggregates at 15 atm. moisture tension				Moisture content	
Z_{zr}	Z_z	e_{zr}	e_z	by wt.	by vol.
$\times 10^6$ dyn.cm. ⁻²		$\times 10^{-2}$ cm.cm. ⁻¹		%	
1.10	0.90	6.06	4.57	7.9	14.8
0.95	0.78	8.71	6.94	19.1	35.0
2.37	1.71	13.68	10.85	21.3	42.5

Table 75. Stress/strain ratio E_{xc} in the polar plane is computed from Equation 158 below and compared with experimental values of E_{xe} ; average rupture stress X_{xrc} is computed using Griffith crack theory and compared with experimentally determined values of X_{xre} ; computed values of e_{xr} , "u" and T are given; all quantities are for Clarion s.l., Webster c.l., and Luton si.c. aggregates in air-dry condition

Soil	$\frac{D/P^a}{D_s}$	clay	K_r	E_{xc}^b	E_{xe}^c	Error ^d
	dimensionless			$\times 10^6 \text{ dyn.cm.}^{-2}$		%
Clarion s.l.	2.185	0.151	23	7.59	7.96	-4.7
Webster c.l.	2.167	0.314	23	15.65	14.66	+6.5
Luton si.c.	2.884	0.520	23	34.50	35.43	-2.7

$$E_x = \frac{D/P}{D_s} \times \text{clay} \times K_r \quad (158)$$

$$\text{where } K_r = 2.30 \times 10^7 \text{ dyn.cm.}^{-2}$$

^aSee list of symbols.

^bSee Equation 103.

^cSee Equation 100.

^dSee Equation 104h.

Table 75. Continued

A	$d^{0.5}$	X_{xrc}^e	X_{xre}^f	Error ^g	e_{xr}^h	"u" ⁱ	T^j
$\text{cm.}^{0.5}$		$\times 10^6$	dyn.cm.^{-2}	%	cm.cm.^{-1}		$\times 10^4$ ergs cm.^{-2}
0.073	0.601	0.922	0.973	-5.4	0.1215	0.52	3.33
0.094	0.610	2.412	2.369	+1.8	0.1541	0.55	10.19
0.119	0.610	6.727	7.129	-5.8	0.1950	0.48	39.43

^eSee Equation 115.^fSee Equation 93.^gSee Equation 106.^hSee Equation 117.ⁱSee Equation 110.^jSee Equation 116.

Table 76. Stress/strain ratio $E_{xc}(2)$ on the polar plane, aggregates at 15 atm. tension computed from Equation 159 below and compared with experimental values of $E_{xe}(2)$; average rupture stress $X_{xrc}(2)$ on the polar plane computed using Griffith crack theory and compared with experimental values of $X_{xre}(2)$; computed values of $e_{xrc}(2)$, "u" and T_2 are also given; results are presented for Clarion s.l., Webster c.l., and Luton si.c. aggregates

Soil	$\frac{D_2 P_1}{D_1 P_2}$ ^a	$\frac{P_1}{P_2}$	$\frac{d_1}{d_2}$	$E_{xe}(1)$	$E_{xc}(2)$ ^b	$E_{xe}(2)$ ^c
	dimensionless			$\times 10^6 \text{ dyn.cm.}^{-2}$		
Clarion s.l.	0.62	0.76	0.97	8.81	4.03	1.74
Webster c.l.	0.29	0.53	0.92	14.81	2.09	0.96
Luton si.c.	0.11	0.34	0.87	32.37	1.05	1.30

$$E_{xc}(2) = E_{xe}(1) \times \left(\frac{D_2 P_1}{D_1 P_2} \right) \times \left(\frac{P_1}{P_2} \right) \times \left(\frac{d_1}{d_2} \right) \quad (159)$$

^aSee list of symbols.

^bSee Equations 118 through 123.

^cSee Equation 100.

Table 76. Continued

A_2	$d_2^{0.5}$	X_{xrc}^d	X_{xre}^e	Error ^f	$e_{xre}(2)^g$	"u ₂ " ^h	T_2^i
	cm. ^{0.5}	$\times 10^6$ dyn.cm. ⁻²		%			$\times 10^4$ ergs cm. ⁻²
.073	0.663	0.191	0.191	0.0	0.1101	0.46	0.73
0.125	0.708	0.169	0.165	+2.4	0.1765	0.49	1.18
0.195	0.712	0.356	0.411	-14.3	0.2738	0.50	4.54

^dSee Equation 124.^eSee Equation 93.^fSee Equation 106.^gSee Equation 126.^hSee Equation 129.ⁱSee Equation 125.

Table 77. Percent stable aggregates^a SA is compared with percent water stable aggregates WS; strain induced by swelling e_{zi}^b is compared with average strain e_z for Clarion s.l., Webster c.l., and Luton si.c. aggregates

Soil	SA	WS	e_{zi}	e_z
	%		cm.cm. ⁻¹	
Clarion s.l.	58.8	58.4	0.0304	0.0489
Webster c.l.	38.0	48.0	0.0867	0.0569
Luton si.c.	66.5	59.6	0.1444	0.0614

^aSee Equation 131.

^bSee Equation 130.

APPENDIX IV

Statistical Analysis

In Table 78, Table 79, and Table 80 analysis of variance over size, density, and size density interaction for percent carbon, percent clay, and percent water stable aggregates respectively is presented for Clarion s.l., Webster c.l., and Luton si.c. Degrees of freedom for error for Clarion s.l. and Webster c.l. have been decreased by 3 from 12 to 9. Some of the size-density subgroups obtained during density separation proved to be very small, consequently shortage of aggregates has resulted in some missing data. Missing data were computed from the formula listed in Snedecor (1957) for a randomized block design. If X is a missing datum then

$$X = \frac{aT + bB - S}{(a-1)(b-1)} \quad (160)$$

a = number of treatments

b = number of blocks

T = sum of items with same treatment as missing item

B = sum of items in the same block as missing item

S = sum of all observed items

The iterative scheme was used since three values were missing and consequently the degrees of freedom for error had to be decreased by three.

In Table 81 through Table 83 approximate analysis of variance for rupture stress, average stress and average strain for Clarion s.l., Webster c.l., and Luton si.c. is presented. This analysis is termed approximate since determination error was used in testing for significance. Furthermore, since the size of the sample varied, unweighted means analysis was

carried out and harmonic mean was used in the analysis of the means. Rupture stress, average stress, and average strain values for two replications (see section on Methods) were combined. Each individual determination was considered a replication. We felt justified in doing so since each aggregate was selected entirely at random from the population. It was also felt that a large sample would be more representative of the population than two smaller ones, and since the variation between individual determinations was very large, it was felt determination error would be a suitable estimator of experimental error used in tests of significance.

Table 78. Percent carbon C analysis of variance over size, density, and size-density interaction for Clarion s.l., Webster c.l., and Luton si.c.

Source	Clarion s.l.			Webster c.l.			Luton si.c.		
	df	MS	F	df	MS	F	df	MS	F
Size	2	0.0272	12.17** ^a	2	0.0710	NS	2	0.0786	37.42**
Density	3	0.1363	61.10**	3	0.3028	7.33**	1	0.3333	158.71**
S x D	6	0.0067	2.98	6	0.1583	3.83*	2	0.0616	29.33**
Error	9	0.0022		9	0.0413		6	0.0021	

^a(**) Significant at 1% level, (*) Significant at 5% level, () Significant at 10% level, (NS) Not significant.

Table 79. Percent clay analysis of variance over size, density, and size-density interaction for Clarion s.l., Webster c.l., and Luton si.c.

Source	Clarion s.l.			Webster c.l.			Luton si.c.		
	df	MS	F	df	MS	F	df	MS	F
Size	2	3.3733	NS ^a	2	0.6547	NS	2	0.1460	NS
Density	3	15.7296	6.00*	3	2.6851	6.09*	1	1.1285	NS
S x D	6	0.8547	NS	6	2.5602	5.81**	2	0.0838	NS
Error	9	2.6197		9	0.4408		6	0.4475	

^a(**) Significant at 1% level, (*) Significant at 5% level, () Significant at 10% level, (NS) Not significant.

Table 80. Percent water stable aggregates WS, analysis of variance over size, density, and size-density interaction for Clarion s.l., Webster c.l., and Luton si.c.

Source	Clarion s.l.			Webster c.l.			Luton si.c.		
	df	MS	F	df	MS	F	df	MS	F
Size	2	36.90	NS ^a	2	579.15	4.49*	2	70.21	6.54*
Density	3	208.92	NS	3	293.53	NS	1	221.88	20.68**
S x D	6	264.38	3.10	6	127.93	NS	2	0.10	NS
Error	9	85.41		9	129.04		6	10.73	

^a(**) Significant at 1% level, (*) Significant at 5% level, () Significant at 10% level, (NS) Not significant.

Table 81. Rupture stress Z_{Zr} dyn.cm.⁻² analysis of variance over size, density, and size-density interaction for Clarion s.l., Webster c.l., and Luton si.c. for aggregates in air-dry condition; all values of MS are $\times 10^6$

Source	Clarion s.l.			Webster c.l.			Luton si.c.		
	df	MS	F	df	MS	F	df	MS	F
Size	2	3.2410	5.55** ^a	2	25.8889	8.74**	2	634.7061	29.12**
Density	3	1.7808	3.05*	3	17.8335	6.02**	1	18.9864	NS
S x D	6	0.9940	NS	6	5.1239	NS	2	10.7709	NS
Error	482	0.5844		466	2.9604		252	21.7977	

^a(**) Significant at 1% level, (*) Significant at 5% level, () Significant at 10% level, (NS) Not significant.

Table 82. Average stress Z_z dyn.cm.⁻² analysis of variance over size, density, and size-density interaction for Clarion s.l., Webster c.l., and Luton si.c., aggregates in air-dry condition; all values for MS are $\times 10^6$

Source	Clarion s.l.			Webster c.l.			Luton si.c.		
	df	MS	F	df	MS	F	df	MS	F
Size	2	3.4203	12.75** ^a	2	27.8455	27.75**	2	275.8923	4.79**
Density	3	0.8111	3.03*	3	7.0442	6.98**	1	8.0055	NS
S x D	6	0.6361	2.37*	6	1.7942	NS	2	5.7115	NS
Error	482	0.2683		466	1.0034		252	5.7540	

^a(**) Significant at 1% level, (*) Significant at 5% level, () Significant at 10% level, (NS) Not significant.

Table 83. Average strain e_z cm.cm.⁻¹ analysis of variance over size, density, and size-density interaction for Clarion s.l., Webster c.l., and Luton si.c. for aggregates in air-dry condition; all values for MS are $\times 10^{-2}$

Source	Clarion s.l.			Webster c.l.			Luton si.c.		
	df	MS	F	df	MS	F	df	MS	F
Size	2	10.4144	38.76** ^a	2	9.8128	38.2**	2	4.5660	18.95**
Density	3	0.5678	2.11	3	0.4418	NS	1	0.0216	NS
S x D	6	0.0712	NS	6	0.1272	NS	2	0.0961	NS
Error	482	0.2687		466	0.2578		252	0.2413	

^a(**) Significant at 1% level, (*) Significant at 5% level, () Significant at 10% level, (NS) Not significant.

APPENDIX V

List of Symbols and Definitions

A	A constant for a soil at a given moisture content, equal to $e_{xrc}/d^{0.5}$ (see Equation 117) in $\text{cm}^{0.5}$.
Aggregate	A number of primary particles of sand, silt and clay connected together in a spatial distribution in the state of equilibrium at a given temperature and moisture content (see Introduction).
Air-dry	Aggregates equilibrated for at least two weeks at 40% (<u>+5</u>) relative humidity and $74^{\circ}\text{F}(\underline{+5}^{\circ})$ temperature.
15 atm.	Aggregates equilibrated on pressure membrane apparatus at 15 atm. moisture tension.
C	Organic carbon content in percent (see Equation 7).
Clay	Clay content in percent (see Equation 8).
Crushing strength	Equivalent to crushing stress Z_{zr} at rupture.
CS	Calculated shift of Weibull lines (see Equation 138), unit: 1 cycle of log scale.
d	Aggregate diameter in cm.
d_1	As above in air-dry condition.
d_2	As above at 15 atm. moisture tension.
Δd	Change in aggregate diameter ($d_2 - d_1$) resulting from increased moisture content.
D	Aggregate bulk density, a ratio: weight of solids/total volume, (see Equations 104d and 48) in g.cm^{-3} .

D_1	As above in air-dry condition (see Equation 45).
D_2	As above at 15 atm. moisture tension (see Equation 122).
D_s	Aggregate particle density, a ratio: weight of solids/volume of solids, (see Equations 104c and 48) in g.cm.^{-3} .
Density group	An assembly of aggregates in the same density range.
E_x	Modulus of elasticity in tension equal to average stress/strain ratio on polar plane in dyn.cm.^{-2} (see Equation 100).
E_{xr}	Same as above except at rupture (see Equations 94 and 95).
E_{xc}	Computed value for the modulus of elasticity in tension on the polar plane in dyn.cm.^{-2} .
$E_{xc}(1)$	Same as above in air-dry condition (see Equation 103).
$E_{xc}(2)$	Same as above except at 15 atm. moisture tension (see Equation 123).
E_{xe}	Experimental value for the modulus of elasticity in tension, stress/strain ratio on the polar plane in dyn.cm.^{-2} .
$E_{xe}(1)$	Same as above in air-dry condition (see Equation 100).
$E_{xe}(2)$	Same as above except at 15 atm. moisture tension (see Equation 100).

E_z	Average modulus of elasticity in compression, stress/strain ratio on equatorial plane in dyn. cm. ⁻² (see Equation 92).
E_{zr}	Same as above but at rupture.
e_x	Strain on the polar plane in cm.cm. ⁻¹ , defined by Equation 90 as a ratio of change in equatorial diameter to the original equatorial diameter.
e_{xr}	As above, at rupture.
e_{xrc}	Computed strain on the polar plane at rupture in cm.cm. ⁻¹ (see Equation 107 or 117).
$e_{xrc}(1)$	Same as above in air-dry condition.
$e_{xrc}(2)$	Same as above at 15 atm. moisture tension.
e_{xre}	Experimental strain on the polar plane in cm.cm. ⁻¹ (see Equation 101).
$e_{xre}(1)$	Same as above in air-dry condition.
$e_{xre}(2)$	Same as above at 15 atm. moisture tension.
e_z	Average strain on the equatorial plane, defined by Equation 90 as a ratio of change in polar diameter to the original polar diameter in cm.cm. ⁻¹ .
e_{zr}	Same as above except at rupture.
e_{zi}	Strain on the equatorial plane induced by swelling in cm.cm. ⁻¹ (see Equation 130).
Equatorial plane	Horizontal plane through the center of an aggregate assumed to be spherical (see Fig. 8).
Equatorial diameter	Diameter of the equatorial plane, (see Fig. 8) in cm.

Error	(Computed value-experimental value)100/((computed value + experimental value)0.5, (see Equations 104h, 106, 108) in percent.
K	Used as a proportionality constant, varies in value among soils and between moisture contents, used in computation of E_{xc} , X_{xrc} and e_{xrc} .
Load axis	As used in this dissertation polar or z-axis of an aggregate (see Fig. 8).
m	Slope of Weibull lines.
Moisture content:	
By weight	Weight of water per unit weight of soil, in percent.
By volume	Volume of water per unit volume of soil in percent.
OS	Observed shift of Weibull lines.
P	Porosity, (volume of voids/total volume) ratio in percent, (see Equations 114a and 49).
P_1	As above in air-dry condition (see Equation 49).
P_2	As above except at 15 atm. moisture tension, (see Equation 121).
ΔP	Change in porosity ($P_2 - P_1$) in percent, (see Equation 120).
Point loads	Loads on a spherical aggregate at the poles (see Fig. 8).
Poisson ratio	A ratio of transverse to longitudinal strain estimated per unit length, produced by the longitudinal stress, (see Equation 85a).
Polar plane	Vertical plane through the center of a spherical

	aggregate (see Fig. 8).
S	Probability of rupture (see Equation 133).
(1-S)	Probability of survival (see Equation 132).
SA	Stable aggregates, exhibiting non-zero stress values at rupture (see Equation 131) in percent.
Size group	An assembly of aggregates in the same size range.
Size-density group	An assembly of aggregates in the same size-density range.
T	Energy of rupture in ergs/cm^{-2} .
T_1	Same as above in air-dry condition (Equation 116).
T_2	Same as above except at 15 atm. moisture tension (Equation 125).
ΔT	Change in energy of rupture ($T_2 - T_1$) in ergs cm^{-2} (see Equations 127, 128).
Tensile strength	Equivalent to tensile stress X_{xr} at rupture.
U	Strain energy (see Equations 111, 112), in erg.cm^{-1} .
u	Poisson ratio (see Equation 85a).
"u"	Values of Poisson ratio computed from experimental data testing the assumption that Poisson ratio for soil aggregates equals approximately 0.50, (see Equations 109 and 110).
Ultimate aggregate	The smallest sized aggregate that has a probability of 0.90 of sustaining average rupture stress for a given soil, in cm., i.e., (1-S) for ultimate sized aggregate is 0.90.
V	Aggregate volume in cm^3 (same as V_{total} below).

ΔV	Change in aggregate volume in cm^3 (see Equation 118).
V_{solids}	Volume of solid material within an aggregate in cm^3 (see Equation 104c).
V_{total}	Aggregate volume in cm^3 (see Equation 104a).
V_{voids}	Volume of voids within an aggregate (see Equation 104a), in cm^3 .
Void ratio	A ratio: (volume of voids/volume of solids), (see Equation 104c).
W_{solids}	Weight of aggregate solid material in g. (see Equation 104d).
WS	Water stable aggregates (see Methods).
Weibull lines	A graph of $1/(1-S)$ against crushing stress at rupture Z_{Zr} , (see Fig. 13).
X_0	Ultimate tensile strength of soil aggregates defined as tensile stress at $S = 0.90$ in dyn.cm^{-2} .
X_x	Average tensile stress on the polar plane in dyn.cm^{-2} (see Equation 88).
X_{xr}	Same as above except at rupture (see Equation 93).
X_{xrc}	Computed value of tensile stress at rupture (see Equations 105 or 115).
$X_{\text{xrc}}(1)$	Same as above in air-dry condition.
$X_{\text{xrc}}(2)$	Same as above except at 15 atm. moisture content.
Z_0	Ultimate crushing strength of soil aggregates defined as crushing stress at $S = 0.90$ in dyn.cm^{-2} (see Equation 136 and Fig. 13), note that when

$$S = 0.90, \log (1/1-S) = 1.$$

 Z_z

Average crushing stress on equatorial plane in
dyn.cm.⁻² (see Equation 84).

 Z_{zr}

Same as above except at rupture (see Equation 84).

Page Numbers of Tables, Figures and Equations

Tables

Table	Page
1	8
2a	36
2b	37
3	39
4	43
5	46
6	50
7	51
8	53
9	59
10	61
11	64
12	71
13	72
14	73
15	78
16	80
17a	82

Table	Page	
17b	90	
18a,18b	131	Discussed on p. 168
19	132	Discussed on p. 170
20	132	Discussed on p. 171
21	133	Discussed on p. 172
22	134	Discussed on p. 179
23	135a	Discussed on p. 180
24	135b	Discussed on p. 185
25	136	Discussed on p. 187
26	137	Discussed on p. 188
27	138	Discussed on p. 189
28,29	139	Discussed on p. 192
30	140	Discussed on p. 193
31	142	Discussed on p. 195
32	143	Discussed on p. 195
33	144	Discussed on p. 197
34	146	Discussed on p. 197
35	147	Discussed on p. 200
36	148	Discussed on p. 201
37	149	Discussed on p. 207
38	150	Discussed on p. 215
39	151	Discussed on p. 217
40	152	Discussed on p. 217
41	153	Discussed on p. 219
42	155	Discussed on p. 219

Table	Page	
43	155	Discussed on p. 224
44	157	Discussed on p. 226
45	158	Discussed on p. 226
46	158	Discussed on p. 227
47	159	Discussed on p. 232
48	159	Discussed on p. 233
49,50	160	Discussed on p. 234
51a	161	Discussed on p. 242
51b	162	
51c	164	
51d	165	
51e	241	
51f	246	
51g	247	
52	264	
53	265	
54	268	
55	269	
56	270	
57	271	
58	272	
59	273	
60	274	
61	275	
62	276	

Table	Page
63	277
64	279
65	280
66	283
67	284
68	285
69	286
70	287
71	288
72	289
73	290
74	292
75	295
76	297
77	299
78,79	302
80,81	303
82,83	304

Figures

Figure	Page
1	11
2	16
3	27
4	47
5	48

Figure	Page
6	49
7	67
8	100
9	106
10	108
11	109
12	110
13	141
14	154

Discussed on p. 193

Discussed on p. 219

Equations

Equation	Page
1	14
2	15
3,4	19
5,6	22
7,8	23
9	31
10a,10b,10c,10d	32
11,12,13a,13b,13c	33
14,15	36
16,17	37
18,19,20	40
21,22,23,24,25	41
26,27	45
28	46

Equation	Page
29	51
30,31,32,33	52
34,35,36,37	62
38,39	64
40,41,42	68
43,44,45,46	69
47,48	70
49	72
50,51	74
52a,52b,53	75
54	82
55,56,57,58,59	84
60,61	85
62,63,64,65,66,67	86
68,69,70	87
71,72	88
73	89
74a,74b,74c,74d,74e	91
74f	92
74g,75,76,77,78	93
79,80	101
81,82,83	102
84,85a	104
85b	105
85c,86	107

Equation	Page
87,88,89	111
90,91	112
92	113
93	114
94,95,96,97,98,99,100,101	115
102,103,104a,104b,104c,104d	116
104e,104f,104g,104h,105,106	117
107,108,109	118
110	119
111,112,113	120
114,115,116,117,118	121
119,120,121,122,123,124,125	122
126,127,128,129,130,131	123
132,133,134,135,136	124
137	125
138,139	126
140	178
141	203
142,143a,143b	204
144	206
145	210
146	239
147	268
148	270
149	272

Equation	Page
150	274
151	283
152	284
153	285
154	286
155	287
156	288
157	289
158	295
159	297
160	300